UNIVERSITÉ DE STRASBOURG

École Doctorale des Sciences de la Vie et de la Santé STRASBOURG

ÉCOLE DOCTORALE 414
Sciences de la vie et de la santé

INSERM U1118

THÈSE présentée par :

Pauline VERCRUYSSE

soutenue le : 28 Septembre 2016

pour obtenir le grade de : **Docteur de l'université de Strasbourg**

Discipline/ Spécialité : Neurosciences

Altérations hypothalamiques dans la Sclérose Latérale Amyotrophique

THÈSE co-dirigée par :

Mr. DUPUIS Luc	Directeur de recherche, Université de Strasbourg
Mme. WITTING Anke	Chercheur, University of Ulm

RAPPORTEURS :

Mr. COURATIER Philippe	Professeur des Universités-Praticien Hospitalier, Université de Limoges
Mr. KABASHI Edor	Chargé de recherches Inserm, ICM, Paris

AUTRES MEMBRES DU JURY :

Mr. CHALLET Etienne	Directeur de recherches, INCI, Strasbourg

Acknowledgement

This thesis would have not been possible without the support I have received over the last four years. I wish to thank the following people.

My sincere and deepest gratitude goes to my supervisor Dr. Luc Dupuis for his continuous support during my Ph.D. His patience, his motivation, his cheerfulness and his knowledge helped me through the rough path of Ph.D., in highest moments and in moments of doubt. He has been a great inspiration for my future research career. His listening, at any time, for research or other topics, built my research knowledge but also grown me as a person. I could not have imagined having a better advisor and mentor for my PhD study.

I would like to thank to my thesis co-supervisor Dr. Anke Witting for her help from Germany. You always had time for me and I really appreciated that.

Besides my advisors, I would like to thank my thesis committee: Dr. Edor Kabashi, Dr. Etienne Challet and Prof. Philippe Couratier for their time and for reviewing my thesis.

My thanks also go to Dr. Jean Philippe Loeffler, who provided me an opportunity to join his team, and who gave me access to the laboratory and research facilities. Without his support, it would not be possible to conduct this research.

I would like also to thank Prof. Albert Ludolph for trusting me and giving me the opportunity to work on my Ph.D. This research would not have possible without his support and his constructive criticism in my work.

I am grateful to Dr Frédérique Rene, Dr. Caroline Rouaux and Dr. Jose-Luis Gonzalez de Aguilar for their insightful comments and questions at every single meeting.

My research has benefited so much from help from Ulm and Lund, thank you to Prof. Jan Kassubek, Dr. Åsa Petersén, Prof. Dietmar Thal, Dr. Martin Gorges, Dr. Hans-Peter Müller, Dr. Sanaz Gabery, Simone Feldengut and all the people that helped me.

A big acknowledgement goes to Sylvie Grosh, Annie Picchinenna and Marie-Jo Ruivo for their technical help all this time in a good mood. I would like to thank Brigitte Kuenemann for always being available every time when we needed you.

My endless acknowledgement goes to Stéphane Dieterlé, Jérôme Sinniger, Hajer El

Oussini and Jelena Scekic-Zahirovic. Stéphane, you have been a great friend, a great companion with your positive mind and your talks, especially about everything except Science. You always have been available for helping me. I will miss lunches and breaks with you! Jérôme, you have been a dynamic and essential part of lab's spirit. I could always count on your technical depth and attention to details. Working with you was exalting, I wish you the best for your future working and personal life. Hajer and Jelena, you were my Ph.D. "buddies" but also some protective mums. Your different and positive way of seeing life changed the person I was. You always have been kind and encouraging with me. Yes, we have managed our PhDs!

There is no way to express how much it meant to me to have been a member of INSERM U1118 laboratory. Special thank to these brilliant friends and colleagues, who inspired me over the many years: Alexandre Henriques (and your special jokes), Mathieu Fischer (and your positive whistling every single day, you endure my thesis writing), Laura Robelin (and your kindness), Gina Picchiarelli (and your smiling positive energy), Robin Waegaert and Thibaut Burg (and your fun), Christine Marques (and your help), Alexia Menuet (and your positive mind). I thank my former lab fellows Lavinia Palamiuc and Aurélia Vernay.

Thank you to those who helped the project as graduate students: Coraline Kostal, Marc-Antoine Goy, Paul Rochet and Florian Parisot.

Last but not least, my acknowledgement goes to my family and friends for your endless love and your support whenever I needed it. After all these years, Aurore and Coralie, all these kilometres were not able to separate us and I hope our strong friendship will last. Annick, Olivier and Grandma, your positivity meant a lot to me. Thomas, tack för dessa år tillbringar tillsammans. I thank my sister, for her listening when I needed it. My biggest thank goes to my mother and my father, with all my love, for your constant support and presence, wherever I have always decided to go. Without your reassuring words, I would not have managed my Ecole d'Ingénieur and my PhD. To anyone that I may have forgotten, I apologize. Thank you as well.

Table of content

Abbreviations

5-HT	5-hrydroxytryptamine (seotonin)
AD	Alzheimer's disease
AgRP	Agouti Realted Peptide
AH	Anterior hypothalamus
ALS	Amyotrophic Lateral Sclerosis
ALSFRS	Amyotrophic Lateral Sclerosis Functional Rating Scale
APOE	Apolipoprotein E
APP	amyloid precursor protein
Arc	Arcuate Nucleus
Aβ	Amyloid beta peptide
BACE	β-Secretase
BDNF	Brain-derived neurotrophic factor
BMI	Body Mass Index
bv-FTD	behavioral variant Fronto-Temporal Dementia
CART	Cocaine and Amphetamine Related Transcript
CCK	Cholecystokinin
CLU	Clusterin
CNS	central nervous system
CRH	Corticotropin-releasing hormone
CSF	Cerebrospinal Fluid
DMN	Dorsomedial Nucleus
DFT	Démence Frontotemporelle (FTD)
DPR	dipeptide repeat
DTI	Diffusion-weighted Magnetic Resonance Imaging
DYRK1A	Dual specificity tyrosine-phosphorylation-regulated kinase 1A
fALS	familial Amyotrophic Lateral Sclerosis
FTD	Fronto Temporal Dementia
FTD	Fronto-Temporal Dementia
FUS	Fused-in Sarcoma
fvFTD	Frontal-Variant Fronto-Temporal Dementia (same as bv-FTD)
GABA	gamma-amino butyric acid
GSK3β	Glycogen synthase kinase 3 beta
HC/HC	High carbohydrate diet hypercaloric
HD	Huntington's disease
HTT	Huntingtin
KI	Knock-in
KO	Knock-out
LHA	Lateral hypothalamus Area
LMN	Lower Motor Neurons
MAPT	Microtubule-associated protein Tau
MCH	Melanin concentrating hormone
MRI	Magnetic Resonance Imaging
MSH	alpha-Melanin stimulating hormone
Nac	Nucleus Accumbens

NLS	Nuclear Localization Signal
NPY	Neuropeptide Y
NTL	Lateral Tuberal Nucleus
ORX	Orexin
OXT	oxytocin
PC	pro-hormone convertase
PD	Parkinson's disease
PET	Positron Emission Tomography
PGRN	progranulin
PH	Posterior hypothalamus
PICALM	phosphatidylinositol binding clathrin assembly protein
PO	preoptic area
POMC	Proopiomelanocortin
PSEN	presenilin 1
PVN	Paraventricular Nucleus
RNA	Ribonuclein Acid
ROS	reactive oxygen species
sALS	sporadic Amyotrophic Lateral Sclerosis
SC	spinal cord
SCN	Suprachiasmatic Nucleus
SLA	Sclérose Latérale Amyotrophique (ALS)
SOD1	Superoxide dismutase 1
SON	Supraoptic nucleus
SorL1	Sortilin-related receptor 1
TARDBP	Tat-Activating Regulatory (TAR) DNA-binding protein
Tau	Tubule-associated unit
TBK1	TRAF Family Member-associated (TANK)-binding Kinase 1
TDP-43	TAR DNA-binding protein 43
TOMM40	Translocase of outer mitochondrial membrane 40
TRH	Thyrotropin-releasing hormone
Trp	Tryptophan
UMN	Upper Motor Neurons
VMN	Ventromedial Nucleus
VTA	Ventral Tegmental Area

Foreword

The goal of my Ph.D. was to identify and characterise the hypothalamic alterations in Amyotrophic Lateral Sclerosis (ALS). Beside motor problems, Amyotrophic Lateral Sclerosis (ALS) is frequently accompanied by weight loss. ALS-related weight loss is an early phenomenon, occurring before onset of motor symptoms in patients. Weight loss is also found in animal models of ALS, and counteracting it through high caloric intake delays motor neuron degeneration. In patients, weight loss is correlated with survival, and a first clinical trial in gastrostomized ALS patients suggested protective effect of high caloric intake. Despite convincing evidence of the importance of weight loss in ALS disease progression, its underlying mechanisms are unknown. Body weight is controlled by a balance between food intake and energy expenditure integrated through a complex network of neuropeptides in the hypothalamus.

In this manuscript, I will first present the mechanisms of regulation of body weight by the hypothalamus. Known hypothalamic defects in other neurodegenerative diseases will be introduced.

In a second part, I will describe the major results obtained during my Ph.D. We have shown the existence of a defect in hypothalamic sub-nuclei network in ALS by indirect evidence in ALS patients and direct evidence in mouse models, (Publication n°1). This alteration seems to be a major cause of food intake alterations in ALS. We were the able to show direct evidence of hypothalamic atrophy in ALS patients by MRI (Publication n°2, submitted). Hypothalamic atrophy correlates with disease stage but also loss of Body Mass Index (BMI). Last, we have identified another alteration in a hypothalamic neuronal population in one mouse model of ALS (Patent application and Publication n°3, in preparation). Complementing the loss of this neuropeptide improved weight loss in this mouse model. Our study thus identifies druggable pathways to treat weight loss in ALS patients besides nutritional interventions.

In a third part, I will discuss the different results and discuss perspectives to this work.

Finally, I have also participated in other studies investigating the role of the serotonergic neurons from brainstem in ALS (Publication n°4 and n°5, in preparation). These papers are included in the Annex of the manuscript.

Introduction

Neurodegenerative diseases are a group of neurological disorders characterized by progressive loss of specific populations of neurons. The third most common neurodegenerative disease worldwide after Alzheimer's and Parkinson's is Amyotrophic Lateral Sclerosis (ALS), the major adult onset motor neuron disease. ALS was first described by Jean-Martin Charcot in 1869, and is thus also known as Charcot's disease. In the USA, ALS is named Lou Gehrig's disease after the famous American baseball player that passed of ALS in the 1960's. The word "Amyotrophic" comes from the Greek, and literally means « no muscle growth » describing the characteristic atrophy of muscle (see below). In ALS, the spinal cord of patients is affected ("sclerosis", hardening of tissues), more precisely in the lateral area, hence the "lateral sclerosis".

I. ALS

A. Symptoms/clinical feature

1. Diagnosis and motor symptoms

ALS is a fatal neurodegenerative disease, with currently no cure. A diagnosis of ALS is traditionally based upon the combined involvement of lower motor neurons and upper motor neurons, as determined using clinical examination. Such diagnosis criteria are currently subject to criticisms (Couratier et al. 2015) and guidelines are regularly published to update the "certainty" of the diagnosis of ALS (Ludolph et al. 2015).

The major initial symptoms of ALS refer to the first site of onset, either spinal (80% of ALS cases) or bulbar (20% of ALS cases) (Zarei et al. 2015; Swinnen & Robberecht 2014) (Figure 1). Spinal symptoms are muscle twitching and/or cramping, followed by muscle weakness leading to muscle atrophy. Bulbar symptoms are speech or swallowing difficulties. Bulbar-onset symptoms are generally followed by limb weakness at later stages. When muscle atrophy becomes too important, death usually occurs shortly as a result of respiratory failure (Zarei et al. 2015). Usually bulbar-onset ALS patients have a shorter prognosis than spinal-onset disease (Couratier et al. 2015).

Figure 1: Site of onset and major ALS symptoms (reproduced from (Swinnen & Robberecht 2014))

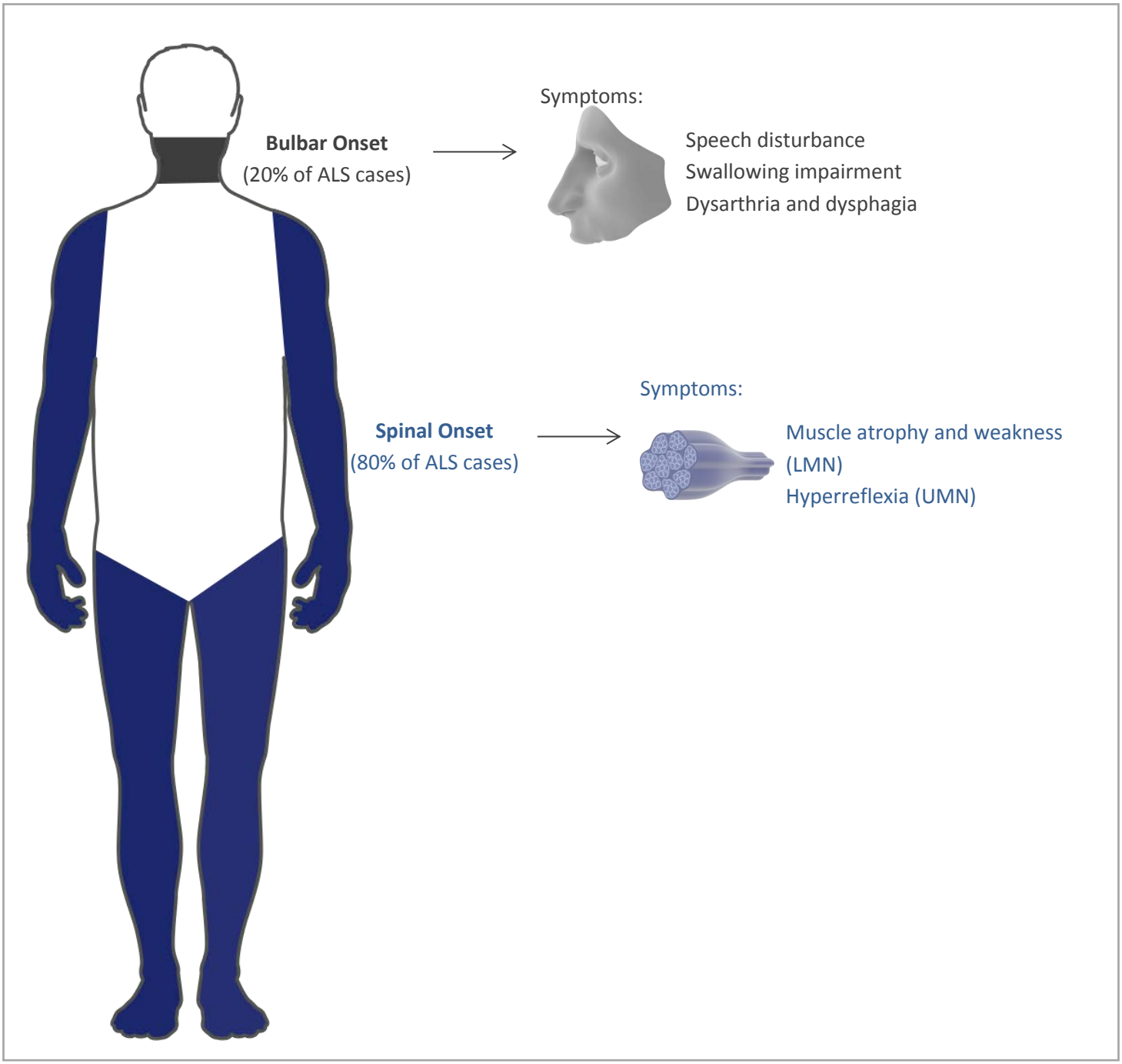

Observed symptoms are linked to the underlying pathology. Indeed, ALS hallmarks include the combined degeneration of Upper Motor Neurons (UMN) and Lower Motor Neurons (LMNs) in brain and spinal cord (Figure 2). UMNs, also called cortico-spinal motor neurons by neuroscientists, carry information from cerebral motor cortex to LMN nuclei located in the brainstem or spinal cord. Spinal cord LMNs innervate all skeletal muscle fibers, while brainstem LMNs control all facial nerves critical, for facial or tongue control for example. Thus, ALS symptoms like muscle fasciculations or muscle atrophy are the direct consequence of Lower Motor Neuron loss. On the contrary, symptoms usually attributed to UMN loss are hyperreflexia or spasticity, which is an excessive and prolonged muscle contraction to a stimulus, and are collectively referred to as UMN syndrome (Zarei et al. 2015).

The follow-up of disease progression in ALS patients is routinely performed by several methods. Besides muscle strength capacity, a score the Amyotrophic Lateral Sclerosis Functional Rating Scale (ALSFRS-R in its revised version) is calculated to measure activities of daily living and global function. This scale consists of 10 questions with 5 possible levels of answer. With this tool, physicians can evaluate functional impairment of the patient in performing common tasks, like writing, walking or cutting food. Decline in ALSFRS-R over time is typical of an evolution of the clinical functional status of patients. It is known that the slope of ALSFRS is correlated with the survival of patients (Gordon et al. 2004).

2. Epidemiology

The onset of ALS is usually difficult to determine precisely and is sometimes assimilated to the time the diagnosis is done, although diagnosis might be certain several months after actual onset. Onset of ALS occurs usually between 50 and 65 years old, with about 5% of ALS cases showing an onset under 30 years old. Patients can survive from months to decades after diagnosis but unfortunately the majority of cases live less than 3 years after onset of the disease. Currently, the incidence rate of the disease is 2.7/100 000 in Europe and North America. Men are slightly more affected than women with a ratio of 1.5:1 cases. In France, everyday there are three to four new ALS cases, leading to a prevalence of 6000 ALS patients in France (Zarei et al. 2015; Couratier et al. 2015).

Figure 2: Schematic representation of Lower Motor Neurons (LMN) and Upper Motor Neurons (UMN) degeneration leading to muscular loss in ALS patients.

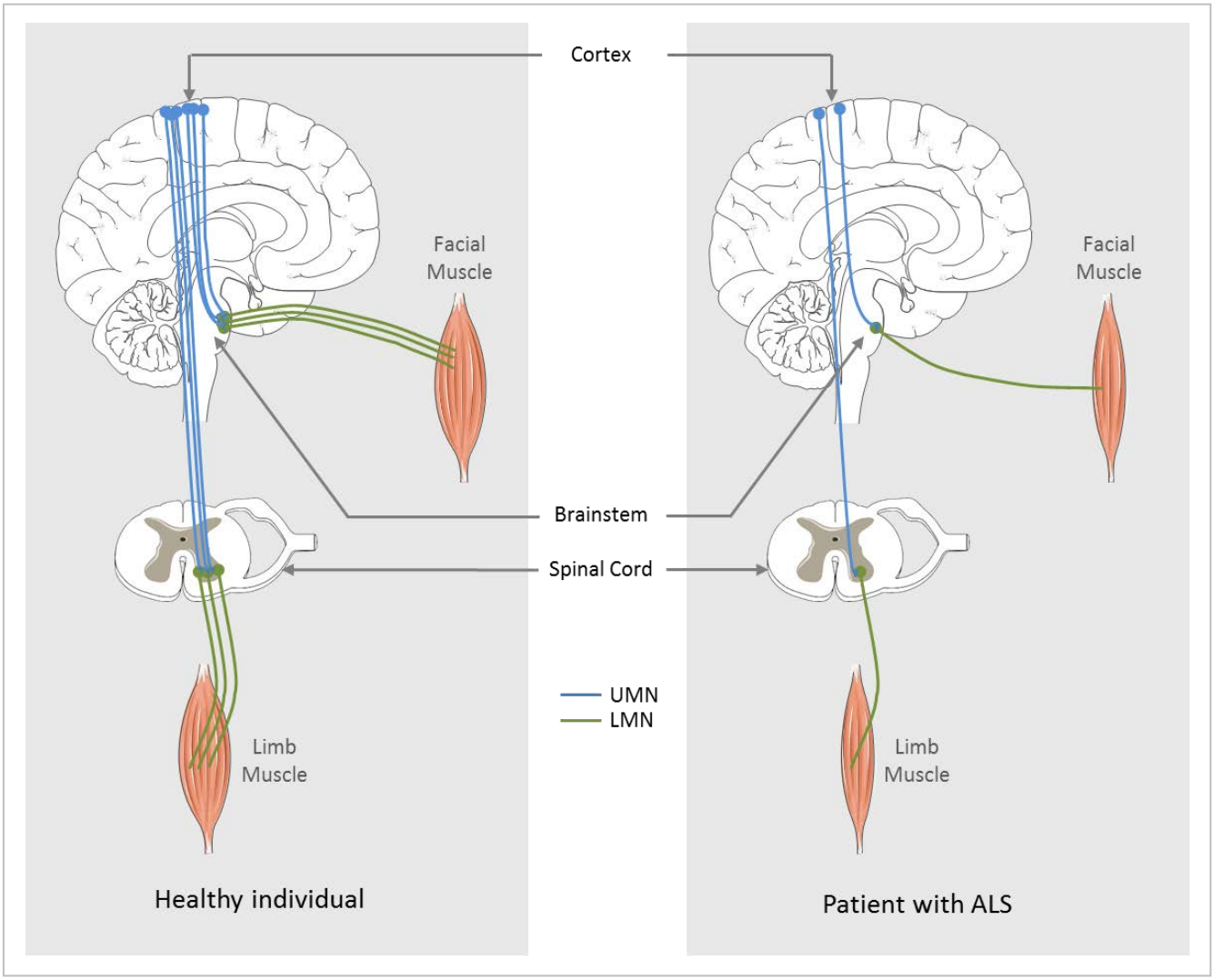

B. Treatment and clinical trials

1. Riluzole

The only FDA approved treatment in ALS is Riluzole (100mg/d).

Riluzole was found positive in one clinical trial in 1996 (Lacomblez et al. 1996), and more recently, the meta-analysis of 3 different clinical trials on Riluzole (Miller et al. 2012), showed a survival effect of 3 months for Riluzole. Symptoms of limb and bulbar function also decline slightly slower. However this drug has also side effects like nausea or asthenia or even alteration of liver function. Moreover, the treatment of Riluzole is under specific conditions: having ALS symptoms less than 5 years, being under 75 years of age and having vital capacity greater than 60%.

2. New drugs for ALS

For the last ten years, 11 human clinical trials yielded negative results, despite seemingly positive results in animal models (see later). The reasons of such failures are unknown. However, it is important to keep in mind that mouse models differ of ALS patients by many different factors. First, preclinical research has been mostly done one single type of mutation in inbred strains, with same genetic background, so they are all homogenous unlike in humans. Further, test of drugs on mice are usually performed before the onset of symptoms. Moreover, many differences of protocols exist between research groups as for the moment there are no standardized protocols. Thus mouse drug studies are useful and necessary, but have to be completed by clinical research before embarking on a randomized clinical trial (Clerc et al. 2016).

C. Genetic

A number of genetic mutations are associated with ALS. Indeed, familial history of ALS is present in 10-15% of cases, termed familial ALS (fALS). The remainder 85-90% of cases are termed sporadic cases, although some sALS cases have been identified with a mutation in an ALS-linked gene (Boillée et al. 2006; Lattante et al. 2015) (Figure 3).

Figure 3: Repartition of ALS gene mutations in sporadic ALS (sALS) and familial ALS (fALS). Modified from (Renton et al. 2014)

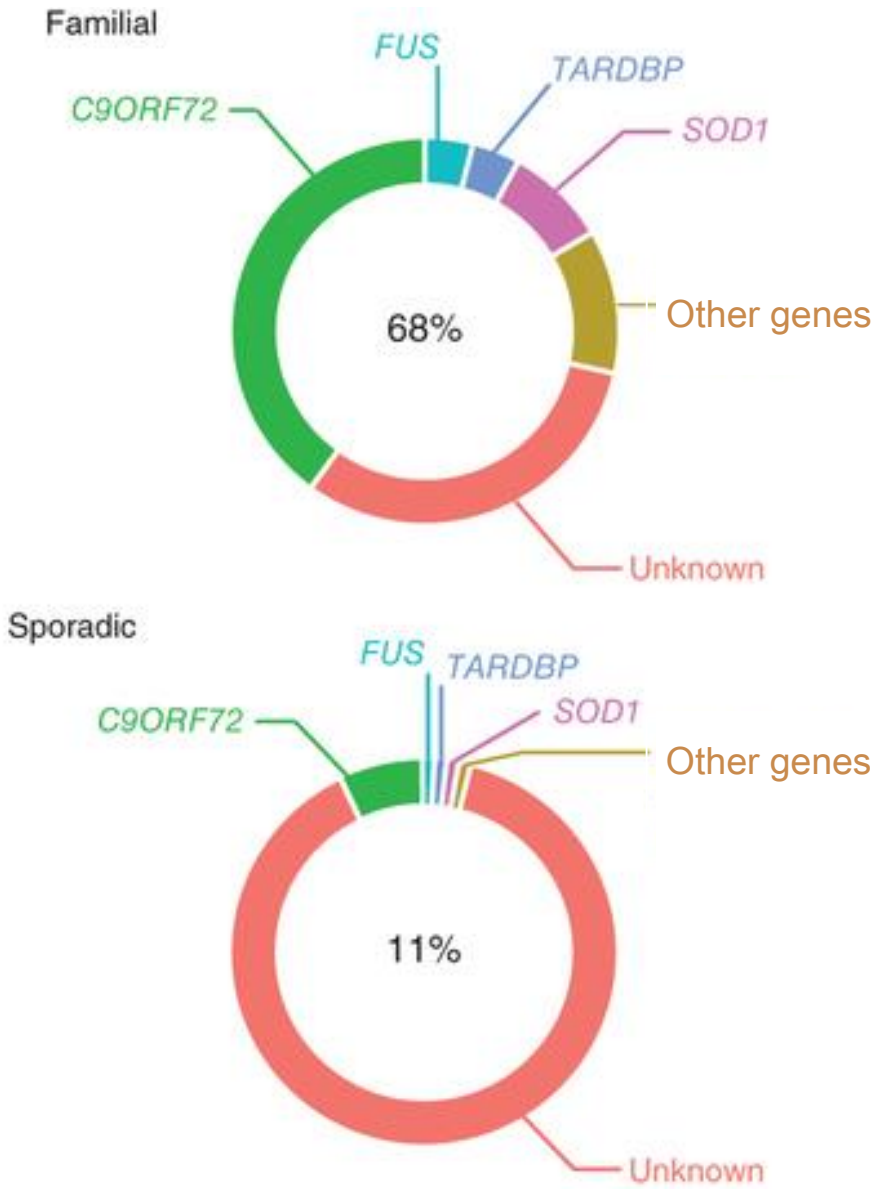

Clinical and pathology features of fALS and sALS are similar, except that the onset of fALS is usually a decade earlier than sALS (Zarei et al. 2015; Couratier et al. 2015). Currently, even if more than 100 genes have been associated with ALS, there are 5 major genes known to be mutated in ALS.

1. Mutations causing ALS

a) SOD1

Mutations in the Cu/Zn Superoxide Dismutase 1 (*SOD1*) gene represent about 1-2% of all ALS cases, and 13% to 20% of fALS cases (Boillée et al. 2006; Lattante et al. 2015). Over 170 mutations in *SOD1* were discovered, distributed throughout all five exons, predominantly leading to missense but also nonsense, deletions, insertions (Lattante et al. 2013).

b) TARDBP/TDP-43

The *TARDBP* gene (Tat-Activating Regulatory (TAR) DNA-binding protein), coding for the TDP-43 (TAR DNA-binding protein 43) protein, is mutated in about 3% of fALS and about 1.5% of sALS (Lattante et al. 2015). For the mutations in this gene, the penetrance is not complete, meaning that some family members of a sALS case are healthy even if they are *TARDBP* mutation carriers (Lattante et al. 2013). It seems that ALS patients with *TDP-43* mutations are more prone to have cognitive deficit (Lattante et al. 2015). Importantly, phosphorylated TDP-43 protein is a major component in neuronal aggregates in sALS, yet no TDP-43 aggregates are found in cases carrying *SOD1* mutations. Details on TDP-43 aggregates are described below.

c) FUS

Mutations in the *FUS* (Fused-in Sarcoma) gene are causing early onset, sometimes juvenile, ALS. The *FUS* gene mutations with proved pathogenicity are mostly found in exons encoding the C-terminal region of the protein. A number of mutations in the N-terminal region of FUS protein were observed in several cases of sALS. In total, 58 different mutations of *FUS* have been discovered, representing about 5% of fALS cases and less than 1% of sALS. *FUS* patients typically present with a juvenile onset of the disease (Lattante et al. 2015). The mutations are mostly missense but also are also found in splicing sites, and can be in frame,

insertion and deletion (Lattante et al. 2013). FUS protein normally shuttles between nucleus and cytoplasm. *FUS* mutations, especially those in the in C-terminal region of the protein that encodes the Nuclear Localization Signal (NLS) of the protein, lead to FUS protein being mislocalized in cytoplasm in ALS patients and mouse models (Scekic-zahirovic et al. 2016).

d) C9ORF72

An expansion of hexanucleotide GGGGCC repeats, in the first intron of the gene *C9ORF72* is associated with ALS cases. In control population, the first intron consists of 20 repeats, while in ALS patients *C9ORF72* repeats expand from 60 to thousands times (Lattante et al. 2015). This mutation is observed in 30% to 50% of fALS cases and 5% to 7% of sALS, representing the most frequent cause of ALS to date. This mutation is also frequent in another neurodegenerative disease, Fronto Temporal Dementia (FTD). About 25% of familial FTD cases and 6% of sporadic FTD cases are due to *C9ORF72* mutation. Thus, *C9ORF72* gene is a typical gene involved in the ALS-FTD continuum (Lattante et al. 2015). Indeed, ALS and FTD patients have some common pathological hallmarks (in particular TDP-43 aggregates), and clinical symptoms overlap. Specifically, 15% to 18% of ALS patients develop FTD symptoms, while 15% of FTD patients also present with motor dysfunction meeting ALS criteria (Lattante et al. 2013).

There are many hypotheses about the mechanism of pathogenesis of *c9orf72* mutation. First, the large expansion in the first intron of the *C9ORF72* gene leads to haploinsufficiency (Ciura et al. 2013; DeJesus-Hernandez et al. 2011). Whether or not, this haploinsufficiency contributes to the pathogenesis, remains controversial (see later). The second hypothesis is that the hexanucleotide repeat pre-mRNA accumulates in the nucleus (leading to so called RNA foci), and sequestering still uncharacterized RNA binding proteins leading to loss of their endogenous function. Third, the mRNA encoding the expansion could be translated by a non-ATG initiated translation (RAN: repeat associated non ATG mediated translation) leading to the production of a series of dipeptide repeat protein (for instance poly(GA), poly(GP) or poly(GR)) from both sense and antisense direction. These RAN products are detected in vivo and form aggregates in patients (Mizielinska & Isaacs 2014; Xiao et al. 2016). The respective contributions of these different mechanisms remain unclear.

e) TBK1

Two recent exome studies identified the *TBK1* (TRAF Family Member-associated (TANK)-binding Kinase 1) gene as causing ALS and FTD (Cirulli et al. 2015; Freischmidt et al. 2015). Importantly, the pathogenicity of these *TBK1* mutations has been recently proven (Freischmidt et al. 2015).

TBK1 mutations are loss of function mutations leading to haploinsufficiency (Cirulli et al. 2015; Freischmidt et al. 2015). In a French study (Cirulli et al. 2015), TBK1 mutation seems to have a frequency of 0,4% to 4% in ALS. Another study (Freischmidt et al. 2015) observed a proportion of 4% of fALS cases with this mutation. This mutation is also related to cognitive impairment and FTD (Freischmidt et al. 2015). The TBK1 protein is a protein kinase involved in autophagy and inflammation, in particular in the clearance of protein aggregates by autophagy and maybe in the autophagosome maturation. TBK1 interacts with two other proteins involved in both autophagy and ALS, namely optineurin and p62, and this pathway could thus be critical in ALS (Freischmidt et al. 2015).

2. Mouse models based on ALS mutations

From these human ALS-associated mutations, a number of mouse models were developed. The first model was a SOD1 based model, published in 1994 (Gurney et al. 1994). Since the years 2000, and the boom of new human gene discoveries in ALS, new models are being developed. However, for the moment, most knowledge on mechanisms of Motor Neuron pathology in ALS stems from SOD1 models (Boillée et al. 2006). Details can be found in Table 1.

a) SOD1

(1) Sod1 (G93A)

In 1994, Gurney et al. (Gurney et al. 1994), developed a transgenic mouse expressing 20 to 24 copies of human fALS mutation *SOD1(G93A)* gene under the human *SOD1* promoter. At 3 to 4 months old, the first signs of limb weakness appear followed by a deterioration of the walking with a reduced stride length. Two weeks later, the mouse is paralyzed in its limbs. Pathologically, a loss of large axons in the ventral motor roots was observed. Moreover, many

vacuoles appear in axons and dendrites of motor neurons in presymptomatic mice (Wong et al. 1995), and these are mostly derived from the mitochondria. Intriguingly, such vacuolar degeneration has never been observed in fALS or sALS human cases, and this was in particular not observed in the motor neurons of *SOD1(G93R)* fALS patients, and likely represents a transgenic artefact. Indeed, Bergemalm and collaborators demonstrated that dismutase competent mutant SOD1, like *Sod1(G93A)*, are extremely stable proteins that lead to artefactual import of the protein in mitochondria (Bergemalm et al. 2010). For this reason, results in *Sod1(G93A)* mice have to be cautiously interpreted and replicated in another mouse model expressing a dismutase incompetent, unstable SOD1 mutant, like G85R or G86R. In our laboratory, we routinely use *Sod1(G86R)* mouse model (Ripps et al. 1995).

(2) Sod1(G86R)

The transgenic *Sod1(G86R)* mouse (Ripps et al. 1995) expressed the same mutation observed on the amino acid residue 85 in some fALS patients, under the endogenous promoter allowing a widespread expression in all tissues. At 3 months old, a loss of motor function start with spastic paralysis in hind limbs and sometimes also in fore limbs associated with muscle wasting. Other symptoms, like metabolic abnormalities, are present and will be described below. The mouse survival is about 4 months. Loss of large spinal motor neurons is one of the degenerative changes that are present (Dupuis et al. 2000). In brainstem and cortex, also cortical motor neurons degenerate.

b) TDP-43/TARDBP

(1) Knock-out of Tardbp

A conditional T*ardbp* knock-out mouse model was generated in 2010 by Chiang et al. (Chiang et al. 2010). TDP-43 protein is necessary for early embryonic development and for this reason a complete *Tdp-43* knock-out adult mouse is not doable. A mouse with the third *Tardbp* exon flanked with loxP sites was crossed with a Rosa26-ErCre mouse generating an adult-inducible *Tardbp*-KO mouse. The loss of the RNA-binding domain encoded by exon 3 leads to a non-functional TDP-43 protein. After induction of the Cre-recombinase with tamoxifen, the

conditional Tardbp-KO mouse died 9 days later. The death is due to a loss of body mass (details below). In this study, there are no details about behaviour or motor neurons loss.

(2) Tdp-43(A315T)

Baloh and collaborators generated the first transgenic mouse line overexpressing the *TDP-43(A315T)* mutation (Wegorzewska et al. 2009) observed in fALS cases, under the control of a mouse prion protein promoter, which allows the expression of the mutation only in the central nervous system. In this line, the expression of the protein mutated TDP-43 is 3 times the level of endogenous TDP-43 protein in the spinal cord and is also high expressed in brain (Guo et al. 2012). At about 4 months of age, the motor functions of these transgenic mice are altered and death occurs at about 5 months of age in male mice (Esmaeili et al. 2013). Interestingly, these mice lose about 20% of lower motor neurons and 50% of upper motor neurons. Intriguingly in this mixed genetic background, female mice die almost one month later (Esmaeili et al. 2013). This gender bias is also present in a pure C57BL/6 background. Cytoplasmic accumulations of ubiquinated proteins, however not of TDP-43, are present in the cortex but has not been observed in several other regions of the Central Nervous System (CNS) (Esmaeili et al. 2013).

Studies in this model need to be carefully interpreted because it has been observed that this model has gastrointestinal tract pathology causing death through intestinal obstruction before any obvious motor neuron degeneration (Esmaeili et al. 2013; Guo et al. 2012). Switching the animals to a gel diet at 30 days of age for males and 80 days of age for females, avoids the development of gastrointestinal problems and the progression of motor phenotype is slower with a longer disease duration (Herdewyn et al. 2014). Nonetheless, the survival extends after disease onset from several weeks to several months with heterogeneity between mice. The rescue of gastrointestinal dysfunction uncovers a motor phenotype, with 20% denervated neuromuscular junctions and a more pronounced loss of motor neurons in cortex in particular larger neurons (Herdewyn et al. 2014).

Another mouse line has been generated in 2014 by Stribl et al. (Stribl et al. 2014). These mice express human *TDP-43(A315T)* under endogenous *Tardpb* promoter, and heterozygous

mice have been studied in the manuscript. These mice did not seem to develop obvious motor deficits, some slight alterations in coordination and walking time. Pathologically, cytoplasmic aggregates positive for ubiquinated TDP-43 were observed in brain and spinal cord. The loss of motor neurons in ventral horn of spinal cord is 10% in mutant mice, consistent with the mild motor phenotype.

c) FUS

(1) *Fus* knock-out or knock-down

Three knock-out mice were developed for the *Fus* gene. First, the *Fus/Tls* -/- (Tls is another name for Fus) (Kuroda et al. 2000), appear sterile in males and females. These mice have normal development except a smaller size. The neuronal phenotype was not studied further.

In 2000, Hicks et al. (Hicks et al. 2000) generated another *Fus* -/- mouse line. These *Fus* -/- mice died within a couple of hours after birth despite seemingly normal development of organs. Due to the early death, no study of the CNS was performed.

Both of these knock-out lines expressed residual FUS protein, and recently, our laboratory participated in the generation and characterization of a third *Fus* -/- mouse strain that is completely devoid of FUS protein (Scekic-zahirovic et al. 2016). These mice die at birth of respiratory insufficiency but do not display loss of large motor neurons.

(2) Fus overexpression of wt or mutant Fus

Mitchell and collaborators generated a transgenic mouse line overexpressing human wt *FUS* under the control of the mouse *Prp* promoter (Mitchell et al. 2013). This mouse model developed tremor followed by progressive hind limb paralysis and death at 12 weeks of age. This was associated with large motor neurons degeneration. It should be noted that this mouse line showed down-regulation of endogenous murine FUS as a consequence of FUS auto-regulation.

(3) Knock-in FUS ΔNLS

More recently, our laboratory developed the first Knock-in model of *FUS* by Scekic-Zahirovic et al. (Scekic-zahirovic et al. 2016). These mice express constitutively a form of *Fus* truncated of its C-terminal NLS (*Fus* ΔNLS), hence retained in the cytoplasm. Homozygous *Fus* ΔNLS -/- mice die shortly after birth due to respiratory insufficiency. The study of heterozygous *Fus* ΔNLS +/- mice showed a mild motor phenotype, with a decrease in the number and size of motor neurons in ventral horn of spinal cord of mutated mice (Scekic-Zahirovic, manuscript in preparation).

d) c9orf72

Several mouse models were developed to answer to the hypothesis of toxicity of *c9orf72* mutation. Indeed, the specificities of *c9orf72* mutation leave open several possibilities, non-mutually exclusive to explain its toxicity.

(1) Hypothesis: loss of function

A first possibility is that haploinsuffiency in endogenous C9ORF72 protein may cause/contribute to ALS. If this were true, then complete loss of *C9ORF72* gene should lead to ALS/FTD. In 2015, Koppers et al. (Koppers et al. 2015) developed a mouse with *c9orf72* loss restricted to neurons. These authors did not observe any difference in motor neurons numbers in spinal cord and no difference of muscle innervation as compared to wild type littermates. They also did not observe signs of astrocytes or microglia activation in brain and spinal cord of these mice, and no signs of TDP-43 pathology. Moreover, motor performance and survival were identical to wt. It seems that the loss of *c9orf72* in neurons is not sufficient to cause ALS.

Complete loss of *C9ORF72* has however large toxic effects to myeloid cells. Indeed, 4 different *c9orf72* strains developed splenomegaly and different symptoms of myeloid cell dysfunction, ranging from defects in macrophages/microglia (ORourke et al. 2016), to defects in B lymphocytes (Sudria-Lopez et al. 2016; Sullivan et al. 2016; Jiang et al. 2016). None of these studies identified a defect in motor neuron after complete loss of *C9ORF72*. Importantly, a 50% loss of *c9orf72* expression in heterozygous mice did not trigger disease. Thus, loss of C9ORF72,

either complete or partial is not sufficient to trigger ALS. These data in mouse models contrast with the toxicity observed upon *c9orf72* knockdown in zebrafish (Ciura et al. 2013). This difference might be due either to species difference or to different effects of knock-out vs knock-down. Further studies are warranted to determine the consequences of C9ORF72 loss.

That loss of *C9ORF72* appears not sufficient to trigger ALS in a mammalian system does not exclude that it could be necessary or a contributing factor. Indeed, several studies have shown that the C9ORF72 protein is necessary for autophagy induction (Sellier et al. 2016; Webster et al. 2016). Thus, loss of *C9ORF72* might sensitize neuronal cells to a stress involving autophagy. Consistently, loss of *C9ORF72* synergized toxicity of mid-sized repeat expansions of *Ataxin 2* (Sellier et al. 2016), a widely documented risk factor of ALS (Figley et al. 2014; Sellier et al. 2016).

(2) Hypothesis: gain of function

A second hypothesis to explain C9ORF72 toxicity is that the expansion would be transcribed and lead to a toxic RNA or this would be translated through atypical non-ATG translation. Thus, this would result in a gain of toxic function.

In Drosophila models, the toxicity of the G4C2 repeats appear independent of RNA itself and caused by arginine rich dipeptide repeat proteins produced from this locus (Mizielinska et al. 2014). Further studies by different groups showed that G4C2 repeats interfered with nucleo-cytoplasmic shuttling to trigger neurodegeneration in Drosophila models (Freibaum et al. 2015; Zhang et al. 2015; Jovicic et al. 2015).

In mouse models, only few transgenic mice have been developed. Two of these mice developed RNA foci and DPR (Dipeptide repeat) pathology but no behavioural abnormalities (Peters et al. 2015; O'Rourke et al. 2015). More recently Jiang et al. (Jiang et al. 2016) created transgenic mice expressing a BAC (bacterial artificial chromosome) with a portion of the *c9orf72* gene, including from exon 1a (the promoter region) to exon 5. Thus these mice do not overexpress the C9ORF72 protein. These authors generated different strains, which expressed about 110 repeats of *c9orf72* and about 450 repeats of *c9orf72*. The expression of the transgene

was found in mice carrying 450 repeats in different parts of brain from 2 months of age, while no expression was observed from mice expressing 110 repeats in any part of brain at any age. In the mouse with 450 repeats, poly(GA), poly(GP) or poly(GR) peptide aggregates were detected in Central Nervous System from 3 months of age, showing that these mice develop typical C9ORF72 pathology. These mice did not develop any problem of motor deficit or weight loss or denervation or motor neurons loss. However, mice with 450 repeats developed some cognitive impairment from the age of 4 months old (memory deficit, anxiety, social interaction deficit). Another publication (Chew et al. 2015), with viral expression of 66(G4C2) repeats without ATG, showed mRNA expression in the Central Nervous System but also in the Spinal Cord associated with dipeptide repeats aggregates. In this model a slight brain atrophy and slight motor impairment was observed, while the overexpression of these proteins was extreme. These publications have shown that, contrary to *c9orf72* loss, the *c9orf72* expanded repeat gain of function in mouse trigger characteristics similar to symptoms of c9orf ALS/FTD. However, further characterization of these different mouse models need to be performed in order to validate their usefulness for preclinical research.

Table 1: Mouse models of ALS and characteristics

(m.: months; w: weeks; d: days; MN: Motor neurons; LMN: Lower Motor Neurons; UMN: Upper Motor Neurons; SC: Spinal Cord; KO: Knock-out; KI: Knock-in)

Model	Genetic construction	Survival	Age of Motor dysfunction	Pathology	Metabolism dysfunction
SOD1	*Sod1(G93A)*	5-6 m.	3-4 m.	-Loss of large MN in SC -Vacuoles in axons and dendrites	-weight loss -hypermetabolism -reduction WAT -reduction leptin
	Sod1(G86R)	4 m.	3 m.	-Loss of large MN in SC -Loss of cortical MN	
TDP-43/ TARDPB	*Tdp-43* KO (inducible)	9 d. after induction	/	/	-weight loss -loss fat mass
	Tdp-43(A315T)	5-6 m.	4 m.	-loss of 20% LMN -loss of 50% UMN -ubiquinated protein aggregates in cortex	-weight loss

Model	Genetic construction	Survival	Age of Motor dysfunction	Pathology	Metabolism dysfunction
TDP-43/ TARDPB *(rest)*	Human *TDP-43(A315T)*		/	-loss of 10% MN in SC -TDP-43 aggregates in brain and spinal cord	-10% weight loss
FUS	KO	Sterile or die a couple of hours after birth			
	wt human *FUS* overexpression	12 w.	10 w.	-loss of large MN	
	KI *Fus* ΔNLS	Die at birth (homozygous)	Mild motor phenotype	-decrease number and size MN in SC	
C9ORF	<u>Loss of function</u>: *c9orf72* KO in neurons	Identical to wt	/	/	
	<u>Gain of function</u>: *c9orf72* BAC (450 repeats)		/	Poly GA/GP/GR aggregates in central nervous system	/

D. Pathology in ALS and brain spreading

A common feature of neurodegenerative diseases is the appearance of ubiquinated misfolded proteins that form aggregates in cytoplasm or nucleus of the CNS. In sALS cases as well as in non-*SOD1* fALS, TDP-43 aggregates are observed in a subset of neurons from the CNS (Neumann et al. 2006; Neumann 2009). p62 aggregation is also observed in various neurodegenerative disease such as ALS linked to *C9ORF72*, and in spinal cord of fALS-*SOD1* mouse model (Gal et al. 2007). A recent study (Nakamura et al. 2015), has shown p62 aggregates in different parts of brain, for example hypothalamus, in a fALS cases with *SOD1* mutation. However between members of the family there was a high heterogeneity in p62 and ubiquitine positive aggregates.

In many other neurodegenerative diseases, including Alzheimer's disease or Parkinson's disease aggregates spread between the different brain regions during disease progression in a stereotypical pattern. Thus, the pathology of these neurodegenerative diseases progress stereotypically, as a function of the anatomy of the CNS. This was in particular shown for phosphorylated Tau in Alzheimer's disease and alpha-synuclein in Parkinson's disease. In these two diseases, Pr. Braak identified different pathological stages, that are now termed Braak stages (Braak & Braak 1991; Braak et al. 2003).

Pr. Braak recently performed similar studies in ALS using phosphorylated TDP-43 aggregates as a marker of disease progression. This led to a staging of ALS pathology in 2013 (Braak et al. 2013; Brettschneider et al. 2013) (Figure 4).

Stage 1: Agranular Motor Cortex (Broadmann area 4&6), Bulbar and Spinal Somatomotor Neurons

Stage 2: precerebellar nuclei of the brainstem

Stage 3: Prefrontal Neocortex and Basal Ganglia

Stage 4: Anteromedial Areas of the Temporal Lobe and the Hippocampal Formation

Figure 4: Model of pTDP-43 spreading in ALS. Reproduced from (Braak et al. 2013)

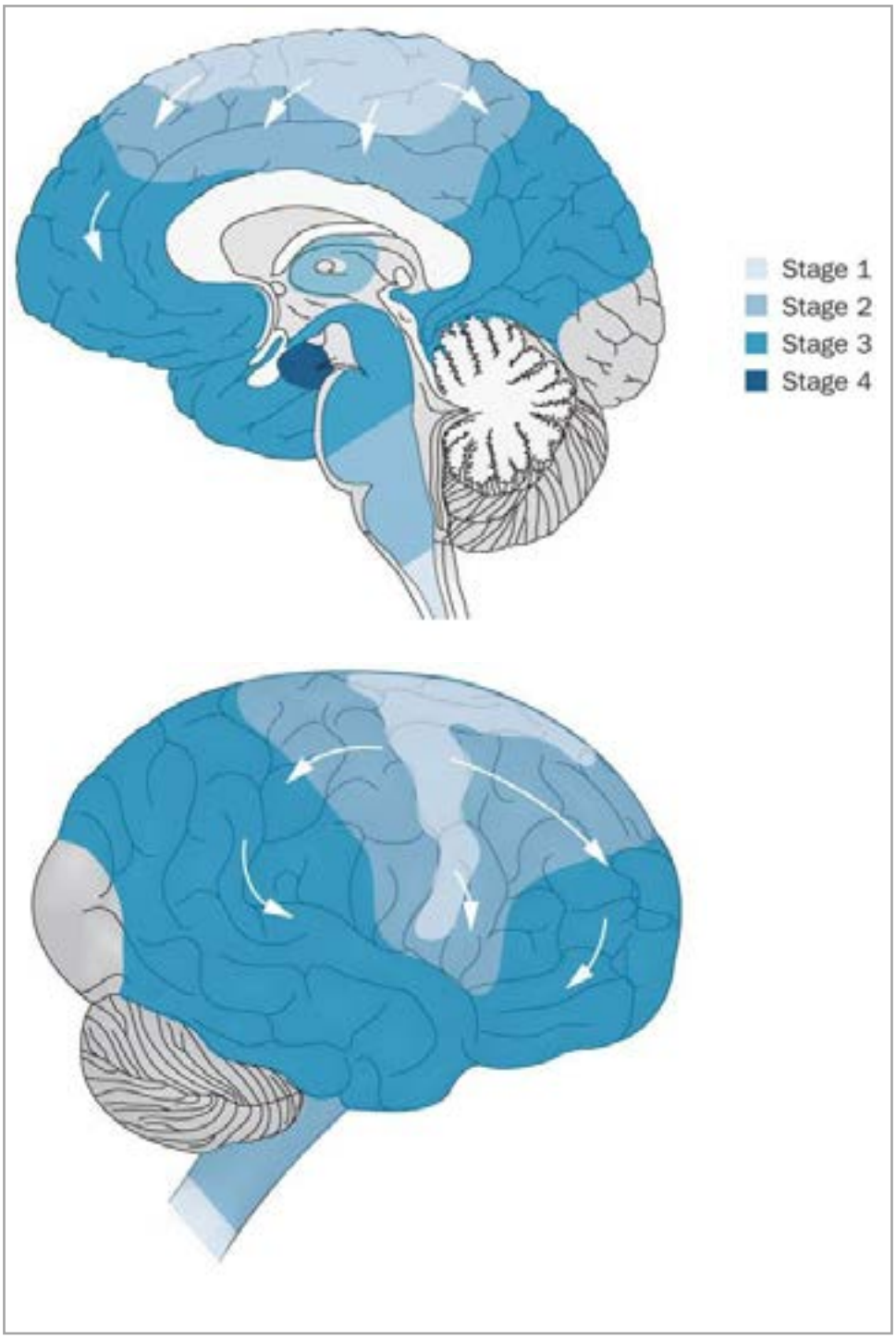

Importantly, these stages are defined post-mortem, and it would be critical to have access to a proxy of pTDP-43 stage using imaging. Kassubek and collaborators used DTI (Diffusion-weighted MRI) to validate the staging system of ALS *in vivo* (Kassubek et al. 2014). In this method, the analysis of the different white matter neuronal tracts by local properties of water diffusion may be indicative of axonal and myelin degeneration. The staging of different tracts involvement are as follows: the corticospinal tract (stage 1), the corticorubral and corticopontine tracts (stage 2), the corticostriatal pathway (stage 3), and the proximal portion of the perforant path (stage 4). This DTI staging method is very useful to determine disease progression in ALS patients.

E. Existence of abnormalities in energy metabolism during ALS

Besides motor neuron degeneration, ALS is associated with other symptoms that are not directly linked with motor neuron loss. In the next section, I will show that ALS is a multi-organ systemic disease characterized by metabolic dysfunction. The balance between the food intake and energy consumption is perturbed, causing weight loss that contributes to disease progression.

1. In patients and mouse models

a) ALS mouse models

In 2004, Dupuis et al. (Dupuis et al. 2004) characterized *Sod1(G86R)* and *Sod1(G93A)* metabolism. Long time before the beginning of motor symptoms, *Sod1* mice have a lower body weight. The lower body weight is due to higher rates of O2 consumption, sign of increased energy expenditure at rest, in both *Sod1* models. In addition, a reduction of the White Adipose Tissue (WAT) leading to a reduction of circulating leptin is observed at a stage without motor problems.

In transgenic *Tdp-43(A315T)* mice, a weight loss was observed at 105 days old, about 10 days before loss of motor functions (Esmaeili et al. 2013). In knock-in *Tdp-43(A315T)* mice from Stribl and collaborators (Stribl et al. 2014), heterozygous *Tdp-43(A315T)+/-* mice showed a 10% weight loss. In conditional *Tdp-43* Knock-Out mice (Chiang et al. 2010), the deletion of TDP-43

led to a large decrease in body weight accompanied by a large decrease in whole body fat mass. This weight loss is caused by a decrease of food intake and an increased fat oxidation accelerating the fat loss in adipocyte. The overexpression of *Tdp-43(A315T)* (Stallings et al. 2013) leads to weight gain before the onset of motor deficit , with an increase of the fat mass in WAT and BAT (Brown Adiposity Tissue). Interestingly, this symptom seems to be due to TDP-43 expression in peripheral target organs (like skeletal muscle, maybe fat) rather than Central Nervous System expression.

b) ALS patients

The weight balance of a healthy individual is explained by an equilibrium between the caloric intake (food) and the energy expenditure (Nau et al. 1995). Weight loss is observed when the individual is not eating enough calories to equilibrate its energy expenditure, leading to decreased lean and fat mass.

In the last 20 years it was shown that ALS patients are generally lean with normal or lower BMI. O'Reilly and collaborators found that lower BMI (Body Mass Index) (18.5 to 23 kg/m^2) from baseline are associated with a higher rate of developing ALS (O'Reilly et al. 2013). Even overweight (BMI from 25 to 29.9kg/m^2) and obese (BMI>30.0kg/m^2) people have lower risk of ALS than healthy BMI people. ALS patients at presymptomatic stage, without motor deficit, have a lower BMI (Huisman et al. 2015). A large European population study (Gallo et al. 2013), have shown that underweight women (BMI<18.5kg/m^2) have a higher risk of dying from ALS and increased BMI in men is associated with a decreased risk of ALS. In ALS, even with an appropriate caloric intake, the patient loses mass (Nau et al. 1995; Vaisman et al. 2009; Kasarskis et al. 1996). This mass loss is not only due to low nutritional intake. Some studies show a loss of lean mass (Nau et al. 1995; Vaisman et al. 2009) or a loss of fat mass (Kasarskis et al. 1996). For example, male ALS patients lose an average of 2.0kg in 6 months (Nau et al. 1995). BMI declines several months before death in males and females (study from 40 months before death) (Kasarskis et al. 1996). In all, weight loss can be considered as an early symptom that progresses over the disease course.

Several causes can explain the energy imbalance in ALS (Figure 5). First, ALS patients consume more energy at rest when normalized by their mass composition. About 50% (Bouteloup et al. 2009) to about 60% of ALS patients (Desport et al. 2005) show hypermetabolism (Vaisman et al. 2009; Wijesekera & Leigh 2009; Kasarskis et al. 1996; Bouteloup et al. 2009; Desport et al. 2005). Hypermetabolism has been demonstrated in patients with familial and sporadic ALS (Dupuis et al. 2011) from early in the disease to all along the disease in a stable manner except at the proximity of death (Desport et al. 2005; Bouteloup et al. 2009). Secondly, about 50% of ALS patients (Dedic et al. 2012) display hyperlipidemia (Dupuis et al. 2008), and glucose intolerance with or without insulin resistance (Dupuis et al. 2011; Pradat et al. 2010). Both factors have been put forward as a cause of weight loss. Thirdly, the progression of motor symptoms to bulbar muscles is a major cause of dysphagia in ALS patients, thus reducing their capacity to eat (Kasarskis et al. 1996; Kühnlein et al. 2008; Vaisman et al. 2009).At presymptomatic stage, ALS patient have a higher daily energy intake than healthy controls, to may compensate for hypermetabolism, but it may raise the risk of hyperlipidemia and insulin resistance (Huisman et al. 2015). But then after diagnosis, pure ALS patients are eating same calories than controls (Ahmed et al. 2016).

For the moment, the only guidelines concerning weight loss in ALS is to set up a supplementary enteral feeding when body weight falls more than 10% of baseline weight (Wijesekera & Leigh 2009).

Figure 5: Comparison of the metabolic balance between healthy individuals and ALS patients.

Reproduced from (Dupuis et al. 2011)

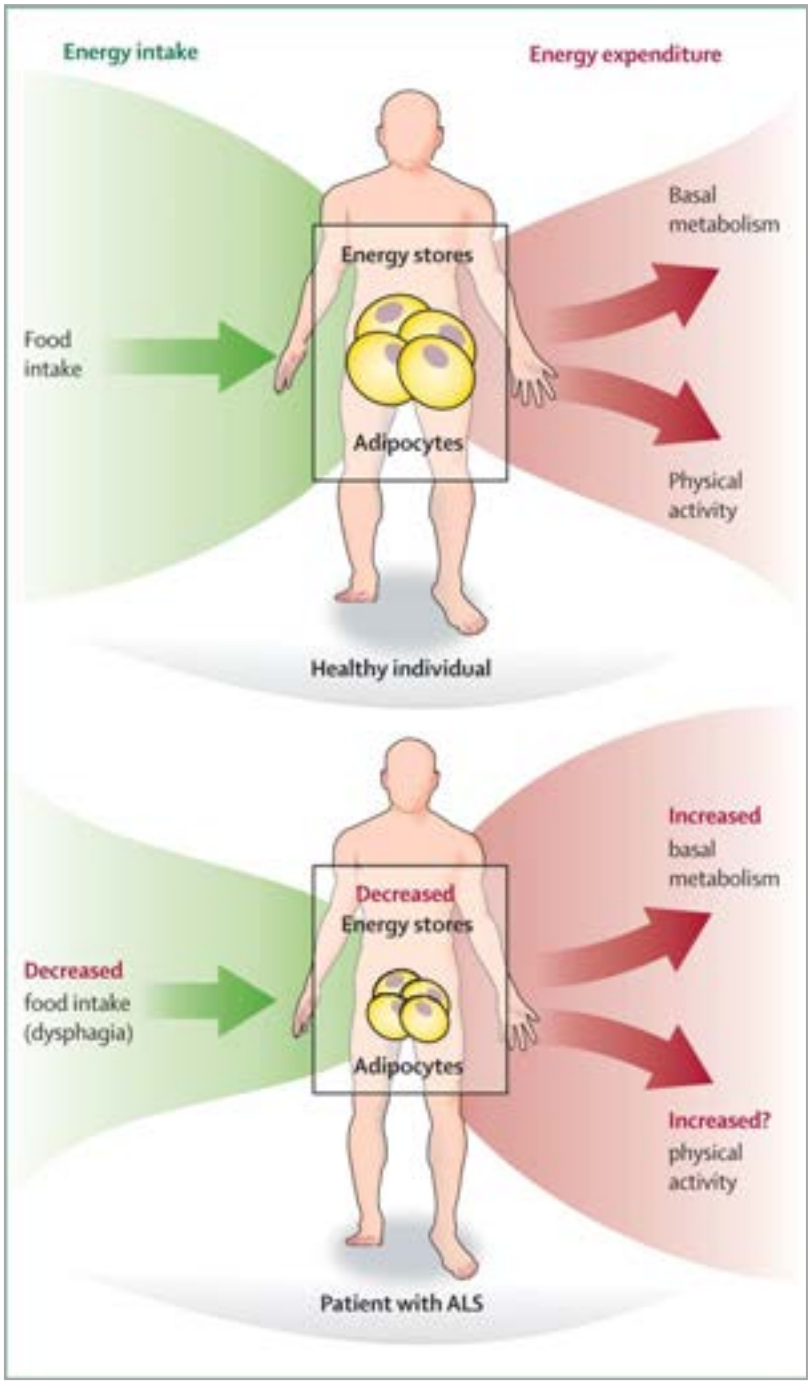

2. Correlation between metabolic problems and survival

Weight loss in ALS can be correlated with several factors. First, in a Korean study, ALS patients negative balance status was negatively correlated with disease severity using ALSFRS (Park et al. 2015). Second, there is a correlation between weight loss and the progression of the disease or the survival of patient (Kasarskis et al. 1996; Dupuis et al. 2011). Indeed, a correlation between BMI and the disease progression has been well established. Higher BMI is correlated with a longer survival (Jawaid et al. 2010; Desport et al. 1999; Wills et al. 2014; Paganoni et al. 2011). For example, moderate obesity BMI=30-35kg/m² is associated with slower disease progression and longer survival (Paganoni et al. 2011; Wills et al. 2014) compared to those with BMI<30kg/m² and those with BMI>35kg/m². Also patients with a loss of more than 1 point of BMI within 2 years have shorter survival and faster rates of disease progression (Jawaid et al. 2010). Indeed there is a correlation between BMI and rate of disease progression in the 2 years after diagnosis (Jawaid et al. 2010). Third, hyperlipidemia appears related with survival (Dupuis et al. 2008) in a manner that appears dependent upon body weight loss (Dedic et al. 2012; Paganoni et al. 2011).

In animal models, dietary rescue of weight loss was evaluated as a neuroprotective strategy. A publication from Dupuis et al. 2004 (Dupuis et al. 2004) has studied the consequence of a fat-enriched high-energy diet on phenotype of *Sod1(G86R)* mice. This increased energy intake was sufficient to compensate for the increased energy expenditure, and to reduce the energy deficit. In the periphery, high-energy diet reverted markers of muscle denervation and prevented loss of motor neurons in the spinal cord. More important, high-fat diet increased the survival of *Sod1(G86R)* of 20%.

In patients, a similar study has been published recently. In a phase 2 trial (Wills et al. 2014), adults with ALS receiving percutaneous enteral nutrition, gained 3 times more weight with high-carbohydrate diet hypercaloric (HC/HC) than control diet (respectively 0,39kg/month and 0,11kg/month). In addition, the decline of ALSFRS score was slower in HC/HC group than control. Moreover, over the 5 month-follow, 43% of the control group died while no HC/HC patient died. However these results have to be interpreted with caution. Indeed, this study

involved only very few patients, with 7 controls and 9 HC/HC, and included only a specific population of patients with advanced disease (percutaneous enteral nutrition). Another clinical trial on a larger and on ALS patients earlier in their disease progression is currently being performed in Germany.

Despite many evidence of importance in ALS disease progression, the mechanisms underlying weight loss and other metabolic abnormalities remain unknown. The objective of this thesis was to investigate whether hypothalamic abnormalities might participate in these phenotypes.

II. Hypothalamic structure

Hypothalamus is a small part of the brain, which regulates several important functions in the body. In general, the hypothalamus is the major integrating centre between signals from the CNS and signals from the periphery to regulate most basic functions, from reproduction to response to stress. A major function of the hypothalamus and the one of interest here is the regulation of food intake and energy expenditure.

The structure of hypothalamus and its role in the control of food intake and weight will be detailed afterwards.

A. Major nuclei of hypothalamus

The hypothalamus is composed of several sub-nuclei. Each of them has different functions. The major nuclei are Suprachiasmatic nucleus, Supraoptic nucleus, Preoptic nucleus, Anterior hypothalamus, Paraventricular nucleus, Dorsomedial nucleus, Ventromedial nucleus, Arcuate nucleus, Lateral hypothalamus area, Posterior hypothalamus and Lateral Tuberal Nucleus. Details can be found in the table 1 and Figure 6.

B. Nuclei implicated in Metabolism and Food Intake

As detailed before, several hypothalamic nuclei are implicated in the control of energy metabolism and food intake. The different nuclei involved are detailed below (Figure 7). It is worth mentioning that the relationships between the different nuclei are not completely characterized.

1. Arcuate Nucleus (Arc) or Infundibular nucleus

The Arcuate Nucleus, or Infundibular Nucleus in Humans, is a nucleus localised at the most ventral part of the hypothalamus, in the medial part bordering the third ventricle. In this nucleus, there are two major neuronal populations: one type of neurons expressing the neuropeptides NPY, ARGP and GABA, and one type of neurons expressing the neuropeptides CART and POMC. Both neuron types express leptin, insulin and ghrelin receptors.

Table 2: Different nuclei of hypothalamus. Information from (Swaab 2004; Ishiwata et al. 2002; Paredes 2003; Chou et al. 2003; Ripps et al. 1995; Morrison & Nakamura 2011; Li et al. 2014)

Nucleus	Functions
Paraventricular Nucleus (PVN)	blood pressure, thermoregulation, food control, parental behaviour, sexual function, stress response, mood control
Preoptic area (PO)	thermoregulation, sexual behaviour
Anterior hypothalamus (AH)	thermoregulation, sexual behaviour
Suprachiasmatic Nucleus (SCN)	Biological rhythms, sexual behaviour, glucose homeostasis
Supraoptic nucleus (SON)	Fluid balance, lactation, parturition
Dorsomedial Nucleus (DMN)	Emotion, body-weight regulation, circadian activity, stress response, thermoregulation
Ventromedial nucleus (VMN)	Feeding, sexual behaviour, aggression, thermoregulation
Arcuate Nucleus/ Infundibular Nucleus (Arc/ Inf)	Weight homeostasis and metabolism, sexual behaviour
Posterior Hypothalamus (PH)	Thermoregulation
Lateral Tuberal Nucleus (NTL) only in primates and human	Feeding behaviour and metabolism
Lateral hypothalamus Area (LHA)	Appetite and body weight control, thermoregulation, blood pressure, sleep

Figure 6: Schematic representation of the localisation of hypothalamic nuclei in Human brain (A; based on (Melmed 1995)**) and in mouse brain (B, based on** (Paxinos & Franklin 2001)**).**
Inf: Infundibular Nucleus; SON: Supraoptic Nucleus; PO: Preoptic Area; AH: Anterior Hypothalamus; PVN: Paraventricular Nucleus; LHA: Lateral Hypothalamus Area; DH: Dorsal Hypothalamus; DMN: Dorsomedial Nucleus; VMN: Ventromedial Nucleus; PH: Posterior Hypothalamus; Arc: Arcuate Nucleus

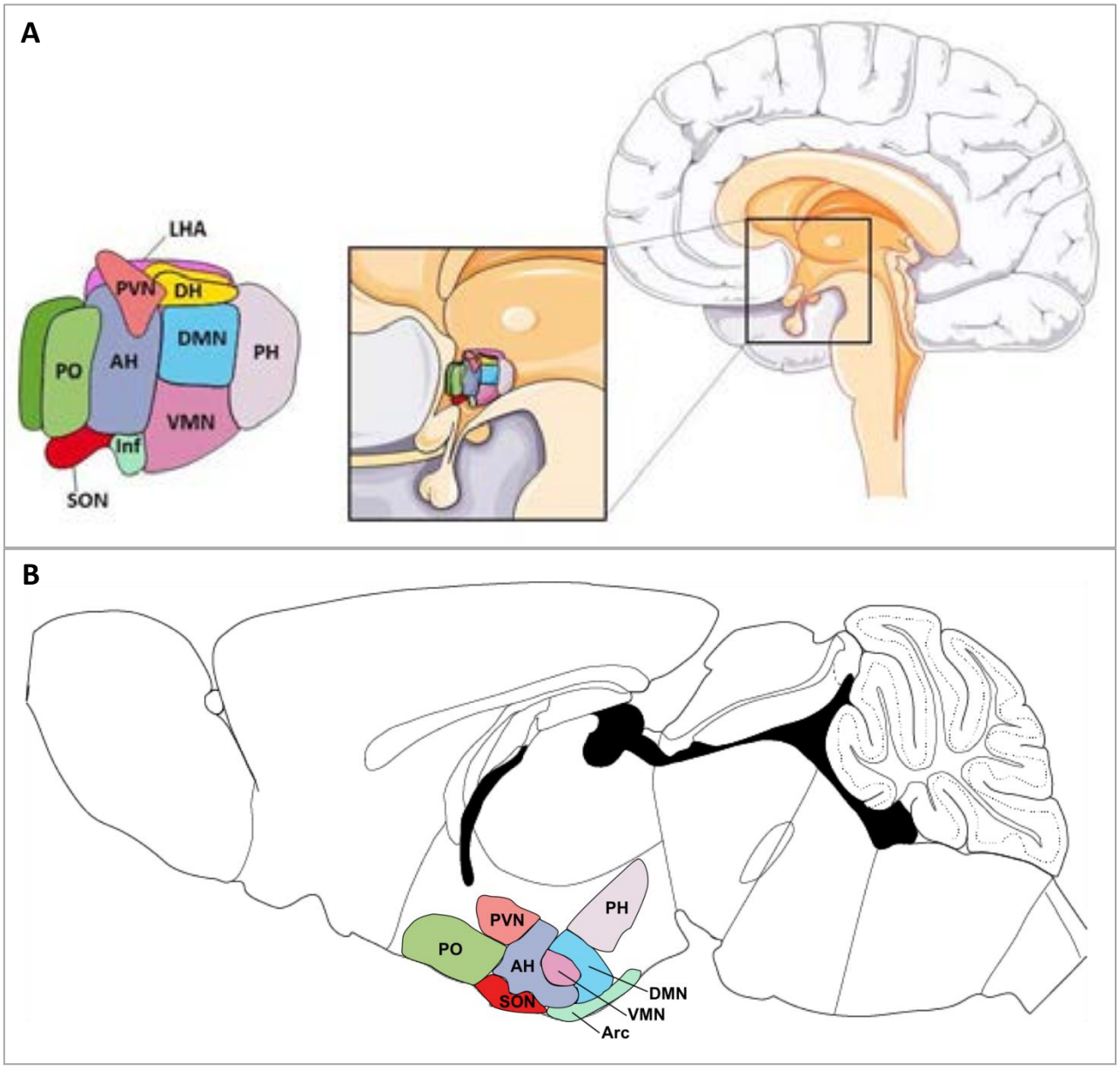

Figure 7: Schematic representation of the interconnectivity between hypothalamic nuclei and with NTS (based on figure from (Yeo & Heisler 2012)**)**

3V: Third ventricle, Arc: Arcuate Nucleus; VMN: Ventromedial Nucleus; DMN: Dorsomedial Nucleus; LHA: Lateral Hypothalamus Area; PVN: Paraventricular Nucleus. NTS: Nucleus of the solitary tract. Projections are indicated with arrows, full (proved) or dash (hypothetic). Neuropeptides that inhibit (-) or stimulate (+) food intake are indicated. POMC: Proopiomelacotin; CART: Cocaine and Amphetamine Regulated Transcript; AgRP: Agouti related peptide; NPY: neuropeptide Y; GABA: gamma-amino butyric acid; BDNF: Brain-derived neurotrophic factor; Neu.:Neurotensin; ORX: Orexin; MCH: Melanin Concentrating Hormone;

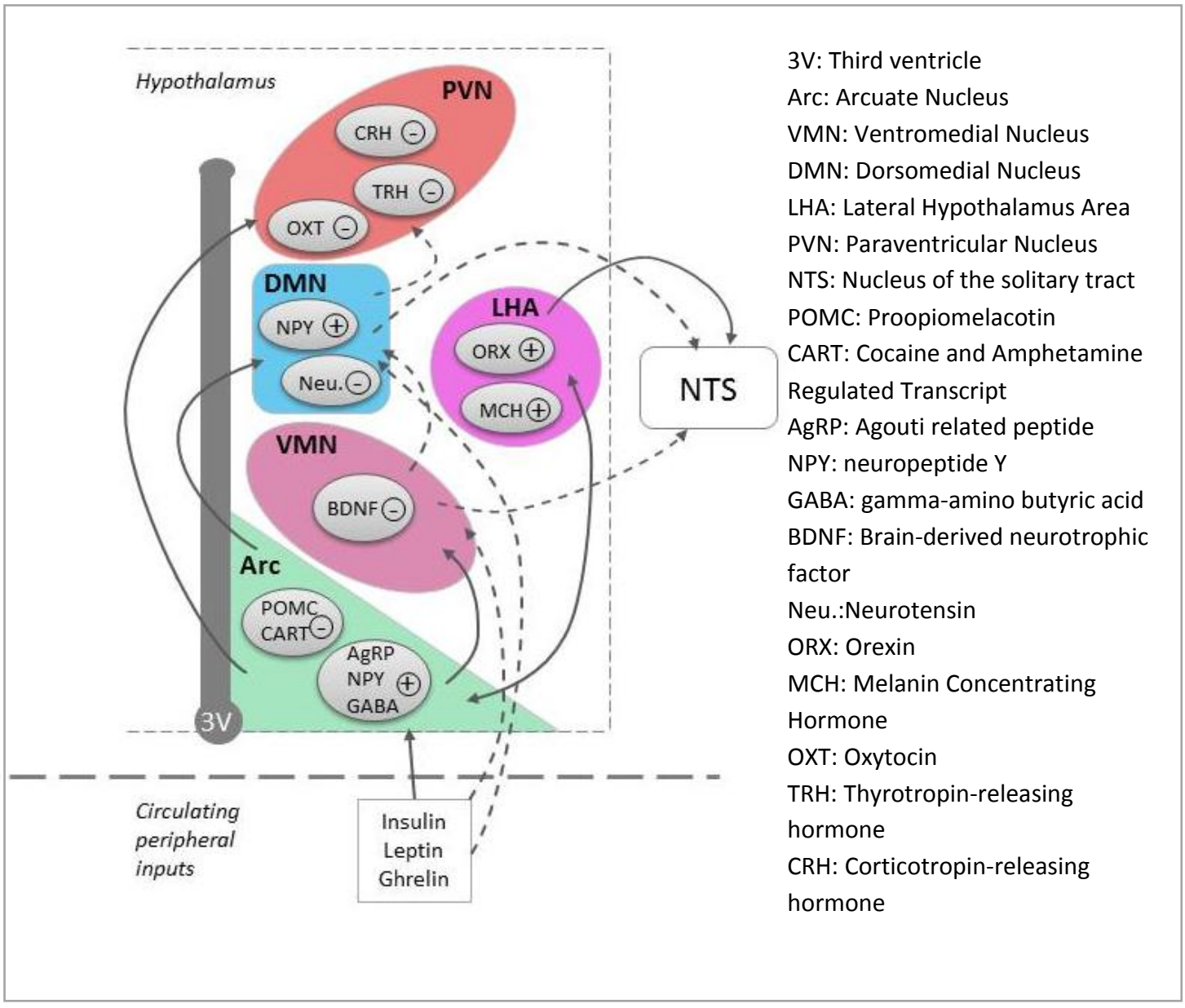

Arcuate Nucleus is the main leptin target in the brain. Partly located outside the blood–brain barrier, large molecules have access to this part of brain (Nilsson et al. 2013). POMC/CART and AgRP/NYP neurons are considered as “first-order neurons” and project to “second-order neurons” located in PVN, DMN, LHA and VMN nuclei (Valassi et al. 2008).

a) AgRP neurons co-express AgRP/NPY/GABA

AgRP neurons from Arcuate Nucleus co-express AgRP, GABA and NPY. Leptin and ghrelin, but also innervation from LH, act on these neurons (Morton et al. 2014). Leptin and insulin inhibit AgRP/NPY neurons, while ghrelin activate these ones (Morton et al. 2014). AgRP neurons project externally from Arc to PVN, VMN, DMN, LHA (Bi et al. 2012; Simpson et al. 2009). 6 NPY receptors are currently known, two of them seemingly important for food intake (NPY1 and NPY5) (Valassi et al. 2008). Moreover NPY neurons also project internally to inhibit POMC neurons via GABA release (Morton et al. 2014; Wilson & Enriori 2015). Activation of AgRP/NPY neurons is able to increase food intake (orexigenic effect), leading to an increase in body weight (Morton et al. 2014; Schwartz et al. 2000). AgRP neuron activation releases AgRP, thus blocking α-MSH action by antagonizing its binding on MC3 and MC4 receptors, (details below), releases GABA, that tonically inhibits POMC neurons, and releases NPY that activates its NPY1 and 5 receptors, all of these actions contributing to weight gain (Simpson et al. 2009; Wilson & Enriori 2015). Recent studies suggest that GABA, NPY and AgRP peptides have slightly different actions on food intake, with GABA and NPY required for acute feeding, while AgRP is required for long-term regulation of feeding (Wilson & Enriori 2015).

b) POMC neurons co-express POMC/CART

POMC neurons from Arcuate Nucleus co-express POMC and CART. Activation of these neurons is possible by leptin, and also by innervation from the LHA (Morton et al. 2014) and serotoninergic projections from the Brainstem (Pollak Dorocic et al. 2014). A leptin deficient state inhibits the expression of POMC and CART (Morton et al. 2014). POMC neurons project to PVN, VMN, DMN and LHA (Bi et al. 2012). POMC is derived from a polypeptide precursor called pre-POMC, which is then cut in several neuropeptides (α-MSH, γ-MSH and β-MSH) (Yeo & Heisler 2012) by the pro-hormone convertase 1/3 and 2 (PC1/3 and PC2) (Hill 2010). The POMC

cleavage peptides bind to MC3 and MC4 receptors in the projection area, thus AgRP and POMC are in competition for acting on these receptors (Simpson et al. 2009). Activation of POMC/CART neurons leads to a decrease of food intake (anorexic effect) and a decrease of weight (Sohn 2015).

c) MC3/MC4 receptor

Melanocortin receptors (MC) family is composed of 5 members, whose only MC3 and MC4 receptors are expressed in the brain. AgRP and α-MSH have an opposite action on these receptors. α-MSH is an agonist, while AgRP is an inverse agonist of MC3/4 receptors, especially MC4 receptor which is constitutively active (Hillebrand et al. 2002). MC4 receptor is highly expressed in the PVN, and its activation induces a reduction of food intake, while its inhibition or its deletion causes a hyperphagia with a reduction of the energy expenditure. The role of MC3 receptor is less clear, nevertheless its deletion causes an increase of the fat content (Simpson et al. 2009).

2. Ventromedial Nucleus (VMN)

The Ventromedial Nucleus (VMN) is considered as the "satiety centre" (Schwartz et al. 2000) and BDNF is the main neuropeptide expressed in this nucleus. VMN neurons are modulated by POMC/NPY neurons from Arc through MC4R, NPY1R, NPY2R, NPY5R receptor (Xu et al. 2003; Gao & Horvath 2007) . VMN is another important mediator of leptin, in addition of Arc through a poorly understood pathway that seems to be independent from the Arc (Gao & Horvath 2007). BDNF neurons project from VMN to DMN, and also maybe to NTS (Xu et al. 2003). The activation of BDNF suppresses food intake, explaining the term of "satiety centre". In case of food deprivation, BNDF is low expressed allowing an increase of food intake (Xu et al. 2003; Simpson et al. 2009).

3. Dorsomedial Nucleus (DMN)

The Dorsomedial Hypothalamus (DMN) is located close to the third ventricle just above the VMN. Neurotensin and NPY neurons are the two main neuronal types from the DMN, and are activated by NPY/AgRP neurons of Arc (Bi et al. 2012) and maybe also by VMN (Xu et al.

2003) and leptin (Hillebrand et al. 2002). According to Bi et al. (Bi et al. 2012), the regulation of NPY in Arc is different from its regulation in DMN: NPY in Arc is under the control of leptin, while NPY in DMN is leptin-independent with no leptin receptor expressed on the surface of NPY neurons. However another study showed leptin-responsive neurons projecting from DMN to PVN (Gautron et al. 2010)**.** Neurotensin is the product of cleavage of the precursor preproneurotensin (Hillebrand et al. 2002). Both neurotensin and NPY neurons project to PVN, and NPY neurons projects externally from hypothalamus to the NTS nucleus of brainstem. Activation of neurotensin neurons cause a reduction of food intake (Bi et al. 2012). On the contrary an activation of NPY neurons leads to an increase of food intake. These neurons have also impact on adiposity tissues and thermogenesis to regulate energy expenditure. Action and connectivity of the DMN within the brain is not well established (Wilson & Enriori 2015).

4. Lateral Hypothalamus Area(LHA)

The lateral hypothalamus area (LHA) is located on the most outer part, all along the hypothalamus even if it is slightly more posterior and is considered as the "hunger centre" (Schwartz et al. 2000). LHA includes two major types of neurons: one type of neuron expressing MCH and one type of neurons expressing orexin A and orexin B (Gao & Horvath 2007; Hillebrand et al. 2002). Orexin A and orexin B, also named hypocretin A and hypocretin B, are products of a common precursor polypeptide, prepro-orexin, after proteolytic processing (Tsujino & Sakurai 2009). MCH and orexin neurons are activated by neuronal projections from Arc. LHA neurons project outside of the hypothalamus in the NTS and VTA (Ventral Tegmental Area), but it also project to Arc in a feedback loop (Morton et al. 2014). MCH and orexin are stimulators of food intake (Gao & Horvath 2007), explaining the term of "hunger centre". This hypothalamic nuclei is considered as the centre of hunger and is linked to food reward (Gatta-Cherifi 2012). Orexin is known to be implicated in the food research behaviour (Gatta-Cherifi 2012). Interestingly, MCH neurons project to the spinal cord and the motor cortex (Bonnavion et al. 2016; Berthoud & Münzberg 2011). The implication of LHA for the reward will be explained below.

5. Paraventricular hypothalamus (PVN)

The Paraventricular Nucleus is located at the border of the third ventricle, above the DMN. The PVN is split into two parts, a medial and a lateral part. The medial part is composed of the TRH and CRH neuroendocrine neurons. In the lateral part, the neuropeptide oxytocin is expressed (Gatta-Cherifi 2012). Projections from VMN, DMN and Arc (Sabatier et al. 2013), activate PVN neurons. Both αMSH/CART and AgRP/NPY can have an action with MC4/3 receptors and NPY Y1/5 receptor expressed in PVN. αMSH/CART activate these neurons, while AgRP/NPY inhibit them (Lechan & Fekete 2006). Some studies showed that leptin could have a direct effect on oxytocin neurons of the PVN, however no clear pathway is known (Wilson & Enriori 2015). Leptin and ghrelin may also have a direct activity on CRH and TRH, yet further investigations are needed. TRH and CRH neurons project outside of the hypothalamus, and even outside the blood brain barrier to have impact on peripheral tissues (Lechan & Fekete 2006). CRH, which causes anorexia (Schwartz et al. 2000), belongs to the HPA (Hypothalamic-pituitary-gonadal) axis and participate to the secretion of glucocorticoids (Ferguson et al. 2009). TRH, which reduces food intake (Schwartz et al. 2000), belongs to the HPT (hypothalamic-pituitary-thyroid) axis and participate in the secretion of thyroid hormone (Ferguson et al. 2009). CRH plays a key role on the circadian rhythm of food intake, fasting-induced refeeding and also thermoregulation, energy expenditure and lyposis. TRH plays a role in the thermoregulation (Hillebrand et al. 2002). On their own, oxytocin neurons project to the pituitary gland, which allows the secretion of oxytocin into the blood (Sabatier et al. 2013) controlling function in uterus (Schwartz et al. 2000). But also oxytocin neurons project to NTS part of brainstem to inhibit the food intake (Sabatier et al. 2013). Oxytocin influences also the gastric emptying (Hillebrand et al. 2002).

C. Upstream control of the hypothalamus: serotonin

The amino acid Tryptophan (Trp) enters the brain by the blood brain barrier and is absorbed by serotoninergic neurons of the Raphe nucleus in Brainstem. After several enzymatic reactions, Trp is converted into serotonin (5-HT) (Voigt & Fink 2015; Donovan & Tecott 2013). Serotoninergic neurons from raphe nucleus project to several nucleus of hypothalamus: Arc,

PVN and LHA. On one hand, POMC neurons of Arc express 5HT2C receptor and 5-HT induce the release of α-MSH. On the other hand 5-HT binds to 5HT1B receptors at the surface of NPY neurons and increase the release of αMSH by supressing the inhibition of AgRP neurons. In the PVN, 5HT1B receptors are expressed and induced satiety. Both receptors inhibit food intake, but 5HT2C affect the frequency of meals, and 5HT1B affects meal duration.

A retrograde label of serotonergic neurons from dorsal raphe revealed a feedback loop from hypothalamus to dorsal raphe (Pollak Dorocic et al. 2014). Innervations of Dorsal Raphe is composed by 20% of orexin neurons from LH, 20% of MCH neurons from LHA and 10% of PVN projections (Donovan & Tecott 2013).

III. Food Intake and Weight control

The control of food intake and weight control are complex regulations, integrating signals from several brain parts as well as signals from the periphery.

A. Stimulating meal

Before the meal onset, the gastric hormone ghrelin is secreted. Ghrelin then binds to ghrelin receptors 1a (GHS-R1a) activating the secretion of AgRP/NPY from AgRP/NPY Arcuate Nucleus neurons (Wilson & Enriori 2015). At the same time, the inhibitory signals of GABA from AgRP/NPY neurons on POMC neurons is lowering the POMC anorexigenic effect (Wilson & Enriori 2015). The feeding is thus stimulated (Morton et al. 2014) (Figure 8).

B. Satiety signals: short-term signals

After food ingestion, the physical distension of the stomach relays a neural satiety signals through vagus nerve from gut and visceral organs to NTS nucleus in brainstem(Donovan & Tecott 2013). Moreover the digestion of fat, protein and glucose stimulates gastrointestinal cells to secretes CCK, GLP1 and hormones (Rui 2013). These hormones act on NTS nucleus. Both signals on NTS are integrated in the sum of signals from hypothalamus and the brain reward system to act on feeding (Figure 8). The short-term signal decreases the meal size and triggers the end of feeding. However, this signal is during the time of meal and has not an important impact on the body weight. Indeed, even if the meal size is reduced, a compensation by an increased meal frequency can appears (Morton et al. 2014).

C. Adiposity signals: long-term signal

1. System of action

Leptin and Insulin are hormones produced respectively by the adipose tissue and the β-cells of pancreas. Their level in plasma is proportional to the body fat content. After entering the Central Nervous System, both hormones act on Arcuate Nucleus to decrease the food intake. The effect of leptin is quantitatively much greater than insulin (Morton et al. 2014; Schwartz et al. 2000) (Figure 8A).

2. Leptin

In a case of weight gain or at mealtime (Figure 8A), a direct and an indirect signal act on the NTS as the satiety centre. First, leptin binds directly to NTS neurons and enhances the indirect signal. Second, by the indirect signal, leptin acts on the leptin receptors at the surface of POMC and AgRP neurons in the Arcuate Nucleus. The fixation on the receptors leads to a stimulation of POMC signals and an inhibition of AgRP signals. Then these neuropeptides act on second-order neurons in the PVN and LH. At this moment the projection from PVN and LHA activate the NTS. The NTS nuclei receive direct and indirect signals from leptin, but also signals from CCK (see before). A hypothalamic signal from NPY neurons of DMN to NTS can also modulate the satiety signal (Bi et al. 2012). Even if the pathway is not clear, it seems that BDNF neurons have also an Arc-independent action on NTS (Gao & Horvath 2007). After the summation of all these signals, NTS sends a satiety signal to reduce food intake. In case of a weight loss (Figure 8B), leptin shows less efficacy on NTS leading to increased meal size. (Morton et al. 2014)

D. Food reward (LHA and leptin)

The LHA receives signals from Arc of hypothalamus but also signals from Nucleus Accumbens (NAc). NAc is located in the basal forebrain. With this sum of signal, LHA influence the VTA composed of dopaminergic neurons and the NTS for the satiety perception. VTA have then projection to NAc to increase the reward of palatable food (Morton et al. 2014). In case of weight loss, the lower level of insulin and leptin with the increased level of ghrelin increases the rewarding properties of food. This action is direct with ghrelin and indirect with leptin and insulin through the LH. If the energy balance is positive, in case of increased weight, the signal of rewarding is reduced associated with a higher satiety signal (Figure 9).

Figure 8: Schematic representation of the food intake regulation in case of positive energy balance (for example after a meal or weight gain, A) and in case of a negative energy balance (for example after fasting or weight loss, B). Based on (Morton et al. 2014).

Effects of different mediators are either reduced (dotted lines) or important (solid line). Signals either inhibit (-) or stimulate (+) food intake. Arc : Arcuate Nucleus ; LHA : Lateral Hypothalamus Area ; PVN : Paraventricular Nucleus ; NTS : Nucleus of the Solitary Tract. POMC : Proopiomelanocortin ; AgRP : Agouti-Related Peptide. CCK : Cholecystokinin.

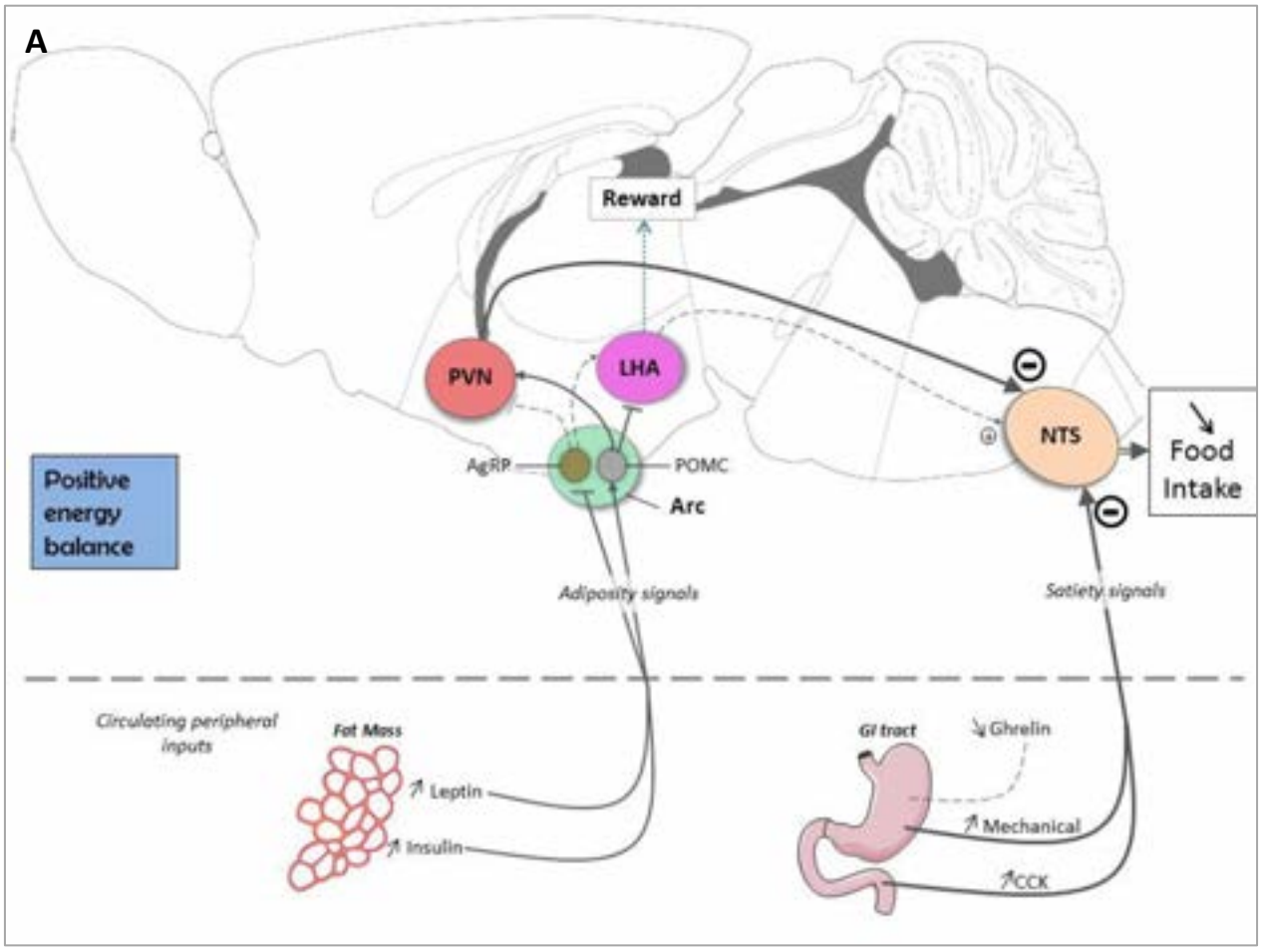

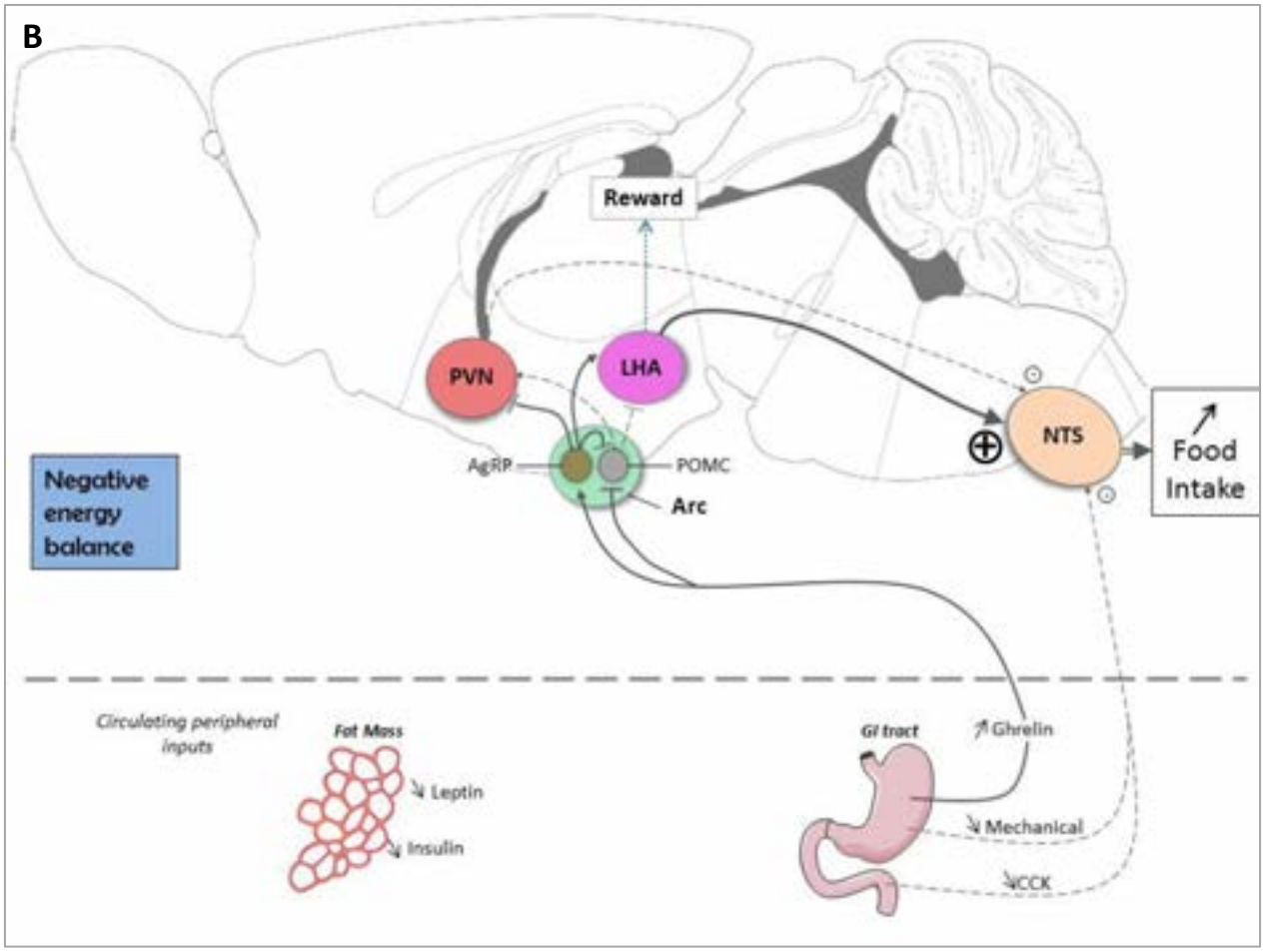
B
Reward
PVN
LHA
NTS
Food Intake
AgRP
POMC
Arc
Negative energy balance
Circulating peripheral inputs
Fat Mass
Leptin
Insulin
GI tract
Ghrelin
Mechanical
CCK

Figure 9: Schematic representation of the network implicated in the reward. Modified from (Morton et al. 2014).
Effects of different effecters are indicated with arrows. Arc : Arcuate Nucleus ; LHA : Lateral Hypothalamus Area ; VTA : Ventral Tegmental Area ; NAc : Nucleus Accumbens

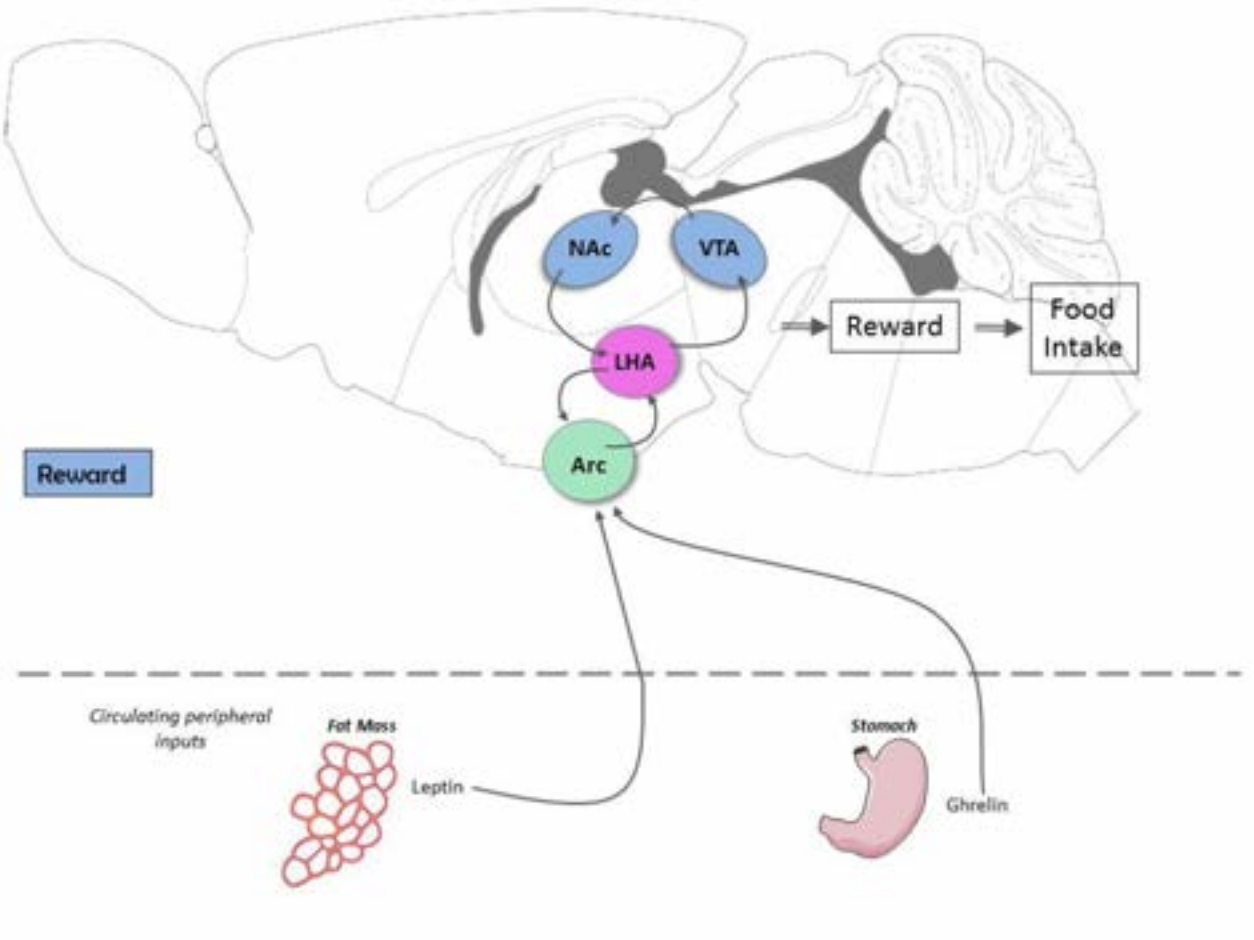

IV. Hypothalamic alterations in neurodegenerative diseases

Main information can be found in Table 2.

A number of hypothalamic alterations have been documented in neurodegenerative diseases.

A. Alzheimer's disease

1. Symptoms and pathology of Alzheimer's disease

Alzheimer's disease (AD) is a neurodegenerative disease with onset at about 65 years of age. The main AD symptoms are a memory loss associated with impairment of certain abilities (speech, personality, judgment, vision, association sensory-motor function) (Castellani et al. 2010). Four Familial genes and 7 risk genes are known. There are respectively APP (amyloid precursor protein), PSEN1 (presenilin 1), PSEN2 (presenilin 2), SorL1 (Sortilin-related receptor 1) and APOE (Apolipoprotein E), GSK3β (Glycogen synthase kinase 3 beta), DYRK1A (Dual specificity tyrosine-phosphorylation-regulated kinase 1A), Tau (Tubule-associated unit), TOMM40 (Translocase of outer mitochondrial membrane 40), CLU (Clusterin), PICALM (phosphatidylinositol binding clathrin assembly protein) (Ballard et al. 2011). Nowadays, there are still difficulties of diagnosis between AD and other Dementia. Using brain MRI scan or PET scan (positron emission tomography scan), physicians are able to detect lesions or disease that can cause or contribute to dementia, and differentiate the diseases. There is no biomarker and the definitive diagnosis of AD can only be pronounced with certainty at post-mortem histological examination (Ballard et al. 2011). APP protein is cleaved by γ- and β- secretase complexes (BACE) leading to several peptide fragments, 1 of them is Aβ peptide. Misregulation of APP proteolytic processing or dysfunction of protein clearance lead to formation of plaques (McGuire & Ishii 2016). Also high level of BACE1 enzyme is measured in AD, and other indications Tau protein can be also be hyperphosphorylated or undergo abnormal post-translational modifications leading to aggregates (McGuire & Ishii 2016). In the brain, accumulation of extracellular amyloid beta (Aβ) deposits and intracellular neurofibrillary tangles of hyperphosphorylated Tau protein cause neuronal dysfunction and neuronal death and are the pathological hallmarks of this disease (Ballard et al. 2011; McGuire & Ishii 2016).

2. Metabolic problems

About 50%-60% of Alzheimer cases show abnormal eating behaviours (Ikeda et al. 2002). Indeed 14% to 80% of AD cases are at risk of under nutrition (Droogsma et al. 2015). Weight loss is recognized as a clinical feature of Alzheimer disease with about 20% to 45% of cases showing this symptom (Droogsma et al. 2015; Aziz et al. 2008). This weight loss occurs usually before the clinical onset then body weight generally increases after diagnosis thanks to treatment or nutritional advice (Droogsma et al. 2015). Importantly, BMI decline in older age is associated with increased risk of developing AD as well as with a faster rate of disease progression (Aziz et al. 2008). Nutritional recommendations are to follow weight and perform a nutritional intervention if weight loss is superior to 5% in 3-6months (Droogsma et al. 2015).

Weight loss and abnormal eating behaviour could be caused by defects in sensory integration or processing, in particular taste or olfaction, or could be side effects of medications (Droogsma et al. 2015). Nevertheless, the apparition of body weight problems before the initial cognitive symptoms suggest that weight loss is intrinsic aspect of AD (McGuire & Ishii 2016).

In addition to weight loss observed in late-life period of AD, the mid-life weight is in correlation with the risk of developing AD. Several studies have shown that mid-life obesity is a risk factor for developing AD, which is in opposition of the protective effect of high BMI in late-life. However, one study indicate that a mid-life obesity decrease AD risk. In one word, it is clear that mid-life BMI influences positively or negatively the risk of developing AD (McGuire & Ishii 2016). In addition to obesity, type 2 diabetes is also associated with increased risk of developing AD. In AD mouse models, insulin resistance induced by high-fat diet exacerbates AD pathology. Several proofs of brain glucose metabolism defects and insulin signalling in AD suggest that AD could be a “type 3 diabetes” (McGuire & Ishii 2016). This connection is also in both ways. Indeed AD patients have a higher prevalence for Type-2 diabetes than control subjects (Janson et al. 2004).

Several studies have highlighted that caloric restriction are beneficial to reduce AD-like pathology and improvement of cognitive impairments in AD mouse model (Ishii & Iadecola 2015).

3. Hypothalamic defects

a) In mouse model

BACE1 is mainly expressed in neurons and its levels are increased in AD. Ablation of this enzyme improves metabolism in high-fat induced obesity or diabetes mouse models. Thus, BACE1 could be a link between AD and type 2 diabetes. In a study (Plucińska et al. 2016), a brain specific human BACE1 KI mouse (called PLB4), is leaner with impairment of glucose homeostasis, leptin, insulin resistance, changes in lipid composition. Moreover a glucose hypometabolism is observed in brain of PLB4 mice at the age of 6 months. More precisely, POMC hypothalamic expression is increased with a higher expression of the receptor MC4, showing a shift towards anorectic signalling. The same team have shown previously that this mouse presents an AD like phenotype without APP mutation, which put forward the possibility of a link of BACE1 enzyme in sporadic AD. This points the implication of hypothalamus in AD and metabolic defects.

Moreover, in an AD mouse model, AD pathology leads to hypothalamic insulin signalling resistance contributing to impaired glucose homeostasis observed in mouse and increased possibility of Type-2 diabetes (Ruiz et al. 2016).

Furthermore, Aβ seems to be able to inhibit leptin expression and leptin receptor activation. Indeed in 2014 Ishii and collaborators (Ishii et al. 2014), showed that in mouse model low level of leptin is caused by excess Aβ, which then causes an inhibition of NPY neurons in the Arcuate Nucleus leading to the decrease in body weight. However, the effects of Aβ on hypothalamic neurons were different in another study: In 2015, Clarke and collaborators (Clarke et al. 2015), have shown that injection of Aβ oligomers in lateral ventricle of wt mice leads to insulin resistance and impaired glucose tolerance 7 days after injection. Metabolic problems are due to the presence of Aβ oligomers in brain and not in the periphery. On hypothalamic primary neurons, Aβ oligomers bind to dendrites of hypothalamic neurons, causing an increase of ROS (reactive oxygen species). Concerning the control of metabolic factors, Aβ oligomers injection causes an increase in food intake but no changes in body weight. Consistent with the increased

food intake, AgRP and NPY expression are increased without changes on their death rate or electrophysiological properties.

Currently, publications show that Aβ interacts with hypothalamus and also hypothalamic input signals (leptin and insulin). The pathway of action and the exact consequences of Aβ on AD and metabolism disease need to be further investigated.

b) In patients

Pathologically, amyloid plaques and neurofibrillary tangles are observed in hypothalamus of AD patients associated with neuronal loss (Ishii & Iadecola 2015). For example LHA and PVN, but also other hypothalamic nuclei, are affected in AD. Concerning hypothalamic neuropeptides, orexin neurons are 40% less numerous in hypothalamus of AD patient in comparison to healthy controls. Level of orexin in Cerebrospinal Fluid (CSF) is in agreement with number of neurons with a decrease of 14% in AD versus controls (Fronczek et al. 2012).

Signals of hypothalamus are leptin and insulin. Like in mouse models, low level of leptin is associated with risk of AD (Holden et al. 2009). Leptin treatment in AD patients is protective for cognition capacities (Ishii & Iadecola 2015). Similar to leptin, insulin resistance seems to regulate Aβ and tau protein. Thus Aβ would disrupt insulin signalling in AD (Kim & Feldman 2015). And insulin treatment is beneficial on AD pathology and cognition (Claxton et al. 2015). Hypothalamus, which is the target of insulin, might be a critical component between diabetes and AD.

Several neuroimaging studies have observed by MRI a hypothalamic atrophy (Ishii & Iadecola 2015). Callen and collaborators, and also Loskutova and collaborators, have shown that hypothalamic volume is reduced of about respectively 10% and 12% (Loskutova et al. 2010; Callen et al. 2001). Hypothalamic atrophy appears in early clinical stages of AD (Loskutova et al. 2010).

B. Fronto-Temporal Dementia (FTD)

1. Symptoms and pathology of disease

Fronto-Temporal Dementia (FTD) is a neurodegenerative disease with an age of onset between 45 years old and 64 years old. The survival of FTD patients is about 2 to 5 years after diagnosis. FTD is characterized by progressive deficits in behaviour, executive function and language. In FTD there are 3 different variants; one of them is behavioural-variant FTD (bv-FTD) with early behavioural and executive deficits. Bv-FTD can sometimes also be called frontal-variant FTD (fvFTD). The bv-FTD patients have some personality changes like stereotypic behaviours, disinhibition (for example interaction with strangers without respect of boundaries), and also sometimes apathy (for example less sympathy toward family and friends) (Neary et al. 2005). Some common genetic mutations cause ALS and FTD like described before. These genes are TDP-43, FUS and c9orf72. Moreover two main genes are identified as pure FTD mutations: MAPT (Microtubule-associated protein Tau) and PGRN (progranulin) (Baker et al. 2006).

2. Changes of eating behaviours in FTD

In FTD, there is a high prevalence of alterations in appetite and food preference. The changes include not only changes in quality but also in the quantity of food ingested. This symptom is present in more than 60% of cases at onset and affects more than 80% of cases during the course of disease (Piguet et al. 2011). All bv-FTD patients show an abnormal eating behaviour (Ikeda et al. 2002; Ahmed et al. 2014). Patients might develop new habits, like eating every day at same time or new oral behaviours such as chewing or smoking. In a recent study measuring food intake at a breakfast meal (Ahmed et al. 2016), bv-FTD patients are eating two times more that control group (1344 calorie intake for bv-FTD versus 603 calorie intake for controls). Bv-FTD patients also have an increased preference for sweet taste, often observed by caregivers by a sweet food-seeking behaviour (Ahmed et al. 2016). Moreover, Ikeda et al. have shown a weight gain, superior to 7.5kg, is observed is 30% of cases in bv-FTD and a weight loss, superior to 7.5kg, is observed in 9% of bv-FTD (Ikeda et al. 2002). Data from Ahmed et al shows that bv-FTD patients have higher BMI (Ahmed et al. 2014; Ahmed et al. 2014; Ahmed et al.

2015). The increased of BMI is less than what would be expected with their increased of food intake. The question of the presence of hypermetabolism in bv-FTD is thus still raised (Ahmed et al. 2016). The hypothesis of a metabolic continuum between FTD and ALS is currently developed: on one end, weight loss, malnutrition, insulin resistance, hypermetabolism in ALS and on the opposite end, insulin resistance, weight gain, maybe hypermetabolism in FTD (Ahmed et al. 2016). ALS patients with cognitive impairment and ALS-FTD patients, whose metabolic characterisation has not been performed, are likely in between the two classical phenotypes.

3. Hypothalamic defects in bv-FTD

A small study from Piguet et al. in 2011 (Piguet et al. 2011), with 16 controls and 18 bv-FTD showed atrophy of the hypothalamus, especially in its posterior part (including the lateral hypothalamus area and dorsomedial nuclei). In this study, the decrease in the hypothalamic volume was about 15% as compared to controls. These authors conclude that hypothalamic atrophy is an early feature of the disease, which appears within the 2 years after diagnosis. Two other recent studies from Bocchetta et al. and Ahmed et al. (Bocchetta et al. 2015; Ahmed et al. 2015), with for the first study 18 controls and 18 bv-FTD, and for the second study with 23 controls and 19 bv-FTD patients, also observed that bv-FTD patients show a smaller hypothalamus as compared to controls (loss of 17 % in Bocchetta et al.).The second study also found that the atrophy is mainly in the posterior part (Ahmed et al. 2015). In the publication of Bocchetta (Bocchetta et al. 2015), the authors were able to segment for sub regions of hypothalamus. Significant atrophy was observed in the subunits containing PVN, DMN and LH/mammillary body. It also has been observed that FTD patients with the highest eating disturbances were the one with the most important atrophy of posterior hypothalamus (Piguet et al. 2011; Ahmed et al. 2015).

2 subtypes of bv-FTD are distinguished on neuropathological criteria, FTD-Tau with Tau positive inclusions in Pick body, and FTD-TDP with TDP-43 positive inclusions. Piguet and collaborators found that FTD-Tau patients have more hypothalamic aggregates than FTD-TDP patients. In FTD-Tau, Tau-immunoreactivity is observed in the overall hypothalamus, while in

FTD-TDP only few inclusions were found in posterior hypothalamus (Piguet et al. 2011). Moreover FTD-Tau patients have a more severe hypothalamic atrophy than FTD-Tau patients versus controls. For the Tau group, neuronal loss was observed, while in the TDP group, even if there is atrophy, no changes were observed in the quantity of neurons. Though there is a neuronal loss in FTD-Tau cases, this was not due to changes in eating peptide neurons (NPY, CART and orexin neurons) (Piguet et al. 2011). Peripheral hormone levels and hypothalamic neuropeptide level were measured in blood of bv-FTD (Ahmed et al. 2015). No changes were observed between bv-FTD and controls for leptin, CCK, ghrelin, PYY and oxytocin. However levels of AgRP in fasting condition were three times higher in bv-FTD in comparison to controls. Indeed AgRP and leptin correlated with BMI.

C. Huntington's disease

1. Symptoms and pathology of disease

Huntington's disease (HD) is a neurodegenerative disease with an age of onset between 35 and 45 years of age, which affects about 4 to 8 patients on 100 000 people (Harper 1992). The survival is about 10 to 25 years after the disease diagnosis (Goodman et al. 2008). Symptoms are a progressive motor dysfunction, with a cognitive decline and a psychiatric disturbance, which can start before the onset of motor signs (Goodman et al. 2008). Criteria of diagnosis are motor signs of chorea, which are involuntary and not controlled movements, dystonia, which is involuntary long muscle contraction during effort, and bradykinesia.

HD is a monogenic disease caused by a repeat expansion in the CAG triplet in exon 1 of Huntingtin (*HTT*) gene leading to an expanded polyglutamine stretch in the protein (Ross & Tabrizi 2011). Short expansions (36 to 39) increases the risk of developing the disease, while expansions superior to 40 repeats leads to complete disease penetrance (McNeil et al. 1997). The length of CAG expansion influences the age of onset (earlier if longer) (Ross & Tabrizi 2011).

2. Metabolic problems

a) In patients

At early stage, short time after diagnosis, HD patients with low motor impairment show a lower BMI than general population (Knowlton et al. 2002; Süssmuth et al. 2015; Marder et al. 2009; Mochel et al. 2007). This seems due to a decreased fat mass because fat-free mass (all components except fat like skeletal muscle, liver and heart) are similar between HD patients and controls. With the advancement of disease, the difference increases leading to a severe weight loss at end stage (Knowlton et al. 2002; Süssmuth et al. 2015). The weight loss is not correlated with motor or cognitive or behavioural decline, showing that is not secondary to hyperactivity or other motor symptoms. Hypermetabolism is one explanation of weight loss in HD (Aziz et al. 2008; Mochel et al. 2007). Patients with early disease stage and mild-moderate stage show increased Total Energy Expenditure (TEE) with an increased basal resting energy expenditure, correlated with disease duration (Goodman et al. 2008; Aziz et al. 2010). It has been shown that HD patients with higher BMI at onset of symptoms have slower decrease of disease progression (Süssmuth et al. 2015; Aziz et al. 2009). Consistent with a pre-morbid origin of weight loss, presymptomatic HD mutations carriers consume more calories (Mochel et al. 2007) to compensate for hypermetabolism. However leptin, ghrelin or insulin were unchanged in HD patients in comparison to controls (Süssmuth et al. 2015).

In 2009, Aziz et al. (Aziz et al. 2009) showed that longer CAG repeats is associated with lower BMI than shorter CAG HD patients. Also, the longer CAG repeat is the faster BMI declines.

b) In mouse models

There are several mouse models for Huntington's disease. Interestingly, the metabolic alterations are different between models.

(1) R6/2

R6/2 mouse is a HD model, with expression of exon 1 of human *HTT* gene under human huntingtin promoter, with 110 to 160 CAG repeats depending of the different strains (van Wamelen et al. 2014). In this model, motor symptoms onset is at the age of 6 weeks of age and

survival ranges from 10 to 13 weeks (Crook & Housman 2011). From 6 weeks old to 7.5 weeks, R6/2 mice consume higher caloric intake than wt mice (van der Burg et al. 2008) and also present hypermetabolism (van der Burg et al. 2008; Goodman et al. 2008). At this age, the increase of energy expenditure is compensated by the increased food intake. From 7.5 weeks old to 9 weeks old, hypermetabolism is still present, but the consumed kilocalories decreased. At this age, consumption of fat deposit or skeletal muscle tissue help to maintains weight (van der Burg et al. 2008). From 9 weeks of age, R6/2 mice lose weight (van der Burg et al. 2008). At this age, mice can no longer compensate hypermetabolism by calories consumed (Aziz et al. 2009; van der Burg et al. 2008). Moreover, higher the number of CAG repeat is, the lower the body weight is and higher is the consumption of energy (Aziz et al. 2009).

(2) BACHD mice

Another important HD mouse model is the BACHD mouse with the expression of full length human *HTT* gene with about 97 CAG repeat length (Crook & Housman 2011). The motor onset is at 2 months old and lifespan is normal (Crook & Housman 2011). At same age as motor onset, BACHD mice have already a higher body weight, due to increased body fat, and keep this difference over time causing an obesity at 4 months old (Hult et al. 2011). Obesity is not due to reduced activity but an increased food intake compared to wt (Hult et al. 2011). The metabolic problem of BACHD mouse could be recapitulated by injecting fragment of mutant htt fragment in hypothalamus (Hult et al. 2011).

3. Hypothalamic defects

a) Hypothalamic volume

Gabery et al. (Gabery et al. 2010) have studied in 2010, the hypothalamic volume of HD patients on post-mortem tissues. After stereological analysis on 9 HD cases and on 8 control cases, a trend toward an 11% atrophy of HD hypothalamus has been observed. In 2015, the same team (Gabery et al. 2015), developed a MRI analysis for estimation of hypothalamic volume based on previous histological analysis of post-mortem tissues. In this paper, reproducible landmarks on MRI, closest from histological landmarks, were described. The analysis was done on 36 presymptomatic HD, 34 symptomatic HD and 33 healthy controls with

2 scans followed from 18 months. Hypothalamic volume was not different between groups with no evolution over 18 months. The pathology of HD hypothalamus seems thus independent from a hypothalamic atrophy.

b) Hypothalamic neurons

(1) In mouse models

(a) R6/2 model

In Arcuate nucleus of R6/2 mice, a progressive decrease of neurons expressing POMC positive neurons, associated with neuron atrophy, and a decrease of CART positive neurons are present. Expression of NPY mRNA is decreased in the whole brain. The number of PVN neurons is decreased, with specially a decrease of neurons expressing oxytocin mRNA and a reduction of oxytocin protein level. Changes were also found in the LH, with a decrease of MCH neurons, a decrease of CART neurons and a severe decrease of 70% of orexin neurons (van Wamelen et al. 2014).

(b) BACHD mouse

In BACHD mice, mRNA level of NPY in the whole brain is reduced. There are no other changes in PVN (van Wamelen et al. 2014). An increase of orexin positive neurons has been observed in LHA (Hult Lundh et al. 2013). However there was no difference of oxytocin or vasopressin neurons between BACHD and wt mice.

(2) In patients

In the Infundibular Nucleus, the equivalent of Arcuate Nucleus in mouse brain, the mRNA level of NPY is not changed. However, there are less NPY neurons in HD hypothalamus. POMC, AgRP and CART are not changed (van Wamelen et al. 2014). Controversies exist about the expression of oxytocin in the PVN. Either the expression was found constant (van Wamelen et al. 2014) or decreased of 45% (Gabery et al. 2010). In the same publication, Gabery et al. found a reduction of 24% in the number of vasopressin neurons (Gabery et al. 2010). Concerning the LH, a decrease of 30% to 38% of orexin positive neurons has been observed, but no changes in MCH neurons (Gabery et al. 2010).

Table 3: Metabolic and hypothalamic dysfunction in neurodegenerative diseases.

Neurodegenerative diseases	Metabolic problems	Hypothalamic volume	Hypothalamic network
Alzheimer's	50%-60% cases with abnormal food intake behaviour 20%-45% cases with weight loss Obesity and type 2 diabetes are risk factor for AD	Decrease of volume (10-12%)	In patients, aggregates and neuronal loss (for example ORX) Leptin and Insulin implication In mouse model, leptin reduction, insulin resistance and NPY/AgRP/POMC changes
FTD	60%-80% bv-FTD cases with abnormal food intake behaviour	Decrease of volume (15% to 17%)	Increase AgRP level in blood Inclusions (TDP or Tau)
Huntington's	Lower BMI Weight loss (hypermetabolism)	No difference	Decrease of NPY (in Arc), Vasopressin, Orexin No change for POMC, AgRP, CART

Results

I. Results #1

A. Résumé – Publication #1

« Alterations in the hypothalamic melanocortin pathway in amyotrophic lateral sclerosis »

Les patients SLA souffrent d'un défaut du métabolisme énergétique. En effet il existe une perte de poids importante dès le début de la maladie qui est due en partie à un hypermétabolisme. Les mêmes observations sont faites chez les souris mutées *Sod1(G86R)* avec une perte de poids et un hypermétabolisme. Cependant les causes et les mécanismes de ce dysfonctionnement ne sont pas connus. Il faut savoir que les études préalables sur le métabolisme énergétique chez les patients SLA sont en général réalisées à un seul temps sans suivi longitudinal. Cependant la régulation du métabolisme est extrêmement dynamique et des essais cliniques, avec une intervention pharmacologique, sont un très bon moyen de suivre les effets métaboliques sur plusieurs mois.

Dans notre étude, nous avons réalisé une analyse *post-hoc* d'échantillons obtenus au cours d'un essai clinique de 2012, où les patients SLA ont été traités avec un antidiabétique la Pioglitazone. La Pioglitazone est très bien connue pour des effets sur le métabolisme chez les patients et chez les modèles murins. Au niveau périphérique, la Pioglitazone a des effets sur l'insuline, la glycémie et les enzymes hépatiques. Au niveau du système nerveux central, la Pioglitazone inhibe le système mélanocortine entrainant un gain de poids de l'ordre de 3 à 5 kg chez l'humain.

Premièrement, dans le sang des patients SLA sous placebo et sous Pioglitazone, nous avons mesuré le niveau d'insuline, de glycémie et des enzymes hépatiques tout au long du traitement sur plusieurs mois. Nous observons l'effet escompté de la Pioglitazone sur ces marqueurs périphériques. Cependant, les patients sous traitement Pioglitazone n'ont pas pris de poids au cours des 20 mois de traitement. Ainsi la Pioglitazone n'a pas d'effet au niveau central chez les patients SLA.

Des travaux précédents avaient montré que la prise de poids sous Pioglitazone est causée par une augmentation de la prise alimentaire. En réalisant une expérience de prise alimentaire sur les souris *Sod1(G86R)*, nous observons que la pioglitazone augmente la prise alimentaire chez les souris sauvages, alors que cette molécule n'a pas le même effet chez les souris mutées.

Le mode d'action de la Pioglitazone consiste en une action sur le système mélanocortine du noyau arqué composé des neurones POMC et AgRP. Nous remarquons qu'il existe un dysfonctionnement de ce système chez plusieurs modèles murins de la SLA. Une baisse de POMC est associée à une augmentation d'AgRP, au niveau de l'expression d'ARNm et de l'expression protéique. Ces régulations anormales sont cohérentes avec une augmentation de la prise alimentaire en réponse au jeûne chez ces souris.

Finalement, nous montré que le dysfonctionnement mélanocortine était en aval d'une perte d'innervation sérotoninergique provenant du tronc cérébral. Compenser cette perte de sérotonine, par intervention pharmacologique, permet un retour à la normal de POMC et une normalisation de l'hyperphagie transitoire en réponse au jeûne.

L'ensemble de ces résultats nous fournit un mécanisme pouvant expliquer le manque d'effet de la Pioglitazone chez les patients SLA. De plus, le dysfonctionnement mélanocortine peut rendre compte de certains défauts métaboliques observés dans la SLA, comme une anomalie du comportement alimentaire. Finalement, cette étude nous montre qu'un traitement pharmaceutique permettant de contrecarrer la perte de poids ne devrait pas cibler le système mélanocortine.

doi:10.1093/brain/aww004 BRAIN 2016: 139; 1106–1122 | 1106

BRAIN
A JOURNAL OF NEUROLOGY

Alterations in the hypothalamic melanocortin pathway in amyotrophic lateral sclerosis

Pauline Vercruysse,[1,2,3] Jérôme Sinniger,[1,2] Hajer El Oussini,[1,2] Jelena Scekic-Zahirovic,[1,2] Stéphane Dieterlé,[1,2] Reinhard Dengler,[4] Thomas Meyer,[5] Stephan Zierz,[6] Jan Kassubek,[3] Wilhelm Fischer,[3] Jens Dreyhaupt,[7] Torsten Grehl,[8] Andreas Hermann,[9] Julian Grosskreutz,[10] Anke Witting,[3] Ludo Van Den Bosch,[11] Odile Spreux-Varoquaux,[12,13,14] the GERP ALS Study Group,[†] Albert C. Ludolph[3] and Luc Dupuis[1,2]

[†]See Appendix 1

Amyotrophic lateral sclerosis, the most common adult-onset motor neuron disease, leads to death within 3 to 5 years after onset. Beyond progressive motor impairment, patients with amyotrophic lateral sclerosis suffer from major defects in energy metabolism, such as weight loss, which are well correlated with survival. Indeed, nutritional intervention targeting weight loss might improve survival of patients. However, the neural mechanisms underlying metabolic impairment in patients with amyotrophic lateral sclerosis remain elusive, in particular due to the lack of longitudinal studies. Here we took advantage of samples collected during the clinical trial of pioglitazone (GERP-ALS), and characterized longitudinally energy metabolism of patients with amyotrophic lateral sclerosis in response to pioglitazone, a drug with well-characterized metabolic effects. As expected, pioglitazone decreased glycaemia, decreased liver enzymes and increased circulating adiponectin in patients with amyotrophic lateral sclerosis, showing its efficacy in the periphery. However, pioglitazone did not increase body weight of patients with amyotrophic lateral sclerosis independently of bulbar involvement. As pioglitazone increases body weight through a direct inhibition of the hypothalamic melanocortin system, we studied hypothalamic neurons producing proopiomelanocortin (POMC) and the endogenous melanocortin inhibitor agouti-related peptide (AGRP), in mice expressing amyotrophic lateral sclerosis-linked mutant SOD1(G86R). We observed lower *Pomc* but higher *Agrp* mRNA levels in the hypothalamus of presymptomatic SOD1(G86R) mice. Consistently, numbers of POMC-positive neurons were decreased, whereas AGRP fibre density was elevated in the hypothalamic arcuate nucleus of SOD1(G86R) mice. Consistent with a defect in the hypothalamic melanocortin system, food intake after short term fasting was increased in SOD1(G86R) mice. Importantly, these findings were replicated in two other amyotrophic lateral sclerosis mouse models based on TDP-43 (*Tardbp*) and FUS mutations. Finally, we demonstrate that the melanocortin defect is primarily caused by serotonin loss in mutant SOD1(G86R) mice. Altogether, the current study combined clinical evidence and experimental studies in rodents to provide a mechanistic explanation for abnormalities in food intake and weight control observed in patients with amyotrophic lateral sclerosis. Importantly, these results also show that amyotrophic lateral sclerosis progression impairs responsiveness to classical drugs leading to weight gain. This has important implications for pharmacological management of weight loss in amyotrophic lateral sclerosis.

1 Inserm U1118, Mécanismes centraux et périphétiques de la neurodégénérescence, Strasbourg, F-67085 France
2 Université de Strasbourg, Faculté de Médecine, UMRS1118, Strasbourg, F-67085 France
3 Department of Neurology, University of Ulm, Germany
4 Department of Neurology, Hannover Medical School, Hannover, Germany
5 Department of Neurology, Charité University Hospital, Berlin, Germany
6 Department of Neurology, University of Halle-Wittenberg, Germany
7 Institute of Epidemiology and Medical Biometry, University of Ulm, Germany

Received July 27, 2015. Revised November 13, 2015. Accepted December 04, 2015. Advance Access publication March 16, 2016

8 Department of Neurology, BG University Hospital Bergmannsheil, Bochum, Germany
9 Department of Neurology, Technische Universität Dresden, and German Center for Neurodegenerative Disease (DZNE), Dresden, Germany
10 Department of Neurology, University Hospital, Jena, Germany
11 Laboratory of Neurobiology, KU Leuven and Vesalius Research Center, VIB, Leuven, Belgium
12 Faculté de Médecine Paris-Ile de France-Ouest, France
13 Université de Versailles Saint-Quentin-en-Yvelines, France
14 Centre Hospitalier Versailles, Le Chesnay, France

Correspondence to: Luc Dupuis,
INSERM U1118, Faculté de médecine, bat 3, 8e etage, 11 rue Humann, 67085 Strasbourg, Cedex, France
E-mail: ldupuis@unistra.fr

Correspondence may also be addressed to: Albert C. Ludolph,
RKU, Universitatsklinik Ulm, Oberer Eselsberg 45, 89081 Ulm, Germany
E-mail: albert-c.ludolph@uni-ulm.de

Keywords: amyotrophic lateral sclerosis; calorie intake; hypothalamus; thiazolinediones; weight loss

Abbreviations: ALS = amyotrophic lateral sclerosis; TZD = thiazolinedione

Introduction

Amyotrophic lateral sclerosis (ALS), the most common adult-onset motor neuron disease, is characterized by the simultaneous degeneration of upper and lower motor neurons, leading to muscle atrophy and paralysis, and death within 3 to 5 years after onset. A subset of ALS cases are of familial origin and five major genes are currently associated with familial ALS (*C9orf72*, *SOD1*, *FUS*, *TARDBP* and *TBK1*) (Leblond *et al.*, 2014; Cirulli *et al.*, 2015; Freischmidt *et al.*, 2015; Lattante *et al.*, 2015). The *SOD1* gene was the first associated with ALS and most ALS mouse models currently used are based upon overexpression of mutant forms of *SOD1* (Gurney *et al.*, 1994; Ripps *et al.*, 1995).

Beyond progressive motor impairment, patients with ALS suffer from major, yet incompletely characterized, defects in energy metabolism (Dupuis *et al.*, 2011). First, ALS is more likely to occur with lower premorbid body fat (Gallo *et al.*, 2013; O'Reilly *et al.*, 2013) or better cardiovascular or physical fitness (Turner *et al.*, 2012; Huisman *et al.*, 2013). Second, weight loss is negatively correlated with survival (Desport *et al.*, 1999; Marin *et al.*, 2011; Paganoni *et al.*, 2011). This weight loss is associated with, and likely caused by, intrinsic hypermetabolism (Desport *et al.*, 2001; Bouteloup *et al.*, 2009), and is exacerbated by dysphagia occurring with bulbar involvement. Third, ALS patients develop abnormalities in lipid (Dupuis *et al.*, 2008; Dorst *et al.*, 2011; Lindauer *et al.*, 2013) and glucose (Pradat *et al.*, 2010) metabolisms. Interestingly, these metabolic alterations are largely replicated in transgenic mice expressing mutant SOD1 (Dupuis *et al.*, 2004; Fergani *et al.*, 2007; Palamiuc *et al.*, 2015). Not much is known on the underlying mechanisms of energy metabolism impairment despite the fact that elucidation of such mechanisms would offer therapeutic strategies to treat weight loss pharmacologically. Furthermore, deciphering the mechanisms of energy metabolism impairment could identify disease-modifying interventions as a hypercaloric diet was recently found to increase survival of patients with ALS under gastrostomy (Wills *et al.*, 2014; Dorst *et al.*, 2015).

Most of the studies to date have characterized energy metabolism in patients with ALS in steady state, at one single time point. The dynamic nature of energy metabolism and its homeostatic regulation thus severely limit the interpretation of these studies. Interventions performed during randomized clinical trials often have metabolic effects, and such studies include long term follow-up of patients for many months. These clinical studies thus provide high-quality information useful to understand the metabolic defects of patients with ALS.

Here, we performed a *post hoc* analysis of samples obtained during the clinical trial of pioglitazone (Dupuis *et al.*, 2012) to characterize energy metabolism of ALS patients on a metabolic challenge. Indeed, pioglitazone, like other thiazolinediones (TZDs), has pleiotropic effects on energy metabolism that have been extremely well characterized in both mouse models and human patients. In the periphery, pioglitazone sensitizes to insulin, leading to decreased glycaemia, and decreases circulating levels of liver enzymes (Promrat *et al.*, 2004; Belfort *et al.*, 2006; Sanyal *et al.*, 2010; DeFronzo *et al.*, 2011). In the CNS, pioglitazone inhibits the hypothalamic melanocortin system to increase food intake (Diano *et al.*, 2011; Lu *et al.*, 2011; Ryan *et al.*, 2011; Long *et al.*, 2014). Specifically, pioglitazone decreases activity of the hypothalamic neurons producing proopiomelanocortin (POMC), the precursor of a number of anorexigenic peptides such as α-MSH (melanocyte stimulating hormone) (Diano *et al.*, 2011; Lu *et al.*, 2011; Ryan *et al.*, 2011; Long *et al.*, 2014). In humans, this leads to a robust (3–5 kg) weight gain that was repeatedly

observed in multiple clinical trials (Promrat *et al.*, 2004; Belfort *et al.*, 2006; Sanyal *et al.*, 2010; DeFronzo *et al.*, 2011). Here, we show that patients with ALS display normal peripheral action of pioglitazone, while they lack weight gain. In transgenic mice expressing mutant SOD1, pioglitazone failed to increase food intake. This was associated with prominent involvement of the hypothalamic melanocortin system, also observed in other mouse models of ALS, independent of mutant SOD1 overexpression. Last, we show that the melanocortin defect occurs downstream of the previously documented serotonin loss (Dentel *et al.*, 2013). Altogether, our analysis of the data from the pioglitazone trial disclosed a previously unanticipated defect in patients with ALS that could account for a subset of ALS-related metabolic defects.

Materials and methods

Patients and treatments

All the biological materials from human ALS patients were sampled as part of the GERP-ALS trial (clinicaltrials.gov reference: NCT00690118) (Dupuis *et al.*, 2012). Briefly, patients with possible, probable (clinically or laboratory-supported) or definite ALS according to the revised version of the El Escorial criteria were considered for enrolment into the study. Included patients displayed onset of progressive weakness within 36 months prior to study and had disease duration of > 6 months and < 3 years (inclusive) with disease onset defined as date of first muscle weakness, excluding fasciculation and cramps. They reached a best-sitting slow vital capacity between 50% and 95% of predicted normal. They were capable of thoroughly understanding the information provided and gave written informed consent. All included patients had been treated with 100 mg riluzole daily for at least 3 months prior to inclusion. Detailed exclusion and inclusion criteria have been described earlier (Dupuis *et al.*, 2012). The study protocol was approved by the ethics committee of the University of Ulm and all other participating centres.

The two treatment groups were 100 mg riluzole plus 45 mg pioglitazone (pioglitazone group) and 100 mg riluzole plus placebo (placebo group). Patients were randomly assigned to one of the two treatment groups and both groups were matched for age, gender and site of onset (Dupuis *et al.*, 2012).

Procedures and biochemical analysis of human samples

After inclusion, patients underwent a screening phase and a treatment phase (18 months), with stepwise increase in dosage (Dupuis *et al.*, 2012). Clinical and physical examinations, blood sampling, and drug compliance were recorded at on-site visits (1, 2, 6, 12 and 18 months after baseline visit). Body weight was recorded at on-site visits, except for 3-, 9- and 15-month time points (telephone contacts). There were no differences in results when excluding these three time points. Routine clinical laboratory tests were performed at each on-site visit (baseline and 1, 2, 6, 12 and 18 months after baseline). All tests were carried out according to standard laboratory procedures at each study centres' locally accredited laboratory, which defined the normal reference range for each analyte. The following laboratory tests were performed using standard methods: alanine aminotransferase (ALAT), aspartate aminotransferase (ASAT), fasting blood glucose. Adiponectin measurements were done in the neurochemical laboratory in Ulm (MSD assay).

Animals

Transgenic mice were housed in the animal facility of the medicine faculty of Strasbourg University, with 12 h/12 h light/dark and unrestricted access to food and water. In all experiments, littermates were used for comparison. Transgenic SOD1(G86R) were maintained in their initial FVB/N genetic background according to previous studies (Dentel *et al.*, 2013). Transgenic mice expressing TDP43(A315T) were previously described and were maintained as heterozygous in their initial C57Bl6/J background (Wegorzewska *et al.*, 2009). Heterozygous $Fus^{\Delta NLS/+}$ are knock-in mice expressing FUS protein deleted from its C-terminal nuclear localization signal (NLS) from one copy of the endogenous *Fus* gene. These mice were generated and maintained in C57Bl6/J background. The motor phenotype of these mice will be described elsewhere (Scekic-Zahirovic, submitted for publication). Tph2-YFP mice were purchased from Jackson laboratories (Bar Harbor; strain 014555) and maintained in their initial genetic background. Female Tph2-YFP mice were crossed with male SOD1(G86R) to generate compound transgenic mice.

For biochemical analysis, animals were sacrificed at the ages indicated at 2 pm, and tissues were quickly dissected, frozen in liquid nitrogen, and stored at $-80°C$ until use. For histological analysis, animals were anaesthetized by intraperitoneal injection of ketamine (Imalgène 1000®, Merial; 90 mg/kg body weight) and xylazine (Rompun 2%®, Bayer; 10 mg/kg body weight) at the ages indicated at 2 pm. After perfusion of 4% paraformaldehyde (v/v PFA, Sigma), brains were removed, stored in the same fixative overnight at 4°C and stored in phosphate-buffered saline (PBS) until used. These experiments were authorized by the local ethical committee of Strasbourg University (CREMEAS).

Drugs and treatments

Pioglitazone (Actos®, Takeda) was dissolved in 10% (v/v) dimethyl sulphoxide (DMSO, Fisher Scientific) and a single oral administration was given by gavage at a dose of 40 mg/kg body weight. Fluoxetine (Sigma) was dissolved in 0.9% (w/v) NaCl (Sigma) and administrated intraperitoneally at a dose of 20 mg/kg body weight.

Measurements of food intake

For the pioglitazone experiment, mice were fasted from 9 am to 3 pm, and pioglitazone was administrated at 3 pm. Food was reintroduced 1 h after gavage and food intake was recorded for 24 h.

For short-term fasting experiments, mice were fasted from 8 am to 3 pm (7 h fasting conditions) or from 2 pm to 3 pm (1 h fasting conditions) and food was reintroduced after 7 h or 1 h

of fasting. Food intake was measured 1 h and 24 h after refeeding.

For fluoxetine experiment, mice were fasted from 1 pm to 2 pm, and fluoxetine was injected at 2 pm. Food was reintroduced 30 min after fluoxetine injection and food intake was measured for 1 h. For biochemical analysis, a second injection of fluoxetine was done after 1 h of feeding and mice were sacrificed 30 min later.

Histology

Fixed brains were included in 6% (w/v) agar (Sigma) and sectioned from Bregma 0.02mm to Bregma −2.90 mm into 40 µm coronal sections on a vibratome. Arcuate nucleus was identified according to Paxinos Brain Atlas. POMC immunohistochemistry was performed on half of the selected brain sections. AGRP and green fluorescent protein (GFP) immunohistochemistries were performed each on anatomically matched sections. Immunohistochemistry was performed on floating sections using standard histological techniques. Endogenous peroxidases were inactivated using 3% (v/v) H_2O_2. For POMC immunohistochemistry, permeabilization and saturation of non-specific sites were done with 0.25% (v/v) Triton™ (Sigma) and 50 mg/ml bovine serum albumin (BSA, Sigma). For GFP immunohistochemistry, permeabilization and saturation of non-specific sites were done with 0.5% (v/v) Triton™ (Sigma) and 5% (v/v) horse serum (Gibco, Life Technologies). For AGRP immunohistochemistry, antigen retrieval with citrate buffer was done before permeabilization and saturation of non-specific sites with 0.5% (v/v) Triton™ (Sigma) and 5%(v/v) horse serum (Gibco, Life Technologies). Rabbit anti-POMC primary antibody (Phoenix Peptide; 1:2000), rabbit anti-AgRP primary antibody (Phoenix Peptide; 1:2000) or rabbit anti-GFP primary antibody (Invitrogen, Life Technologies, 1:1000) were incubated overnight at room temperature. Biotinylated donkey anti-Rabbit secondary antibody (Jackson; 1:500) was incubated for 90 min at room temperature. Staining was performed using Vectastain Elite ABC kit (Vector). After revelation with 3,3'-diaminobenzidine (DAB, Sigma; 0.5 mg/ml), sections were mounted and images of all sections were taken.

For quantification, bright-field images of lower brain part for POMC and AgRP stainings or bright-field images of right arcuate nucleus part for GFP staining were acquired with a Nikon DS –Ri1 camera attached to a Nikon microscope (Nikon Eclipse E800) fitted with a Plan Apo 4× lens (N.A. = 0.20, Nikon) and a plan Apo 10× lens (N.A. = 0.45, Nikon), respectively. White balance, gain, exposure, and light settings were kept the same when acquiring all images of a given staining.

Image analysis

An operator blinded to the genotype quantified all experiments. Total numbers of POMC-positive cell bodies in the arcuate nucleus were determined for each animal and normalized per section. Quantification of GFP staining and AGRP staining was processed to binary images using NIH ImageJ as described previously (Grider *et al.*, 2006). Briefly, after changing tiff images to 8-bit images, images were inverted and processed with Feature J plugin for ImageJ (version 1.50d) to select the smallest Hessian values and « smoothing scale » of 1.0. The resulting images were transformed into binary images by thresholding. Threshold was determined on one cut and same threshold was applied to every image. Occupied area for AGRP or GFP staining was measured.

RNA extraction and quantitative reverse transcription-polymerase chain reaction

RNA was extracted from mouse hypothalami using TRIzol® reagent (Life Technologies). After reverse transcription with iScript™ reverse transcription Supermix for RT-qPCR (Bio-Rad), cDNA was obtained from 1 µg of RNA. Messenger RNA levels were obtained by quantitative PCR using Sso Advanced Universal SYBR Green Supermix (Bio-Rad) with corresponding sense and antisense primers. Standard curves were constructed by amplifying serial dilutions of cDNA. Starting quantities of samples were calculated with Bio-Rad software. Messenger RNA levels of genes of interest were normalized to expression levels of the 18S ribosomal, *Tbp* and *Pola2* RNA housekeeping genes using GeNorm (Vandesompele *et al.*, 2002). Primer sequences are shown in Supplementary Table 1.

Serotonin levels

Hypothalamic serotonin levels were measured using high performance liquid chromatography, as previously described (Dentel *et al.*, 2013).

Statistical analysis

For statistical analyses in ALS patients, group comparisons were performed using mixed effects regression model analysis by the Institute of Epidemiology and Medical Biometrics at the University of Ulm using the statistical software package SAS Version 9.2 under Windows.

For animal experiments, comparison of two groups was performed using unpaired Student's *t*-test, except for experiments with pioglitazone in which paired *t*-test was used. Comparison of three or four groups was performed using one-way ANOVA and Tukey *post hoc* test. Statistics in animal experiments were performed using Prism version 6.0.

All results from analysis were regarded as hypothesis generating only. All statistical tests were carried out two-sided at a significance level of 5%.

Results

Normal peripheral response to pioglitazone in patients with ALS

We took advantage of data collected during the pioglitazone GERP-ALS trial to investigate energy metabolism in ALS patients in response to pioglitazone.

In this clinical trial, 219 patients with ALS were enrolled and randomly allocated to either placebo ($n = 110$; bulbar: $n = 33$, spinal: $n = 77$), or pioglitazone ($n = 109$;

bulbar: $n = 32$, spinal: $n = 77$) treatment after stratification based on site of onset (bulbar or spinal) (Dupuis *et al.*, 2012).

The metabolic effects of TZDs, including pioglitazone are well understood in models and their effects are largely described in patients (Fig. 1A and Supplementary Table 2). Pioglitazone treatment is known to increase levels of adiponectin, an adipose-derived hormone through direct transcriptional activation of the adiponectin gene in adipocytes (Maeda *et al.*, 2001). Consistently, pioglitazone treatment increased the levels of circulating adiponectin 4-fold in patients with ALS after 6 months of treatment, and this was maintained after 12 months of treatment (Fig. 1B). Pioglitazone decreases glycaemia through hepatic and skeletal muscle PPARγ (encoded by *PPARG*). In patients with ALS, pioglitazone decreased glycaemia (Fig. 1C), although this effect was milder than observed in other populations, including non-diabetic patients (Belfort *et al.*, 2006; Sanyal *et al.*, 2010; DeFronzo *et al.*, 2011). Consistent with a direct action on liver, pioglitazone decreased levels of ASAT and more robustly levels of ALAT (Fig. 1D and E). In all, pioglitazone displayed the expected metabolic effects on adipocytic, muscular, and hepatic biomarkers, and was likely able to activate PPARγ in these tissues.

Pioglitazone does not lead to weight gain in patients with ALS

TZDs are also known to act in hypothalamic melanocortin neurons to promote feeding (Diano *et al.*, 2011; Long *et al.*, 2014), and this activation of PPARγ in melanocortin neurons is responsible for the robust weight gain associated with TZD treatment (Lu *et al.*, 2011; Ryan *et al.*, 2011; Long *et al.*, 2014). Thus, the evolution of body weight upon pioglitazone treatment represents a reliable proximal marker of PPARγ action in hypothalamic melanocortin neurons. In ALS patients, pioglitazone had no effect on weight loss (Fig. 2A), or body mass index (BMI) (Fig. 2B and Supplementary Table 2). Increased weight in response to pioglitazone is due to increased food intake, and a subset of ALS patients experience dysphagia. However, pioglitazone had also no effect on BMI and weight loss when considering spinal onset patients (Fig. 2C and D), or patients with preserved everyday life during at least 6 months (results from EuroQoL EQ-5D questionnaire, Fig. 2E and F). Lastly, patients with preserved bulbar function during at least 6 months after inclusion [as assessed using ALS functional rating scale-revised (FRS-R) bulbar subscale] did not lose weight, yet pioglitazone had no effect on their BMI (Fig. 2G and H). Importantly, there were no differences among groups for intake of drugs affecting body weight and food intake, in particular anti-epileptics, anti-diabetics, anti-psychotics or selective serotonin reuptake inhibitors (Supplementary Table 4). Thus, pioglitazone did not increase weight in ALS patients, and this was not related with dysphagia nor confounded by intake of other drugs.

Pioglitazone does not increase food intake in mutant SOD1 mice

We hypothesized that the lack of weight gain for patients with ALS under pioglitazone was due to defects in stimulating food intake. To test this hypothesis, we used transgenic mice expressing mutant SOD1(G86R) (SOD1m mice) as a model of ALS and examined food intake in response to pioglitazone. In rodents, pioglitazone has various effects on food intake depending on genetic background, dose, route and associated diet (Diano *et al.*, 2011; Ryan *et al.*, 2011; Long *et al.*, 2014). Using a protocol (Fig. 3A) adapted from Ryan *et al.* (2011), we observed that a single oral dose of pioglitazone (40 mg/kg) increased food intake by 10–15% in wild-type FVB/N mice (Fig. 3B and C). However, food intake was not increased in littermate SOD1m mice either 1 month before motor symptoms (Fig. 3 B) or at disease onset (Fig. 3C). Thus, pioglitazone was not able to increase food intake in SOD1m mice.

Defects in melanocortin neurons in mutant SOD1 mice

Hypothalamic melanocortin neurons constitute the primary target of TZDs to promote food intake (Diano *et al.*, 2011; Long *et al.*, 2014). The melanocortin system mainly comprises two antagonistic neuronal types located in the arcuate nucleus: POMC neurons, which secrete the anorexigenic peptide alpha melanocyte-stimulating hormone (αMSH), and AGRP neurons, which promote food intake, mostly through production of AGRP, an endogenous αMSH antagonist. *Pomc* mRNA levels were 2-fold lower in SOD1m mice at 75 days of age (Fig. 4A) or at onset (Fig. 4B), whereas *Agrp* mRNA levels were higher in non-symptomatic mice, but not at onset (Fig. 4A and B). This involvement of the melanocortin system was relatively selective, as we did not observe expression changes in multiple neuropeptides involved in energy homeostasis, in particular CART (*Cartpt*), NPY, CRF (*Crh*), AVP, TRH, galanin (GAL), somatostatin (SST) and BDNF. Importantly however, we observed decreased expression of MCH (*Pmch*) at both ages, and orexin, at onset (Fig. 4C). Consistent with decreased POMC expression, we observed ~30% fewer POMC-positive neurons in the arcuate nucleus of SOD1m mice as compared with their wild-type littermates at 75 days of age and almost 50% fewer at onset (Fig. 5). Furthermore, we observed increased density of AGRP-positive fibres in arcuate nucleus as well as in projection regions present on the same sections such as dorso-medial hypothalamus and lateral hypothalamus (Fig. 6). In all, the melanocortin system appears shifted towards decreased melanocortin tone in SOD1m mice.

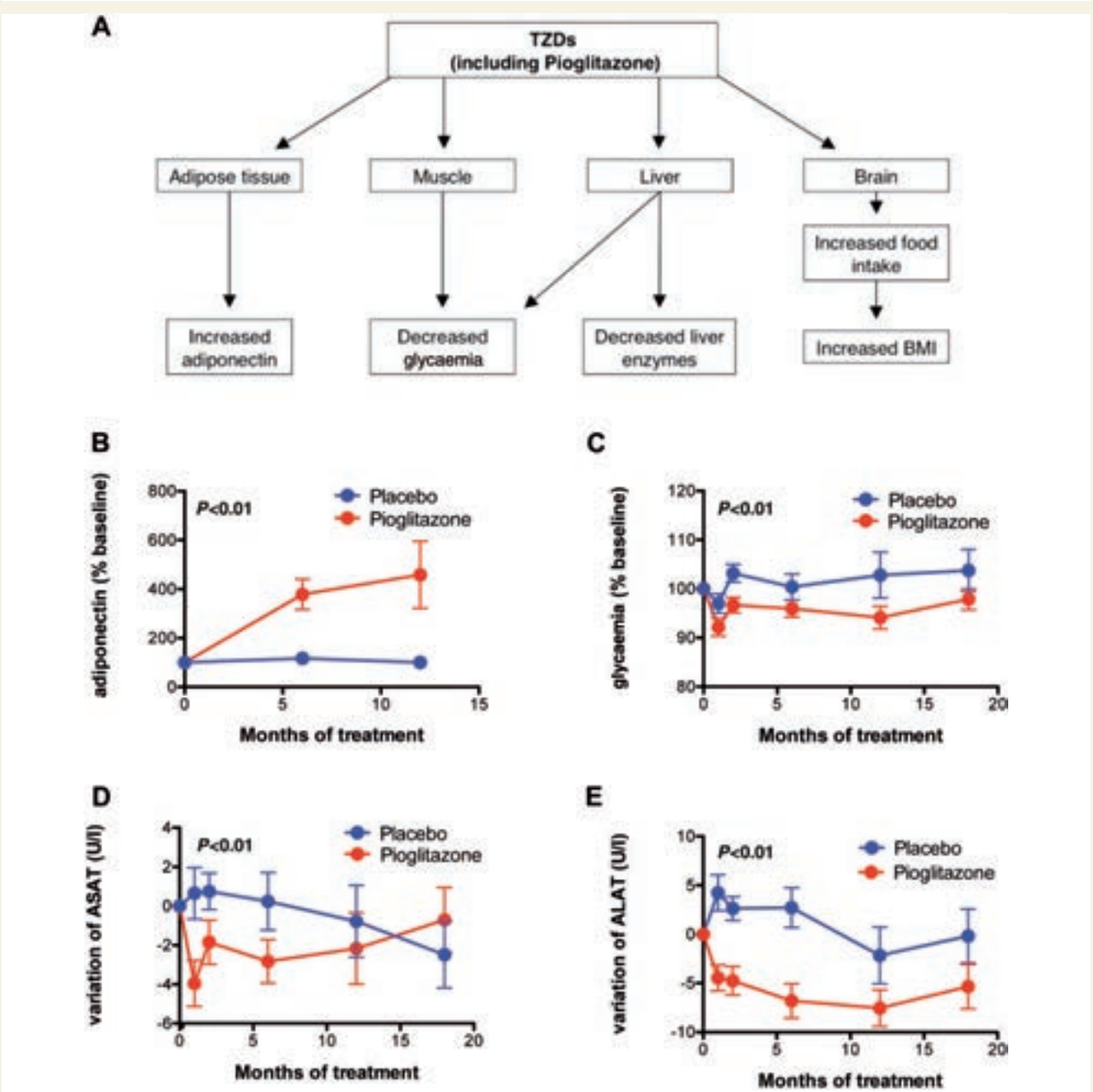

Figure 1 Effects of pioglitazone on peripheral biomarkers in ALS patients. (**A**) Summary of metabolic effects of pioglitazone (and TZDs) in humans. (**B**–**E**) Changes in plasma adiponectin (% from the baseline, **B**), glycaemia (% from the baseline, **C**), circulating aspartate amino-transferase (ASAT, changes in U/l from the baseline, **D**), and alanine amino-transferase (ALAT, changes in U/l from the baseline, **E**). Pioglitazone treated patients are significantly different from placebo treated patients for these items as assessed using a mixed effects regression model analysis. Data are presented as mean and standard error (SE).

Multiple ALS mouse models display functional and molecular alterations in hypothalamic melanocortin system

We then asked whether the observed melanocortin defects translated into functional abnormalities. Indeed, the combination of decreased POMC with increased AgRP is usually found in situations of promotion of food intake, such as during fasting or in the case of leptin deficiency (Mizuno *et al.*, 1998, 1999; Ziotopoulou *et al.*, 2000), and compromised melanocortin system is likely to affect food intake behaviour, in particular during refeeding (Perez-Tilve *et al.*, 2010). Thus, we measured food intake after short-term fasting in SOD1m mice. Consistent with decreased POMC levels, 1 h food intake of SOD1m mice was 2-fold higher than wild-type littermates after 7 h (Fig. 7A) or 1 h (Fig. 7B)

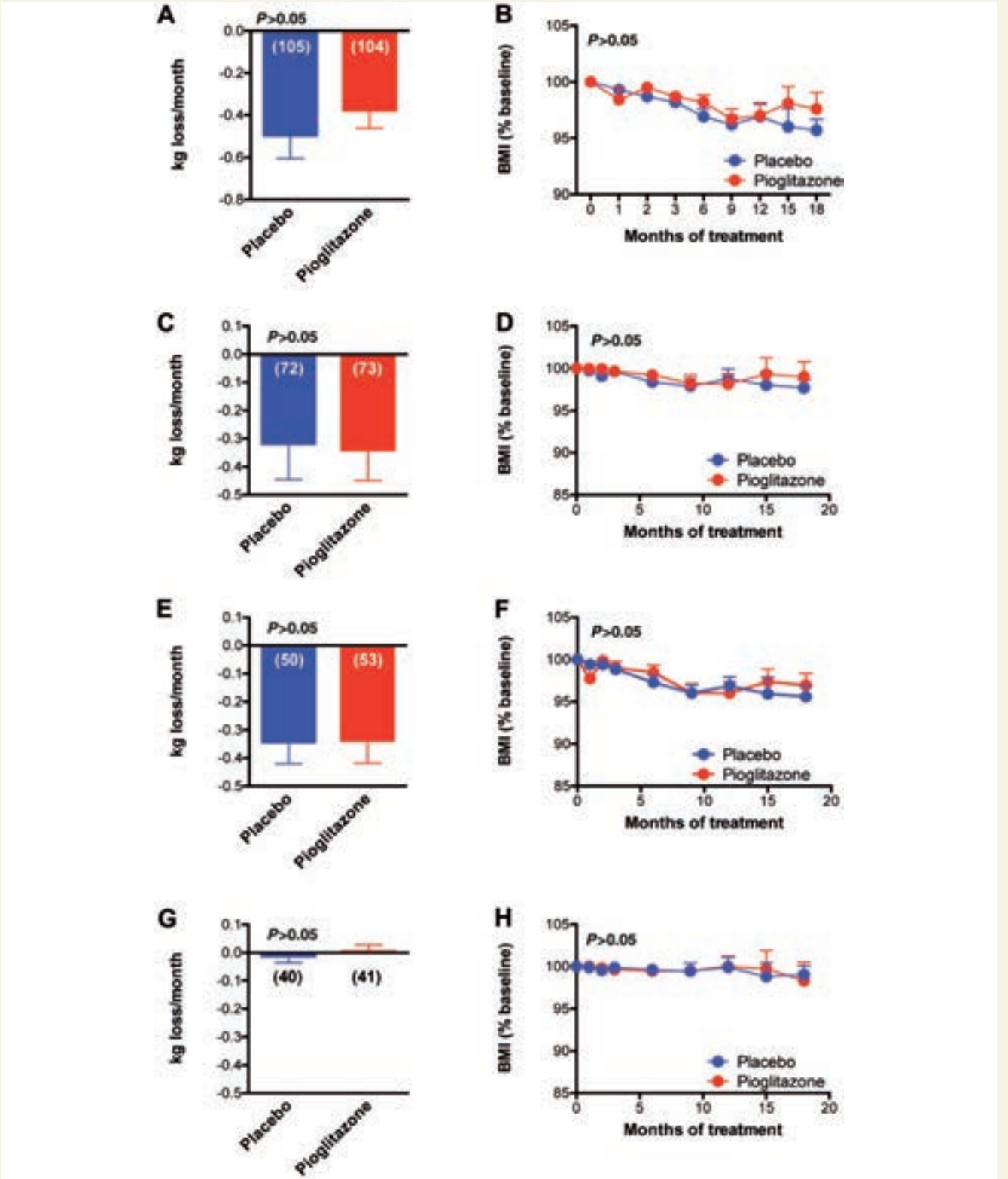

Figure 2 Effects of pioglitazone on weight loss in ALS patients. Weight loss (kg loss per month, **A**, **C**, **E** and **G**) and changes in BMI from the baseline (**B**, **D**, **F** and **H**) in the whole ALS population (**A** and **B**), spinal onset patients (**C** and **D**), in patients with relatively preserved quality of life (**E** and **F**) and in patients with preserved bulbar function (**G** and **H**). To select the patients with preserved quality of life, we used the results from the EuroQoL questionnaire to identify patients that had no or only few problems with their everyday life. Selected patients answered that they had either no or few problems in their everyday life during at least 6 months after their allocation to a group. To select the patients with preserved bulbar function, we used the results from ALS-FRS-R bulbar subscale and selected patients with a score equal or superior to 10 (maximum: 12) 6 months after inclusion. No significant difference is noted for these items. Data are presented as mean and SE.

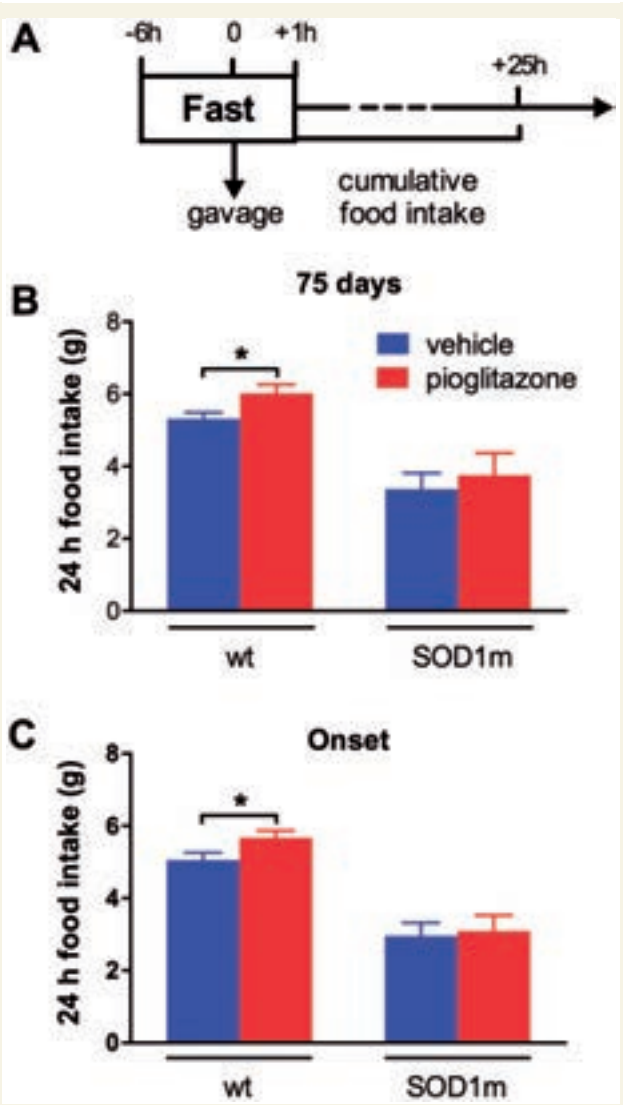

Figure 3 No effect of piogliotazone on SOD1m mice food intake. (**A**) Experimental scheme: pioglitazone was provided *per os* after 6 h of fasting. Food was reintroduced 1 h after gavage, and food intake recorded for the next 24 h. (**B** and **C**) Food intake after pioglitazone treatment in SOD1(G86R) mice (SOD1m) and control littermates (wt) at 75 days of age ($n = 12$, **B**) and symptom onset ($n = 13$, **C**), either treated with vehicle (blue) or pioglitazone 40 mg/kg body weight (red).$^{*}P < 0.05$, Paired Student's *t*-test for the drug. Data are presented as mean and SE.

of fasting. Mutations in *SOD1* only account for 20% of familial ALS cases, and alterations in hypothalamic melanocortin pathways could be SOD1-specific. However, *Pomc* mRNA levels were decreased in transgenic mice expressing A315T mutant *Tardbp* (Wegorzewska *et al.*, 2009) (Fig. 7C), and these mice also displayed transient hyperphagia in response to fasting (Fig. 7D). Last, *Pomc* mRNA levels tended to be lower in 10-month-old knock-in mice expressing a truncated FUS protein retained in the cytoplasm ($Fus^{\Delta NLS/+}$ mice) (Fig. 7E) (Scekic-Zahirovic, submitted for publication), and $Fus^{\Delta NLS/+}$ mice displayed increased food intake after short-term fasting as compared with their littermates (Fig. 7F). Thus, abnormal food intake behaviour and defects in the melanocortin system are hallmarks of ALS mouse models.

Involvement of serotonin loss in melanocortin defects associated with ALS

We then sought to understand the mechanisms underlying melanocortin defects in ALS. POMC neurons are affected by multiple stressors that could ultimately underlie the observed defects. We did not observe changes in expression of a series of genes related with oxidative or endoplasmic reticulum stress (e.g. gp47, splicing of *Xbp1* mRNA), peroxisome biogenesis [*Gpx1*, catalase (*Cat*)] or mitochondrial function (*Mfn2*; not shown) indirectly suggesting that neither overt oxidative stress, nor endoplasmic reticulum stress, nor defective peroxisomal biogenesis, nor mitochondrial abnormalities might account for decreased POMC neuronal counts. We hypothesized that the previously observed serotonin neuron degeneration (Turner *et al.*, 2005; Dentel *et al.*, 2013) could contribute to the observed melanocortin defects. Indeed, serotonin is known to promote POMC expression in arcuate nucleus through the 5-HT_{2C} receptor (encoded by *HTR2C*) (Heisler *et al.*, 2006; Lam *et al.*, 2008). Interestingly, serotonin levels tended to decrease at onset in the hypothalamus of SOD1m mice (Fig. 8A). To determine whether loss of serotonin axons occurred in the arcuate nucleus, we crossed SOD1m mice with Tph2-YFP mice, expressing yellow fluorescent protein (YFP) under the control of the *Tph2* promoter targeting expression in central serotonin neurons (Zhao *et al.*, 2011). We observed a sharp and profound decrease in the density of YFP-positive fibres in the arcuate nucleus of SOD1m mice, as compared with their littermates (Fig. 8B). Hypothalamic 5-HT_{2C} expression was increased suggesting that the hypothalamus sought to compensate for loss of serotonergic innervation (Fig. 8C). To probe for serotonergic involvement in defects of the melanocortin system, we used fluoxetine, a selective serotonin reuptake inhibitor to rescue serotonin signalling, using previously published doses and protocols (Kaur and Kulkarni, 2002; Liou *et al.*, 2012). Interestingly fluoxetine pretreatment completely abrogated the increased food intake in response to short-term fasting (Fig. 8D) and increased *Pomc* mRNA levels back to normal in SOD1m mice (Fig. 8E). Fluoxetine had no effect on *Agrp* upregulation (Fig. 8E). Thus, loss of serotonin innervation is contributing to the melanocortin defects observed in SOD1m mice.

Discussion

In this combined mouse and human study, we showed that ALS is associated with defects in the melanocortin system,

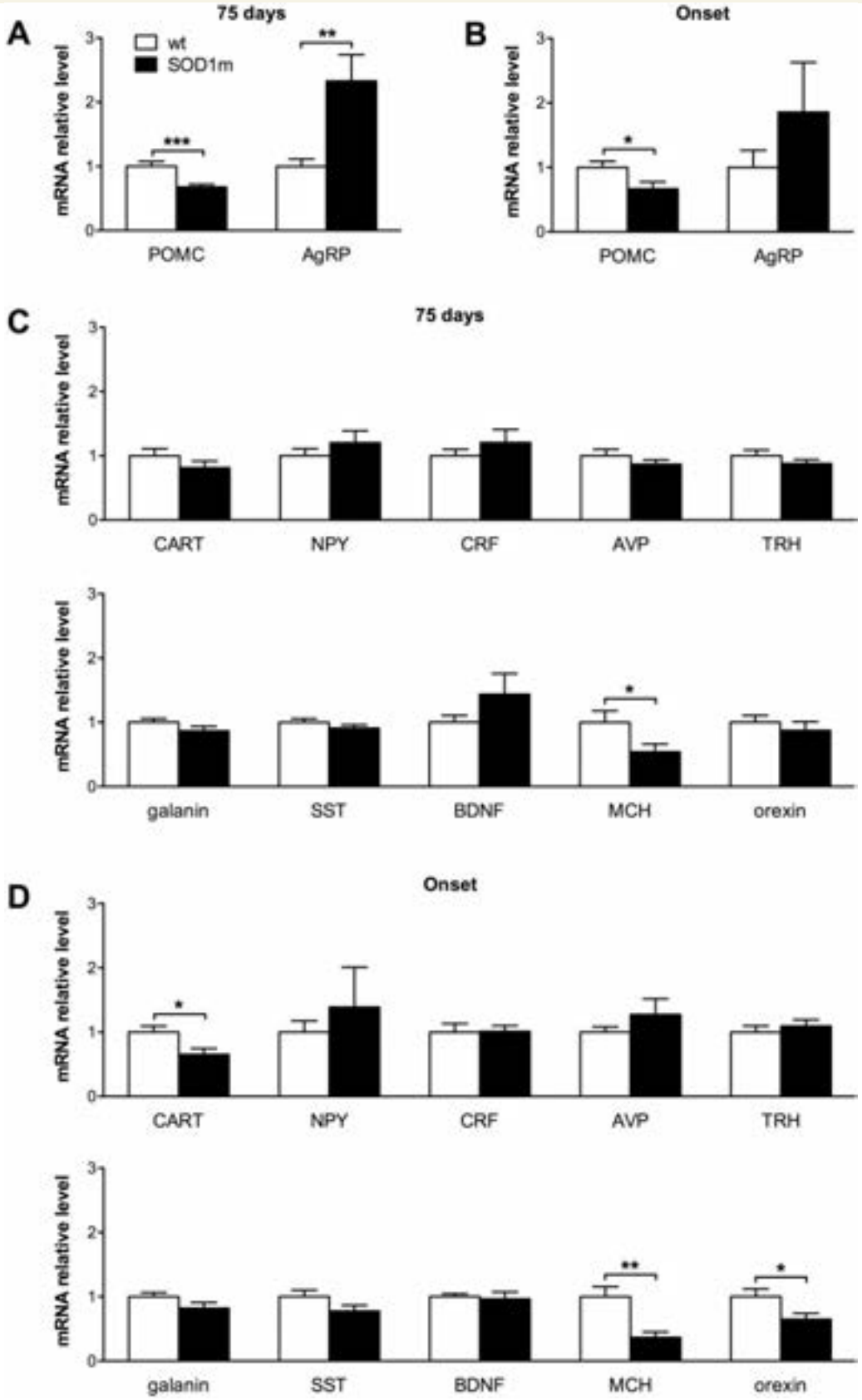

Figure 4 Altered melanocortin-related gene expression in SOD1m mice. (**A** and **B**) Messenger RNA levels of *Pomc* and *Agrp* in the hypothalamus of SOD1(G86R) mice (black, SOD1m) and control littermates (white, wt) at 75 days of age ($n = 15$, **A**) and symptom onset ($n = 11$, **B**). $^{*}P < 0.05$. $^{**}P < 0.005$. $^{***}P < 0.0005$, Student's *t*-test. Data are presented as mean and SE. (**C** and **D**) Messenger RNA levels of hypothalamic neuropeptides in the hypothalamus of SOD1(G86R) mice (black columns, SOD1m) and control littermates (white columns, wt) at 75 days of age ($n = 15$, **C**) and symptom onset ($n = 11$, **D**). $^{*}P < 0.05$; $^{**}P < 0.005$, Student's *t*-test. Data are presented as mean and SE.

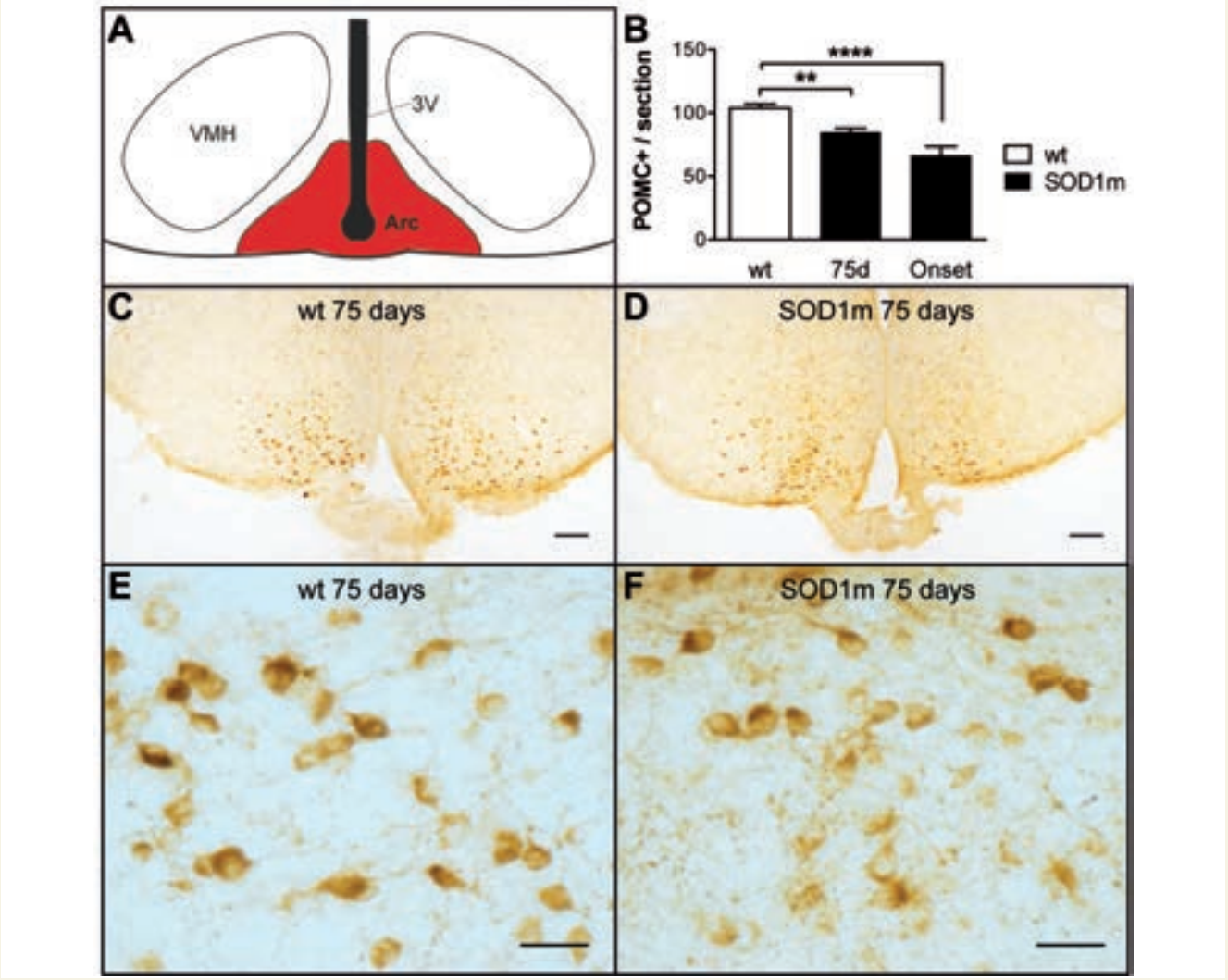

Figure 5 Decreased POMC-positive neurons in SOD1m mice. (**A** and **B**) Quantification of POMC neurons in the arcuate nucleus. The whole region was sectioned and half of these sections were stained for POMC immunohistochemistry after identification of arcuate nucleus according to Paxinos Brain Atlas (scheme of identified regions, in red, **A**). Total numbers of POMC-positive cell bodies in the arcuate nucleus were determined in SOD1m mice at 75 days of age ($n = 8$, **B–F**) and at symptom onset ($n = 7$, **B**) as compared with their wild-type littermates. $^{**}P < 0.005$, $^{****}P < 0.0001$, one-way ANOVA followed by Tukey *post hoc* test. Data are presented as mean and SE. (**C–F**) Representative images are shown for SOD1(G86R) mice (**D** and **F**) and control littermates (**C** and **E**) at 75 days of age at two magnifications. Scale bar = 200 μm (**C** and **D**); 20 μm (**E** and **F**).

the major hypothalamic circuit controlling food intake and energy expenditure. Pioglitazone did not increase weight in ALS patients, thus providing indirect evidence of altered hypothalamic melanocortin pathway. Pathological and functional deficits of melanocortin system were found in ALS mouse models directly demonstrating these defects. These findings further extend the spectrum of defects in ALS and provide a mechanistic explanation for a subset of metabolic signs observed in these patients. Our study also has important implications for the design of therapies to target weight loss in this disease.

We first observed that pioglitazone did not increase body weight or slow down weight loss in patients with ALS. This was a surprising observation as progressive weight gain has been repeatedly observed in all clinical trials of pioglitazone in multiple non-neurological diseases (Promrat *et al.*, 2004; Belfort *et al.*, 2006; Sanyal *et al.*, 2010; DeFronzo *et al.*, 2011). Despite this lack of weight gain, ALS patients under pioglitazone displayed all other biomarkers of efficacy, including decreased glycaemia, decreased circulating liver enzymes or increased adiponectin, thus ruling out that patients with ALS simply did not respond to the drug. Interestingly, a series of recent studies dissected out how TZDs lead to weight gain through activation of PPARγ in hypothalamic POMC neurons leading to increased food intake (Diano *et al.*, 2011; Lu *et al.*, 2011; Ryan *et al.*, 2011; Long *et al.*, 2014). Consistent with the notion that pioglitazone hypothalamic response was blunted in

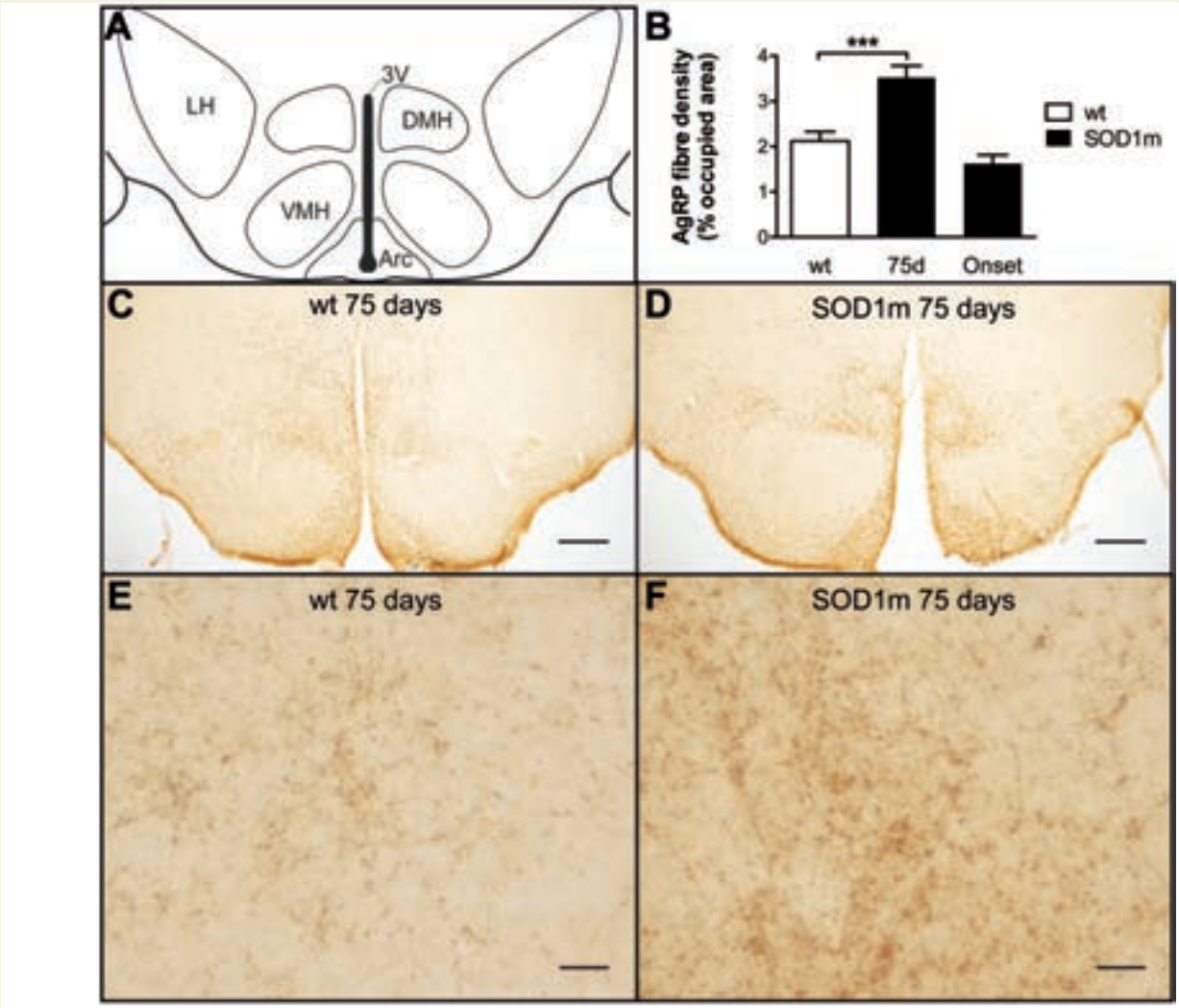

Figure 6 Defect in AGRP neurons in SOD1m mice. (**A** and **B**) Quantification of AGRP immunoreactive neurites in the hypothalamus. For each animal, one section (Bregma −1.58 mm) was identified according to Paxinos Brain Atlas (**A**, scheme of identified regions) and stained for AGRP immunohistochemistry. AGRP fibre density was determined in SOD1m mice at 75 days of age ($n = 7$, **B** and **F**) and at symptom onset ($n = 4$, **B**) as compared with their wild-type littermates. $^{***}P < 0.001$, one-way ANOVA followed by Tukey *post hoc* test. Data are presented as mean and SE. (**C–F**) Representative images are shown for SOD1(G86R) mice (**D** and **F**) and control littermates (**C** and **E**) at 75 days of age at two magnifications. Scale bar = 200 μm (**C** and **D**), 20 μm (**E** and **F**).

ALS patients, pioglitazone was not able to promote food intake in SOD1m mice. Indeed, the melanocortin system is dramatically affected in these mice, with decreased POMC expression and loss of POMC positive neurons; similar alterations were observed in TDP-43- and FUS-based mouse models pointing out that such defects are a general feature in ALS. As pioglitazone decreases the activity of POMC neurons thus increasing food intake (Diano *et al.*, 2011), we propose that the already decreased melanocortin tone in ALS prevents the silencing of POMC neurons by pioglitazone. Consistent with this, SOD1 mice displayed hyperphagia in response to short-term fasting, an orexigenic stimulus that also leads to decreased POMC neuronal activity (Perez-Tilve *et al.*, 2010; Diano *et al.*, 2011). Thus, our results point to a general decrease in melanocortin tone in ALS, leading to both a lack of response to TZDs, and abnormal food intake behaviour in response to fasting.

What is the contribution of impaired melanocortin system to the metabolic phenotypes associated with ALS? The melanocortin system exerts multiple actions on energy metabolism, either dependent on or independent of food intake. First, an expected consequence of decreased melanocortin tone is increased energy intake, especially in response to an orexigenic stimulus such as food deprivation. This is indeed what has been observed in multiple transgenic mouse models of ALS, suggesting that the defect in the melanocortin system translates into a functional deficit. Furthermore, consistent with the observed melanocortin defect, we previously observed slightly increased cumulative food intake in SOD1m mice (Dupuis *et al.*, 2004).

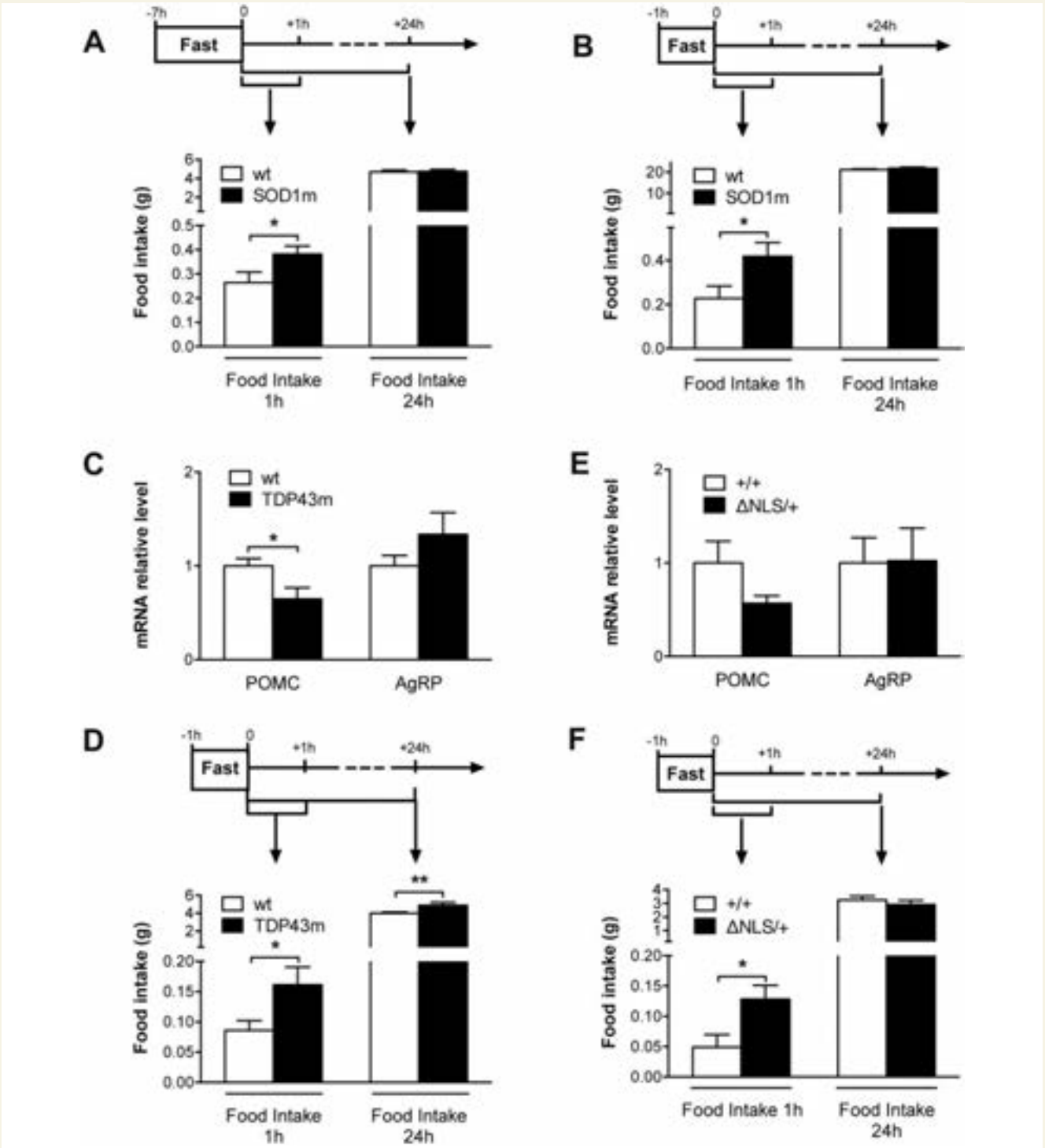

Figure 7 Multiple ALS mouse models display functional and molecular alterations in hypothalamic melanocortin system. (**A** and **B**) Food intake was measured for 1 h, after either 7 h (**A**) or 1 h (**B**) of fasting in SOD1(G86R) mice (black columns, SOD1m) and control littermates (white columns, wt) at 75 days of age ($n = 10$ and $n = 14$, respectively, for **A** and **B**). $^{*}P < 0.05$, Student's *t*-test. Data are presented as mean and SE. (**C**) Messenger RNA levels of *Pomc* and *Agrp* in the hypothalamus of transgenic mice expressing A315T TDP-43 mutation (black columns, TDP43m) and control littermates (white columns, wt) at non-symptomatic stage ($n = 6$). Unpaired *t*-test. $^{*}P < 0.05$. (**D**) Food intake was measured 1 h after refeeding in TDP43m mice ($n = 8$). $^{*}P < 0.05$, $^{**}P < 0.01$, Multiple *t*-test. Data are presented as mean and SE. (**E**) Messenger RNA levels of *Pomc* and *Agrp* in the hypothalamus of transgenic mice *Fus* ΔNLS/+ knock-in mice (black columns, ΔNLS/+) and control littermates (white columns, +/+) at 10 months of age ($n = 4$). Data are presented as mean and SE. (**F**) Food intake was measured 1 h after refeeding in ΔNLS/+ mice ($n = 10$) at 10 months of age. $^{*}P < 0.05$, Student's *t*-test. Data are presented as mean and SE.

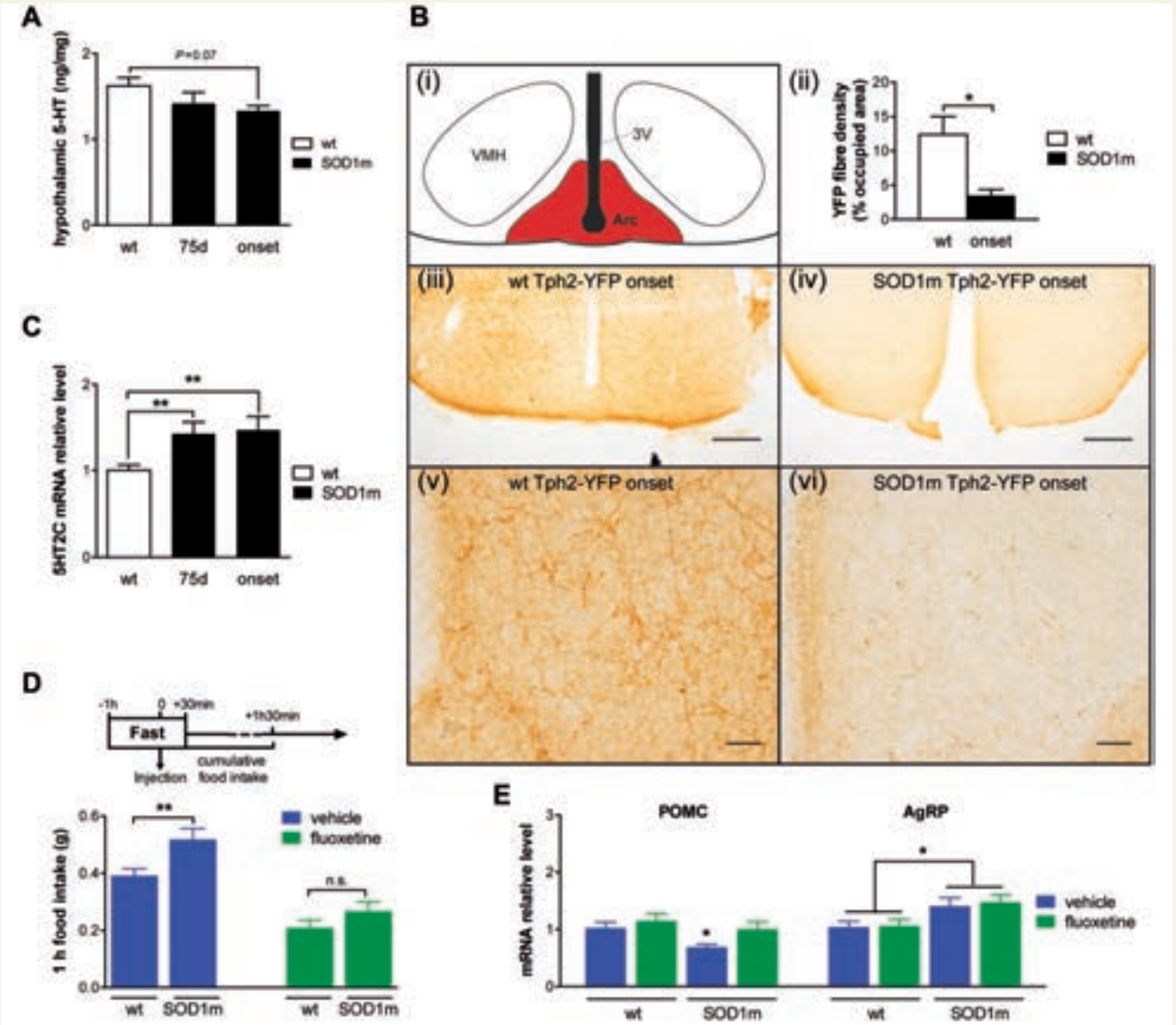

Figure 8 Involvement of serotonin loss in melanocortin defects of mutant SOD1 mice. (**A**) Serotonin levels in the hypothalamus of SOD1(G86R) mice (black columns, SOD1m) and control littermates (white columns, wt) ($n = 5$ at 75 days and $n = 5$ at onset). One-way ANOVA followed by Tukey *post hoc* test. Data are presented as mean and SE. (**B**) Serotonergic innervation in the arcuate nucleus. GFP immunohistochemistry was performed on Tph2-YFP mice on arcuate nucleus cuts after identification on Paxinos Brain Atlas (**i**, scheme of identified regions, in red, in the upper left column). Representative images are shown for SOD1(G86R) Tph2-YFP mice and control littermates at onset at two magnifications. Scale bar = 200 μm (**iii**, **iv**), 20 μm (**v** and **vi**). Serotonergic fibre densities in the arcuate nucleus were quantified by a blind observer as described previously (Grider *et al.*, 2006) in SOD1m mice at symptom onset (**ii**–**vi**, $n = 4$) as compared with their wild-type littermates. $^{*}P < 0.05$, Student's *t*-test. Data are presented as mean and SE. (**C**) Messenger RNA levels of *Htr2c* (5-HT_{2C} receptor) in the hypothalamus of SOD1(G86R) mice (black, SOD1m) at 75 days of age and onset and in control littermates (white, wt) ($n = 8$). $^{**}P < 0.01$, one-way ANOVA. Data are presented as mean and SE. (**D**) Food intake was measured 1 h after refeeding in SOD1(G86R) mice (SOD1m) at 80 days of age and control littermates (wt) after fluoxetine 20 mg/kg body weight (red) or vehicle (blue) injection ($n = 38$). $^{**}P < 0.005$, Multiple *t*-test. Data are presented as mean and SE. (**E**) Messenger RNA levels of *Pomc* and *Agrp* in the hypothalamus of SOD1(G86R) mice (SOD1m) and control littermates (wt) at 85 days of age after fluoxetine 20 mg/kg body weight (red) or vehicle (blue) injection ($n = 20$). $^{*}P < 0.05$, one-way ANOVA. Data are presented as mean and SE.

The situation in ALS patients is less clear with respect to energy intake due to a relative lack of studies reporting dietary intake accurately and to confounding effects of dysphagia in advanced ALS patients. However, two case-control studies reported that increased dietary fat intake was associated with ALS (Nelson *et al.*, 2000; Huisman *et al.*, 2015). Moreover, Huisman *et al.* (2015) and collaborators observed that presymptomatic daily energy intake was increased in ALS patients as compared with controls, and this would be consistent with both melanocortin

impairment and lack of weight gain under pioglitazone. Second, the melanocortin defect could be responsible for alterations in peripheral metabolic pathways. Indeed, the melanocortin system regulates peripheral lipid metabolism in rodents, by activating cholesterol reuptake by the liver (Perez-Tilve *et al.*, 2010) and reduces hepatic lipogenesis (Leckstrom *et al.*, 2011) independently of food intake. In the same line, the melanocortin system is controlling glucose metabolism and insulin response (Obici *et al.*, 2001). Interestingly, ALS patients have been reported to display increased circulating cholesterol levels (Dupuis *et al.*, 2008), and glucose intolerance (Pradat *et al.*, 2010). Third, the melanocortin defect could impair regulation of the autonomic nervous system (Sohn *et al.*, 2013), and autonomic abnormalities have sometimes been found in ALS patients (Baltadzhieva *et al.*, 2005). The relationships between these different phenotypes and melanocortin defects are unclear and will have to be clarified in further studies. Importantly, the observed melanocortin defect is unable to explain the weight loss associated with ALS, as, on the contrary, the increased orexigenic drive triggered by POMC deficiency likely compensates for weight loss by increasing food intake. Other mechanisms, either peripheral or central, have still to be identified to explain weight loss.

What causes the melanocortin defect in ALS? A first obvious potential mechanism is energy deficit. Indeed, SOD1m mice display weight loss due to hypermetabolism, leading to decreased fat mass. These mice also display decreased circulating insulin and leptin levels (Dupuis *et al.*, 2004). Ablation of leptin in *ob/ob* mice or fasting is indeed sufficient to cause decreased *Pomc* mRNA (Mizuno *et al.*, 1998, 1999; Ziotopoulou *et al.*, 2000). However, leptin levels are only decreased by 30% in 75-day-old mice (Dupuis *et al.*, 2004), an age at which we already observe strong *Pomc* mRNA decreases. We and others had previously observed serotonin loss in ALS (Turner *et al.*, 2005; Dentel *et al.*, 2013), and we hypothesized that this contributed to melanocortin impairment in SOD1m mice. Indeed, serotonin is a major activator of POMC neurons through the 5-HT_{2C} receptor, and this occurs through direct electrical stimulation (Heisler *et al.*, 2002) but also trough transcriptional activation (Zhou *et al.*, 2007; Lam *et al.*, 2008; Xu *et al.*, 2008). Consistently, loss of 5-HT_{2C} receptor leads to decreased *Pomc* mRNA in the hypothalamus (Wang and Chehab, 2006). Our observation of restoration of *Pomc* mRNA levels, as well as reversal of transient hyperphagia in SOD1m mice by fluoxetine argues for serotonin loss being a primary cause of melanocortin defect. This, however, does not exclude that direct modulation of electrical activity by either decreased leptin or other cues, either extrinsic or intrinsic, further exacerbate the observed defect. Brain serotonin system is itself affected by organismal energy status (Dwarkasing *et al.*, 2015; Zemdegs *et al.*, 2015) and our data do not exclude that defects in serotonin levels found in ALS patients and models is caused, or contributed by, weight loss and hypermetabolism. Consistent with this notion, decreasing leptin, whose major action is on the melanocortin system, was able to revert partial weight loss and increased energy expenditure in SOD1m mice (Lim *et al.*, 2014), suggesting that the melanocortin system can be further inhibited by leptin ablation.

What are the consequences of our current findings in ALS? There are at least three consequences of our finding for ALS research. First, melanocortin impairment seems to be a general event occuring in sporadic ALS patients, as well as in animal models caused by disparate mutations leading to ALS. Interestingly, a series of recent studies demonstrated the occurence of similar hypothalamic abnormalities in FTD (Piguet *et al.*, 2011; Ahmed *et al.*, 2014*a*, *b*, 2015), and in particular, increased AGRP (Ahmed *et al.*, 2015). Thus, melanocortin impairment appears associated with overall ALS/FTD continuum. It remains to be determined how melanocortin impairment relates with motor neuron degeneration in ALS. Second, this study reinforces the notion of systemic involvement in ALS. That melanocortin impairment appears downstream of serotonin loss, also brings about the notion that circuitry dysfunction might contribute to aspects of ALS phenotype. How these serotonin and melanocortin defects might be related to the spreading of TDP-43 aggregates (Brettschneider *et al.*, 2013) remains to be resolved. Second, these results have consequences for the design of pharmacological strategies to combat weight loss in ALS. Weight loss in ALS is likely to be multi-factorial, with primary causes such as hypermetabolism, and bulbar involvement, and could be exacerbated secondary to other symptoms such as deficit in upper limbs or depression. Treating weight loss could identify disease-modifying interventions as a hypercaloric diet was recently found to increase survival of ALS patients under gastrostomy (Wills *et al.*, 2014; Dorst *et al.*, 2015). Many drugs that could be used to prevent weight loss, including atypical antipsychotics (e.g. olanzapine) inhibit POMC neurons (Kirk *et al.*, 2009; Weston-Green *et al.*, 2012; Lian *et al.*, 2014). Drugs targeting the cannabinoid system increase body weight by increasing beta-endorphin release from POMC neurons (Koch *et al.*, 2015). As beta-endorphin is derived from POMC, which is decreased in ALS mice, it appears likely that cannabinoids might not be able to promote food intake through this mechanism in ALS. Thus, our current study provides a note of caution for the use of these drugs to counteract weight loss in the specific context of ALS patients, and suggest that disease progression might impair responsiveness of ALS patients to classical drugs leading to weight gain. A number of neural pathways controlling energy homeostasis have not yet been studied in the context of ALS and could be potential targets for treating weight loss (Morton *et al.*, 2014). First, pathways involved in the emergency response to glucose deprivation (glucopaenia) such as NPY might be useful, although the precise neurochemical pathways still need to be elucidated. Second, drugs affecting food reward might be of interest to improve the attractability of food during the disease. Last, the existence of emergency neuronal circuits involved in stress-

induced anorexia was recently elucidated. Inhibiting these pathways in ALS might also be a possible target for treating weight loss (Morton *et al.*, 2014). Alternatively, and besides pharmacological treatments, increasing caloric density of the diet is likely an efficient strategy to counteract weight loss (Wills *et al.*, 2014; Dorst *et al.*, 2015), although current results do not allow us to determine whether lipid enriched or carbohydrate enriched would be more efficient.

In all, our *post hoc* analysis of the pioglitazone trial revealed that the melanocortin system is profoundly altered in ALS, and that this might be important for understanding and preventing impairment of energy metabolism in ALS patients.

Acknowledgements

We acknowledge the technical help of Marie Jo Ruivo, Annie Picchinenna, Coraline Kostal, Marc Antoine Goy and Paul Rochet.

Funding

This work was supported by Association de recherche sur la SLA (ARSLA) and Fondation Thierry Latran (SpastALS, to LD). Work in our laboratories is supported by ALS Association Investigator Initiated Award (grants 2235, 3209 and 8075; to L.D.); the Frick Foundation (award 2013 to L.D.); Association Française contre les Myopathies (grant #18280; to L.D.); Virtual Helmholtz Institute "RNA dysmetabolism in ALS and FTD VI-510" (WP2, to L.D., A.W., A.C.L. and A.H.); Fondation « recherche sur le cerveau » (call 2015, to L.D.). Research leading to these results has received funding from the European Community's Health Seventh Framework Programme (FP7/2007-2013; EuroMOTOR grant agreement n° 259867).

Supplementary material

Supplementary material is available at *Brain* online.

References

Ahmed RM, Irish M, Kam J, van Keizerswaard J, Bartley L, Samaras K, et al. Quantifying the eating abnormalities in frontotemporal dementia. JAMA Neurol 2014a; 71: 1540–6.

Ahmed RM, Latheef S, Bartley L, Irish M, Halliday GM, Kiernan MC, et al. Eating behavior in frontotemporal dementia: peripheral hormones vs hypothalamic pathology. Neurology 2015; 85: 1310–7.

Ahmed RM, MacMillan M, Bartley L, Halliday GM, Kiernan MC, Hodges JR, et al. Systemic metabolism in frontotemporal dementia. Neurology 2014b; 83: 1812–8.

Baltadzhieva R, Gurevich T, Korczyn AD. Autonomic impairment in amyotrophic lateral sclerosis. Curr Opin Neurol 2005; 18: 487–93.

Belfort R, Harrison SA, Brown K, Darland C, Finch J, Hardies J, et al. A placebo-controlled trial of pioglitazone in subjects with nonalcoholic steatohepatitis. N Engl J Med 2006; 355: 2297–307.

Bouteloup C, Desport JC, Clavelou P, Guy N, Derumeaux-Burel H, Ferrier A, et al. Hypermetabolism in ALS patients: an early and persistent phenomenon. J Neurol 2009; 256: 1236–42.

Brettschneider J, Del Tredici K, Toledo JB, Robinson JL, Irwin DJ, Grossman M, et al. Stages of pTDP-43 pathology in amyotrophic lateral sclerosis. Ann Neurol 2013; 74: 20–38.

Cirulli ET, Lasseigne BN, Petrovski S, Sapp PC, Dion PA, Leblond CS, et al. Exome sequencing in amyotrophic lateral sclerosis identifies risk genes and pathways. Science 2015; 347: 1436–41.

DeFronzo RA, Tripathy D, Schwenke DC, Banerji M, Bray GA, Buchanan TA, et al. Pioglitazone for diabetes prevention in impaired glucose tolerance. N Engl J Med 2011; 364: 1104–15.

Dentel C, Palamiuc L, Henriques A, Lannes B, Spreux-Varoquaux O, Gutknecht L, et al. Degeneration of serotonergic neurons in amyotrophic lateral sclerosis: a link to spasticity. Brain 2013; 136(Pt 2): 483–93.

Desport JC, Preux PM, Magy L, Boirie Y, Vallat JM, Beaufrere B, et al. Factors correlated with hypermetabolism in patients with amyotrophic lateral sclerosis. Am J Clin Nutr 2001; 74: 328–34.

Desport JC, Preux PM, Truong TC, Vallat JM, Sautereau D, Couratier P. Nutritional status is a prognostic factor for survival in ALS patients. Neurology 1999; 53: 1059–63.

Diano S, Liu ZW, Jeong JK, Dietrich MO, Ruan HB, Kim E, et al. Peroxisome proliferation-associated control of reactive oxygen species sets melanocortin tone and feeding in diet-induced obesity. Nat Med 2011; 17: 1121–7.

Dorst J, Dupuis L, Petri S, Kollewe K, Abdulla S, Wolf J, et al. Percutaneous endoscopic gastrostomy in amyotrophic lateral sclerosis: a prospective observational study. J Neurol 2015; 262: 849–58.

Dorst J, Kühnlein P, Hendrich C, Kassubek J, Sperfeld AD, Ludolph AC. Patients with elevated triglyceride and cholesterol serum levels have a prolonged survival in Amyotrophic Lateral Sclerosis. J Neurol 2011; 258: 613–7.

Dupuis L, Corcia P, Fergani A, Gonzalez De Aguilar JL, Bonnefont-Rousselot D, Bittar R, et al. Dyslipidemia is a protective factor in amyotrophic lateral sclerosis. Neurology 2008; 70: 1004–9.

Dupuis L, Dengler R, Heneka MT, Meyer T, Zierz S, Kassubek J, et al. A randomized, double blind, placebo-controlled trial of pioglitazone in combination with riluzole in amyotrophic lateral sclerosis. PLoS One 2012; 7: e37885

Dupuis L, Oudart H, Rene F, Gonzalez de Aguilar JL, Loeffler JP. Evidence for defective energy homeostasis in amyotrophic lateral sclerosis: benefit of a high-energy diet in a transgenic mouse model. Proc Natl Acad Sci USA 2004; 101: 11159–64.

Dupuis L, Pradat PF, Ludolph AC, Loeffler JP. Energy metabolism in amyotrophic lateral sclerosis. Lancet Neurol 2011; 10: 75–82.

Dwarkasing JT, Boekschoten MV, Argiles JM, van Dijk M, Busquets S, Penna F, et al. Differences in food intake of tumour-bearing cachectic mice are associated with hypothalamic serotonin signalling. J Cachexia Sarcopenia Muscle 2015; 6: 84–94.

Fergani A, Oudart H, Gonzalez De Aguilar JL, Fricker B, Rene F, Hocquette JF, et al. Increased peripheral lipid clearance in an animal model of amyotrophic lateral sclerosis. J Lipid Res 2007; 48: 1571–80.

Freischmidt A, Wieland T, Richter B, Ruf W, Schaeffer V, Muller K, et al. Haploinsufficiency of TBK1 causes familial ALS and frontotemporal dementia. Nat Neurosci 2015; 18: 631–6.

Gallo V, Wark PA, Jenab M, Pearce N, Brayne C, Vermeulen R, et al. Prediagnostic body fat and risk of death from amyotrophic lateral sclerosis: the EPIC cohort. Neurology 2013; 80: 829–38.

Grider MH, Chen Q, Shine HD. Semi-automated quantification of axonal densities in labeled CNS tissue. J Neurosci Methods 2006; 155: 172–9.

Gurney ME, Pu H, Chiu AY, Dal Canto MC, Polchow CY, Alexander DD, et al. Motor neuron degeneration in mice that express a human Cu,Zn superoxide dismutase mutation. Science 1994; 264: 1772–5.

Heisler LK, Cowley MA, Tecott LH, Fan W, Low MJ, Smart JL, et al. Activation of central melanocortin pathways by fenfluramine. Science 2002; 297: 609–11.

Heisler LK, Jobst EE, Sutton GM, Zhou L, Borok E, Thornton-Jones Z, et al. Serotonin reciprocally regulates melanocortin neurons to modulate food intake. Neuron 2006; 51: 239–49.

Huisman MH, Seelen M, de Jong SW, Dorresteijn KR, van Doormaal PT, van der Kooi AJ, et al. Lifetime physical activity and the risk of amyotrophic lateral sclerosis. J Neurol Neurosurg Psychiatry 2013; 84: 976–81.

Huisman MH, Seelen M, van Doormaal PT, de Jong SW, de Vries JH, van der Kooi AJ, et al. Independent associations of presymptomatic body mass index, and consumption of fat and alcohol with amyotrophic lateral sclerosis. JAMA Neurol 2015; 72: 1155–62.

Kaur G, Kulkarni SK. Evidence for serotonergic modulation of progesterone-induced hyperphagia, depression and algesia in female mice. Brain Res 2002; 943: 206–15.

Kirk SL, Glazebrook J, Grayson B, Neill JC, Reynolds GP. Olanzapine-induced weight gain in the rat: role of 5-HT2C and histamine H1 receptors. Psychopharmacology 2009; 207: 119–25.

Koch M, Varela L, Kim JG, Kim JD, Hernandez-Nuno F, Simonds SE, et al. Hypothalamic POMC neurons promote cannabinoid-induced feeding. Nature 2015; 519: 45–50.

Lam DD, Przydzial MJ, Ridley SH, Yeo GS, Rochford JJ, O'Rahilly S, et al. Serotonin 5-HT2C receptor agonist promotes hypophagia via downstream activation of melanocortin 4 receptors. Endocrinology 2008; 149: 1323–8.

Lattante S, Ciura S, Rouleau GA, Kabashi E. Defining the genetic connection linking amyotrophic lateral sclerosis (ALS) with frontotemporal dementia (FTD). Trends Genet 2015; 31: 263–73.

Leblond CS, Kaneb HM, Dion PA, Rouleau GA. Dissection of genetic factors associated with amyotrophic lateral sclerosis. Exp Neurol 2014; 262 (Pt B): 91–101.

Leckstrom A, Lew PS, Poritsanos NJ, Mizuno TM. Central melanocortin receptor agonist reduces hepatic lipogenic gene expression in streptozotocin-induced diabetic mice. Life Sciences 2011; 88: 664–9.

Lian J, Huang XF, Pai N, Deng C. Betahistine ameliorates olanzapine-induced weight gain through modulation of histaminergic, NPY and AMPK pathways. Psychoneuroendocrinology 2014; 48: 77–86.

Lim MA, Bence KK, Sandesara I, Andreux P, Auwerx J, Ishibashi J, et al. Genetically altering organismal metabolism by leptin-deficiency benefits a mouse model of amyotrophic lateral sclerosis. Hum Mol Genet 2014; 23: 4995–5008.

Lindauer E, Dupuis L, Muller HP, Neumann H, Ludolph AC, Kassubek J. Adipose Tissue Distribution Predicts Survival in Amyotrophic Lateral Sclerosis. PLoS One 2013; 8: e67783.

Liou YJ, Chen CH, Cheng CY, Chen SY, Chen TJ, Yu YW, et al. Convergent evidence from mouse and human studies suggests the involvement of zinc finger protein 326 gene in antidepressant treatment response. PLoS One 2012; 7: e32984

Long L, Toda C, Jeong JK, Horvath TL, Diano S. PPARgamma ablation sensitizes proopiomelanocortin neurons to leptin during high-fat feeding. J Clin Invest 2014; 124: 4017–27.

Lu M, Sarruf DA, Talukdar S, Sharma S, Li P, Bandyopadhyay G, et al. Brain PPAR-gamma promotes obesity and is required for the insulin-sensitizing effect of thiazolidinediones. Nat Med 2011; 17: 618–22.

Maeda N, Takahashi M, Funahashi T, Kihara S, Nishizawa H, Kishida K, et al. PPARgamma ligands increase expression and plasma concentrations of adiponectin, an adipose-derived protein. Diabetes 2001; 50: 2094–9.

Marin B, Desport JC, Kajeu P, Jesus P, Nicolaud B, Nicol M, et al. Alteration of nutritional status at diagnosis is a prognostic factor for survival of amyotrophic lateral sclerosis patients. J Neurol Neurosurg Psychiatry 2011; 82: 628–34.

Mizuno TM, Kleopoulos SP, Bergen HT, Roberts JL, Priest CA, Mobbs CV. Hypothalamic pro-opiomelanocortin mRNA is reduced by fasting and [corrected] in ob/ob and db/db mice, but is stimulated by leptin. Diabetes 1998; 47: 294–7.

Mizuno TM, Makimura H, Silverstein J, Roberts JL, Lopingco T, Mobbs CV. Fasting regulates hypothalamic neuropeptide Y, agouti-related peptide, and proopiomelanocortin in diabetic mice independent of changes in leptin or insulin. Endocrinology 1999; 140: 4551–7.

Morton GJ, Meek TH, Schwartz MW. Neurobiology of food intake in health and disease. Nat Rev Neurosci 2014; 15: 367–78.

Nelson LM, Matkin C, Longstreth WT Jr, McGuire V. Population-based case-control study of amyotrophic lateral sclerosis in western Washington State. II. Diet Am J Epidemiol 2000; 151: 164–73.

O'Reilly EJ, Wang H, Weisskopf MG, Fitzgerald KC, Falcone G, McCullough ML, et al. Premorbid body mass index and risk of amyotrophic lateral sclerosis. Amyotroph Lateral Scler Frontotemporal Degener 2013; 14: 205–11.

Obici S, Feng Z, Tan J, Liu L, Karkanias G, Rossetti L. Central melanocortin receptors regulate insulin action. J Clin Invest 2001; 108: 1079–85.

Paganoni S, Deng J, Jaffa M, Cudkowicz ME, Wills AM. Body mass index, not dyslipidemia, is an independent predictor of survival in amyotrophic lateral sclerosis. Muscle Nerve 2011; 44: 20–4.

Palamiuc L, Schlagowski A, Ngo ST, Vernay A, Dirrig-Grosch S, Henriques A, et al. A metabolic switch toward lipid use in glycolytic muscle is an early pathologic event in a mouse model of amyotrophic lateral sclerosis. EMBO Mol Med 2015; 7: 526–46.

Perez-Tilve D, Hofmann SM, Basford J, Nogueiras R, Pfluger PT, Patterson JT, et al. Melanocortin signaling in the CNS directly regulates circulating cholesterol. Nat Neurosci 2010; 13: 877–82.

Piguet O, Petersen A, Yin Ka Lam B, Gabery S, Murphy K, Hodges JR, et al. Eating and hypothalamus changes in behavioral-variant frontotemporal dementia. Ann Neurol 2011; 69: 312–9.

Pradat PF, Bruneteau G, Gordon PH, Dupuis L, Bonnefont-Rousselot D, Simon D, et al. Impaired glucose tolerance in patients with amyotrophic lateral sclerosis. Amyotroph Lateral Scler 2010; 11: 166–71.

Promrat K, Lutchman G, Uwaifo GI, Freedman RJ, Soza A, Heller T, et al. A pilot study of pioglitazone treatment for nonalcoholic steatohepatitis. Hepatology 2004; 39: 188–96.

Ripps ME, Huntley GW, Hof PR, Morrison JH, Gordon JW. Transgenic mice expressing an altered murine superoxide dismutase gene provide an animal model of amyotrophic lateral sclerosis. Proc Natl Acad Sci USA 1995; 92: 689–93.

Ryan KK, Li B, Grayson BE, Matter EK, Woods SC, Seeley RJ. A role for central nervous system PPAR-gamma in the regulation of energy balance. Nat Med 2011; 17: 623–6.

Sanyal AJ, Chalasani N, Kowdley KV, McCullough A, Diehl AM, Bass NM, et al. Pioglitazone, vitamin E, or placebo for nonalcoholic steatohepatitis. N Engl J Med 2010; 362: 1675–85.

Sohn JW, Harris LE, Berglund ED, Liu T, Vong L, Lowell BB, et al. Melanocortin 4 receptors reciprocally regulate sympathetic and parasympathetic preganglionic neurons. Cell 2013; 152: 612–9.

Turner MR, Rabiner EA, Hammers A, Al-Chalabi A, Grasby PM, Shaw CE, et al. [11C]-WAY100635 PET demonstrates marked 5-HT1A receptor changes in sporadic ALS. Brain 2005; 128(Pt 4): 896–905.

Turner MR, Wotton C, Talbot K, Goldacre MJ. Cardiovascular fitness as a risk factor for amyotrophic lateral sclerosis: indirect evidence from record linkage study. J Neurol Neurosurg Psychiatry 2012; 83: 395–8.

Vandesompele J, De Preter K, Pattyn F, Poppe B, Van Roy N, De Paepe A, et al. Accurate normalization of real-time quantitative RT-PCR data by geometric averaging of multiple internal control genes. Genome Biol 2002; 3: research0034.

Wang B, Chehab FF. Deletion of the serotonin 2c receptor from transgenic mice overexpressing leptin does not affect their lipodystrophy but exacerbates their diet-induced obesity. Biochem Biophys Res Commun 2006; 351: 418–23.

Wegorzewska I, Bell S, Cairns NJ, Miller TM, Baloh RH. TDP-43 mutant transgenic mice develop features of ALS and frontotemporal lobar degeneration. Proc Natl Acad Sci USA 2009; 106: 18809–14.

Weston-Green K, Huang XF, Deng C. Alterations to melanocortinergic, GABAergic and cannabinoid neurotransmission associated with olanzapine-induced weight gain. PLoS One 2012; 7: e33548.

Wills AM, Hubbard J, Macklin EA, Glass J, Tandan R, Simpson EP, et al. Hypercaloric enteral nutrition in patients with amyotrophic lateral sclerosis: a randomised, double-blind, placebo-controlled phase 2 trial. Lancet 2014; 383: 2065–72.

Xu Y, Jones JE, Kohno D, Williams KW, Lee CE, Choi MJ, et al. 5-HT2CRs expressed by pro-opiomelanocortin neurons regulate energy homeostasis. Neuron 2008; 60: 582–9.

Zemdegs J, Quesseveur G, Jarriault D, Penicaud L, Fioramonti X, Guiard BP. High fat diet-induced metabolic disorders impairs serotonergic function and anxiety-like behaviours in mice. Br J Pharmacol 2015. Advance Access published on October 16, 2015, doi: 10.1111/bph.13343.

Zhao S, Ting JT, Atallah HE, Qiu L, Tan J, Gloss B, et al. Cell type-specific channelrhodopsin-2 transgenic mice for optogenetic dissection of neural circuitry function. Nat Methods 2011; 8: 745–52.

Zhou L, Sutton GM, Rochford JJ, Semple RK, Lam DD, Oksanen LJ, et al. Serotonin 2C receptor agonists improve type 2 diabetes via melanocortin-4 receptor signaling pathways. Cell Metab 2007; 6: 398–405.

Ziotopoulou M, Erani DM, Hileman SM, Bjorbaek C, Mantzoros CS. Unlike leptin, ciliary neurotrophic factor does not reverse the starvation-induced changes of serum corticosterone and hypothalamic neuropeptide levels but induces expression of hypothalamic inhibitors of leptin signaling. Diabetes 2000; 49: 1890–6.

Appendix 1

Collaborators: GERP ALS Study Group

All centres were located in Germany. Investigators are listed by alphabetical order of centre and investigator:

Berlin (Department of Neurology, Charité University Hospital): Nadja Borisow; Theresa Holm; Andre Maier; Thomas Meyer; Bochum (Department of Neurology, University Hospital Bergmannsheil): Paula Budde; Torsten Grehl; Kai Gruhn; Bonn (Department of Neurology, University Hospital of Bonn): Malte Bewersdorff; Michael Heneka; Dresden (Department of Neurology, University Hospital Carl Gustav Carus, Technische Universität Dresden): Andreas Hermann; Alexander Storch; Göttingen (Department of Neurology, University Hospital of Göttingen): Tobias Frank; Bettina Göricke; Jochen Weishaupt; Halle (Department of Neurology, University Hospital of Halle/Saale): Katharina Eger; Frank Hanisch; Stephan Zierz; Hannover (Department of Neurology and Clinical Neurophysiology, Hannover Medical School (MHH), University Clinic): Anna-Lena Boeck; Reinhard Dengler; Sonja Koerner; Katja Kollewe; Susanne Petri; Jena (Department of Neurology, University Hospital Jena): Julian Grosskreutz; Tino Prell; Thomas Ringer; Jan Zinke; Munich (Department of Neurology, University of Munich): Johanna Anneser; Gian Domenico Borasio; Christine Chahli; Andrea S. Winkler; Muenster (Department of Neurology, University of Muenster): Matthias Boentert; Bianca Stubbe-Draeger; Peter Young; Regensburg (Department of Neurology, University of Regensburg): Ulrich Bogdahn; Steffen Franz; Verena Haringer; Norbert Weidner; Rostock (Department of Neurology, University of Rostock): Reiner Benecke; Stefanie Meister; Johannes Prudlo; Matthias Wittstock; Ulm (Department of Neurology, University of Ulm): Johannes Dorst; Corinna Hendrich; Albert C. Ludolph; Anne-Dorte Sperfeld; Ulrike Weiland; Wiesbaden (Department of Neurology, Neurological clinic, DKD): Sabine Neidhardt; Berthold Schrank; Wurzburg (Department of Neurology, University of Wurzburg): Marcus Beck; Peter Kraft; Klaus Toyka; Jochen Ulzheimer; Carsten Wessig.

Supplementary Table 1: primers used for RT-qPCR

Target	forward primer	reverse primer
18s	F-TCTGATAAATGCACGCATCC	R-GCCATGCATGTCTAAGTACGC
AgRP	F- CAGGCTCTGTTCCCAGAGTT	R- TCTAGCACCTCCGCCAAA
AVP	F- TCTGACATGGAGCTGAGACAG	R- GAAGCAGCCCAGCTCGT
BDNF	F- GCCTTTGGAGCCTCCTCTAC	R- GCGGCATCCAGGTAATTTT
CART	F- CGAGAAGAAGTACGGCCAAG	R- CTGGCCCCTTTCCTCACT
CRH	F- GAGGCATCCTGAGAGAAGTCC	R- TGTTAGGGGCGCTCTCTTC
Galanin	F- AGAAGAGAGGTTGGACCCTGA	R- GAGGCCATGCTTGTCGCTAA
MCH	F-GCAGAAAGATCCGTTGTCGC	R-CGGATCCTTTCAGAGCGAGG
NPY	F- CCGCTCTGCGACACTACAT	R- TGTCTCAGGGCTGGATCTCT
NTS	F-AGCCCTGGAGGCAGATCTAT	R-CCAAGACGGAGGACTTGCTT
Orexin	F-CTTCAGGCCAACGGTAACCA	R-GGTGCTAAAGCGGTGGTAGT
PC1	F- GCTGGTGTGTCTCTGATCTTG	R- GAGTCCAACCTCTTTGCTCCA
PC2	F- AAAATACCACCCACCGGCAA	R- CCAGGTAGCGGACGAAGTTT
POMC	F- AGTGCCAGGACCTCACCA	R- CAGCGAGAGGTCGAGTTTG
POL2	F-GCTGGGAGACATAGCACCA	R-TTACTCCCCTGCATGGTCTC
SST	F- GGGCATCATTCTCTGTCTGG	R- GGGCATCATTCTCTGTCTGG
TBP	F-CCAATGACTCCTATGACCCCTA	R-CAGCCAAGATTCACGGTAGAT
TRH	F- TGCAGAGTCTCCACCTTGC	R- GGGGATACCAGTTAGCACGA

Supplementary Table 2: numbers of patients for Figure 1

	0	1	2	6	12	18
Adiponectin						
Placebo	58			58	38	
Pioglitazone	57			56	35	
Glycemia						
Placebo	100	84	90	70	47	41
Pioglitazone	104	89	95	79	44	44
ASAT						
Placebo	104	92	93	76	46	43
Pioglitazone	106	98	96	79	48	47
ALAT						
Placebo	104	92	93	76	46	44
Pioglitazone	107	99	97	80	48	47

Supplementary Table 3: numbers of patients for Figure 2

	0	1	2	3	6	9	12	15	18
Total									
Placebo	105	94	94	84	77	67	52	32	55
Pioglitazone	104	94	98	86	80	69	48	30	55
Spinal onset									
Placebo	72	64	65	56	53	46	37	24	37
Pioglitazone	72	66	67	56	56	47	34	20	40
Preserved QoL									
Placebo	50	47	48	45	49	45	36	20	36
Pioglitazone	53	49	50	47	49	45	35	21	40
Preserved bulbar function									
Placebo	40	38	39	37	39	35	30	21	26
Pioglitazone	42	40	41	39	41	34	28	18	30

Supplementary Table 4: intake of drugs affecting body weight and food intake

The number of patients taking the corresponding class of drug is shown. P value was calculated using Fisher's exact – test

Class of drugs	**n total**	**Pioglitazone**	**Placebo**	**p-value**
anti-epileptics	9	3	6	0.50
anti-diabetics	3	1	2	1.00
anti-psychotics	4	4	0	0.12
SSRIs	37	20	17	0.72

I. Results #2

A. Résumé – Publication #2

« Posterior hypothalamic volume is related to weight loss in amyotrophic lateral sclerosis»

La Sclérose Latérale Amyotrophique et la Démence Frontotemporale sont considérées comme les extrêmes d'un continuum génétique et pathologique. En effet des patients SLA présentent des symptômes légers de DFT, et des patients DFT ont une pathologie du motoneurone au cours de leur maladie.

Une sous catégorie des DFT, les bv-DFT (variant comportemental de la DFT), représentant 60% des patients DFT, présentent des anomalies du comportement alimentaire. Des études suggèrent que l'origine de ce dysfonctionnement réside dans l'hypothalamus. Entre autres, des études IRM ont montrées une atrophie de l'hypothalamus jusqu'à 15%, plus particulièrement dans la partie postérieure chez les patients bv-DFT.

Des problèmes du métabolisme énergétique sont aussi une caractéristique très importante chez les patients SLA, avec une perte de poids et un hypermétabolisme. De plus, il est connu que contrecarrer la perte de poids dans un modèle murin de SLA permet d'augmenter la survie. Récemment, une altération du comportement alimentaire, moins importante que chez les bv-DFT, a été mise en évidence chez des patients SLA. Nous avons également montré qu'il y a des problèmes hypothalamiques dans cette maladie. Cependant aucune étude volumétrique de l'hypothalamus n'a a été faite à ce jour. La question qui se posait était de savoir si une atrophie de l'hypothalamus chez les patients SLA pouvait être à l'origine des problèmes métaboliques.

Dans notre étude, nous avons mesuré le volume hypothalamique de 279 patients SLA et 98 contrôles. Nous avons montré qu'il y avait une atrophie modeste, mais significative, de l'hypothalamus dans la SLA, préférentiellement dans la partie postérieure. Nous avons montré que cette atrophie apparaît au milieu du processus pathologique présent dans le cerveau (staging de Braak), et non dès le début. De plus une corrélation existe entre l'atrophie hypothalamique et la perte de poids préalable à l'examen. Nos résultats, en accord avec d'autres études pathologiques, indiquent qu'une atteinte de l'hypothalamus est présente chez les patients SLA et qu'elle serait plus dans les noyaux de la partie postérieure de l'hypothalamus.

Posterior hypothalamic volume is related to weight loss in amyotrophic lateral sclerosis

Pauline Vercruysse[1,2,3]*, Martin Gorges[3]*, Hans-Peter Müller[3], Hans-Jürgen Huppertz[4], Angela Rosenbohm[3], Gabriele Nagel[5], Åsa Petersén[6], Albert C. Ludolph[3], Jan Kassubek[3#] & Luc Dupuis[1,2#]

* shared first authorship

shared senior authorship

[1]INSERM UMR-S1118, faculté de médecine, Strasbourg, 67085 France.

[2]Université de Strasbourg, fédération de Médecine Translationnelle, Strasbourg, France.

[3]Department of Neurology, University of Ulm, Germany.

[4]Swiss Epilepsy Centre, Klinik Lengg, Zurich, Switzerland.

[5] Institute of Epidemiology and Medical Biometry, Ulm University, Ulm, Germany

[6] Translational Neuroendocrine Research Unit, Department of Experimental Medical Sciences, Lund University, Sweden.

* Corresponding author: ldupuis@unistra.fr; jan.kassubek@uni-ulm.de

Abstract (<250 words)

Background:

Decreased hypothalamic volume related to abnormal food intake behaviour has been observed in behavioral variant frontotemporal dementia (bvFTD). Similar volumetric studies are lacking for amyotrophic lateral sclerosis (ALS), although hypothalamic dysfunction was recently postulated to be involved in abnormal eating behaviour of ALS animal models. Here, our objective was to study the relationships between hypothalamic volume, weight loss and functional status in ALS patients.

Methods:

High resolution 3-dimensional T1-weighted magnetic resonance imaging (MRI)images from 270 ALS patients (30 patients with familial ALS) and 98 matched healthy controls were registered for manual delineation of the hypothalamus using a well-established landmark-based procedure. The raters were blinded to the clinical status, and intra/inter-rater reliability showed robust and reproducible measurements. The volume of the hypothalamus, in total or subdivided in its anterior and posterior parts, was normalized to the intracranial volume and adjusted with age. Correlation analysis were performed with weight loss before and after MRI, metabolic hormones (leptin, adiponectin), and disease progression markers such as ALSFRS-R. Pathologically defined ALS-stages were determined *in vivo* by diffusion tensor imaging.

Results

We observed a moderate atrophy of the hypothalamus in ALS patients (-4.0%, p=0.019) which was more pronounced in the posterior part of the hypothalamus (-5.1%, p=0.003). Interestingly, this atrophy was more severe in familial ALS patients (-7.2%, p=0.020) as compared with sporadic cases (-3.4%, p=0.039) and more pronounced in patients in advanced stages (-5.7%, p=0.005) as determined using DTI. Posterior hypothalamic volume, and to a lesser extent total hypothalamic volume, was correlated with weight loss before MRI, but neither with weight loss after MRI, circulating levels of leptin or adiponectin nor with ALS-FRS-R.

Conclusions

Reduced posterior hypothalamic volume in ALS patients appears to be associated with prior weight loss.

Introduction

Amyotrophic lateral sclerosis (ALS) and frontotemporal dementia (FTD) are commonly considered as part of a pathophysiological continuum. Both diseases clinically overlap, with a subset of ALS patients developing moderate FTD-like symptoms, and, conversely, FTD patients motor neuron involvement during the time course of the disease. Moreover, ALS and FTD patients also share mutations in identical genes and similar neuropathology [1-4], in contrast the longitudinal course of both diseases differ [5-7]

A major symptom of the behavioural (bv) form of FTD (60% of FTD cases) consists of an alteration in appetite and food preference of patients, in particular a marked preference for sucrose-rich foods [8-11]. In bvFTD, this is associated with marked hyperphagia, leading to weight gain[8, 12]. Peripheral hormones appear normally regulated in bvFTD patients[13], suggesting that overeating is due to central abnormalities in food intake behaviour. Indeed, levels of AgRP, a strongly orexigenic hypothalamic neuropeptide, were increased in bvFTD patients[9] and several MRI-based studies have observed up to 15% atrophy of the hypothalamus, especially of its posterior part, in bvFTD patients[9, 10, 14]. Thus, disease progression of bvFTD involves hypothalamic atrophy potentially leading to abnormal eating behaviour[15].

Disturbed energy metabolism is also a hallmark of ALS. ALS patients are generally lean with normal or low BMI preceding onset of motor symptoms[16, 17]. The extent of weight loss[18-21], as well as metabolic status, evaluated by circulating lipids [22, 23] or fat distribution[24] are prognostic markers of ALS. The causes of weight loss in ALS are multifactorial and include dysphagia and hypermetabolism[15, 25]. Importantly, increasing energy content of the diet increased survival of ALS mouse models[26], and showed efficacy in a pilot clinical trial in gastrostomized ALS patients[27] as well as in a longitudinal register of PEG-implanted patients[28]. Recently, ALS patients were shown to display altered eating behavior similar, yet milder, to bvFTD patients[29, 30]. Suggestive of a hypothalamic involvement in ALS, AgRP levels were increased in mouse models of ALS, while levels of its antagonist pro-opiomelanocortin (POMC) were decreased[31], and two studies observed pathological abnormalities in the hypothalamus of ALS patients[32, 33]. Indeed, ALS patients did not gain weight in response to pioglitazone, a drug known to increase food intake through hypothalamic relays[31, 34].

In spite of this clinical information, there is no information available on hypothalamic volume in ALS patients, and it remains unknown whether any hypothalamic atrophy in humans could be related to metabolic problems typical of ALS. Here, we performed a MRI-based analysis of the hypothalamic volume in 270 ALS

cases in comparison to 98 healthy controls in order to determine whether ALS patients presented hypothalamic atrophy which could be correlated to metabolic status, functional status and survival in ALS.

Subjects and methods

Study samples

All subjects were recruited from the Department of Neurology, University of Ulm, Germany and provided their written informed consent according to institutional guidelines approved by the Ethics Committee of the University of Ulm (reference #19/12). Patients were included in the German Motor Neuron Disease Network. Patients with ALS (*N*=270) underwent MRI scans at enrollment (for details of the scanning protocols, see *MRI acquisition*), together with standardized clinical-neurological and laboratory examinations, distant from less than 3 months of the MRI session. The diagnosis of all patients was made by a motor neuron disease specialist according to the El Escorial diagnostic criteria[35, 36]. None of the ALS patients had any history of other neurological or psychiatric disorders. Thirty patients presented familial ALS having a genetic form of either *C9ORF72* (*N*=19), *SOD1* (*N*=8), or *FUS* (*N*=3), and the remaining 240 ALS patients were considered as sporadic ALS cases. For 61 patients, information on serum adiponectin and leptin concentrations were available.

MRI data and demographic characteristics of matched healthy controls (*N*=98) for comparison were obtained from a normal database. None had a history of neurological or psychiatric disease or other medical conditions. Detailed clinical characteristics and demographic features of all participants are summarized in **Table 1**.

MRI acquisition

The study utilized two different protocols for whole-brain based morphological data and diffusion tensor imaging (DTI) acquisition.

The data for 77 ALS patients and 41 controls were acquired at a 3.0 Tesla MRI scanner (Allegra Siemens Medical, Erlangen, Germany). Morphological data were obtained using a high-resolution 3-D T_1-weighted magnetization-prepared gradient echo image (MPRAGE) sequence (192 sagittal slices, no gap, 1.0x1.1x1.0mm^3 voxels, 256x192x256 matrix, *TE*=4.7ms, *TR*=2200ms). The DTI study protocol consisted of

49 gradient directions, including one *b*0 gradient direction (no gap, 2.2mm^3 iso-voxels, 96x128x52 matrix, *TE*=85ms, *TR*=7600ms, *b*=1000 s/mm^2).

The data for 193 ALS patients and 57 controls were acquired at a 1.5 Tesla clinical MRI scanner (Symphony, Siemens Medical, Erlangen, Germany). Morphological data were obtained using a high-resolution 3-D T_1-weighted magnetization-prepared gradient echo image (MPRAGE) sequence (144 sagittal slices, no gap, 1.0x1.2x1.0mm^3 voxels, 256x192x256 matrix, *TE*=4.2ms, *TR*=1600ms). The DTI study protocol consisted of 52 gradient directions, including four *b*0 gradient directions (no gap, voxelsize 2.0x2.0x2.8 mm3, 128x128x64 matrix, *TE*=95ms, *TR*=8000ms, *b*=1000 s/mm^2).

Hypothalamic volumetry

High resolution MPRAGE images, resampled and rigidly registered into a standardized grid, were used for manual delineation of the hypothalamus in the coronal plane using a well-established landmark-based procedure (Gabery et al., 2015). To this end, volumetric analyses of the hypothalamus, global brain and intra-cranial volume were performed.

The Tensor Imaging and Fiber Tracking (TIFT) software package [37] was used for volumetric analysis of the hypothalamus for each of the 368 subjects in a three-step processing pipeline: (1) rigid body normalization, (2) spatial up-sampling into a study-specific grid, and (3) manual delineation of the left and right hemispheric hypothalamus. In particular, rigid body normalization was performed along the anterior commissure (AC)—posterior commissure (PC) axis such that the coronal cutting plane was perpendicular with respect to the AC—PC axis. The rigid body transformation approach (i) preserves the amount of hypothalamic volume, (ii) corrects for individual-based tilt of the head in order to ensure coronal slicing in a common space for all subjects, and (iii) minimizes potential partial volume effects. The delineation of the hypothalamus (for details see *Hypothalamic delineation procedure)* was performed on equidistantly spaced coronal slices (up-sampled slice thickness of 0.5mm) within an up-sampled in-plane resolution of 62.5x62.5 µm^2. We are aware that up-sampling did not fully overcome the problem of limited native resolution, but higher isotropic in-plane resolution improved considerably accuracy in identifying landmarks and borders used to calculate the hypothalamic volume.

Prior to the analysis, all 368 datasets were randomized such that the raters were blinded to all demographic and clinical features. Gray matter and intracranial volume (ICV) were directly determined by the build-in “Tissue Volumes” utility of the MATLAB (R2014b, The MathWorks, Inc., Natick, Massachusetts, USA) based

Statistical Parametric Mapping 12 (SPM12) software (Wellcome Trust Centre for Neuroimaging, London, UK)[38].

Hypothalamic delineation procedure

The hypothalamus was manually delineated in the coronal plane using a robust and highly reproducible technique established by Gabery et al.[39] based on well-defined boundaries visualized in coronal sections of human postmortem hypothalamic tissue[40]. Briefly, the most anterior coronal slice was defined when the optic chiasm was first seen to be attached to the ventral part of the septal area (**Figure 1A**) and the most posterior slice was determined by the coronal section where the fornix appears to be merged with the mammillary nucleus (**Figure 1C**, **right panel**). The superior border was defined as a straightline between the hypothalamic sulcus and the most lateral edge of the optical tract (**Figure 1C**) for all slices. The hypothalamus was medially bounded by the third ventricle, the inferior border was defined by the junction of the optical chiasm for the anterior part, and by the border of the cerebrospinal fluid for the more posterior slices (**Figure 1C**). The optical tract was excluded from all slices. This well-established delineation procedure achieves a high level of reproducibility which is the most critical factor of the measurements in a large cohort. Hence, we did not perform morphometric analysis of hypothalamic subregions since the anatomical borders of the nuclei are difficult to define in both MRI data (**Figure 1**) and histological sections[40].

Volumetric analysis

A medial border in the coronal plane was defined in order to separate the hypothalamus into an anterior and posterior part such that the anterior and posterior part comprised the same number of coronal slices. The underlying technique for anterior-posterior segmentation (**Figure 1B**) was adapted from Piguet and collaborators[10], given the distinct structural connectivity and potentially ALS-related selective vulnerability of the hypothalamus [31]. All volumes, i.e. (1) the total volume including the left and right hemispherical part of the hypothalamus, (2) the volumes for the anterior, and (3) posterior hypothalamus, were normalized to the mean intracranial volume of the whole study population to correct for individual differences in overall brain size and adjusted for age by using age as a covariate.

Intra-inter rater reliability

Prior to the hypothalamus delineation for all 368 subjects included in the analysis, an intra- and inter-rater reliability analysis was performed to ensure robustness and reproducibility for the hypothalamus volume

delineation. Both raters (PV and MG) repeated each assessment of the hypothalamic volume three times in 12 pseudo-randomly selected subjects comprising 3 ALS patients and 3 controls measured at 1.5T, and 3 ALS patients and 3 controls measured at 3.0T. The total of 12x3=36 data sets were randomized prior to the volumetric analysis such that both raters were completely blinded to both clinical data and measurement protocols. The coefficient of variation (CV=mean volume of three scans/standard deviation of three scans) was 2.2±0.9 (range 0.4-3.4) for the first rater and 1.8±0.9 (0.8-3.6) for the second rater; CV<4% was considered as acceptable[39]. The intraclass correlation coefficient (ICC) between the two raters was >0.9 (*N*=12, Pearson's *r*=0.93, *p*<0.0001), indicating robust and highly reproducible hypothalamic volume measurement in accordance with others [10, 14, 39]. The MRI protocol (either 1.5T or 3.0T) did not influence the volumetric analysis.

Assessing disease status using DTI

We used the well-established fiber tract-based DTI staging procedure introduced by our group [41] in order to classify *in vivo* the disease stage of all ALS patients using the DTI data. The DTI-based fiber tracking uses a hypothesis-guided tract of interest-based approach corresponding to the neuropathological *p*TDP43 pathology propagation model[5] and measures potential white matter pathway involvement of the corticospinal, -pontine, and -rubral tract as well as the corticostriatal pathway and the perforant path. Patients presenting structural abnormalities exclusively in the corticospinal tract were classified as ALS stage 1; patients presenting stage 1 plus structural abnormalities in corticopontine tract and corticorubral tract were classified as ALS stage 2; patients presenting stage 2 plus corticostriatal pathway damage were classified as ALS stage 3, and patients presenting stage 3 plus damage in the perforant path were classified as ALS stage 4. [36]

Statistics

The statistical software package Prism (GraphPad, USA) was used for statistical data analysis. ALS patients and controls were contrasted using the unpaired Student's *t*-test. One-way analyses of variance (ANOVA) was performed in cases of three or more groups, followed in the event of significance ($p<0.05$) by unpaired Student's *t*-test for post-hoc analysis. Spearman's rank order correlation coefficient was used to study possible relationships between volumetric measures and clinical scores for the patient groups. All statistical tests were 2 sided with $p<0.05$ indicating statistical significance.

Results

In this retrospective study, 270 ALS and 98 controls were included in the data analysis. There were no significant differences in age and sex between ALS patients and controls. Age at onset, proportion of sites of onset, and proportion of familial cases were representative of a typical ALS population (**Table 1**). Median value of ALS-FRS-R was 41, suggesting that the majority of patients included were relatively early in their disease course.

Hypothalamic volumes (**Figure 1**) of 270 ALS patients (mean 735±109 mm^3) were significantly smaller (unpaired Student's t=-2.35, p=0.019) by 4.0% than those of 98 healthy controls (mean 766±116 mm^3, **Figure 2A**). This atrophy was most marked in the 30 familial ALS cases (710±103 mm^3) included, mostly with *C9ORF72* and *SOD1* mutations (vs controls: -7.2%, t=-2.36, p=0.020) compared with 240 sporadic cases (738±110 mm^3, vs controls: -3.4%, t=-2.07, p=0.039) (**Figure 2B**). The posterior hypothalamus as defined by Piguet and collaborators[10], but not the anterior hypothalamus (p=0.683), was smaller in ALS patients than in healthy controls (-5.1%, t=-2.97, p=0.003) (**Figure 2C**). Thus ALS is associated with a moderate atrophy of the posterior hypothalamus.

To determine the selectivity of the observed atrophy, we measured whole brain volume (WBV) on the same MRI scans, and observed atrophy of the whole brain at a similar level as the hypothalamic volumes in ALS patients as compared with healthy controls (**Figure 3A**). Consistent with a relationship between hypothalamic volume, brain atrophy and disease progression, ALS patients in DTI Stages 3-4 showed a more pronounced atrophy of total or posterior hypothalamus (-5.7%, p=0.005) than ALS patients in DTI stages 1-2 (-4.9%, p=0.029) compared with healthy controls (**Figure 3B-C**). Thus, hypothalamic atrophy is related with disease progression.

Hypothalamic volume, either total or posterior, did not appear to correlate with metabolic indices at the time of MRI, such as circulating levels of leptin (**Figure S1A-B**) or adiponectin (**Figure S1C-D**), two hormones that are closely related with the individual's metabolic status. There was also no correlation between hypothalamic volumes and body mass index at the time of MRI (**Figure S1E-F**). However, total hypothalamic volume was correlated with monthly changes in BMI before MRI (Spearman rank order correlation r=0.22, p=0.016; **Figure 4A**). This was more pronounced for the posterior hypothalamic volume (r= 0.26, p= 0.005,

Spearman correlation, **Figure 4B**), but not observed for whole brain volume (**Figure 4C**). There were no relationships between total or posterior hypothalamic volume and monthly changes in BMI after the MRI (not shown). Contrastingly, there were no correlations between ALS-FRS-R and hypothalamic volumes (**Figure S2A-B**), while brain volume was highly correlated with ALS-FRS-R (**Figure S2C**). Thus, hypothalamic volume of ALS patients is related with brain atrophy and previous weight loss, and this relationship is mostly due to morphological alterations in the posterior hypothalamus.

Discussion

In this study, we provide evidence that the total volume of the hypothalamus in ALS patients is moderately reduced compared with controls. The volume loss resulted from a pronounced atrophy of the posterior part of hypothalamus which is correlated with weight loss preceding the MRI. These findings have consequences for our understanding of energy metabolism defects in ALS.

To our knowledge, this represents the largest study of hypothalamic volumetry in a disease, with 270 cases studied and compared to 98 healthy controls. Previous studies included an order of magnitude less cases and were performed in bvFTD[9, 10, 14], psychiatric diseases [42, 43] and Huntington's disease[39] (HD). We used the delineation technique previously validated by Gabery and collaborators [39] that proved to display very high intra-rater and inter-rater reliability in our hands, and all the analysis were performed upon complete blinding to the disease status. In particular, our method is very conservative in the determination of hypothalamic volume, as it excludes mammillary bodies and optical tracts, regions that are sometimes included in other studies[9, 10, 14]. This likely underlies the difference between the hypothalamic volumes in controls in our study (mean value: 759 mm^3) as compared with the study by Bocchetta et al. (mean value: 944 mm^3). Despite these technical differences, it is important to note that the different studies converge for their conclusions. For instance, our study identified 7% atrophy in fALS cases, mostly *C9ORF72* expansion carriers, and this is similar to the hypothalamic atrophy observed in bvFTD patients carrying a *C9ORF72* expansion[14]. It is interesting to note that it was shown in morphological studies that C9ORF72 positive cases show more extensive neuropathology, including cell death, than sporadic ALS cases. We chose not to further subdivide the hypothalamus into subregions, mostly because the boundaries between the different nuclei are difficult to define in both MRI data (**Figure 1**) and histological sections[40].

The first major result of our study is that the posterior hypothalamic volume is atrophied in ALS. The atrophy of the hypothalamus was similar to the atrophy of the whole brain arguing against a region-selective process of degeneration in ALS and suggesting that the hypothalamic atrophy could be secondary to the spreading of the disease, rather than a primary event. In this respect, hypothalamic atrophy occurs between stage 2 and stage 3, as defined by DTI [41]. In the neuropathological studies of Braak and collaborators, the hypothalamus was not systematically studied. It is thus possible that hypothalamic atrophy occurs as the secondary consequence of the spreading of p-TDP43 proteinopathy in this region that would occur in stage 3, as

proposed by Braak and collaborators[5, 44]. Consistent with this hypothesis, pTDP43 pathology was observed in the hypothalamus of a subset of ALS patients that also had basal forebrain pathology and could therefore be classified as Stage 3/4 ALS patients according to Braak staging of ALS[33]. It should be noted that our current study does not exclude that the hypothalamus could be affected in earlier stage ALS patients, as selective degeneration of one of the many neuronal types of the hypothalamus would not necessarily translate into a loss of hypothalamic volume. More detailed pathological analysis of the hypothalamus in ALS patients should be conducted and compared with Braak staging.

The observed hypothalamic atrophy in ALS patients was quantitatively more important than in HD[39], but much less severe than what was previously observed in bvFTD patients[8, 10, 11]. However, a similar atrophy was observed in *C9ORF72* carriers between studies[8, 10, 11]. This would be consistent with a major role of the hypothalamus in eating abnormalities that are pronounced in bvFTD patients and correlated with hypothalamic volume[8, 10, 11], and milder in ALS patients, as detected in a series of recent studies[29, 30] as well as in animal models[26, 31].

We used a similar strategy as Piguet and collaborators to identify the posterior and anterior hypothalamus[10], as these authors identified a preferential atrophy of the posterior hypothalamus in bvFTD. In the present study, we observed a more pronounced atrophy of the posterior hypothalamus in ALS patients. The posterior part of the hypothalamus as defined here includes most of the lateral hypothalamus area, as well as dorsomedial, ventromedial and posterior hypothalamic nuclei, and it is therefore not possible to assign the observed atrophy to a specific hypothalamic nucleus. However, the atrophy of the posterior hypothalamus is consistent with the recent observation of pTDP43 pathology in the lateral hypothalamus of ALS patients[33]. Our results are thus consistent with ALS and FTD showing similar patterns of damage inspite of showing a neuropathologically different course, affecting preferentially the posterior part of the hypothalamus. The extent of hypothalamic involvement potentially underlying the differences in terms of eating behaviour.

A second major result of our study is that hypothalamic atrophy, even if moderate, is correlated with the pre-existing weight loss of ALS patients but not with future weight loss. It has been repeatedly shown that weight loss is a very early process in ALS patients, and is even premorbid[16, 17]. Our correlation analysis suggests that this early weight loss might be related, as a cause or a consequence, to an involvement of the hypothalamus. Importantly, there was no correlation between whole brain atrophy and weight loss, suggesting that hypothalamus is selectively associated with weight loss. The lack of correlation between

hypothalamic volume and future weight loss could be the consequence of dietary management of ALS patients, including percutaneous endoscopic gastrostomy, as well as progression of dysphagia, i.e. potential modifiers of weight loss during disease progression. Hypothalamic volumes appeared unrelated with functional motor impairment, while at contrast, brain atrophy was. This suggests that weight loss and progression of motor symptoms are two distinct processes, resulting from differential propagation of the pathology between patients, according to the centrifugal model of disease propagation proposed by Braak and coworkers [5, 44].

Summarizing, we provide here evidence that the posterior part of the hypothalamus of ALS patients is atrophied, especially in ALS patients in stages 3 and 4, and that this atrophy relates to the extent of pre-existing weight loss. The large cohorts with 270 ALS patients included in the analysis as well as their *in vivo* DTI-based staging characterization reinforce our conclusions. Further prospective studies should be initiated, combining dietary evaluation, longitudinal follow up of metabolism, and MRI and CSF puncture to strengthen these results. Since counteracting weight loss could be a valuable strategy to improve the survival of ALS patients[27, 28], our study suggests that the identification of the precise hypothalamic alterations could help in designing targeted strategies to combat weight loss in these patients.

Acknowledgements

We thank Sanaz Gabery, Raphael Peter and Kornelia Günther for their help in data collection.

This work was supported by fondation « recherche sur le cerveau » (call 2015, to LD), Fondation Thierry Latran (SpastALS, to LD) and ARSla (call 2016, to LD). Work in our laboratories is supported by ALS Association Investigator Initiated Award (grants 2235, 3209 and 8075; to LD); the Frick Foundation (award 2013 to LD); Association Française contre les Myopathies (grant #18280; to LD); Virtual Helmholtz Institute “RNA dysmetabolism in ALS and FTD” (WP2, to LD and ACL); the Swedish Research Council (ÅP).

Table 1: demographic features of patients and controls

	ALS (*n*=270)	**healthy controls (*n*=98)**	***p*-value**
gender (male/female)	**158/112**	**50/48**	0.234[a]
age (years)	**62** (54-71), 19-86	**62** (54-68), 38-81	0.366[b]
disease duration (month)	**12** (8-24), 1-180	NA	-
age at onset (years)	**62** (52-70), 19-85	NA	-
familial ALS/sporadic ALS	**30/240**	NA	-
ALS-FRS-R[c]	**41** (35-45), 15-48	NA	-
site of onset (bulbar/cervical/lumbar)	**72/99/99**	NA	-
leptin (ng/ml)	**7** (3-13), 1-74	NA	-
adiponectin (µg/ml)	**10** (6-14), 2-31	NA	-
weight (kg)	**76** (68-85), 40-120	-	-
body mass index (kg/m^2)	**26** (23-28), 16-36)	-	-

Data are shown as median (interquartile range, Q1-Q3), min—max. All values were computed using the MATLAB® (The Mathworks Inc, Natick, MA, USA) based 'Statistics Toolbox'.

[a]Fisher's exact test.

[b]Mann-Whitney-*U* test.

[c]ALSFRS-R, revised ALS Functional Rating Scale (maximum score 48, falling with increasing physical impairment)

NA, not applicable.

Figure legends

Figure 1: Volumetric analysis of the hypothalamus. Example of the delineation of the hypothalamus in one representative healthy subject (female, 58 years) based on 1.5T high-resolution magnetization-prepared gradient echo image (MPRAGE) data (voxel size: 1.0x1.2x1.0 mm^3). (**A**) Coronal slice through the most anterior part of the hypothalamus and example of delineation for the left-hemispheric part (resampled in-plane resolution 62.5x62.5 μm^2). (**B**) Delineation was performed on a consecutive sequence of coronal slices in anterior-posterior direction at a resampled slice thickness of 0.5 mm. Then, the hypothalamus was subdivided into an anterior and posterior part using the criteria reported by Piguet et al. [10](**C**) Consecutive sequence of each second coronal slice in anterior-posterior direction showing the boundaries (yellow line) used to delineate the hypothalamus according to technique by Gabery et al.[39] The hypothalamic sulcus (*) and the lateral edge of the optical tract (+) were used as landmarks; the most anterior slice (left panel) was defined where the optic chiasm was attached to the ventral part of the septal area and the most posterior slice (right panel) was defined where the fornix (fx) appears to be merged with the mammillary body (MB). The optical tract (OT) was excluded from all slices. AC=anterior commissure; 3V=third ventricle.

Figure 2: Moderate hypothalamic atrophy in ALS

A: Volume of the hypothalamus in healthy controls (HC, *n* = 98) and ALS patients (n = 270),* *p*=0.019..

B: Volume of the hypothalamus in healthy controls (*n* = 98), familial ALS patients (fALS, *n* = 30) and sporadic ALS cases (sALS, *n*=240), fALS versus healthy controls (**p*=0.02), and psALS versus healthy controls (*p*=0.039).

C: Volume of the anterior and posterior hypothalamus in healthy controls (*n* = 98) and ALS patients (*n* = 270), ***p*=0.003.

All volumes (shown as mean±std) are corrected for the intracranial volume (ICV) and adjusted for age.

Figure 3: Hypothalamic atrophy is related to disease progression and general brain atrophy in ALS

A : ICV corrected whole brain volume relative (in cm^3) in healthy controls (HC, *n* = 98) and ALS patients (*n* = 270), *** *p*<0.001.

B-D: ICV corrected hypothalamic volume (in mm^3, B), posterior hypothalamic volume (in mm^3, C) and WBV (in mm^3, D) in healthy controls (HC) and ALS patients stratified by DTI stages. *p<0.05, **p<0.01, ***p<0.001.

Figure 4: Hypothalamic atrophy is related to previous weight loss in ALS

A-C : Spearman rank order correlations of hypothalamic volume (A), posterior hypothalamic volume (B) and ICV-corrected whole brain volume (C) with the rate of BMI change between onset of symptoms and MRI.

Figure S1: Hypothalamic atrophy in MRI is not related to metabolic status

A-B: correlations of ICV-corrected hypothalamic volume (A) and posterior hypothalamic volume (B) with circulating leptin, p>0.05.

C-D: correlations of ICV-corrected hypothalamic volume (C) and ICV-corrected posterior hypothalamic volume (D) with circulating adiponectin. Spearman correlation test, p>0.05

E-F: correlations of ICV-corrected hypothalamic volume (E) and ICV-corrected posterior hypothalamic volume (F) with BMI, p>0.05).

All correlations were studied using Spearman rank order correlation.

Figure S2: Hypothalamic atrophy is not related with functional status in ALS

A-C: Spearman rank order correlations of ICV-corrected (A) and posterior hypothalamic volume (B) and whole brain volume (C) with ALS-FRS-R.

References:

1. Lattante S, Ciura S, Rouleau GA, Kabashi E. Defining the genetic connection linking amyotrophic lateral sclerosis (ALS) with frontotemporal dementia (FTD). Trends Genet. 2015 May;31(5):263-73.
2. Ludolph AC, Brettschneider J, Weishaupt JH. Amyotrophic lateral sclerosis. Curr Opin Neurol. 2012 Oct;25(5):530-5.
3. Ling SC, Polymenidou M, Cleveland DW. Converging mechanisms in ALS and FTD: disrupted RNA and protein homeostasis. Neuron. 2013 Aug 7;79(3):416-38.
4. Swinnen B, Robberecht W. The phenotypic variability of amyotrophic lateral sclerosis. Nat Rev Neurol. 2014 Nov;10(11):661-70.
5. Braak H, Brettschneider J, Ludolph AC, Lee VM, Trojanowski JQ, Del Tredici K. Amyotrophic lateral sclerosis--a model of corticofugal axonal spread. Nat Rev Neurol. 2013 Dec;9(12):708-14.
6. Brettschneider J, Arai K, Del Tredici K, et al. TDP-43 pathology and neuronal loss in amyotrophic lateral sclerosis spinal cord. Acta Neuropathol. 2014 Sep;128(3):423-37.
7. Brettschneider J, Del Tredici K, Irwin DJ, et al. Sequential distribution of pTDP-43 pathology in behavioral variant frontotemporal dementia (bvFTD). Acta Neuropathol. 2014 Mar;127(3):423-39.
8. Ahmed RM, Irish M, Kam J, et al. Quantifying the eating abnormalities in frontotemporal dementia. JAMA Neurol. 2014 Dec;71(12):1540-6.
9. Ahmed RM, Latheef S, Bartley L, et al. Eating behavior in frontotemporal dementia: Peripheral hormones vs hypothalamic pathology. Neurology. 2015 Oct 13;85(15):1310-7.
10. Piguet O, Petersen A, Yin Ka Lam B, et al. Eating and hypothalamus changes in behavioral-variant frontotemporal dementia. Ann Neurol. 2011 Feb;69(2):312-9.
11. Ahmed RM, Irish M, Henning E, et al. Assessment of Eating Behavior Disturbance and Associated Neural Networks in Frontotemporal Dementia. JAMA Neurol. 2016 Mar 1;73(3):282-90.
12. Ahmed RM, MacMillan M, Bartley L, et al. Systemic metabolism in frontotemporal dementia. Neurology. 2014 Nov 11;83(20):1812-8.
13. Woolley JD, Khan BK, Natesan A, et al. Satiety-related hormonal dysregulation in behavioral variant frontotemporal dementia. Neurology. 2014 Feb 11;82(6):512-20.
14. Bocchetta M, Gordon E, Manning E, et al. Detailed volumetric analysis of the hypothalamus in behavioral variant frontotemporal dementia. J Neurol. 2015 Dec;262(12):2635-42.
15. Ahmed RM, Irish M, Piguet O, et al. Amyotrophic lateral sclerosis and frontotemporal dementia: distinct and overlapping changes in eating behaviour and metabolism. Lancet Neurol. 2016 Mar;15(3):332-42.
16. Gallo V, Wark PA, Jenab M, et al. Prediagnostic body fat and risk of death from amyotrophic lateral sclerosis: the EPIC cohort. Neurology. 2013 Feb 26;80(9):829-38.
17. O'Reilly EJ, Wang H, Weisskopf MG, et al. Premorbid body mass index and risk of amyotrophic lateral sclerosis. Amyotrophic lateral sclerosis & frontotemporal degeneration. 2013 Apr;14(3):205-11.
18. Desport JC, Preux PM, Truong TC, Vallat JM, Sautereau D, Couratier P. Nutritional status is a prognostic factor for survival in ALS patients. Neurology. 1999 Sep 22;53(5):1059-63.
19. Marin B, Desport JC, Kajeu P, et al. Alteration of nutritional status at diagnosis is a prognostic factor for survival of amyotrophic lateral sclerosis patients. J Neurol Neurosurg Psychiatry. 2011 Jun;82(6):628-34.
20. Paganoni S, Deng J, Jaffa M, Cudkowicz ME, Wills AM. Body mass index, not dyslipidemia, is an independent predictor of survival in amyotrophic lateral sclerosis. Muscle Nerve. 2011 Jul;44(1):20-4.
21. Jawaid A, Murthy SB, Wilson AM, et al. A decrease in body mass index is associated with faster progression of motor symptoms and shorter survival in ALS. Amyotroph Lateral Scler. 2010 May 26.
22. Dupuis L, Corcia P, Fergani A, et al. Dyslipidemia is a protective factor in amyotrophic lateral sclerosis. Neurology. 2008 Mar 25;70(13):1004-9.
23. Henriques A, Blasco H, Fleury MC, et al. Blood Cell Palmitoleate-Palmitate Ratio Is an Independent Prognostic Factor for Amyotrophic Lateral Sclerosis. PLoS One. 2015;10(7):e0131512.
24. Lindauer E, Dupuis L, Muller HP, Neumann H, Ludolph AC, Kassubek J. Adipose Tissue Distribution Predicts Survival in Amyotrophic Lateral Sclerosis. PLoS One. 2013;8(6):e67783.
25. Dupuis L, Pradat PF, Ludolph AC, Loeffler JP. Energy metabolism in amyotrophic lateral sclerosis. Lancet Neurol. 2011 Jan;10(1):75-82.
26. Dupuis L, Oudart H, Rene F, Gonzalez de Aguilar JL, Loeffler JP. Evidence for defective energy homeostasis in amyotrophic lateral sclerosis: benefit of a high-energy diet in a transgenic mouse model. Proc Natl Acad Sci U S A. 2004 Jul 27;101(30):11159-64.
27. Wills AM, Hubbard J, Macklin EA, et al. Hypercaloric enteral nutrition in patients with amyotrophic lateral sclerosis: a randomised, double-blind, placebo-controlled phase 2 trial. Lancet. 2014 Feb 27.

28. Dorst J, Dupuis L, Petri S, et al. Percutaneous endoscopic gastrostomy in amyotrophic lateral sclerosis: a prospective observational study. J Neurol. 2015;262(4):849-58.
29. Ahmed RM, Caga J, Devenney E, et al. Cognition and eating behavior in amyotrophic lateral sclerosis: effect on survival. J Neurol. 2016 Jun 3.
30. Huisman MH, Seelen M, van Doormaal PT, et al. Effect of Presymptomatic Body Mass Index and Consumption of Fat and Alcohol on Amyotrophic Lateral Sclerosis. JAMA Neurol. 2015 Oct;72(10):1155-62.
31. Vercruysse P, Sinniger J, El Oussini H, et al. Alterations in the hypothalamic melanocortin pathway in amyotrophic lateral sclerosis. Brain. 2016 Apr;139(Pt 4):1106-22.
32. Nakamura M, Bieniek KF, Lin WL, et al. A truncating SOD1 mutation, p.Gly141X, is associated with clinical and pathologic heterogeneity, including frontotemporal lobar degeneration. Acta Neuropathol. 2015 Jul;130(1):145-57.
33. Cykowski MD, Takei H, Schulz PE, Appel SH, Powell SZ. TDP-43 pathology in the basal forebrain and hypothalamus of patients with amyotrophic lateral sclerosis. Acta neuropathologica communications. 2014;2:171.
34. Dupuis L, Dengler R, Heneka MT, et al. A randomized, double blind, placebo-controlled trial of pioglitazone in combination with riluzole in amyotrophic lateral sclerosis. PLoS One. 2012;7(6):e37885.
35. Brooks BR, Miller RG, Swash M, Munsat TL. El Escorial revisited: revised criteria for the diagnosis of amyotrophic lateral sclerosis. Amyotroph Lateral Scler Other Motor Neuron Disord. 2000 Dec;1(5):293-9.
36. Ludolph A, Drory V, Hardiman O, et al. A revision of the El Escorial criteria - 2015. Amyotrophic lateral sclerosis & frontotemporal degeneration. 2015;16(5-6):291-2.
37. Muller HP, Unrath A, Ludolph AC, Kassubek J. Preservation of diffusion tensor properties during spatial normalization by use of tensor imaging and fibre tracking on a normal brain database. Phys Med Biol. 2007 Mar 21;52(6):N99-109.
38. Malone IB, Leung KK, Clegg S, et al. Accurate automatic estimation of total intracranial volume: a nuisance variable with less nuisance. Neuroimage. 2015 Jan 1;104:366-72.
39. Gabery S, Georgiou-Karistianis N, Lundh SH, et al. Volumetric analysis of the hypothalamus in Huntington Disease using 3T MRI: the IMAGE-HD Study. PLoS One. 2015;10(2):e0117593.
40. Gabery S, Murphy K, Schultz K, et al. Changes in key hypothalamic neuropeptide populations in Huntington disease revealed by neuropathological analyses. Acta Neuropathol. 2010 Dec;120(6):777-88.
41. Kassubek J, Muller HP, Del Tredici K, et al. Diffusion tensor imaging analysis of sequential spreading of disease in amyotrophic lateral sclerosis confirms patterns of TDP-43 pathology. Brain. 2014 Jun;137(Pt 6):1733-40.
42. Tognin S, Rambaldelli G, Perlini C, et al. Enlarged hypothalamic volumes in schizophrenia. Psychiatry Res. 2012 Nov 30;204(2-3):75-81.
43. Terlevic R, Isola M, Ragogna M, et al. Decreased hypothalamus volumes in generalized anxiety disorder but not in panic disorder. J Affect Disord. 2013 Apr 25;146(3):390-4.
44. Brettschneider J, Del Tredici K, Toledo JB, et al. Stages of pTDP-43 pathology in amyotrophic lateral sclerosis. Ann Neurol. 2013 Jul;74(1):20-38.

Figures

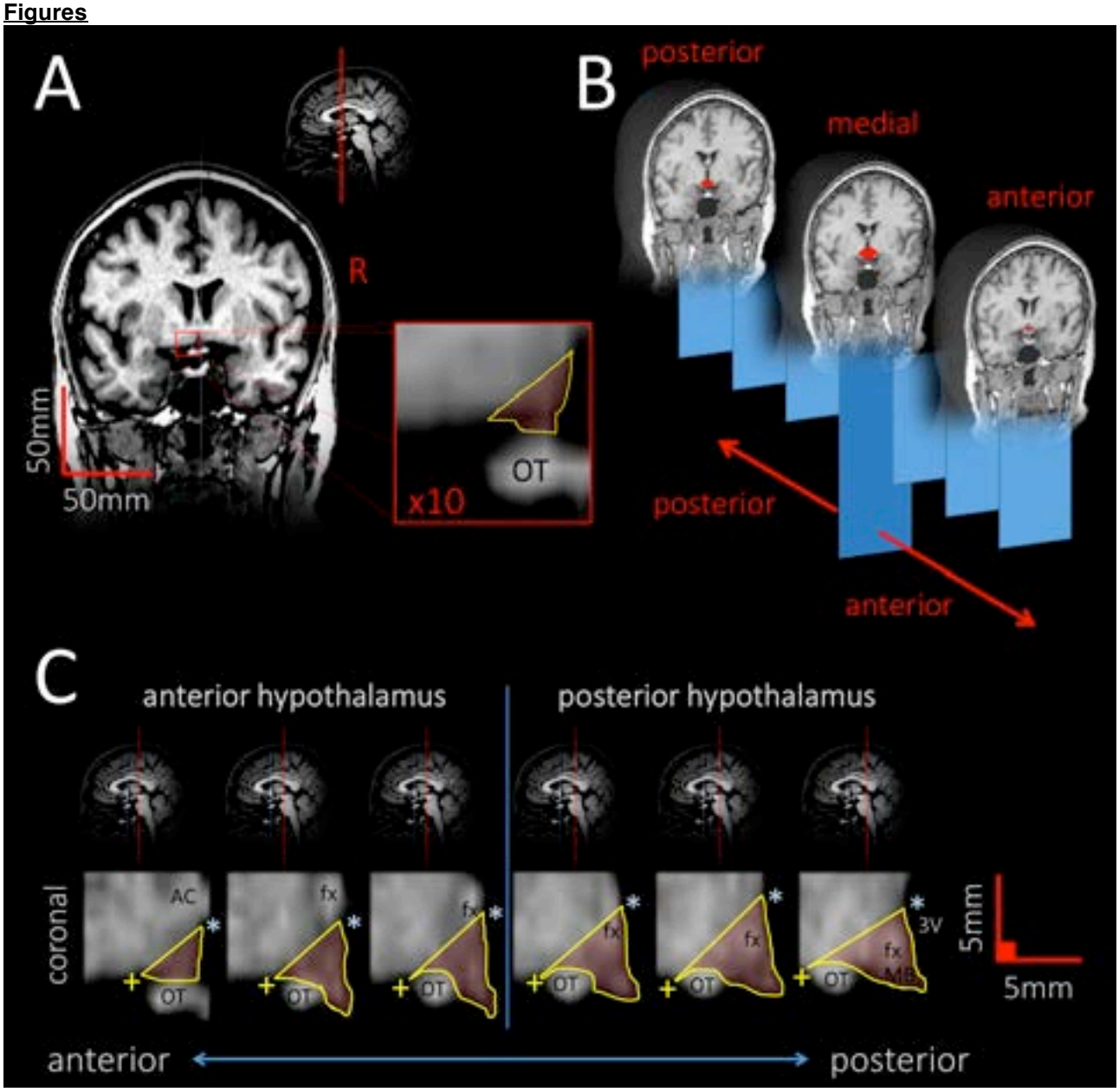

Figure 1: Volumetric analysis of the hypothalamus. Example of hypothalamus delineation in one representative healthy subject (female, 58 years) based on 1.5T high-resolution magnetization-prepared gradient echo image (MPRAGE) data (voxel size: 1.0x1.2x1.0 mm^3). (**A**) Coronal slice through the most anterior part of the hypothalamus and example of delineation for the left-hemispheric part (resampled in-plane resolution 62.5x62.5 μm^2). (**B**) Delineation was performed on a consecutive sequence of coronal slices in anterior-posterior direction at a resampled slice thickness of 0.5 mm. Then, the hypothalamus was subdivided into an anterior and posterior part using the criteria reported by Piguet et al. [7](**C**) Consecutive sequence of each second coronal slice in anterior-posterior direction showing the boundaries (yellow line) used to delineate the hypothalamus according to technique by Gabery et al.[35] The hypothalamic sulcus (*) and the lateral edge of the optical tract (+) were used as landmarks; the most anterior slice (left panel) was defined where the optic chiasm was attached to the ventral part of the septal area and the most posterior slice (right panel) was defined where the fornix (fx) appears to be merged with the mammilary body (MB). The optical tract (OT) was excluded from all slices. AC=anterior commissure; 3V=third ventricle.

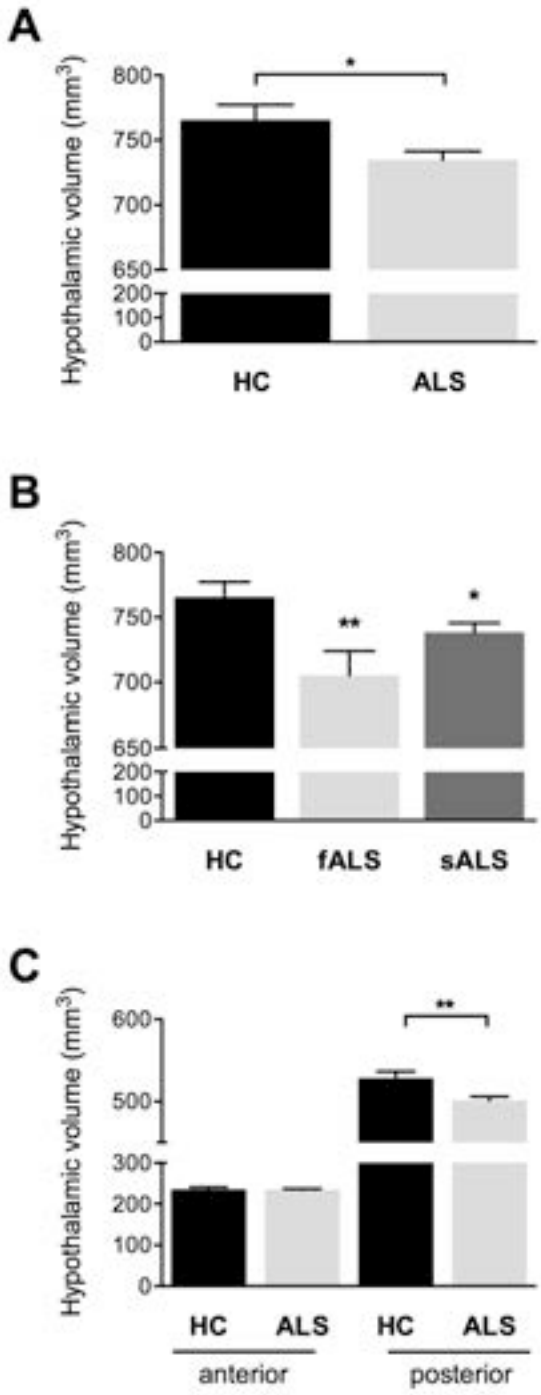

Figure 2: modest hypothalamic atrophy in ALS

A: ICV corrected volume of the hypothalamus (in mm^3) in healthy controls (HC, *n* = 98) and ALS patients (n = 270) (mean +/- SEM),* *p*=0.019..

B: ICV corrected volume of the hypothalamus (in mm^3) in healthy controls (*n* = 98), familial ALS patients (fALS, *n* = 30) and sporadic ALS cases (sALS, *n*=240), * p = 0.02 fALS versus healthy controls, and p=0.039 sALS versus healthy controls.

C: ICV corrected volume of the anterior and posterior hypothalamus (in mm^3) in healthy controls (*n* = 98) and ALS patients (*n* = 270), ***p*=0.002.

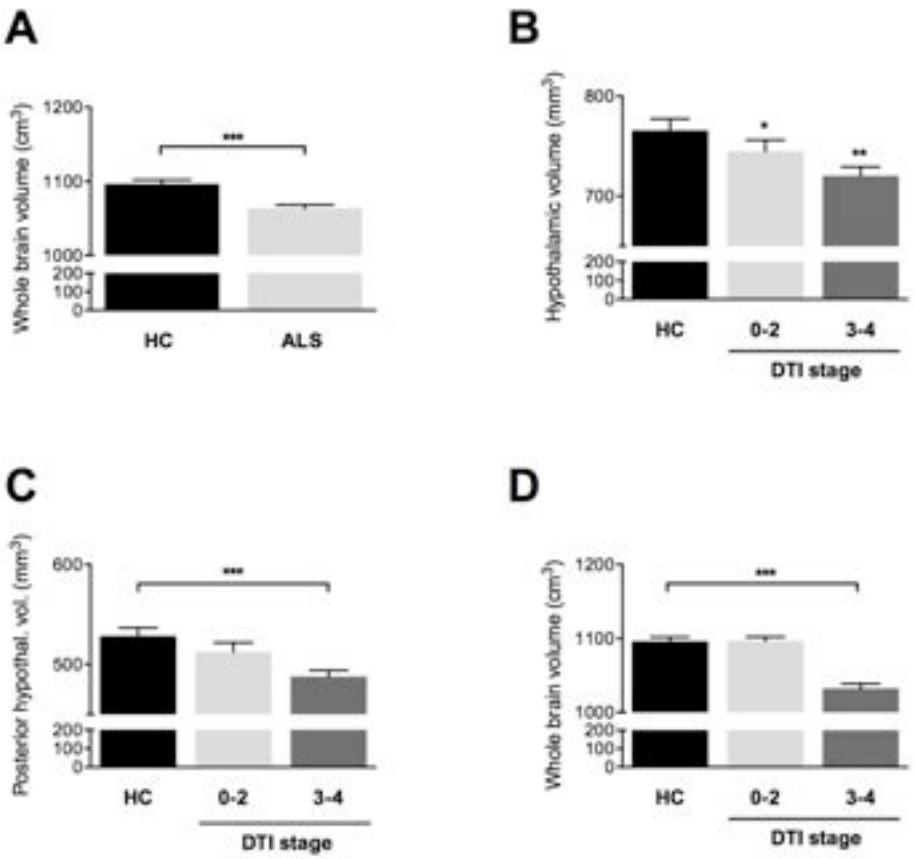

Figure 3: hypothalamic atrophy is related with disease progression and brain atrophy in ALS
A : ICV corrected whole brain volume relative (in cm^3) in healthy controls (HC, $n = 98$) and ALS patients ($n = 270$), *** $p<0.001$.
B-D: ICV corrected hypothalamic volume (in mm^3, B), posterior hypothalamic volume (in mm^3, C) and WBV (in mm^3, D) in healthy controls (HC) and ALS patients stratified by DTI stages. *$p<0.05$, **$p<0.01$, ***$p<0.001$.

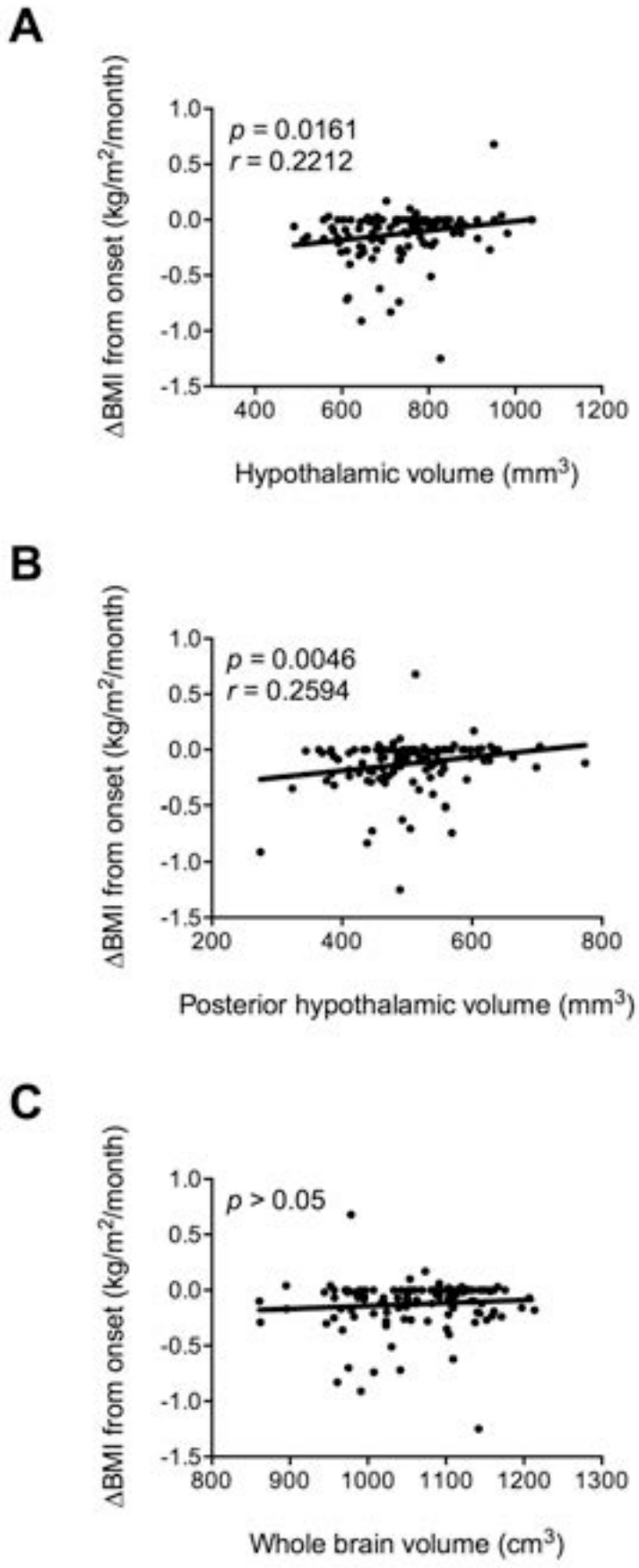

Figure 4: hypothalamic atrophy is related with previous weight loss in ALS
A-C : correlations of hypothalamic volume (in mm^3, A), posterior hypothalamic volume (in mm^3, B) and ICV corrected whole brain volume (in cm^3, C) with the rate of BMI change between onset of symptoms and MRI (expressed in kg/m^2/month). N=118, Spearman correlation test.

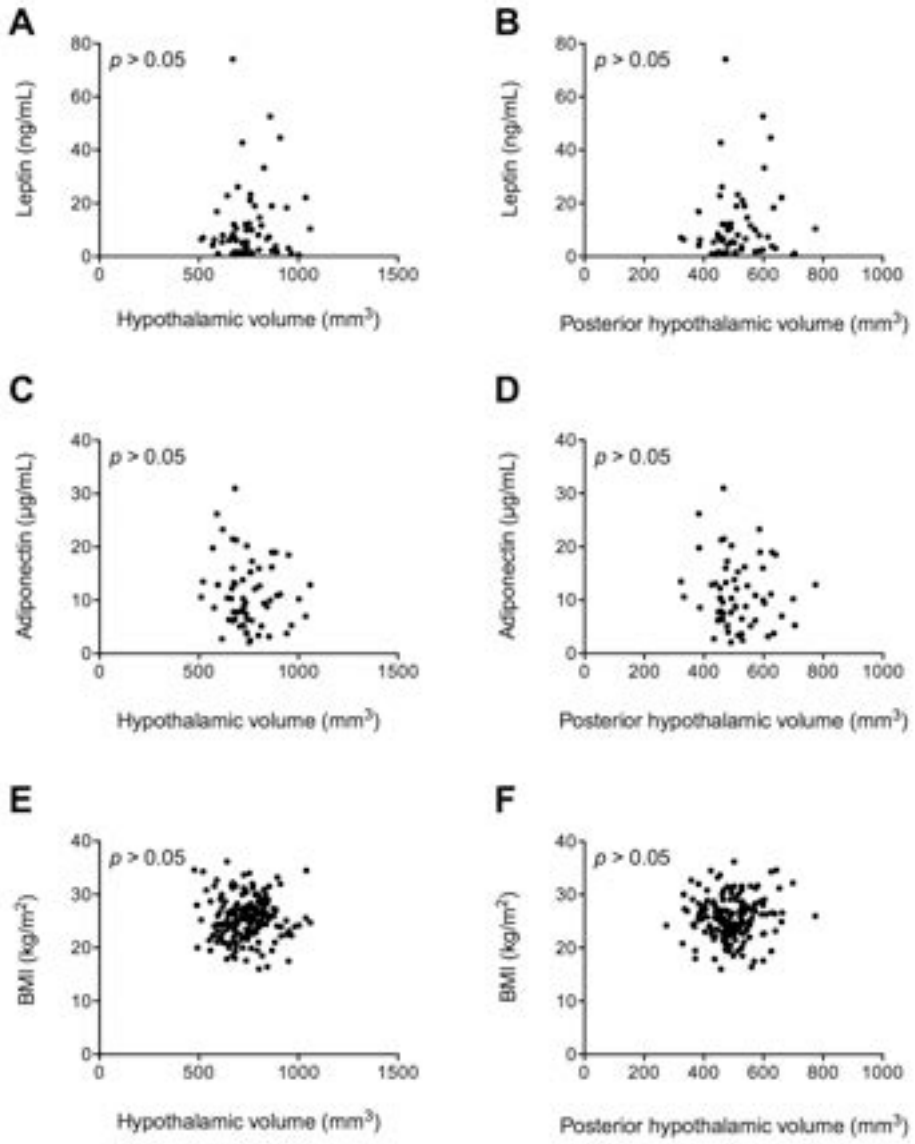

Figure S1: hypothalamic atrophy is not related with metabolic status at MRI
A-B: correlations of ICV-corrected hypothalamic volume (in mm^3, A) and posterior hypothalamic volume (in mm^3, B) with circulating leptin (ng/mL). Spearman correlation test, p>0.05
C-D: correlations of ICV-corrected hypothalamic volume (in mm^3, C) and ICV-corrected posterior hypothalamic volume (in mm^3, D) with circulating adiponectin (μg/mL). Spearman correlation test, p>0.05
E-F: correlations of ICV-corrected hypothalamic volume (in mm^3, E) and ICV-corrected posterior hypothalamic volume (in mm^3, F) with BMI (in kg/m^2) . Spearman correlation test, p>0.05

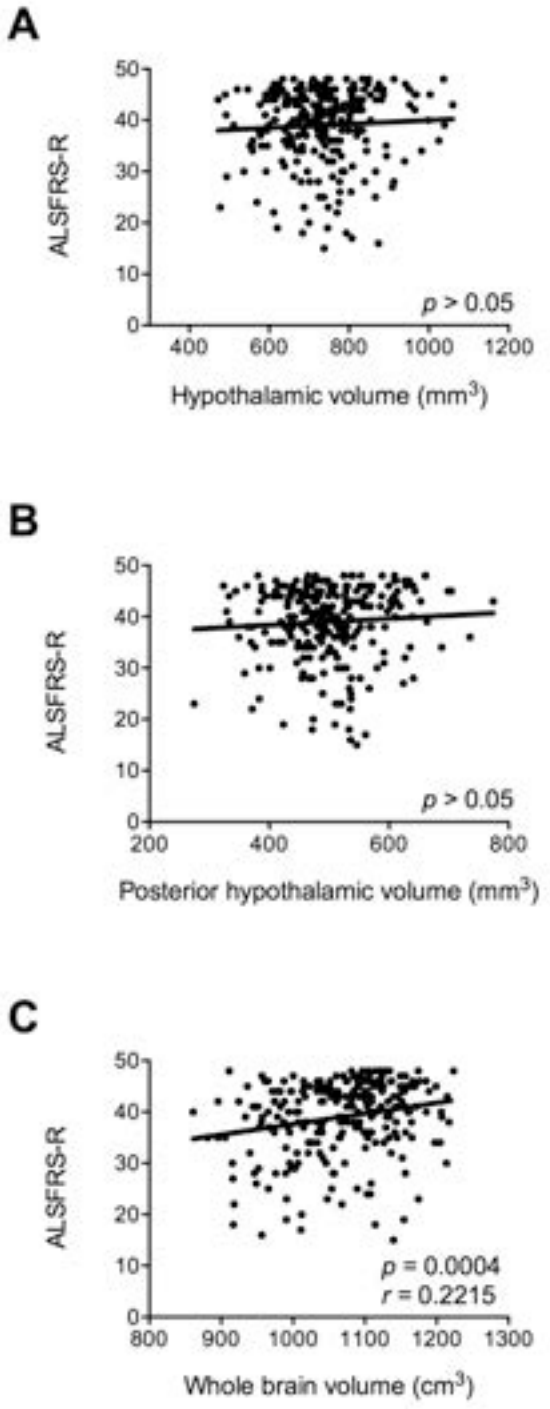

Figure S2: hypothalamic atrophy is not related with functional status in ALS
A-C : correlations of ICV-corrected (in mm^3, A) and posterior hypothalamic volume (in mm^3, B) and whole brain volume (in cm^3, C) with ALS-FRS-R. N=255, Spearman correlation test.

I. Results #3

A. Résumé – Publication #3

« Melanin-concentrating hormone (MCH) rescues weight loss in an animal model of amyotrophic lateral sclerosis»

Associée aux symptômes moteurs, la perte de poids est un symptôme majeur de la Sclérose Latérale Amyotrophique. L'importance de cette perte de poids est corrélée à la survie, et la contrecarrer permet d'améliorer la survie. Cependant, les mécanismes sont inconnus et aucune approche thérapeutique n'existe pour traiter ce symptôme important.

Dans cette publication, notre objectif était d'identifier le mécanisme de la perte de poids, pour permettre de concevoir une approche thérapeutique.

Nos travaux précédents avaient montré une atteinte du système mélanocortine du noyau arqué pouvant être à l'origine de l'anomalie du comportement alimentaire (Publication 1). Cependant, l'implication de l'hypothalamus dans la perte de poids n'était pas connue.

Avec notre étude volumétrique, nous avons montré que la partie postérieure de l'hypothalamus, comprenant 4 noyaux, était la plus atteinte et liée à la perte de poids (Publication 2). De plus, une étude précédente avait mis en évidence une pathologie précisément dans l'un de ces noyaux, l'hypothalamus latéral (LHA). Ainsi nous voulions savoir si ce noyau précis avait un lien avec la perte de poids dans un modèle murin de la SLA.

Tout d'abord, nous avons montré que le LHA est spécifiquement atteint dans la SLA chez les patients et dans le modèle murin. En accord avec l'étude précédente, nous avons trouvé des agrégats pathologiques pTDP-43 dans le LHA, mais pas dans le noyau arqué chez les patients SLA. Des agrégats p62 et Ubiquitine ont été observés dans le LHA, mais pas dans le noyau arqué, des modèles murins dès un âge non symptomatique. Cependant, les deux types neuronaux les mieux documentés du LHA, les neurones MCH et neurones Orexin, ne développent que peu d'agrégats pathologiques. Ensuite, nous avons mis en évidence une perte des neurones MCH dès un âge non symptomatique. Enfin, nous avons injecté par icv le neuropeptide MCH pour compenser cette perte. Le traitement a permis d'augmenter le poids des souris *Sod1(G86R)*. Nous pouvons donc affirmer que la perte de MCH est la cause

de la perte de poids dans un modèle murin. Notre étude permet d'identifier une cible thérapeutique pour traiter la perte de poids dans la SLA.

---Manuscript in preparation---

Melanin-concentrating hormone (MCH) rescues weight loss in an animal model of amyotrophic lateral sclerosis

Pauline Vercruysse, Jérôme Sinniger, Stéphane Dieterlé, Dietmar R. Thal, Albert C. Ludolph & Luc Dupuis

Abstract

Amyotrophic lateral sclerosis (ALS) is associated with profound weight loss that is negatively associated with survival. The neural mechanisms underlying weight loss in ALS remain unknown, and we recently showed that atrophy of the hypothalamus was correlated with weight loss. The hypothalamus includes a complex network of neuropeptides expressed in different nuclei that collectively regulate energy balance. Here, we show that ALS patients display ALS-related TDP-43 pathology in the lateral hypothalamic area (LHA) nuclei, but not in the arcuate nucleus. Consistently, p62 and ubiquitin aggregates progressively accumulate in neurons of the LHA and ventro-medial nuclei in transgenic mice expressing ALS-associated SOD1(G86R) mutation, but these aggregates were absent from the arcuate nucleus. Numbers of lateral hypothalamic neurons producing melanin-concentrating hormone (MCH), a neuropeptide involved in feeding behavior and energy balance, were decreased in SOD1(G86R) mice. Importantly, continuous icv delivery of a low non orexigenic dose of MCH allowed to completely rescue weight loss of SOD1(G86R) mice, while not modifying body weight of wild type mice. Thus, MCH neurons, located in the LHA, are affected during disease progression, significantly contributing to weight loss in ALS.

Introduction

Amyotrophic lateral sclerosis (ALS), also called Lou Gehrig's disease or Charcot's disease, is a rapidly progressive, invariably fatal neurological disease affecting motor neurons. The average life expectancy after the diagnosis is approximately 2 years, making it one of the most fatal neurological diseases associated with the highest unmet medical need.

Motor symptoms of ALS are frequently accompanied by weight loss that can be pronounced and is clinically explained by a combination of dysphagia and hypermetabolism[1, 2]. Even before onset of motor symptoms, ALS patients are generally lean with normal or low BMI[3, 4]. The magnitude of weight loss[5-8] as well as multiple metabolic indices [9-11] are tightly associated with the survival of patients. Importantly, counteracting weight loss through increased energy content of the diet increased survival of ALS mouse models[12], and showed efficacy in a pilot clinical trial in gastrostomized ALS patients[13]. Despite this clinical relevance, the biological mechanisms underlying weight loss remain unknown and consequently there is no pharmacological approach to treat ALS associated weight loss.

The hypothalamus is the major regulatory center of energy homeostasis in human brain[14, 15]. Central and peripheral signals are integrated by a complex network of neuropeptidergic neurons located in a subset of hypothalamic nuclei, including the arcuate nucleus, the Paraventricular Nucleus (PVN), the Dorsomedial Nucleus (DMN), the Ventromedial Nucleus (VMN) and the Lateral Hypothalamic area (LHA)[14, 15]. Recently, we showed that the melanocortin pathway, the major pathway controlling food intake in the arcuate nucleus is altered in both mouse models and ALS patients[16]. Indeed, levels of AgRP, a potent orexigenic

neuropeptide, were increased, while levels of its antagonist pro-opiomelanocortin (POMC) were decreased in a mouse model of ALS[16]. ALS patients did not gain weight in response to pioglitazone, a drug known to increase food intake through relays in the arcuate nucleus[16, 17]. The melanocortin pathway could thus be a major player in the altered eating behaviour of ALS patients[18, 19], yet it remains unclear whether and how altered hypothalamic signaling could be involved in weight loss.

Most recently, we performed a volumetric analysis of an extended cohort of ALS patients and compared to controls. We observed a moderate atrophy of the hypothalamus, prominently in its posterior part, that was correlated with previous weight loss. The posterior part of the hypothalamus includes most of the LHA, as well as dorsomedial, ventromedial and posterior hypothalamic nuclei, and our study could therefore not assign the observed atrophy to a specific hypothalamic nucleus. However, the atrophy of the posterior hypothalamus is consistent with the recent observation of pTDP43 pathology in the LHA of ALS patients[20].

Here, we show that the LHA is selectively affected in ALS, and that the loss of one its neuropeptidergic neuronal type, MCH neurons, is instrumental in the development of weight loss. This finding identifies a druggable pathway to treat weight loss in ALS.

Materials and Methods

Patients

10 ALS patients and 10 non ALS, non neurological controls from the brain bank of the department of Neurology of Ulm were included in the pathology study. Details on the disease of these cases are included in Table 1. All patients and controls gave informed consent for research.

Animals

Transgenic mice were housed in the animal facility of the medicine faculty of Strasbourg University, with 12 h/12 h of light/dark and unrestricted access to food and water. In all experiments, littermates were used for comparison. Transgenic SOD1(G86R) were maintained in their initial FVB/N genetic background according to previous studies[21].

For histological analysis, animals were anesthetized by intraperitoneal injection of ketamine (Imalgène 1000®, Merial, Lyon France; 90 mg/kg body weight) and xylazine (Rompun 2% ®, Bayer, Leverkusen, Germany; 10 mg/kg body weight) at the ages indicated at 2PM. After perfusion of 4% paraformaldehyde (v/v PFA, Sigma, St Louis, MO, USA), brains were removed, stored in the same fixative overnight at 4°C and stored in phosphate buffered saline (PBS) until used. These experiments were authorized by the local ethical committee of Strasbourg University (CREMEAS).

Drugs and treatments

MCH (Sigma, St Louis, MO, USA) was administrated by IntraCerebral Injection (ICV) using continuous delivery through Alzet osmotic mini-pumps (see below). Artificial Cerebro-Spinal Fluid (a-CSF) was used as vehicle in ICV experiment. aCSF was composed of 119mM NaCl, 26.2mM $NaHCO_3$, 2.5mM KCl, 1mM NaH2PO4, 1.3mM $MgCl_2$, 10mM glucose, 2.5mM $CaCl_2$.

Surgery

75 days old-mice were anesthetized with ketamine and xylazine (respectively 90mg/kg from Imalgene 1000, Merial, Lyon, France and 10mg/kg from Rompun 2%, Bayer, Puteaux, France).Prior to the surgery, 50µL of lidocaine (21.33mg/mL, Xylovet, Ceva, Libourne, France) was injected under the skin at the place of the head skin incision. A sterile brain infusion cannula of Brain Infusion Kit 3 (28-gauge; Alzet, Palo Alto, CA) was stereotaxically implanted into the left lateral ventricle. When a flat skull position was used, the stereotaxic coordinates were 0.4 mm posterior to the bregma, 0.8 mm left lateral to the midline, and 2.0 mm from the surface of the skull. The cannulas were fixed to the skull with instant adhesive gel (loctite 454). The infusion cannula was connected to an osmotic minipump (Alzet, model no. 2002) that was pre-filled with MCH (0.1mg/mL) or vehicle (aCSF) and had polyvinyl chloride tubing. The mini-pump was then implanted under the skin of the back, and care was taken to clean wound properly with antiseptics. Prior to the implantation, pumps and Brain Infusion Kit were prepared at a depth of 2.0mm and according manufacter's recommendation especially with overnight

incubation at 37°C in 0.9% saline solution. Body weight and daily food intake were measured daily between 11am and 1pm during 13 days.

Histology of mouse brain

Fixed brains were included in 6% (w/v) agar (Sigma, St Louis, MO, USA) and sectioned from Bregma 0.02mm to Bregma -2.90mm into 40µm coronal sections on a vibratome. Lateral hypothalamus was identified according to Paxinos Brain Atlas. p62, ubiquitine, MCH (Melanin Concentrating Hormone), ORX (Orexin), NeuN immunohistochemistries were performed on anatomically matched floating sections using standard histological techniques. Sections were treated in citrate buffer (1mM, pH6) at 80°C. Permeabilization and saturation of nonspecific sites were done with 0.5%(v/v) Triton (Sigma, St Louis, MO, USA), 5% (v/v) Horse serum (Gibco, Oukland, New-Zeland) and 50mg/ml Bovine Albumin Serum (BSA, Sigma, St Louis, MO, USA). Guinea Pig anti-p62 primary antibody (Progen, Heidelberg, Germany; 1:100) or mouse anti-ubiquitine primary antibody (Millipore, Billerica, MO, USA; 1:200) were incubated overnight at room temperature with goat anti-orexin primary antibody (Santa-Cruz Biotechnology, Dallas, TX, USA; 1:200) and rabbit anti-MCH primary antibody (Phoenix Peptide, Burlingame, CA, USA; 1:1000) or with rabbit anti-NeuN primary antibody (Millipore, Darmstadt, Germany; 1:1000). Alexa-594 donkey anti-Guinea Pig secondary antibody (Jackson, West Grove, PA, USA; 1:500) or Alexa-594 donkey anti-Mouse secondary antibody (Molecular Probes, Thermo Fisher Scientific, Waltham, MO, USA; 1:500) were incubated with during 90 minutes at room temperature with Alexa-488 donkey anti-Goat secondary antibody (Bethyl, Montgomery, TX, USA; 1:500) and Cy3 donkey anti-Rabbit secondary antibody (Jackson, West Grove, PA, USA; 1:500) or Alexa-488

donkey anti-rabbit secondary antibody (Jackson, West Grove, PA, USA; 1:500).

Quantification of MCH neurons

To quantify MCH neuronal numbers, immunohistochemistry was performed on one every two sections over the whole lateral hypothalamic area. Immunohistochemistry was performed on floating sections using standard histological techniques. Endogenous peroxidases were inactivated using 3% (v/v) H_2O_2. Permeabilization and saturation of nonspecific sites were done with 0.25%(v/v) Triton (Sigma, St Louis, MO, USA) and 50mg/ml Bovine Albumin Serum (BSA, Sigma, St Louis, MO, USA). Rabbit anti-MCH primary antibody (Phoenix Peptide, Burlingame, CA, USA; 1:2000) was incubated overnight at room temperature. Biotinylated donkey anti-Rabbit secondary antibody (Jackson, West Grove, PA, USA; 1:500) was incubated during 90 minutes at room temperature. Staining was performed using Vectastain Elite ABC kit (Vector, Burlingame, CA, USA). After revelation with 3,3'-Diaminobenzidine (DAB, Sigma, St Louis, MO, USA; 0.5mg/ml), sections were mounted and images of all sections were taken.

Imaging and quantification of immunofluorescence and immunohistochemistry

For immunofluorescence, Z-Stack images (3µm optical section) were acquired using apotome module (Zeiss 2) on Zeiss microscope (AX10, Imager M2) equipped with 10× objective (NA 0.45) and a Hamamatsu camera (C11440) with tiles option of Zeiss module. Higher magnification images were obtained using Z-stack images (1µm optical section) of lateral hypothalamic

aggregates with 63x oil-objective (NA 1.4). Gain, exposure, and light settings were kept the same when acquiring all images of a given staining. Total of p62 or ubiquitine aggregates were determined for each section with Alexa 594 channel picture on ImageJ software (version 1.50i). Colocalization of aggregates and neurons was determined for each section with Alexa 594 channel, Cy3 channel and Alexa 488 channel pictures on Zeiss Zen software (blue edition).

For immunohistochemistry, Bright-field images of lower brain part were acquired with a Nikon DS –Ri1 camera attached to a Nikon microscope (Nikon Eclipse E800) fitted with respectively a Plan Apo 4x lens (N.A.=0.20) and a plan Apo 10x lens (N.A.=0.45). White balance, gain, exposure, and light settings were kept the same when acquiring all images. Total numbers of MCH positive cell bodies in the arcuate nucleus were determined for each animal and normalized per section.

All quantifications were performed by an operator blinded to the genotype or disease status.

Histology of human brain

Paraffin included human hypothalamus were sectioned in 70µm sections according to the method previously described [22]

Every 10 cuts, after deparaffination, free-floating sections were processed immunohistochemically. Endogenous peroxidases were inactivated using 3% (v/v) H_2O_2. Antigen retrieval with performic acid buffer was done in steamer during 30 minutes before permeabilization and saturation of nonspecific sites with 0.25%(v/v) Triton (Sigma, St Louis, MO,

USA) and 50mg/ml Bovine Albumin Serum (BSA, Sigma, St Louis, MO, USA). Rabbit anti-pTDP43 (kindly provided by Pr Braak, 1:10000) primary antibody was incubated overnight at room temperature. Biotinylated donkey anti-Rabbit secondary antibody (1:200) and was incubated during 90 minutes at room temperature. Staining was performed using Vectastain Elite ABC kit (Vector, Burlingame, CA, USA). After revelation with 3,3'-Diaminobenzidine (DAB, Sigma, St Louis, MO, USA; 0.5mg/ml), sections were dehydrated and mounted [22].

Statistical analysis

For all experiments, comparison of two groups was performed using unpaired Student's t-test, except for p62 and ubiquitine aggregates quantification performed using t-test with nonparametric test. Comparison of three or four groups was performed using One-way ANOVA and Tukey *post-hoc* test. Statistics were performed using Prism version 6.0.

All results from analysis were regarded as hypothesis generating only. All statistical tests were carried out two-sided at a significance level of 5%.

Results

pTDP-43 inclusions in the lateral hypothalamus of ALS patients

In order to characterize the pathological alterations in the hypothalamus in ALS, we stained hypothalamic sections of ALS patients (n=10) and controls (n=10) for phosphorylated TDP43 (pTDP43), the major component of ubiquitin positive inclusions in ALS[23, 24]. We barely observed pTDP43 pathology in the infidibulate nucleus (arcuate nucleus in humans), while pTDP43 inclusions were common in the LHA (Figure 1A-C). Quantification of the frequency of pTDP43 pathology using a semi-quantitative scale revealed a prominent pTDP43 pathology in the LHA and a complete preservation of the arcuate nucleus (Figure 1D). Thus, the lateral hypothalamic area is selectively affected over other hypothalamic nuclei in ALS.

Progressive development of p62 and Ubiquitin inclusions in the lateral hypothalamus of SOD1(G86R) mice

In order to extend these initial findings, we studied the hypothalamic pathology of a transgenic mouse model of ALS, expressing ALS-associated SOD1(G86R) mutation. These mice do not develop TDP-43 positive inclusions, but rather inclusions positive for p62, a ubiquitin binding protein that accumulates upon UPS or autophagic dysfunction. In a manner analogous to pTDP43 pathology in ALS patients, p62 positive aggregates were observed primarily in the LHA of mutant SOD1 mice at 75 days of age, an age showing mild weight loss and no motor symptoms (Figure 2A). p62 inclusions were also observed in the ventro-medial nucleus (VMN).

The number of p62 positive inclusions exponentially increased at 90 days of age (early symptomatic) and 105 days of age (symptomatic) in LHA and VMN, while p62 inclusions were neither observed in the arcuate nucleus nor in the dorso-medial nucleus (DMN) (Figure 2A-B). Identical results were obtained when using ubiquitin as a marker of protein inclusions (Figure 3). Thus, the LHA is early and selectively affected during ALS in both patients and mouse models.

Protein aggregates in the LHA are neuronal but rarely observed in MCH or orexin neurons

We then sought to determine whether specific neuronal types are affected by the disease in the LHA. Two major neuropeptidergic populations are present in the LHA, namely orexin (ORX) and melanin-concentrating hormone (MCH) neurons. We performed triple labelling with ORX, MCH and either p62 or ubiquitin antibodies. Intriguingly, the vast majority of p62 or ubiquitin positive inclusions were neither ORX nor MCH positive (Figure 3A). A small percentage of inclusions occurred in ORX neurons (Figure 3B) and we barely detected inclusions in MCH neurons (Figure 3B). These aggregates were however mostly found in NeuN positive neurons or displayed typical neuronal morphology even if negative for NeuN (Figure 4). Thus, ALS pathology affects neurons of the LHA that are mostly not MCH or ORX neurons.

Loss of MCH expressing neurons in SOD1(G86R) mice

We then sought to determine whether MCH or ORX neurons were affected by the disease. Since previous results[16] showed an early and sustained downregulation of MCH in the hypothalamus

of SOD1(G86R) mice[16], we focused our efforts on MCH and counted the number of MCH positive neurons in the LHA of SOD1(G86R) mice (Figure 5A). Consistent with the previously observed decreased MCH expression, we observed about 30% less MCH-positive neurons in the LHA of SOD1(G86R) mice as compared with their wild type littermates at 75 days of age and almost 50% less at onset (Figure 5B-F). Indeed, MCH-positive neurons showed in general overall decreased MCH immunoreactivity (Figure 5E-F).

Complementation with icv delivered MCH rescues weight loss in SOD1(G86R) mice

We then asked whether the loss of MCH could be responsible for weight loss in SOD1(G86R) mice. To answer this question, 75 days old SOD1(G86R) mice and control littermates were implanted surgically implanted with a cannula stereotactically inserted in the lateral ventricle. The cannula was connected with osmotic mini-pumps filled either with vehicle (aCSF) or with MCH allowing a constant delivery of MCH at a rate of 1,2ug/day during 13 days intra-cerebro ventricularly. Importantly, this dose is 3 times lower than doses known to increase food intake[25]. MCH ICV administration led to sustained increased weight gain in mutant SOD1 mice (Figure 7A), but not in wild type controls (figure 7A). Indeed, daily weight gain of MCH-treated SOD1m mice was similar to the weight gain of wild type mice (Figure 7B). Consistent with the low dose delivered, we did not observe increases in food intake in any group (Figure 7C), suggesting that MCH restored energy balance through an effect on energy expenditure rather than on food intake. Thus, MCH complementation is sufficient to revert weight loss in ALS mice.

Discussion

Our current study brings about two major results. First, the lateral hypothalamus is selectively affected in ALS, both in patients and animal models. Second, MCH neurons, located in the LHA, are affected during ALS, and MCH complementation is sufficient to rescue weight loss in mutant SOD1 mice. These two major results have consequences for our understanding of disease pathogenesis, and provide avenues to pharmacologically target weight loss in ALS.

Our first important result is that only a subset of hypothalamic nuclei are affected during ALS disease. In patients, pTDP43 aggregates were found in LHA and not in Arcuate Nucleus, another key nucleus for energy homeostasis. This observation is completely consistent with the report of Cykowski and collaborators who also observed pTDP43 pathology in the LHA of ALS patients[20], while Nakamura and collaborators recently observed hypothalamic pathology in a patient carrying a *SOD1* mutation[26]. We previously showed that the hypothalamus was atrophied in a large cohort of ALS patients, and this atrophy was mostly posterior, a region that includes notably the LHA (Vercruysse, submitted). Thus, our current study confirms these initial observations in patients, and extends them to an animal model of ALS, SOD1(G86R) mice that displayed similar selective involvement of a subset hypothalamic nuclei. In mice, p62 and ubiquitin positive aggregates were observed mostly in the LHA and VMN, but spared completely the arcuate nucleus or the DMN. Importantly, these inclusions were observed at non-symptomatic ages, and exponentially increased with disease progression. Thus, hypothalamic involvement is early and selective in mouse models. In this respect, it is important to note that,

despite species differences as well as differences in etiology, SOD1(G86R) mice reliably replicated the pattern of hypothalamic pathology observed in patients.

We then sought to characterize in more details the affected neurons. The two major neuronal types of the LHA are MCH and orexin neurons. However, neither MCH nor orexin neurons were the major neuronal type developing prominent p62 or ubiquitin inclusions. Many of the cells developing p62/Ubiquitin positive aggregates were either of neuronal morphology or expressing the neuronal marker NeuN. Besides MCH and orexin neurons, the LHA also includes a number of other neuronal types, in particular neurons expressing the leptin receptor (LepRb), mostly co-expressing the neurotensin peptide[27]. Interestingly, most of these LepRb expressing neurons express also the melanocortin receptor MC4R [28], suggesting that the development of p62 or ubiquitin pathology could be downstream of the melanocortin impairment we previously observed in the mouse model[16]. Further studies are required to elucidate the identity of these affected neurons as several other GABAergic neuronal populations have been postulated to exist in the LH[27].

Despite MCH neurons did not develop p62 or ubiquitin inclusions, they were severely affected by the disease process. Indeed, our previous results identified an early and sustained downregulation of MCH mRNA[16], and we now show that this downregulation translates into a progressive loss of MCH positive neurons in the LHA. Loss of MCH leads to leanness, that is mostly caused by increased energy expenditure, and associated with hypophagia in a mixed background[29, 30]. Consistently, loss of MCH, lead to decreased hypothalamic POMC levels[29], increased energy expenditure in obese mice as well as in aged mice[31, 32], while injection or overexpression of MCH triggered obesity[33], decreased energy expenditure [34] and sympathetic

tone[35]. It is noteworthy that weight loss[12], increased energy expenditure[12] and decreased hypothalamic POMC levels[16] are also typical features of SOD1(G86R) mice, and we hypothesized that the weight loss of SOD1(G86R) mice could be caused by MCH loss. Importantly, the weight loss of SOD1(G86R) mice was completely rescued by MCH icv delivery, and this effect was not due to hyperphagia as we did not observe increased food intake in our cohort of mice. Several mechanisms could account for the shift in metabolism in MCH-treated SOD1(G86R) mice. In particular, MCH administration was most likely able to decrease ALS-linked hypermetabolism. It is also possible that MCH re-orientated lipid metabolism through the sympathetic nervous system[36]. Further studies are required to elucidate the mechanisms of protection by MCH in ALS mice, and determine whether MCH delivery also modifies the motor symptoms developed by SOD1(G86R) mice.

A major question arising from our results is how MCH neurons, and more generally LHA, are involved in ALS progression. According to the centrifugal model of diseases pathogenesis by Braak and collaborators[24, 37], pTDP-43 pathology spreads from the motor cortex to anatomically connected regions. It is noteworthy that MCH neurons are anatomically connected to the sensory-motor cortex [38], and, in general, the LHA is densely connected to the cortex as well as to many other brain and spinal cord areas[27, 39]. The observation of hypothalamic atrophy in stage 3/4 ALS patients both in DTI-staging (Vercruysse, submitted) and in pathology studies [20], would be consistent with involvement of the LHA as a secondary consequence of disease progression. Our current results, together with previous efforts from our group (Vercruysse, submitted) and others [20], suggest that this propagation of ALS disease to the LHA is the major

cause of weight loss in ALS. This suggests that agonizing the MCH receptors could treat weight loss in ALS patients, and this is relevant as drugs known to increase food intake through the melanocortin pathway were inefficient in increasing weight in ALS patients[16]. Thus, our current study identifies a selective hypothalamic pathology, that opens new avenues to treat weight loss in ALS patients in a disease relevant manner.

Table 1:

	Age	Sex	Cause of death
ALS	68	M	ALS
	75	M	ALS
	57	M	ALS
	43	M	ALS
	61	F	ALS
	50	M	ALS
	75	M	ALS
	74	M	ALS
	63	M	ALS
	84	M	ALS
control	46	M	Cardiac insufficiency
	45	M	Myocardial infarct
	76	M	Cardiac insufficiency
	63	F	Multiple Sclerosis
	74	M	Myocardial infarct
	55	M	Epilepsie
	57	M	Infection
	58	F	Lung cancer
	66	M	Myocardial infarct
	73	M	Lung cancer

Figures

Figure 1: pTDP43 pathological staining in the lateral hypothalamus of post-mortem patient tissues

(A,B,C): Representative images are shown for ALS patients (scale bar 10µm).(D): pTDP43 staining in the lateral hypothalamus Area (LHA) and Arcuate Nucleus (Arc) were scored by a blind observer in ALS post mortem patient tissues as compared with their control patient tissues (n=10). * p<0.05, Student's t-test. Data are presented as mean and SE.

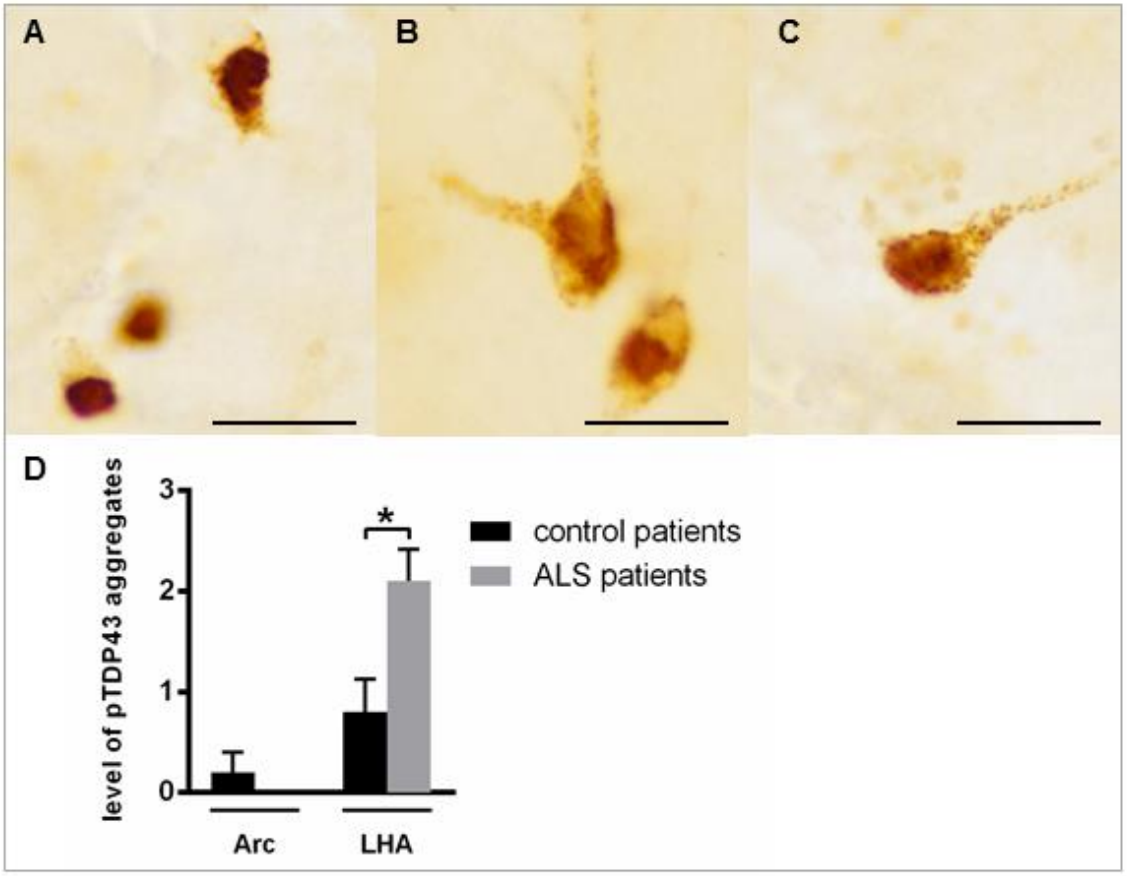

Figure 2: p62 pathological aggregates in hypothalamus of mice.
p62 immunohistochemistry was performed on selected sections after identification of area of hypothalamus according to Paxinos Brain Atlas (A, right column). Representative images are shown for SOD1 (G86R) (b,c,d) mice and control littermates (a) at 75 days (a, b), 90 days (c) and 105 days (d) (scale bar 500 μm). Positions of aggregates compared to Paxinos Atlas (A, right column) indicated the spreading of p62 aggregates from lateral hypothalamus area (LHA) at 75 days to Ventro Medial Nucleus (VMN) at 90 days and to the rest of hypothalamus at 105 days. p62 aggregates were counted by a blind observer in SOD1(G86R) mice at three different ages as compared with their wt littermates (B, 75 days: n=7; 90 days: n=8; 105 days n=4). * $p<0.05$, Student's t-test. Data are presented as mean and SEM.

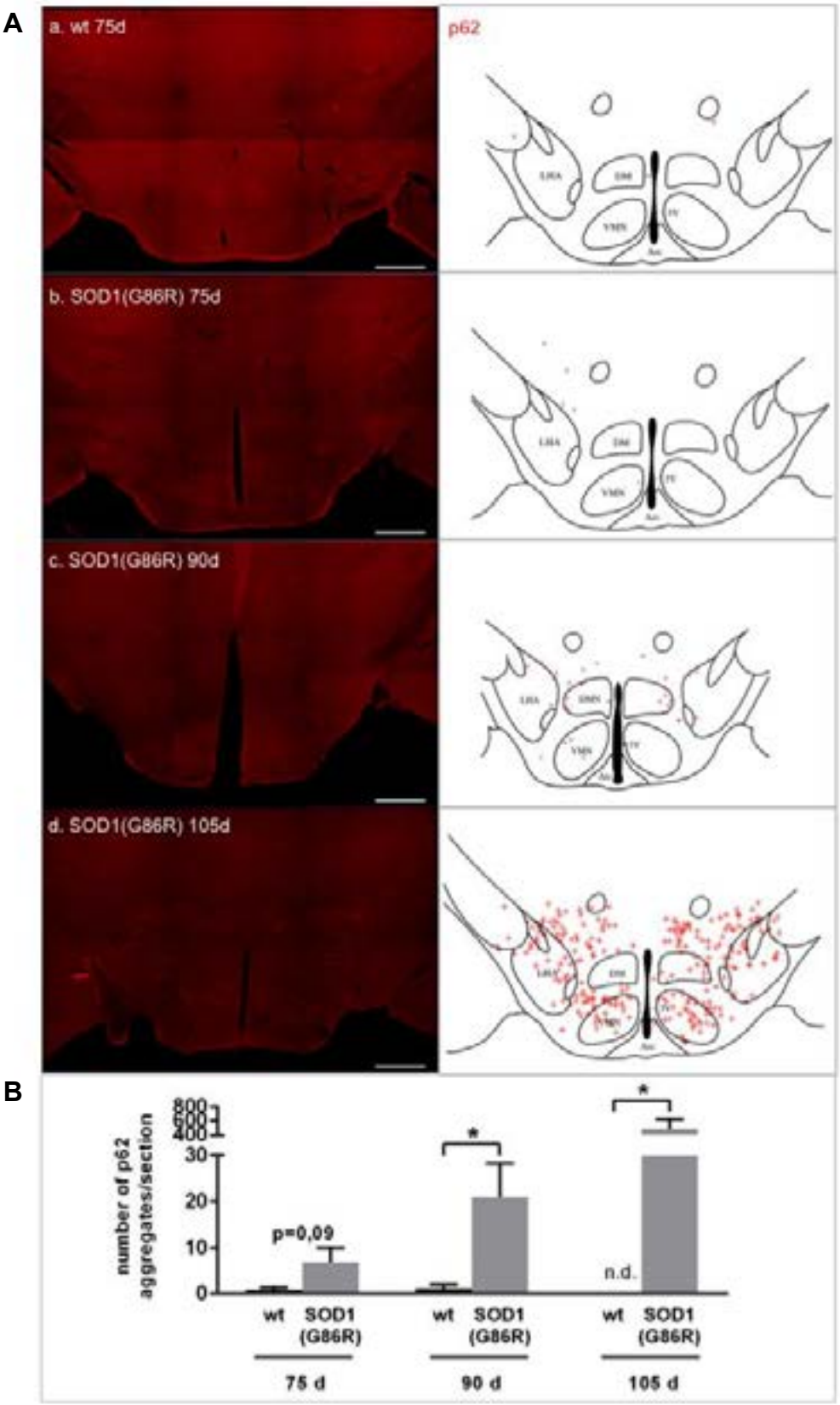
A
a. wt 75d
p62
b. SOD1(G86R) 75d
c. SOD1(G86R) 90d
d. SOD1(G86R) 105d
B
number of p62 aggregates/section
800
600
400
30
20
10
0
p=0,09
*
*
n.d.
wt
SOD1 (G86R)
wt
SOD1 (G86R)
wt
SOD1 (G86R)
75 d
90 d
105 d

Figure 3: Ubiquitin pathological aggregates in hypothalamus of mice.
Ubiquitin immunohistochemistry was performed on selected sections after identification of area of hypothalamus according to Paxinos Brain Atlas (A, right column). Representative images are shown for SOD1 (G86R) (b,c,d) mice and control littermates (a) at 75 days (a, b), 90 days (c) and 105 days (d) (scale bar 500 µm). Positions of aggregates compared to Paxinos Atlas (A, right column) indicated the spreading of ubiquitine aggregates from lateral hypothalamus area(LHA) at 75 days to Ventro Medial Nucleus (VMN) at 90 days and to the rest of hypothalamus at 105 days. Ubiquitine aggregates were counted by a blind observer in SOD1(G86R) mice at three different ages (75 days, 90 days and 105 days) as compared with their wt littermates (B, 75 days: n=5; 90 days: n=6; 105 days n=4). * $p<0.05$, Student's t-test. Data are presented as mean and SE.

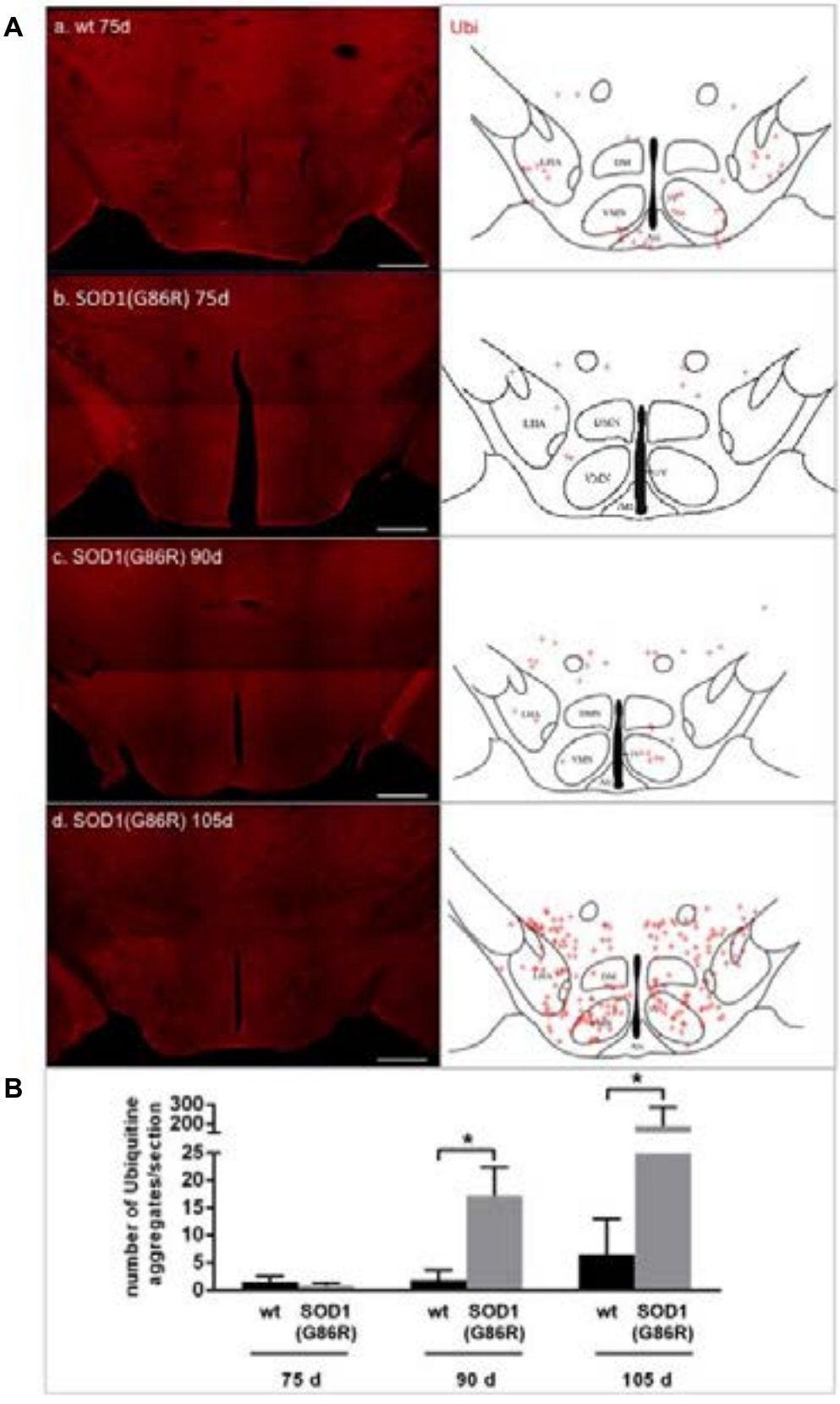
A
a. wt 75d
Ubi
b. SOD1(G86R) 75d
c. SOD1(G86R) 90d
d. SOD1(G86R) 105d
B
number of Ubiquitine aggregates/section
300
200
25
20
15
10
5
0
wt
SOD1 (G86R)
75 d
90 d
105 d
*

Figure 4: the majority of aggregates are neither in orexin nor in MCH neurons in the LHA.

A: Representative apotome images of neurons from LHA stained with p62 antibody (red, a1-a8) or ubiquitin antibody (red b1-b8) co-stained with MCH antibody (cyan) and orexin antibody (green) in SOD1(G86R) mice at 105 days (scale bar: 20µm). Few p62 aggregates (a1-a4) or ubiquitine aggregates (b1-b4) were present in orexin positive neurons. Most p62 aggregates (a5-a8) and ubiquitine aggregates (b5-b8) were however neither in MCH nor in orexin positive neurons.
B: Quantification of p62 positive neurons (top panel) and ubiquitin positive neurons (bottom panel) in SOD1(G86R) mice at three different ages (75 days, 90 days and 105 days) by a blind observer. (for top panel: 75 days: n=7; 90 days: n=8; 105 days n=4; for bottom panel: 75 days: n=5; 90 days: n=6; 105 days n=4). Data are presented as mean and SE.

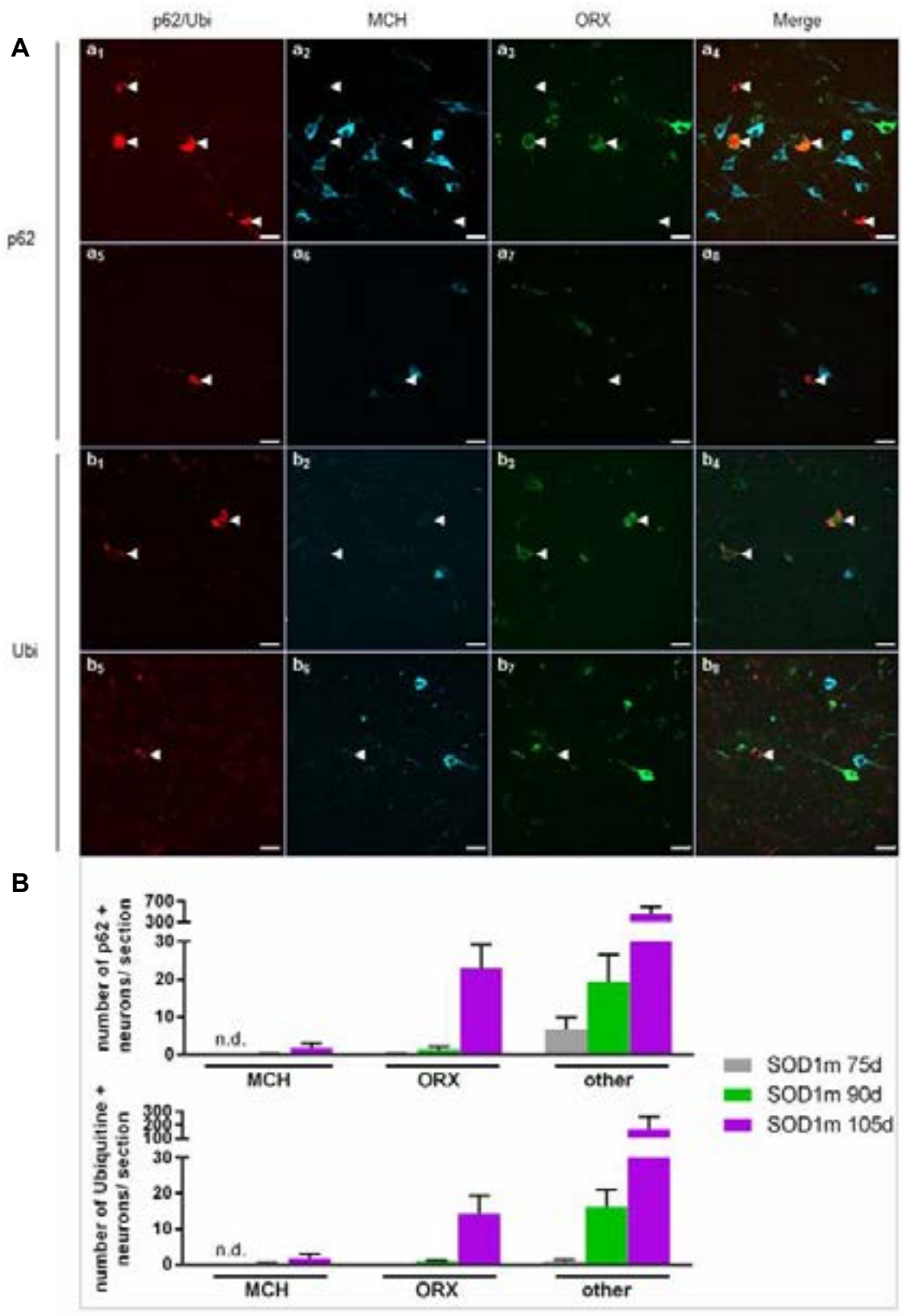
A
p62/Ubi
MCH
ORX
Merge
p62
Ubi
B
number of p62 + neurons/ section
number of Ubiquitine + neurons/ section
n.d.
MCH
ORX
other
SOD1m 75d
SOD1m 90d
SOD1m 105d

Figure 5: p62 and ubiquitin aggregates are present in NeuN positive and NeuN negative cells in the LHA

Representative apotome images of LHA sections stained with p62 antibody (red, a1-a6) or ubiquitine antibody (red, b1-b6) associated with NeuN antibody (green) in SOD1(G86R) mice at 90 days (scale bar: 20µm). Many p62 (a1-a3) or ubiquitin aggregates (b1-b3) were present in NeuN positive neurons. However, we also observed p62 (a4-a6) and ubiquitin aggregates (b4-b6) in NeuN negative cells that displayed neuronal morphology.

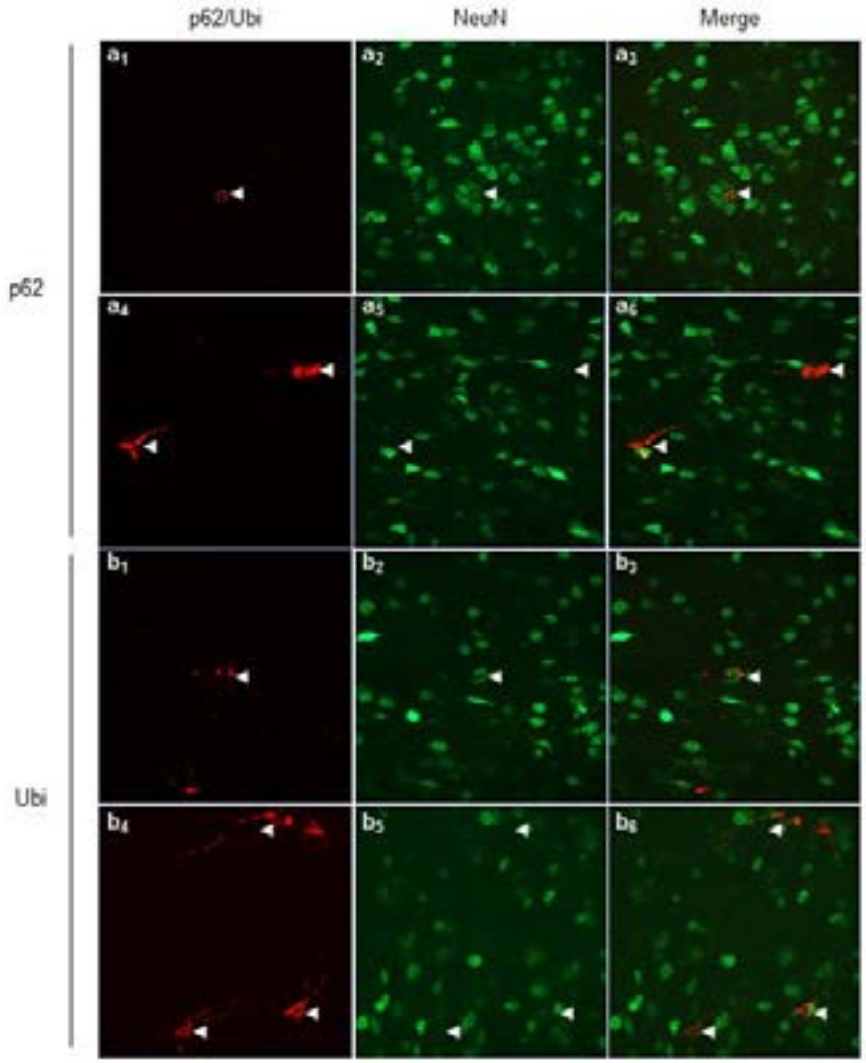

Figure 6: Defect in MCH neurons in SOD1(G86R) mice.
Quantification of MCH neurons in the LHA of SOD1(G86R) mice. LHA was identified according to Paxinos Brain Atlas (scheme of identified regions, in red, A). Representative images are shown for SOD1(G86R) mice and control littermates at 75 days of age at two magnifications (scale bar 500 µm (middle row), 30µm (lower row)). Total numbers of MCH positive cell bodies in the lateral hypothalamus were determined in SOD1(G86R) mice at 75 days of age (n=8, B-F) and at symptom onset (n=7, B) as compared with their wt littermates.

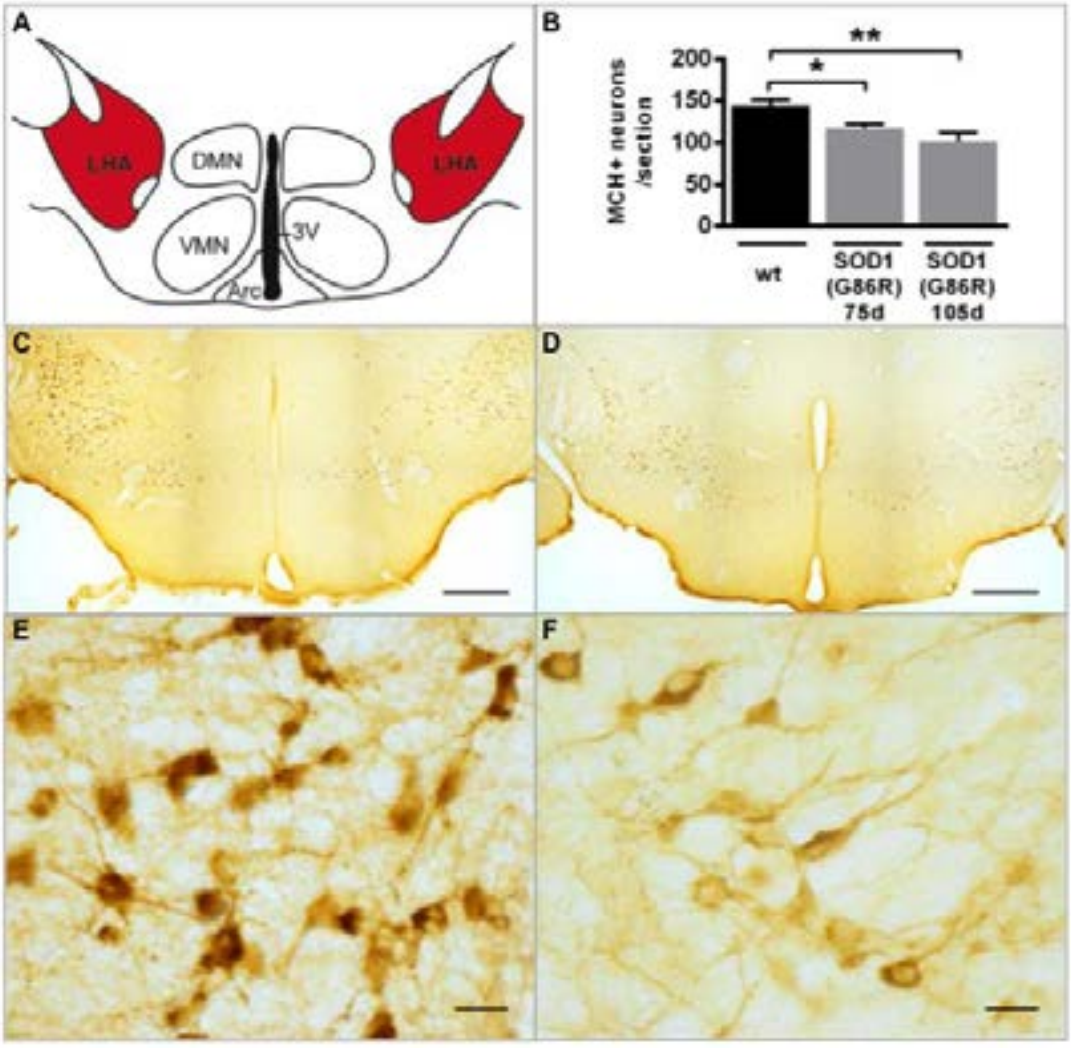

Figure 7: MCH ICV delivery rescues weight loss of SOD1(G86R) mice.

A: Body weight curves of SOD1(G86R) mice (SOD1(G86R), n=13) and wt littermate mice (wt, n=16) at 75 days of age at surgery, after Intra Cerebro Ventricular cannulation (ICV) and constant infusion of MCH (1.2µg/day, red) or vehicle (blue) with an osmotic pump. * $p<0.05$, Two way ANOVA. Data are presented as mean and SE.

B: weight gain per week for mice presented in A. * $p<0.05$, two-way ANOVA. Data are presented as mean and SE.

B: Cumulative food intake over 14 days for mice presented in A. No significant difference is observed.

Data are presented as mean and SE.

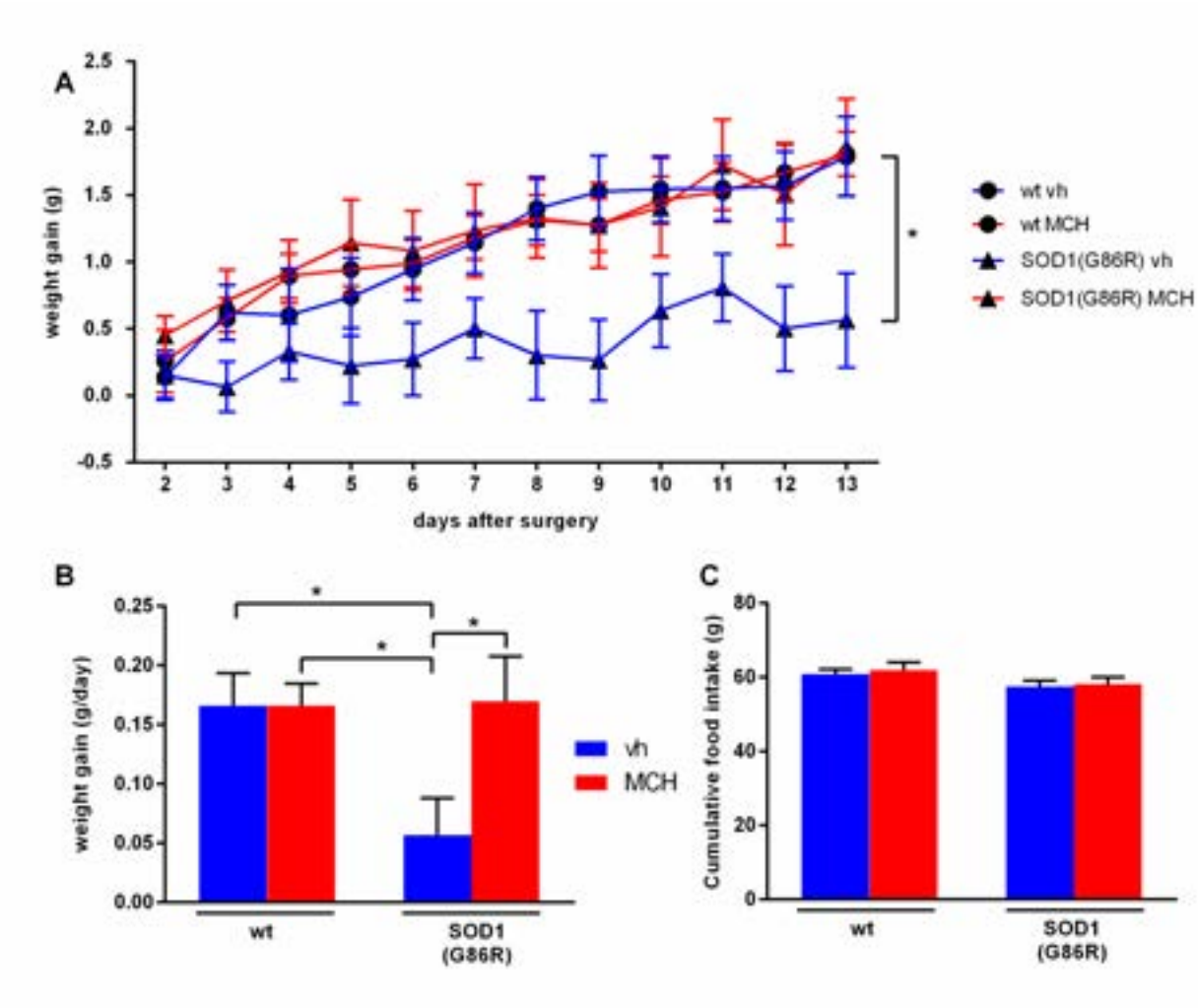

References

1. Dupuis L, Pradat PF, Ludolph AC, Loeffler JP. Energy metabolism in amyotrophic lateral sclerosis. Lancet Neurol. 2011 Jan;10(1):75-82.
2. Ahmed RM, Irish M, Piguet O, et al. Amyotrophic lateral sclerosis and frontotemporal dementia: distinct and overlapping changes in eating behaviour and metabolism. Lancet Neurol. 2016 Mar;15(3):332-42.
3. Gallo V, Wark PA, Jenab M, et al. Prediagnostic body fat and risk of death from amyotrophic lateral sclerosis: the EPIC cohort. Neurology. 2013 Feb 26;80(9):829-38.
4. O'Reilly EJ, Wang H, Weisskopf MG, et al. Premorbid body mass index and risk of amyotrophic lateral sclerosis. Amyotrophic lateral sclerosis & frontotemporal degeneration. 2013 Apr;14(3):205-11.
5. Desport JC, Preux PM, Truong TC, Vallat JM, Sautereau D, Couratier P. Nutritional status is a prognostic factor for survival in ALS patients. Neurology. 1999 Sep 22;53(5):1059-63.
6. Marin B, Desport JC, Kajeu P, et al. Alteration of nutritional status at diagnosis is a prognostic factor for survival of amyotrophic lateral sclerosis patients. J Neurol Neurosurg Psychiatry. 2011 Jun;82(6):628-34.
7. Paganoni S, Deng J, Jaffa M, Cudkowicz ME, Wills AM. Body mass index, not dyslipidemia, is an independent predictor of survival in amyotrophic lateral sclerosis. Muscle Nerve. 2011 Jul;44(1):20-4.
8. Jawaid A, Murthy SB, Wilson AM, et al. A decrease in body mass index is associated with faster progression of motor symptoms and shorter survival in ALS. Amyotroph Lateral Scler. 2010 May 26.
9. Dupuis L, Corcia P, Fergani A, et al. Dyslipidemia is a protective factor in amyotrophic lateral sclerosis. Neurology. 2008 Mar 25;70(13):1004-9.
10. Henriques A, Blasco H, Fleury MC, et al. Blood Cell Palmitoleate-Palmitate Ratio Is an Independent Prognostic Factor for Amyotrophic Lateral Sclerosis. PLoS One. 2015;10(7):e0131512.
11. Lindauer E, Dupuis L, Muller HP, Neumann H, Ludolph AC, Kassubek J. Adipose Tissue Distribution Predicts Survival in Amyotrophic Lateral Sclerosis. PLoS One. 2013;8(6):e67783.
12. Dupuis L, Oudart H, Rene F, Gonzalez de Aguilar JL, Loeffler JP. Evidence for defective energy homeostasis in amyotrophic lateral sclerosis: benefit of a high-energy diet in a transgenic mouse model. Proc Natl Acad Sci U S A. 2004 Jul 27;101(30):11159-64.
13. Wills AM, Hubbard J, Macklin EA, et al. Hypercaloric enteral nutrition in patients with amyotrophic lateral sclerosis: a randomised, double-blind, placebo-controlled phase 2 trial. Lancet. 2014 Feb 27.
14. Yeo GS, Heisler LK. Unraveling the brain regulation of appetite: lessons from genetics. Nat Neurosci. 2012 Oct;15(10):1343-9.
15. Morton GJ, Meek TH, Schwartz MW. Neurobiology of food intake in health and disease. Nat Rev Neurosci. 2014 Jun;15(6):367-78.
16. Vercruysse P, Sinniger J, El Oussini H, et al. Alterations in the hypothalamic melanocortin pathway in amyotrophic lateral sclerosis. Brain. 2016 Apr;139(Pt 4):1106-22.
17. Dupuis L, Dengler R, Heneka MT, et al. A randomized, double blind, placebo-controlled trial of pioglitazone in combination with riluzole in amyotrophic lateral sclerosis. PLoS One. 2012;7(6):e37885.
18. Ahmed RM, Caga J, Devenney E, et al. Cognition and eating behavior in amyotrophic lateral sclerosis: effect on survival. J Neurol. 2016 Jun 3.
19. Huisman MH, Seelen M, van Doormaal PT, et al. Effect of Presymptomatic Body Mass Index and Consumption of Fat and Alcohol on Amyotrophic Lateral Sclerosis. JAMA Neurol. 2015 Oct;72(10):1155-62.

20. Cykowski MD, Takei H, Schulz PE, Appel SH, Powell SZ. TDP-43 pathology in the basal forebrain and hypothalamus of patients with amyotrophic lateral sclerosis. Acta neuropathologica communications. 2014;2:171.
21. Dentel C, Palamiuc L, Henriques A, et al. Degeneration of serotonergic neurons in amyotrophic lateral sclerosis: a link to spasticity. Brain. 2013 Feb;136(Pt 2):483-93.
22. Feldengut S, Del Tredici K, Braak H. Paraffin sections of 70-100 mum: a novel technique and its benefits for studying the nervous system. J Neurosci Methods. 2013 May 15;215(2):241-4.
23. Neumann M, Sampathu DM, Kwong LK, et al. Ubiquitinated TDP-43 in frontotemporal lobar degeneration and amyotrophic lateral sclerosis. Science. 2006 Oct 6;314(5796):130-3.
24. Brettschneider J, Del Tredici K, Toledo JB, et al. Stages of pTDP-43 pathology in amyotrophic lateral sclerosis. Ann Neurol. 2013 Jul;74(1):20-38.
25. Ito M, Gomori A, Ishihara A, et al. Characterization of MCH-mediated obesity in mice. Am J Physiol Endocrinol Metab. 2003 May;284(5):E940-5.
26. Nakamura M, Bieniek KF, Lin WL, et al. A truncating SOD1 mutation, p.Gly141X, is associated with clinical and pathologic heterogeneity, including frontotemporal lobar degeneration. Acta Neuropathol. 2015 Jul;130(1):145-57.
27. Bonnavion P, Mickelsen L, Fujita A, de Lecea L, Jackson AC. Hubs and spokes of the lateral hypothalamus: cell types, circuits and behaviour. J Physiol. 2016 Jun 15.
28. Cui H, Sohn JW, Gautron L, et al. Neuroanatomy of melanocortin-4 receptor pathway in the lateral hypothalamic area. J Comp Neurol. 2012 Dec 15;520(18):4168-83.
29. Shimada M, Tritos NA, Lowell BB, Flier JS, Maratos-Flier E. Mice lacking melanin-concentrating hormone are hypophagic and lean. Nature. 1998 Dec 17;396(6712):670-4.
30. Ludwig DS, Mountjoy KG, Tatro JB, et al. Melanin-concentrating hormone: a functional melanocortin antagonist in the hypothalamus. Am J Physiol. 1998 Apr;274(4 Pt 1):E627-33.
31. Segal-Lieberman G, Bradley RL, Kokkotou E, et al. Melanin-concentrating hormone is a critical mediator of the leptin-deficient phenotype. Proc Natl Acad Sci U S A. 2003 Aug 19;100(17):10085-90.
32. Jeon JY, Bradley RL, Kokkotou EG, et al. MCH-/- mice are resistant to aging-associated increases in body weight and insulin resistance. Diabetes. 2006 Feb;55(2):428-34.
33. Ludwig DS, Tritos NA, Mastaitis JW, et al. Melanin-concentrating hormone overexpression in transgenic mice leads to obesity and insulin resistance. J Clin Invest. 2001 Feb;107(3):379-86.
34. Glick M, Segal-Lieberman G, Cohen R, Kronfeld-Schor N. Chronic MCH infusion causes a decrease in energy expenditure and body temperature, and an increase in serum IGF-1 levels in mice. Endocrine. 2009 Dec;36(3):479-85.
35. Egwuenu EJ, Fong AY, Pilowsky PM. Intrathecal melanin-concentrating hormone reduces sympathetic tone and blocks cardiovascular reflexes. Am J Physiol Regul Integr Comp Physiol. 2012 Sep 15;303(6):R624-32.
36. Imbernon M, Beiroa D, Vazquez MJ, et al. Central melanin-concentrating hormone influences liver and adipose metabolism via specific hypothalamic nuclei and efferent autonomic/JNK1 pathways. Gastroenterology. 2013 Mar;144(3):636-49 e6.
37. Braak H, Brettschneider J, Ludolph AC, Lee VM, Trojanowski JQ, Del Tredici K. Amyotrophic lateral sclerosis--a model of corticofugal axonal spread. Nat Rev Neurol. 2013 Dec;9(12):708-14.
38. Elias CF, Sita LV, Zambon BK, Oliveira ER, Vasconcelos LA, Bittencourt JC. Melanin-concentrating hormone projections to areas involved in somatomotor responses. J Chem Neuroanat. 2008 Mar;35(2):188-201.
39. Berthoud HR, Munzberg H. The lateral hypothalamus as integrator of metabolic and environmental needs: from electrical self-stimulation to opto-genetics. Physiol Behav. 2011 Jul 25;104(1):29-39.

Discussion

Cette dernière partie du manuscrit est consacrée à la discussion du projet et des différents résultats obtenus au cours de la thèse. Premièrement, nous discuterons de l'atteinte sélective de l'hypothalamus dans la Sclérose Latérale Amyotrophique (SLA). Deuxièmement, nous nous concentrerons sur les causes de la perte de poids et les anomalies du comportement, en comparaison avec la Démence Fronto Temporale (DFT). Troisièmement, nous discuterons des causes du dysfonctionnement hypothalamique. Finalement, nous nous pencherons sur les stratégies thérapeutiques découlant des résultats de cette thèse.

Depuis la caractérisation de la SLA en 1874, cette maladie a été considérée par les cliniciens comme une dégénérescence exclusive des motoneurones supérieurs et inférieurs causant une paralysie progressive. Cependant de plus en plus d'études récentes montrent que la SLA est une maladie beaucoup plus large qu'une simple atteinte motrice, et que d'autres symptômes causés par une atteinte systémique sont particulièrement importants pour la survie et/ou la qualité de vie des patients SLA.

Il a été clairement établi que les patients SLA souffrent, en plus de leur symptômes moteurs, d'un défaut du métabolisme énergétique causant une perte de poids (Dupuis et al. 2011). Le mécanisme sous-tendant la dérégulation du poids chez les patients SLA reste non caractérisé. Ce travail de thèse suggère que des altérations hypothalamiques en sont la cause.

I. Atteinte sélective de l'hypothalamus

Le lien entre SLA et un faible indice de masse corporel (IMC) avant le déclenchement des symptômes moteurs a été documenté récemment par des études épidémiologiques (Gallo et al. 2013; O'Reilly et al. 2013). De plus la corrélation négative entre perte de poids et survie avait été précédemment montrée (Desport et al. 1999; Marin et al. 2011; Paganoni et al. 2011). La présence d'un hyper-métabolisme chez les patients SLA était également avérée (Kasarskis et al. 1996; Dupuis et al. 2011). Cependant les mécanismes du dérèglement de l'homéostasie du métabolisme énergétique étaient inconnus.

Durant ma thèse, nous avions comme but d'explorer les possibles altérations hypothalamiques dans des modèles murins de SLA ainsi que chez les patients atteints de SLA.

Nous avons montré qu'il existait une atteinte spécifique de l'hypothalamus. De façon intéressante, les altérations anatomopathologiques dans l'hypothalamus ne concernent qu'un nombre restreint de noyaux.

Nous avons tout d'abord observé une atrophie préférentielle de la partie postérieure de l'hypothalamus, contenant la majeure partie de l'hypothalamus latéral ainsi que les noyaux dorsomediaux, ventromediaux et postérieurs. Cette étude IRM, sur un grand nombre de patients, est en accord avec une publication récente qui montre un processus pathologique localisé dans l'hypothalamus latéral de patients SLA (Cykowski et al. 2014). Nous avons de plus confirmé ces résultats anatomo-pathologiques en observant des agrégats TDP43 uniquement dans l'hypothalamus latéral des patients, mais pas dans le noyau arqué.

Nous avons ensuite confirmé l'implication spécifique de la partie postérieure de l'hypothalamus dans le modèle *Sod1(G86R).* Nous avons observé des agrégats p62 et ubiquitine principalement dans l'hypothalamus latéral et dans le noyau ventromedial, c'est à dire deux régions qui sont incluses dans la partie atrophiée de l'hypothalamus des patients SLA. De ce fait, nos deux études sont très cohérentes entre elles. Il existe donc une similitude entre les processus pathologiques chez les patients et les modèles murins ce qui renforce l'utilité des modèles animaux dans la recherche préclinique sur la SLA.

Nous n'avons observé que très peu d'agrégats dans le noyau Arqué. Cependant, notre publication dans Brain identifie de manière indirecte chez le patient et de manière directe chez la souris une altération du système melanocortine du noyau Arqué de l'hypothalamus. Ce changement du système POMC et AgRP (baisse de POMC et augmentation AgRP) explique le manque d'action de la molécule antidiabétique Pioglitazone sur le poids des patients SLA, et est associé plutôt aux altérations de la prise alimentaire qu'à la perte de poids. Notre interprétation est que ces changements du système mélanocortine sont essentiellement une réponse compensatoire à la perte de poids, augmentant la prise alimentaire. Il s'agit donc d'une altération fonctionnelle, et pas dégénérative.

Nous avons pu montrer que, même si les neurones MCH du LHA ne présentent pas d'agrégats pathologiques chez la souris, ils sont impliqués dans la SLA. En effet, nous avons observé une perte d'expression d'ARNm accompagné par une baisse du nombre de neurones MCH positifs dès un âge non symptomatique. Les neurones orexine semblent moins affectés au niveau de l'expression du gène, avec une perte d'ARNm plus tardive, mais il existe cependant un certain nombre de neurones orexine qui développent des agrégats. Il est possible que les neurones MCH soient plus sensibles à la toxicité des agrégats protéiques et qu'ils dégénèrent plus rapidement quand ceux-ci se développent, ce qui expliquerait pourquoi moins de neurones MCH persistent à la fin de la maladie, et que ceux restant sont préservés de la présence d'agrégats. A l'inverse, il ne peut être exclu que les neurones MCH ne développent pas d'agrégats. Le rôle des neurones à orexine reste à préciser dans la SLA.

La grande majorité du processus pathologique dans le modèle murin est localisé dans des neurones du LHA qui ne sont ni MCH ni orexin positifs et qui restent à identifier. Il est important de noter que les populations neuronales du LHA ne sont pas encore bien caractérisées. En effet, le LHA comprend d'autres neurones que les neurones MCH ou orexine, notamment des neurones exprimant à leur surface des récepteurs à la leptine (Bonnavion et al. 2016). Il faut noter que la plupart de ces neurones du LHA exprimant le récepteur à la leptine, expriment aussi des récepteurs MC4 (Cui et al. 2012). Ainsi leur pathologie observée pourrait être une conséquence du dysfonctionnement du système melanocortinergique. L'implication de ces neurones dans le réseau hypothalamique, ainsi que leur implication dans le processus de la SLA sont à éclaircir.

II. Cause de la perte de poids et anomalies du comportement alimentaire

La masse corporelle est le résultat de la balance entre la prise alimentaire et la dépense énergétique. Le déséquilibre de la balance énergétique dans la SLA est bien connu. Avant même le développement de la maladie, un IMC faible augmente le risque de développer une SLA (O'Reilly et al. 2013). De plus au cours de la maladie les patients perdent du poids (Nau et al. 1995), avec soit une perte de masse graisseuse (Kasarskis et al. 1996) ou une perte de masse

sèche (Nau et al. 1995; Vaisman et al. 2009). Cette perte de masse peut être expliquée par un hypermétabolisme (Vaisman et al. 2009; Wijesekera & Leigh 2009; Kasarskis et al. 1996; Bouteloup et al. 2009; Desport et al. 2005), par une hyperlipidémie (Dupuis et al. 2008) ou une intolérance au glucose avec ou sans résistance à l'insuline (Dupuis et al. 2011; Pradat et al. 2010) et par une dysphagie. Les mécanismes causant ces déréglements n'étaient pas connus. Nous avons montré tout d'abord que fournir du MCH en intra-cérébro-ventriculaire permet de compenser la perte de poids dans le modèle *Sod1(G86R)*. Ce réequilibrage de la balance énergétique n'est pas dû à une hyperphagia, mais vraisembablement à la baisse de l'hypermetabolisme présent dans la SLA. Ainsi avec ce modèle murin, nous pouvons dire que la cause de la perte de poids dans la SLA est dûe au dysfonctionnement des neurones à MCH du LHA. Nous avons par ailleurs des preuves indirectes du lien entre LHA et perte de poids chez les patients SLA. En effet, l'atrophie de l'hypothalamus postérieur chez les patients est corrélée avec la perte de poids existante avant l'IRM. Le volume ne corrèle pas avec la perte de poids future, cela pouvant venir du traitement alimentaire qui est fourni aux patients. L'atrophie du reste du cerveau chez les patients SLA ne corrèle quand à elle pas avec la perte de poids mais avec la progression des symptomes moteurs. Cette observation suggère que la perte de poids, associée à l'atteinte hypothalamique, et la progression des symptômes moteurs, associée à l'atrophie cérébrale, principalement corticale, sont deux processus distincts.

En parallèle de la perte de poids, les patients SLA ont des anomalies du comportement alimentaire. A un stade présymptomatique, les patients SLA consomme plus de calories que les contrôles sains (Huisman et al. 2015). De plus il semblerait que les patients SLA mangent plus de graisse (Nelson et al. 2000). Ces comportements pourraient être le reflet du défaut melanocortine que nous avons observé. En effet la baisse de POMC, associé à l'augmentation d'AgRP, est visible dans les situations de prise alimentaire comme après un jeûne (Mizuno et al. 1998). Le déficit physiologique du noyau Arqué entrainerait une augmentation de la prise alimentaire. L'apport calorique au début de la maladie permettrait de contrecarrer l'hypermetabolisme dû au dysfonctionnement de l'hypothalamus latéral. Avec la progression de la maladie, et la progression de la pathologie du LHA, la compensation de l'hypermetabolisme n'est plus suffisante pour maintenir la balance du poids.

Les patients DFT semblent partager de nombreux points communs avec les patients SLA du point de vue métabolique (Figure 10). De leur côté, les patients bv-FTD ont un IMC plus élevé que les contrôles et ont tendance a prendre du poids au cours de la maladie (Ahmed et al. 2014; Ahmed et al. 2014; Ahmed et al. 2015). Chez les patients bv-FTD, le symptôme majeur concernant le métabolisme est une altération de l'appétit ainsi qu'un changement des préférences alimentaires. La grande majorité des patients bv-FTD présentent ces symptômes (Piguet et al. 2011), avec par exemple lors du petit déjeuner une prise alimentaire deux fois plus calorique que les contrôles (Ahmed et al. 2016). Etonnament les patients bv-FTD prennent du poids car ils mangent plus, mais l'augmentation de leur IMC devrait être encore plus important au vu de la prise alimentaire. Ainsi un hypermétabolisme léger pourrait freiner la prise de poids (Ahmed et al. 2016). Au niveau hypothalamique, une atrophie sévère de l'hypothalamus, et plus spécifiquement de la partie postérieure, est présente chez les patients bv-FTD (Ahmed et al. 2014; Piguet et al. 2011; Ahmed et al. 2016). Plus les anomalies alimentaires sont importantes, plus l'atrophie est avancée. De plus le sous groupe de patients bv-FTD avec une expansion C9ORF72 ont une atrophie d'environ 7%, similaire aux patients SLA C9ORF72. L'atrophie pourrait être dû à une pathologie pTDP-43 ou Tau observée dans des tissus post-mortem (Piguet et al. 2011). Le noyau arqué est aussi atteint avec une augmentation du neuropeptide orexigenique AgRP, dont le niveau est corrélé avec IMC, dans le sang des patients bv-FTD. De la même façon que les observations chez les patients SLA, les patients bv-FTD ont des changements du systeme mélanocortin qui pourrait être à l'origine des défauts de la prise alimentaire.

Figure 10 : Représentation schématique des problèmes métaboliques et des dysfonctionnements hypothalamiques chez des patients SLA (ALS) et DFT (FTD).
POMC: Proopiomelacotin; AgRP: Agouti related peptide; ORX: Orexin; MCH: Melanin Concentrating Hormone.

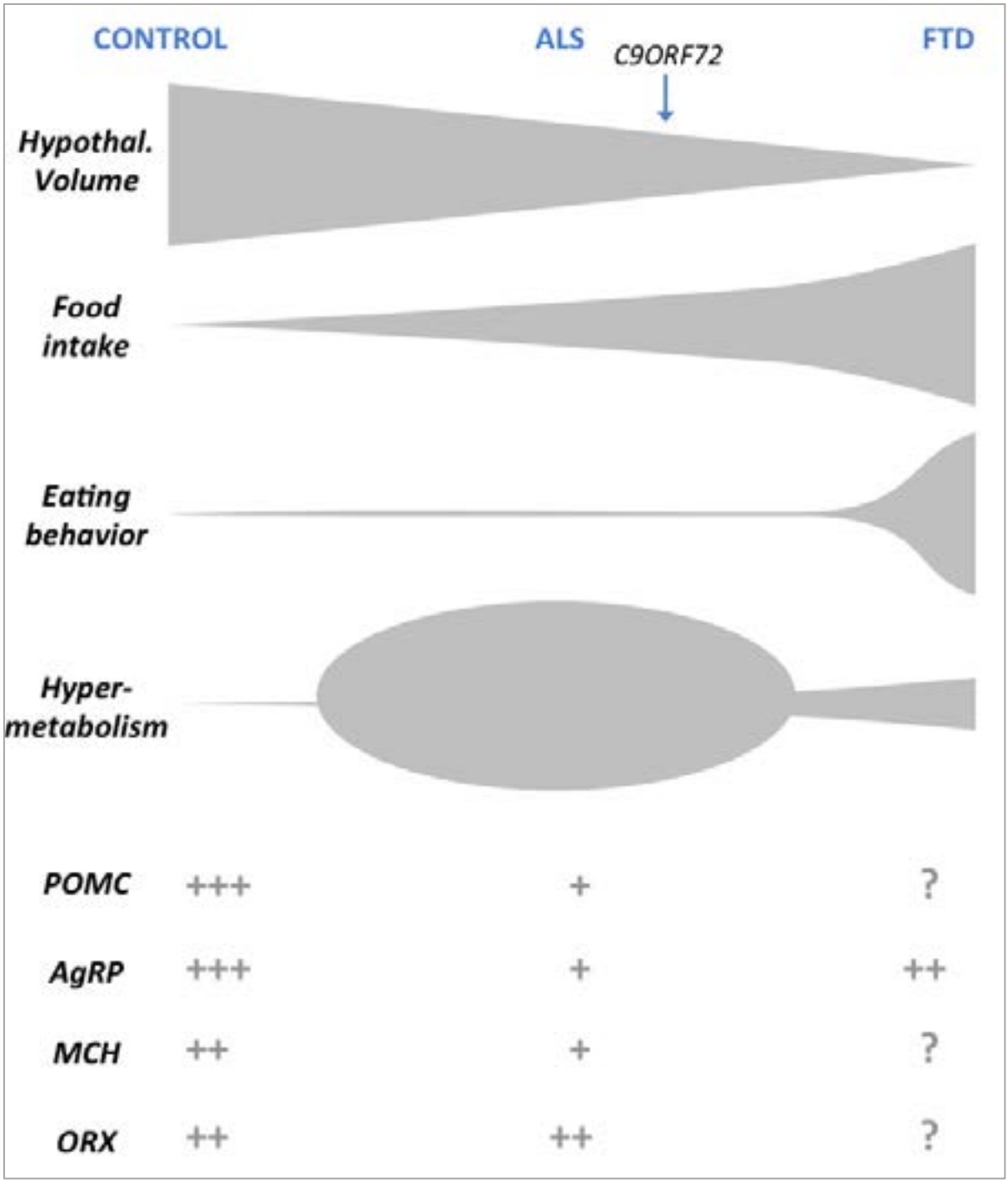

Ce dysfonctionnement est associé à un processus pathologique dans la partie postérieure de l'hypothalamus qui pourrait être à l'origine d'un hypermetabolisme. Ces nouvelles études montrent que le continuum SLA-FTD, qui existe au niveau génétique et antomopathologique, se prolonge au niveau métabolique (Ahmed et al. 2016). Dans ces deux tableaux extrèmes d'une seule et même maladie, l'hypothalamus serait atteint dans les même régions mais à des stades différents.

III. Causes du dysfonctionnement hypothalamique

Une question importante est l'origine de ce dysfonctionnement hypothalamique dans la SLA.

Une étude du laboratoire (Dentel et al. 2013) a montré une baisse de la sérotonine produite dans le tronc cérébral chez les patients SLA, ainsi que chez un modèle murin *Sod1*. L'hypothalamus est sous le contrôle d'une innervation des neurones sérotoninergiques (Voigt & Fink 2015; Donovan & Tecott 2013). Il était connu au préalable que les souris dépourvues de sérotonine au niveau central développe des déficits énergétiques avec un hypermétabolisme (Yadav et al. 2009). Nous avons montré dans notre première étude que l'anomalie du système mélanocortinergique était, au moins en partie, dû à une perte d'innervation sérotoninergique du noyau arqué. Il a aussi été montré récemment dans le laboratoire que la dégénérescence de neurones sérotoninergiques est un processus « cell autonomous » (El Oussini, en préparation, Annexe publication #5). Enlever la toxicité SOD1 spécifiquement dans les neurones sérotoninergiques permet de restaurer la dégénérescence, en particulier dans le noyau arqué. En plus d'intervenir dans les problèmes de poids, la dégénérescence des neurones sérotoninergiques entrainerait le processus de spasticité, qui est bénéfique pour retarder la paralysie. Il semblerait que la sérotonine, par l'intermédiaire de son récepteur 5-HT2B exprimé à la surface des microglies, est un élément important dans la vitesse de propagation de la maladie (El Oussini et al. 2016, Annexe publication #4). La question de l'impact de la sérotonine sur les défauts du LHA reste ouverte.

Le processus pathologique impliquant l'hypothalamus pourrait aussi trouver son origine dans d'autres parties du cerveau. Nous avons montré que l'atrophie de l'hypothalamus est

similaire à celle observée dans l'ensemble du cerveau. Il n'y a pas un processus spécifique à l'hypothalamus, mais celui-ci entrerait plus dans un processus global d'impact sur le cerveau. L'atrophie hypothalamique se situe chez les patients de stades 3 et 4 dans le « staging de Braak ». Braak et collaborateurs (Braak et al. 2013) ont montré qu'il existe une propagation de la pathologie pTDP-43 chez les patients SLA, partant du cortex moteur (stade 1) et se diffusant dans les autres régions du cerveau (stades 2-3-4). De plus il est connu que les neurones du LHA sont connectés avec le cortex moteur (Berthoud & Münzberg 2011). Ainsi on peut soulever l'hypothèse que la maladie commencerait dans le cortex moteur, puis elle irait atteindre les zones connectées comme l'hypothalamus latéral, dont la pathologie serait une conséquence secondaire de la maladie. Dû à cette propagation, l'hypothalamus latéral subirait un dysfonctionnement et un début de pathologie, qui entrainerait à long terme une atrophie. L'étude du changement de connectivité de l'hypothalamus avec le cortex moteur, au cours de l'évolution de la maladie, à l'aide de l'imagerie DTI serait d'une aide précieuse pour comprendre l'intégration de l'ensemble du cerveau. De plus nous avons observé de fortes similarités de l'atteinte du LHA par la SLA entre les patients et les souris *Sod1(G86R)*. Une étude complète de l'ensemble des connections du LHA, ainsi que de ses caractéristiques neuronales, ferait avancer la question de la perte de poids dans la SLA.

Le tronc cérébral, ainsi que le cortex moteur, ont de nombreuses connectivités avec d'autres parties du cerveau. Nous ne pouvons donc pas ignorer que le dysfonctionnement hypothalamique pourrait aussi provenir d'autres structures cérébrales.

IV. Stratégies thérapeutiques

Grâce notre analyse post-hoc d'un essai clinique, nous savons que les molécules dont le mode d'action est une inhibition de POMC, comme la Pioglitazone, ne pourront pas être efficaces pour le traitement de la perte de poids dans la SLA. De plus, les traitements visant le système cannabinoïde, permettant une libération de la beta endorphine des neurones POMC (Koch et al. 2015), ne fonctionneront pas. La beta endorphine est un sous-produit de POMC, qui est baissé dans le cas de la SLA.

Nous savons que dans le modèle murin *Sod1(G86R)*, une injection de MCH par icv permet de contrecarrer la perte de poids. Ainsi un agoniste des récepteurs MCH pourrait être une cible thérapeutique efficace. Malheureusement, dans le domaine public il n'existe pas d'agoniste spécifique de MCH testé *in vivo* autre que le neuropeptide endogène. Pour notre expérience chez les souris, nous étions obligés de faire une opération icv car la molécule ne passe pas la barrière hémato encéphalique.

Dans la littérature, le lien entre perte de poids et survie dans la SLA est bien connu. En effet, augmenter le poids des souris *Sod1(G86R)* par un régime riche en matière grasse permet de prévenir la dénervation musculaire, la perte des motoneurones, ainsi que d'augmenter la survie de 20% (Dupuis et al. 2004). De plus l'étude préalable sur des patients avec un régime hyper calorique (Wills et al. 2014) est aussi encourageante. L'étude d'un régime hyper calorique sur la survie est en cours sur un plus grand nombre de patients. Ainsi la question se pose aussi de l'impact du traitement MCH sur l'amélioration des symptômes moteurs et sur la survie. Pour commencer, une étude à plus long terme sur les souris *Sod1(G86R)* serait à envisager. Il est important de préciser que l'utilisation d'une pompe reliée à une canule, comme dans le papier 3, n'est pas adaptée à notre avis à une étude de survie. En effet la pompe en sous-cutanée pendant plusieurs semaines est une source de gêne et de stress pour la souris. Une injection icv d'un virus entrainant une augmentation de l'expression de MCH pourrait être une meilleure option. Après injection du virus, la survie ainsi que l'évolution des symptômes moteurs serait suivie par plusieurs tests de force musculaire et de démarche. De surcroit la question de la synergie entre un régime hyper calorique et un traitement MCH se pose. Tout laisse à penser

que ces deux traitements peuvent fonctionner en synergie pour multiplier les effets de chacun. MCH permet de réduire l'hyper-métabolisme et le régime alimentaire permet d'augmenter l'apport calorique.

En conclusion, pour pouvoir traiter au mieux la perte de poids dans la SLA, il serait nécessaire de développer une molécule agoniste des récepteurs MCH et de faire ce traitement en plus d'un régime alimentaire adapté.

Conclusion

Pour conclure, nos résultats ont démontrés un dysfonctionnement de sous-régions spécifiques de l'hypothalamus (Figure 11). Nous avons observé une atteinte du noyau arqué, ainsi qu'une atteinte de l'hypothalamus latéral. Par une étude chez le patient et dans des modèles murins de SLA, nous avons mis en évidence que le déséquilibre du système melanocortin entraine des anomalies du comportement alimentaire. Faisant partie d'un réseau dans le cerveau, nous savons que ce défaut hypothalamique est en partie au moins la conséquence d'une atteinte sérotoninergique. Par deux études, une chez le patient et une majoritairement dans un modèle murin, nous savons que l'hypothalamus latéral est sévèrement atteint dans la SLA. Cette pathologie entraine un hypermétabolisme responsable de la perte de poids observée. De plus nous avons pu soulever l'hypothèse que ce défaut est aussi la conséquence d'un réseau de connections avec le cortex moteur. Ainsi l'implication de l'hypothalamus latéral ne serait qu'un processus secondaire dans la propagation de la maladie. Cependant, nos études suggèrent que la perte de poids est un phénomène à part entière, ne dépendant pas de la perte musculaire. Finalement, nous savons que traiter la perte de poids ne doit pas intervenir par une action sur le système melanocortin. Notre dernière étude nous met sur la voie d'un traitement qui pourrait être utile pour contrecarrer la perte de poids chez les patients SLA, en agissant sur les neurones MCH.

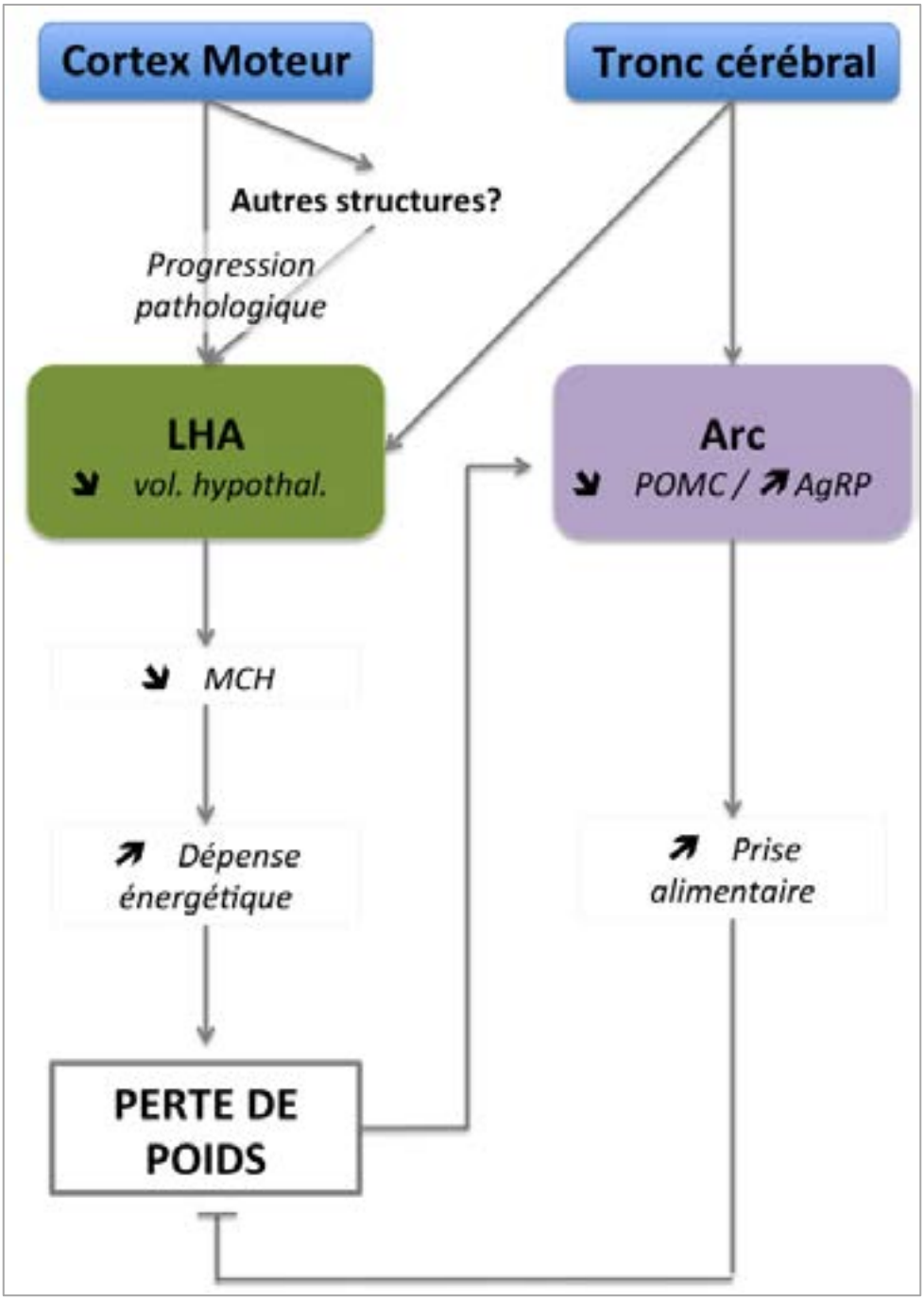

Figure 11 : Schéma de travail des résultats obtenus pendant la thèse.
POMC: Proopiomelacotin; AgRP: Agouti related peptide; MCH: Melanin Concentrating Hormone ; vol. hypothal. : volume hypothalamique.

Bibliography

Ahmed, R. M., J. Caga, E. Devenney, S. Hsieh, L. Bartley, E. Highton-Williamson, E. Ramsey, et al. 2016. “Cognition and Eating Behavior in Amyotrophic Lateral Sclerosis: Effect on Survival.” *Journal of Neurology*, June. Springer Berlin Heidelberg.

Ahmed, R. M., E. Mioshi, J. Caga, M. Shibata, M. Zoing, L. Bartley, O. Piguet, J. R. Hodges, and M. C. Kiernan. 2014. “Body Mass Index Delineates ALS from FTD: Implications for Metabolic Health.” *Journal of Neurology* 261 (9): 1774–80.

Ahmed, Rebekah M, Muireann Irish, Jonathan Kam, Jolanda van Keizerswaard, Lauren Bartley, Katherine Samaras, John R Hodges, and Olivier Piguet. 2014. “Quantifying the Eating Abnormalities in Frontotemporal Dementia.” *JAMA Neurology* 71 (12): 1540.

Ahmed, Rebekah M, Muireann Irish, Olivier Piguet, Glenda M Halliday, Lars M Ittner, Sadaf Farooqi, John R Hodges, and Matthew C Kiernan. 2016. “Amyotrophic Lateral Sclerosis and Frontotemporal Dementia: Distinct and Overlapping Changes in Eating Behaviour and Metabolism.” *The Lancet Neurology* 15 (3). Elsevier Ltd: 332–42.

Ahmed, Rebekah M, Sahar Latheef, Lauren Bartley, Muireann Irish, Glenda M Halliday, Matthew C Kiernan, John R Hodges, and Olivier Piguet. 2015. “Eating Behavior in Frontotemporal Dementia.” *Neurology* 85 (15): 1310–17.

Ahmed, Rebekah M., Muireann Irish, Elana Henning, Nadene Dermody, Lauren Bartley, Matthew C. Kiernan, Olivier Piguet, Sadaf Farooqi, and John R. Hodges. 2016. “Assessment of Eating Behavior Disturbance and Associated Neural Networks in Frontotemporal Dementia.” *JAMA Neurology* 73 (3): 282.

Aziz, N Ahmad, Hanno Pijl, M. Frolich, Marieke Snel, Trea C M Streefland, Ferdinand Roelfsema, and Raymund a C Roos. 2010. “Systemic Energy Homeostasis in Huntington’s Disease Patients.” *Journal of Neurology, Neurosurgery & Psychiatry* 81 (11): 1233–37.

Aziz, N. A., M. A. van der Marck, H. Pijl, M. G M Olde Rikkert, B. R. Bloem, and R. A C Roos. 2008. “Weight Loss in Neurodegenerative Disorders.” *Journal of Neurology* 255 (12): 1872–80.

Baker, Matt, Ian R Mackenzie, Stuart M Pickering-Brown, Jennifer Gass, Rosa Rademakers, Caroline Lindholm, Julie Snowden, et al. 2006. “Mutations in Progranulin Cause Tau-Negative Frontotemporal Dementia Linked to Chromosome 17.” *Nature* 442 (7105): 916–19.

Ballard, Clive, Serge Gauthier, Anne Corbett, Carol Brayne, Dag Aarsland, and Emma Jones. 2011. “Alzheimer’s Disease.” *The Lancet* 377 (9770). Elsevier Ltd: 1019–31.

Bergemalm, Daniel, Karin Forsberg, Vaibhav Srivastava, Karin S. Graffmo, Peter M. Andersen, Thomas Brännström, Gunnar Wingsle, and Stefan L. Marklund. 2010. “Superoxide Dismutase-1 and Other Proteins in Inclusions from Transgenic Amyotrophic Lateral

Sclerosis Model Mice." *Journal of Neurochemistry* 114 (2): 408–18.

Berthoud, Hans Rudi, and Heike Münzberg. 2011. "The Lateral Hypothalamus as Integrator of Metabolic and Environmental Needs: From Electrical Self-Stimulation to Opto-Genetics." *Physiology and Behavior* 104 (1). Elsevier Inc.: 29–39.

Berthoud, Hans-Rudi, and Heike Münzberg. 2011. "The Lateral Hypothalamus as Integrator of Metabolic and Environmental Needs: From Electrical Self-Stimulation to Opto-Genetics." *Physiology & Behavior* 104 (1). Elsevier Inc.: 29–39.

Bi, Sheng, Yonwook J. Kim, and Fenping Zheng. 2012. "Dorsomedial Hypothalamic NPY and Energy Balance Control." *Neuropeptides* 46 (6). Elsevier Ltd: 309–14.

Bocchetta, Martina, Elizabeth Gordon, Emily Manning, Josephine Barnes, David M. Cash, Miklos Espak, David L. Thomas, et al. 2015. "Detailed Volumetric Analysis of the Hypothalamus in Behavioral Variant Frontotemporal Dementia." *Journal of Neurology* 262 (12). Springer Berlin Heidelberg: 2635–42.

Boillée, Séverine, Christine Vande Velde, and Don W. Cleveland. 2006. "ALS: A Disease of Motor Neurons and Their Nonneuronal Neighbors." *Neuron* 52 (1): 39–59.

Bonnavion, Patricia, Laura Mickelsen, Akie Fujita, Luis de Lecea, and Alexander C. Jackson. 2016. "Hubs and Spokes of the Lateral Hypothalamus: Cell Types, Circuits and Behaviour." *The Journal of Physiology* 1 (June): 1–34.

Bouteloup, C., J.-C. Desport, P. Clavelou, N. Guy, H. Derumeaux-Burel, A. Ferrier, and P. Couratier. 2009. "Hypermetabolism in ALS Patients: An Early and Persistent Phenomenon." *Journal of Neurology* 256 (8): 1236–42.

Braak, H, and E Braak. 1991. "Neuropathological Stageing of Alzheimer-Related Changes." *Acta Neuropathologica* 82 (4): 239–59.

Braak, Heiko, Johannes Brettschneider, Albert C Ludolph, Virginia M Lee, John Q Trojanowski, and Kelly Del Tredici. 2013. "Amyotrophic Lateral Sclerosis—a Model of Corticofugal Axonal Spread." *Nature Reviews Neurology* 9 (12). Nature Publishing Group: 708–14.

Braak, Heiko, Kelly Del Tredici, Udo Rüb, Rob A.I de Vos, Ernst N.H Jansen Steur, and Eva Braak. 2003. "Staging of Brain Pathology Related to Sporadic Parkinson's Disease." *Neurobiology of Aging* 24 (2): 197–211.

Brettschneider, Johannes, Kelly Del Tredici, Jon B. Toledo, John L. Robinson, David J. Irwin, Murray Grossman, Eunran Suh, et al. 2013. "Stages of pTDP-43 Pathology in Amyotrophic Lateral Sclerosis." *Annals of Neurology* 74 (1): 20–38.

Callen, D J, S E Black, F Gao, C B Caldwell, and J P Szalai. 2001. "Beyond the Hippocampus: MRI

Volumetry Confirms Widespread Limbic Atrophy in AD." *Neurology* 57 (C): 1669–74.

Castellani, Rudy J., Raj K. Rolston, and Mark A. Smith. 2010. "Alzheimer Disease." *Disease-a-Month* 56 (9). Elsevier Inc.: 484–546.

Chew, Jeannie, Tania F Gendron, Mercedes Prudencio, Hiroki Sasaguri, Y.-J. Zhang, Monica Castanedes-Casey, Chris W Lee, et al. 2015. "C9ORF72 Repeat Expansions in Mice Cause TDP-43 Pathology, Neuronal Loss, and Behavioral Deficits." *Science* 348 (6239): 1151–54.

Chiang, P.-M., J Ling, Y H Jeong, D L Price, S M Aja, and P C Wong. 2010. "Deletion of TDP-43 down-Regulates Tbc1d1, a Gene Linked to Obesity, and Alters Body Fat Metabolism." *Proceedings of the National Academy of Sciences* 107 (37): 16320–24.

Chou, Thomas C, Thomas E Scammell, Joshua J Gooley, Stephanie E Gaus, Clifford B Saper, and Jun Lu. 2003. "Critical Role of Dorsomedial Hypothalamic Nucleus in a Wide Range of Behavioral Circadian Rhythms." *The Journal of Neuroscience : The Official Journal of the Society for Neuroscience* 23 (33): 10691–702.

Cirulli, Elizabeth T, Brittany N Lasseigne, Slavé Petrovski, Peter C Sapp, Patrick A Dion, Claire S Leblond, Julien Couthouis, et al. 2015. "Exome Sequencing in Amyotrophic Lateral Sclerosis Identifies Risk Genes and Pathways." *Science* 347 (6229): 1436–41.

Ciura, Sorana, Serena Lattante, Isabelle Le Ber, Morwena Latouche, Hervé Tostivint, Alexis Brice, and Edor Kabashi. 2013. "Loss of Function of C9orf72 Causes Motor Deficits in a Zebrafish Model of Amyotrophic Lateral Sclerosis." *Annals of Neurology* 74 (2)

Clarke, Julia R, N. M. Lyra e Silva, Claudia P Figueiredo, Rudimar L Frozza, Jose H Ledo, Danielle Beckman, Carlos K Katashima, et al. 2015. "Alzheimer-Associated A Oligomers Impact the Central Nervous System to Induce Peripheral Metabolic Deregulation." *EMBO Molecular Medicine* 7 (2): 190–210.

Claxton, Amy, Laura D. Baker, Angela Hanson, Emily H. Trittschuh, Brenna Cholerton, Amy Morgan, Maureen Callaghan, Matthew Arbuckle, Colin Behl, and Suzanne Craft. 2015. "Long-Acting Intranasal Insulin Detemir Improves Cognition for Adults with Mild Cognitive Impairment or Early-Stage Alzheimer's Disease Dementia." *Journal of Alzheimer's Disease* 44 (3): 897–906.

Clerc, Pascaline, Scott Lipnick, and Catherine Willett. 2016. "A Look into the Future of ALS Research." *Drug Discovery Today* 21 (6). Elsevier Ltd: 939–49.

Couratier, P., P. Corcia, G. Lautrette, M. Nicol, P.-M. Preux, and B. Marin. 2016. "Epidemiology of Amyotrophic Lateral Sclerosis: A Review of Literature." *Revue Neurologique* 172 (1). Elsevier Masson SAS: 37–45.

Crook, Zachary R., and David Housman. 2011. “Huntington’s Disease: Can Mice Lead the Way to Treatment?” *Neuron* 69 (3). Elsevier Inc.: 423–35.

Cui, Huxing, Jong-Woo Sohn, Laurent Gautron, Hisayuki Funahashi, Kevin W Williams, Joel K Elmquist, and Michael Lutter. 2012. “Neuroanatomy of Melanocortin-4 Receptor Pathway in the Lateral Hypothalamic Area.” *The Journal of Comparative Neurology* 520 (18): 4168–83.

Cykowski, Matthew D, Hidehiro Takei, Paul E Schulz, Stanley H Appel, and Suzanne Z Powell. 2014. “TDP-43 Pathology in the Basal Forebrain and Hypothalamus of Patients with Amyotrophic Lateral Sclerosis.” *Acta Neuropathologica Communications* 2 (1): 171.

DeJesus-Hernandez, Mariely, Ian R. Mackenzie, Bradley F. Boeve, Adam L. Boxer, Matt Baker, Nicola J. Rutherford, Alexandra M. Nicholson, et al. 2011. “Expanded GGGGCC Hexanucleotide Repeat in Noncoding Region of C9ORF72 Causes Chromosome 9p-Linked FTD and ALS.” *Neuron* 72 (2). Elsevier Inc.: 245–56.

Dentel, Christel, Lavinia Palamiuc, Alexandre Henriques, Béatrice Lannes, Odile Spreux-Varoquaux, Lise Gutknecht, Frédérique René, et al. 2013. “Degeneration of Serotonergic Neurons in Amyotrophic Lateral Sclerosis: A Link to Spasticity.” *Brain : A Journal of Neurology* 136 (Pt 2): 483–93.

Desport, J C, P M Preux, TC C Truong, JM M Vallat, D Sautereau, and P Couratier. 1999. “Nutritional Status Is a Prognostic Factor for Survival in ALS Patients.” *Neurology* 53 (5): 1059–1059.

Desport, Jean-Claude, Frédéric Torny, Mathieu Lacoste, Pierre-Marie Preux, and Philippe Couratier. 2006. “Hypermetabolism in ALS: Correlations with Clinical and Paraclinical Parameters.” *Neurodegenerative Diseases* 2 (3-4): 202–7.

Djousse, L., B Knowlton, L A Cupples, K Marder, I Shoulson, and R H Myers. 2002. “Weight Loss in Early Stage of Huntington’s Disease.” *Neurology* 59 (9): 1325–30.

Donovan, Michael H, and Laurence H Tecott. 2013. “Serotonin and the Regulation of Mammalian Energy Balance.” *Frontiers in Neuroscience* 7 (March): 36.

Droogsma, E, D van Asselt, and P P De Deyn. 2015. “Weight Loss and Undernutrition in Community-Dwelling Patients with Alzheimer’s Dementia.” *Zeitschrift Für Gerontologie Und Geriatrie* 48 (4): 318–24.

Dupuis, L, P Corcia, A Fergani, J. -L. Gonzalez De Aguilar, D Bonnefont-Rousselot, R Bittar, D Seilhean, et al. 2008. “Dyslipidemia Is a Protective Factor in Amyotrophic Lateral Sclerosis.” *Neurology* 70 (13): 1004–9.

Dupuis, L., H. Oudart, F. Rene, J.-L. G. de Aguilar, and J.-P. Loeffler. 2004. “Evidence for Defective

Energy Homeostasis in Amyotrophic Lateral Sclerosis: Benefit of a High-Energy Diet in a Transgenic Mouse Model." *Proceedings of the National Academy of Sciences* 101 (30): 11159–64.

Dupuis, Luc, Marc de Tapia, Frédérique René, Bernadette Lutz-Bucher, Jon W Gordon, Luc Mercken, Laurent Pradier, and Jean-Philippe Loeffler. 2000. "Differential Screening of Mutated SOD1 Transgenic Mice Reveals Early Up-Regulation of a Fast Axonal Transport Component in Spinal Cord Motor Neurons." *Neurobiology of Disease* 7 (4): 274–85.

Dupuis, Luc, Pierre-François Pradat, Albert C Ludolph, and Jean-Philippe Loeffler. 2011. "Energy Metabolism in Amyotrophic Lateral Sclerosis." *The Lancet Neurology* 10 (1): 75–82.

El Oussini, Hajer, Hanna Bayer, Jelena Scekic-Zahirovic, Pauline Vercruysse, Jérôme Sinniger, Sylvie Dirrig-Grosch, Stéphane Dieterlé, et al. 2016. "Serotonin 2B Receptor Slows Disease Progression and Prevents Degeneration of Spinal Cord Mononuclear Phagocytes in Amyotrophic Lateral Sclerosis." *Acta Neuropathologica* 131 (3). Springer Berlin Heidelberg: 465–80.

Esmaeili, Mohammad A., Marzieh Panahi, Shilpi Yadav, Leah Hennings, and Mahmoud Kiaei. 2013. "Premature Death of TDP-43 (A315T) Transgenic Mice due to Gastrointestinal Complications prior to Development of Full Neurological Symptoms of Amyotrophic Lateral Sclerosis." *International Journal of Experimental Pathology* 94 (1): 56–64.

Ferguson, Alastair V, Kevin J Latchford, and Willis K Samson. 2008. "The Paraventricular Nucleus of the Hypothalamus – a Potential Target for Integrative Treatment of Autonomic Dysfunction." *Expert Opinion on Therapeutic Targets* 12 (6): 717–27.

Figley, Matthew D., Anna Thomas, and Aaron D. Gitler. 2014. "Evaluating Noncoding Nucleotide Repeat Expansions in Amyotrophic Lateral Sclerosis." *Neurobiology of Aging* 35 (4). Elsevier Ltd: 936.e1–936.e4.

Freibaum, Brian D, Yubing Lu, Rodrigo Lopez-Gonzalez, Nam Chul Kim, Sandra Almeida, Kyung-Ha Lee, Nisha Badders, et al. 2015. "GGGGCC Repeat Expansion in C9orf72 Compromises Nucleocytoplasmic Transport." *Nature* 525 (7567): 129–33.

Freischmidt, Axel, Thomas Wieland, Benjamin Richter, Wolfgang Ruf, Veronique Schaeffer, Kathrin Müller, Nicolai Marroquin, et al. 2015. "Haploinsufficiency of TBK1 Causes Familial ALS and Fronto-Temporal Dementia." *Nature Neuroscience* 18 (5): 631–36.

Fronczek, Rolf, Sarita van Geest, Marijke Frölich, Sebastiaan Overeem, Freek W C Roelandse, Gert Jan Lammers, and Dick F. Swaab. 2012. "Hypocretin (Orexin) Loss in Alzheimer's Disease." *Neurobiology of Aging* 33 (8). Elsevier Inc.: 1642–50.

Gabery, Sanaz, Nellie Georgiou-Karistianis, Sofia Hult Lundh, Rachel Y. Cheong, Andrew Churchyard, Phyllis Chua, Julie C. Stout, Gary F. Egan, Deniz Kirik, and Åsa Petersén. 2015. "Volumetric Analysis of the Hypothalamus in Huntington Disease Using 3T MRI: The IMAGE-HD Study." Edited by Jan Kassubek. *PLOS ONE* 10 (2): e0117593.

Gabery, Sanaz, Karen Murphy, Kristofer Schultz, Clement T. Loy, Elizabeth McCusker, Deniz Kirik, Glenda Halliday, and Åsa Petersén. 2010. "Changes in Key Hypothalamic Neuropeptide Populations in Huntington Disease Revealed by Neuropathological Analyses." *Acta Neuropathologica* 120 (6): 777–88.

Gal, J, A.-L. Strom, R Kilty, F Zhang, and H Zhu. 2007. "p62 Accumulates and Enhances Aggregate Formation in Model Systems of Familial Amyotrophic Lateral Sclerosis." *Journal of Biological Chemistry* 282 (15): 11068–77.

Gallo, Valentina, Petra A. Wark, Mazda Jenab, Neil Pearce, Carol Brayne, Roel Vermeulen, Peter M. Andersen, et al. 2013. "Prediagnostic Body Fat and Risk of Death from Amyotrophic Lateral Sclerosis: The EPIC Cohort." *Neurology* 80 (9): 829–38.

Gao, Qian, and Tamas L Horvath. 2007. "Neurobiology of Feeding and Energy Expenditure." *Annual Review of Neuroscience* 30 (1): 367–98.

Gatta-Cherifi, B. 2012. "Neurobiologie de La Prise Alimentaire." *Médecine Des Maladies Métaboliques* 6 (2). Elsevier Masson SAS: 115–19.

Gautron, Laurent, Michael Lazarus, Michael M. Scott, Clifford B. Saper, and Joel K. Elmquist. 2010. "Identifying the Efferent Projections of Leptin-Responsive Neurons in the Dorsomedial Hypothalamus Using a Novel Conditional Tracing Approach." *The Journal of Comparative Neurology* 518 (11): 2090–2108.

Gilbert, G. J. 2009. "Weight loss in Huntington disease increases with higher CAG repeat number." *Neurology* 73 (7): 572–572.

Goodman, Anna O.G., Peter R. Murgatroyd, Gema Medina-Gomez, Nigel I. Wood, Nicholas Finer, Antonio J. Vidal-Puig, A. Jennifer Morton, and Roger A. Barker. 2008. "The Metabolic Profile of Early Huntington's Disease- a Combined Human and Transgenic Mouse Study." *Experimental Neurology* 210 (2): 691–98.

Gordon, Paul H, Robert G Miller, and Dan H Moore. 2004. "ALSFRS-R." *Amyotrophic Lateral Sclerosis and Other Motor Neuron Disorders* 5 (sup1): 90–93.

Guo, Yansu, Qian Wang, Kunxi Zhang, Ting An, Pengxiao Shi, Zhongyao Li, Weisong Duan, and Chunyan Li. 2012. "HO-1 Induction in Motor Cortex and Intestinal Dysfunction in TDP-43 A315T Transgenic Mice." *Brain Research* 1460 (June). Elsevier B.V.: 88–95.

Gurney, M., Haifeng Pu, A. Chiu, M. Dal Canto, C. Polchow, D. Alexander, Jan Caliendo, et al.

1994. “Motor Neuron Degeneration in Mice That Express a Human Cu,Zn Superoxide Dismutase Mutation.” *Science* 264 (5166): 1772–75.

Harper, Peter S. 1992. “The Epidemiology of Huntington’s Disease.” *Human Genetics* 89 (4): 365–76.

Herdewyn, Sarah, Carla Cirillo, Ludo Van Den Bosch, Wim Robberecht, Pieter Vanden Berghe, and Philip Van Damme. 2014. “Prevention of Intestinal Obstruction Reveals Progressive Neurodegeneration in Mutant TDP-43 (A315T) Mice.” *Molecular Neurodegeneration* 9 (1): 24.

Hicks, Geoffrey G, Nagendra Singh, Abudi Nashabi, Sabine Mai, Gracjan Bozek, Ludger Klewes, Djula Arapovic, et al. 2000. “Fus Deficiency in Mice Results in Defective B-Lymphocyte Development and Activation, High Levels of Chromosomal Instability and Perinatal Death.” *Nature Genetics* 24 (2): 175–79.

Hill, Jennifer W. 2010. “Gene Expression and the Control of Food Intake by Hypothalamic POMC / CART Neurons.” *The Open Neuroendocrinology Journal* 3: 21–27.

Hillebrand, J.J.G., D. de Wied, and R.a.H. Adan. 2002. “Neuropeptides, Food Intake and Body Weight Regulation: A Hypothalamic Focus.” *Peptides* 23 (12): 2283–2306.

Holden, Karen F., Karla Lindquist, Frances A. Tylavsky, Caterina Rosano, Tamara B. Harris, and Kristine Yaffe. 2009. “Serum Leptin Level and Cognition in the Elderly: Findings from the Health ABC Study.” *Neurobiology of Aging* 30 (9): 1483–89.

Huisman, Mark H. B., Meinie Seelen, Perry T. C. van Doormaal, Sonja W. de Jong, Jeanne H. M. de Vries, Anneke J. van der Kooi, Marianne de Visser, H. Jurgen Schelhaas, Leonard H. van den Berg, and Jan H. Veldink. 2015. “Effect of Presymptomatic Body Mass Index and Consumption of Fat and Alcohol on Amyotrophic Lateral Sclerosis.” *JAMA Neurology* 72 (10): 1155.

Hult Lundh, Sofia, Nathalie Nilsson, Rana Soylu, Deniz Kirik, and A. Petersen. 2013. “Hypothalamic Expression of Mutant Huntingtin Contributes to the Development of Depressive-like Behavior in the BAC Transgenic Mouse Model of Huntington’s Disease.” *Human Molecular Genetics* 22 (17): 3485–97.

Hult, Sofia, Rana Soylu, Tomas Björklund, Bengt F. Belgardt, Jan Mauer, Jens C. Brüning, Deniz Kirik, and Åsa Petersén. 2011. “Mutant Huntingtin Causes Metabolic Imbalance by Disruption of Hypothalamic Neurocircuits.” *Cell Metabolism* 13 (4): 428–39.

Ikeda, M., J. Brown, A J Holland, R. Fukuhara, and J R Hodges. 2002. “Changes in Appetite, Food Preference, and Eating Habits in Frontotemporal Dementia and Alzheimer’s Disease.” *Journal of Neurology, Neurosurgery, and Psychiatry* 73 (4): 371–76.

Ishii, Makoto, and Costantino Iadecola. 2015. “Metabolic and Non-Cognitive Manifestations of Alzheimer’s Disease: The Hypothalamus as Both Culprit and Target of Pathology.” *Cell Metabolism* 22 (5). Elsevier Inc.: 761–76.

Ishii, Makoto, Gang Wang, Gianfranco Racchumi, Jonathan P. Dyke, and Costantino Iadecola. 2014. “Transgenic Mice Overexpressing Amyloid Precursor Protein Exhibit Early Metabolic Deficits and a Pathologically Low Leptin State Associated with Hypothalamic Dysfunction in Arcuate Neuropeptide Y Neurons.” *Journal of Neuroscience* 34 (27): 9096–9106.

Ishiwata, Takayuki, Hiroshi Hasegawa, Toru Yazawa, Minoru Otokawa, and Yasutsugu Aihara. 2002. “Functional Role of the Preoptic Area and Anterior Hypothalamus in Thermoregulation in Freely Moving Rats.” *Neuroscience Letters* 325 (3): 167–70.

Janson, J., T. Laedtke, J. E. Parisi, P. O’Brien, R. C. Petersen, and P. C. Butler. 2004. “Increased Risk of Type 2 Diabetes in Alzheimer Disease.” *Diabetes* 53 (2): 474–81.

Jawaid, Ali, Santosh B Murthy, Andrew M Wilson, Salah U Qureshi, Moath J Amro, Michael Wheaton, Ericka Simpson, et al. 2010. “A Decrease in Body Mass Index Is Associated with Faster Progression of Motor Symptoms and Shorter Survival in ALS.” *Amyotrophic Lateral Sclerosis* 11 (6): 542–48.

Jiang, Jie, Qiang Zhu, Tania F. Gendron, Shahram Saberi, Melissa McAlonis-Downes, Amanda Seelman, Jennifer E. Stauffer, et al. 2016. “Gain of Toxicity from ALS/FTD-Linked Repeat Expansions in C9ORF72 Is Alleviated by Antisense Oligonucleotides Targeting GGGGCC-Containing RNAs.” *Neuron* 90 (3). Elsevier Inc.: 535–50.

Jovičić, Ana, Jerome Mertens, Steven Boeynaems, Elke Bogaert, Noori Chai, Shizuka B Yamada, Joseph W Paul, et al. 2015. “Modifiers of C9orf72 Dipeptide Repeat Toxicity Connect Nucleocytoplasmic Transport Defects to FTD/ALS.” *Nature Neuroscience* 18 (9): 1226–29.

Kasarskis, E J, S Berryman, J G Vanderleest, a R Schneider, and C J McClain. 1996. “Nutritional Status of Patients with Amyotrophic Lateral Sclerosis: Relation to the Proximity of Death.” *The American Journal of Clinical Nutrition* 63 (1): 130–37.

Kassubek, Jan, H.-P. Muller, Kelly Del Tredici, Johannes Brettschneider, Elmar H. Pinkhardt, D. Lule, S. Bohm, Heiko Braak, and Albert C. Ludolph. 2014. “Diffusion Tensor Imaging Analysis of Sequential Spreading of Disease in Amyotrophic Lateral Sclerosis Confirms Patterns of TDP-43 Pathology.” *Brain* 137 (6): 1733–40.

Kim, Bhumsoo, and Eva L Feldman. 2015. “Insulin Resistance as a Key Link for the Increased Risk of Cognitive Impairment in the Metabolic Syndrome.” *Experimental & Molecular Medicine* 47 (3). Nature Publishing Group: e149.

Koch, Marco, Luis Varela, Jung Dae Jae Geun Kim, Jung Dae Jae Geun Kim, Francisco Hernández-Nuño, Stephanie E. Simonds, Carlos M. Castorena, et al. 2015. “Hypothalamic POMC Neurons Promote Cannabinoid-Induced Feeding.” *Nature* 519 (7541): 45–50.

Koppers, Max, Anna M. Blokhuis, Henk-Jan Westeneng, Margo L. Terpstra, Caroline A C Zundel, Renata Vieira de Sá, Raymond D. Schellevis, et al. 2015. “C9orf72 Ablation in Mice Does Not Cause Motor Neuron Degeneration or Motor Deficits.” *Annals of Neurology* 78 (3): 426–38.

Kostic Dedic, Svetlana I, Zorica Stevic, Velimir Dedic, Vidosava Rakocevic Stojanovic, Milena Milicev, and Dragana Lavrnic. 2012. “Is Hyperlipidemia Correlated with Longer Survival in Patients with Amyotrophic Lateral Sclerosis?” *Neurological Research* 34 (6): 576–80.

Kühnlein, Peter, Hans-Jürgen Gdynia, Anne-Dorte Sperfeld, Beate Lindner-Pfleghar, Albert Christian Ludolph, Mario Prosiegel, and Axel Riecker. 2008. “Diagnosis and Treatment of Bulbar Symptoms in Amyotrophic Lateral Sclerosis.” *Nature Clinical Practice Neurology* 4 (7): 366–74.

Kuroda, M. 2000. “Male Sterility and Enhanced Radiation Sensitivity in TLS-/- Mice.” *The EMBO Journal* 19 (3): 453–62.

Lacomblez, L, G Bensimon, P N Leigh, P Guillet, and V Meininger. 1996. “Dose-Ranging Study of Riluzole in Amyotrophic Lateral Sclerosis. Amyotrophic Lateral Sclerosis/Riluzole Study Group II.” *Lancet (London, England)* 347 (9013): 1425–31.

Lattante, Serena, Sorana Ciura, Guy A. Rouleau, and Edor Kabashi. 2015. “Defining the Genetic Connection Linking Amyotrophic Lateral Sclerosis (ALS) with Frontotemporal Dementia (FTD).” *Trends in Genetics* 31 (5). Elsevier Ltd: 263–73.

Lattante, Serena, Guy A. Rouleau, and Edor Kabashi. 2013. “TARDBP and FUS Mutations Associated with Amyotrophic Lateral Sclerosis: Summary and Update.” *Human Mutation* 34 (6): 812–26.

Lechan, Ronald M., and Csaba Fekete. 2006. “The TRH Neuron: A Hypothalamic Integrator of Energy Metabolism.” In *Progress in Brain Research*, 153:209–35.

Li, Jingcheng, Zhian Hu, and Luis de Lecea. 2014. “The Hypocretins/orexins: Integrators of Multiple Physiological Functions.” *British Journal of Pharmacology* 171 (2): 332–50.

Loskutova, Natalia, Robyn A. Honea, William M. Brooks, and Jeffrey M. Burns. 2010. “Reduced Limbic and Hypothalamic Volumes Correlate with Bone Density in Early Alzheimer’s Disease.” *Journal of Alzheimer’s Disease : JAD* 20 (1): 313–22.

Ludolph, Albert, Vivian Drory, Orla Hardiman, Imaharu Nakano, John Ravits, Wim Robberecht, and Jeremy Shefner. 2015. “A Revision of the El Escorial Criteria - 2015.” *Amyotrophic*

Lateral Sclerosis and Frontotemporal Degeneration 16 (5-6): 291–92.

Marder, K., H. Zhao, S. Eberly, C. M. Tanner, D. Oakes, and I. Shoulson. 2009. "Dietary Intake in Adults at Risk for Huntington Disease: Analysis of PHAROS Research Participants." *Neurology* 73 (5): 385–92.

Marin, B, J C Desport, P Kajeu, P Jesus, B Nicolaud, M Nicol, P M Preux, and P Couratier. 2011. "Alteration of Nutritional Status at Diagnosis Is a Prognostic Factor for Survival of Amyotrophic Lateral Sclerosis Patients." *Journal of Neurology, Neurosurgery & Psychiatry* 82 (6): 628–34.

McGuire, Matthew J., and Makoto Ishii. 2016. "Leptin Dysfunction and Alzheimer's Disease: Evidence from Cellular, Animal, and Human Studies." *Cellular and Molecular Neurobiology* 36 (2). Springer US: 203–17.

McNeil, S M, A Novelletto, J Srinidhi, G Barnes, I Kornbluth, M R Altherr, J J Wasmuth, J F Gusella, M E MacDonald, and R H Myers. 1997. "Reduced Penetrance of the Huntington's Disease Mutation." *Human Molecular Genetics* 6 (5): 775–79.

Melmed, Shlomo. 1995. *The Pituitary*. *Endocrine*.

Miller, Robert G, J D Mitchell, and Dan H Moore. 2012. "Riluzole for Amyotrophic Lateral Sclerosis (ALS)/motor Neuron Disease (MND)." In *Cochrane Database of Systematic Reviews*, edited by Robert G Miller. Chichester, UK: John Wiley & Sons, Ltd.

Mitchell, Jacqueline C., Philip McGoldrick, Caroline Vance, Tibor Hortobagyi, Jemeen Sreedharan, Boris Rogelj, Elizabeth L. Tudor, et al. 2013. "Overexpression of Human Wild-Type FUS Causes Progressive Motor Neuron Degeneration in an Age- and Dose-Dependent Fashion." *Acta Neuropathologica* 125 (2): 273–88.

Mizielinska, S., S. Gronke, T. Niccoli, C. E. Ridler, E. L. Clayton, A. Devoy, T. Moens, et al. 2014. "C9orf72 Repeat Expansions Cause Neurodegeneration in Drosophila through Arginine-Rich Proteins." *Science* 345 (6201): 1192–94.

Mizielinska, Sarah, and Adrian M. Isaacs. 2014. "C9orf72 Amyotrophic Lateral Sclerosis and Frontotemporal Dementia." *Current Opinion in Neurology* 27 (5): 515–23.

Mizuno, Tooru M., Steven P. Kleopoulos, Hugo T. Bergen, James L. Roberts, Catherine A. Priest, and Charles V. Mobbs. 1998. "Hypothalamic pro-Opiomelanocortin mRNA Is Reduced by Fasting in Ob/ob and Db/db Mice, but Is Stimulated by Leptin." *Diabetes* 47 (2): 294–97.

Mochel, Fanny, Perrine Charles, François Seguin, Julie Barritault, Christiane Coussieu, Laurence Perin, Yves Le Bouc, et al. 2007. "Early Energy Deficit in Huntington Disease: Identification of a Plasma Biomarker Traceable during Disease Progression." Edited by Ulrich Mueller.

PLoS ONE 2 (7): e647.

Morrison, Shaun F. 2011. “Central Neural Pathways for Thermoregulation.” *Frontiers in Bioscience* 16 (1): 74.

Morton, Gregory J, Thomas H Meek, and Michael W Schwartz. 2014. “Neurobiology of Food Intake in Health and Disease.” *Nature Reviews Neuroscience* 15 (6). Nature Publishing Group: 367–78.

Nakamura, Masataka, Kevin F. Bieniek, Wen-Lang Lin, Neill R. Graff-Radford, Melissa E. Murray, Monica Castanedes-Casey, Pamela Desaro, et al. 2015. “A Truncating SOD1 Mutation, p.Gly141X, Is Associated with Clinical and Pathologic Heterogeneity, Including Frontotemporal Lobar Degeneration.” *Acta Neuropathologica* 130 (1). Springer Berlin Heidelberg: 145–57.

Nau, Karen L., Mark B. Bromberg, Dallas A. Forshew, and Victor L. Katch. 1995. “Individuals with Amyotrophic Lateral Sclerosis Are in Caloric Balance despite Losses in Mass.” *Journal of the Neurological Sciences* 129 (SUPPL.): 47–49.

Neary, David, Julie Snowden, and David Mann. 2005. “Frontotemporal Dementia.” *The Lancet. Neurology* 4 (11). Elsevier Ltd: 771–80.

Nelson, LM, C Matkin, WT Jr Longstreth, and V. McGuire. 2000. “Population-Based Case-Control Study of Amyotrophic Lateral Sclerosis in.” *Am J Epidemiol.* 151 (2): 164–73.

Neumann, Manuela. 2009. “Molecular Neuropathology of TDP-43 Proteinopathies.” *International Journal of Molecular Sciences* 10 (1): 232–46.

Neumann, Manuela, Deepak M. Sampathu, Linda K. Kwong, Adam C. Truax, Matthew C. Micsenyi, Thomas T. Chou, Jennifer Bruce, et al. 2006. “Ubiquitinated TDP-43 in Frontotemporal Lobar Degeneration and Amyotrophic Lateral Sclerosis.” *Science* 314 (5796): 130–33.

Nilsson, Ida A K, Charlotte Lindfors, Martin Schalling, Tomas Hökfelt, and Jeanette E. Johansen. 2013. “Anorexia and Hypothalamic Degeneration.” *Vitamins and Hormones* 92: 27–60.

O’Reilly, Éilis J., Hao Wang, Marc G. Weisskopf, Kathryn C. Fitzgerald, Guido Falcone, Marjorie L. McCullough, Michael Thun, Yikyung Park, Laurence N. Kolonel, and Alberto Ascherio. 2013. “Premorbid Body Mass Index and Risk of Amyotrophic Lateral Sclerosis.” *Amyotrophic Lateral Sclerosis and Frontotemporal Degeneration* 14 (3): 205–11.

O’Rourke, J G, L. Bogdanik, A Yáñez, D. Lall, A. J. Wolf, A. K. M. G. Muhammad, R. Ho, et al. 2016. “C9orf72 Is Required for Proper Macrophage and Microglial Function in Mice.” *Science (New York, N.Y.)* 351 (6279): 1324–29.

O'Rourke, Jacqueline G., Laurent Bogdanik, A.K.M.G. Muhammad, Tania F. Gendron, Kevin J. Kim, Andrew Austin, Janet Cady, et al. 2015. "C9orf72 BAC Transgenic Mice Display Typical Pathologic Features of ALS/FTD." *Neuron* 88 (5). Elsevier Inc.: 892–901.

Paganoni, Sabrina, Jing Deng, Matthew Jaffa, Merit E.. Cudkowicz, and Anne-Marie Wills. 2011. "Body Mass Index, Not Dyslipidemia, Is an Independent Predictor of Survival in Amyotrophic Lateral Sclerosis." *Muscle & Nerve* 44 (1): 20–24.

Paredes, Raúl G. 2003. "Medial Preoptic Area/anterior Hypothalamus and Sexual Motivation." *Scandinavian Journal of Psychology* 44 (3): 203–12.

Park, Yongsoon, Jinhee Park, Yeonsun Kim, Heejoon Baek, and Seung Hyun Kim. 2015. "Association between Nutritional Status and Disease Severity Using the Amyotrophic Lateral Sclerosis (ALS) Functional Rating Scale in ALS Patients." *Nutrition (Burbank, Los Angeles County, Calif.)* 31 (11-12). Elsevier Inc.: 1362–67.

Paxinos, George, and Keith B. J. Franklin. 2001. *The Mouse Brain in Stereotaxic Coordinates*. 2nd edition

Peters, Owen M., Gabriela Toro Cabrera, Helene Tran, Tania F. Gendron, Jeanne E. McKeon, Jake Metterville, Alexandra Weiss, et al. 2015. "Human C9ORF72 Hexanucleotide Expansion Reproduces RNA Foci and Dipeptide Repeat Proteins but Not Neurodegeneration in BAC Transgenic Mice." *Neuron* 88 (5). Elsevier Ltd: 902–9.

Piguet, Olivier, Asa Petersén, Bonnie Yin Ka Lam, Sanaz Gabery, Karen Murphy, John R. Hodges, and Glenda M. Halliday. 2011. "Eating and Hypothalamus Changes in Behavioral-Variant Frontotemporal Dementia." *Annals of Neurology* 69 (2): 312–19.

Plucińska, Kaja, Ruta Dekeryte, David Koss, Kirsty Shearer, Nimesh Mody, Phillip D. Whitfield, Mary K. Doherty, et al. 2016. "Neuronal Human BACE1 Knockin Induces Systemic Diabetes in Mice." *Diabetologia* 59 (7): 1513–23.

Pollak Dorocic, Iskra, Daniel Fürth, Yang Xuan, Yvonne Johansson, Laura Pozzi, Gilad Silberberg, Marie Carlén, and Konstantinos Meletis. 2014. "A Whole-Brain Atlas of Inputs to Serotonergic Neurons of the Dorsal and Median Raphe Nuclei." *Neuron* 83 (3): 663–78.

Pradat, Pierre-Francois, Gaelle Bruneteau, Paul H Gordon, Luc Dupuis, Dominique Bonnefont-Rousselot, Dominique Simon, Francois Salachas, et al. 2010. "Impaired Glucose Tolerance in Patients with Amyotrophic Lateral Sclerosis." *Amyotrophic Lateral Sclerosis : Official Publication of the World Federation of Neurology Research Group on Motor Neuron Diseases* 11 (1-2): 166–71.

Renton, Alan E, Adriano Chiò, and Bryan J Traynor. 2014. "State of Play in Amyotrophic Lateral Sclerosis Genetics." *Nature Neuroscience* 17 (1). Nature Publishing Group: 17–23.

Ripps, M E, G W Huntley, P R Hof, J H Morrison, and J W Gordon. 1995. “Transgenic Mice Expressing an Altered Murine Superoxide Dismutase Gene Provide an Animal Model of Amyotrophic Lateral Sclerosis.” *Proceedings of the National Academy of Sciences of the United States of America* 92 (3): 689–93.

Ross, Christopher A., and Sarah J. Tabrizi. 2011. “Huntington’s Disease: From Molecular Pathogenesis to Clinical Treatment.” *The Lancet. Neurology* 10 (1). Elsevier Ltd: 83–98.

Rui, Liangyou. 2013. “Brain Regulation of Energy Balance and Body Weight.” *Reviews in Endocrine & Metabolic Disorders* 14 (4): 387–407.

Ruiz, Henry H, Tiffany Chi, Claudia Lindtner, Wilson Hsieh, Andrew C Shin, Michelle Ehrlich, Sam Gandy, and Christoph Buettner. 2016. “Increased Susceptibility to Metabolic Dysregulation in a Mouse Model of Alzheimer’s Disease Is Associated with Impaired Hypothalamic Insulin Signaling and Elevated BCAA Levels.” *Alzheimer’s & Dementia : The Journal of the Alzheimer's Association*, February. Elsevier Inc., 1–11.

Sabatier, Nancy, Gareth Leng, and John Menzies. 2013. “Oxytocin, Feeding, and Satiety.” *Frontiers in Endocrinology* 4 (March): 35.

Scekic-Zahirovic, Jelena, Oliver Sendscheid, Hajer El Oussini, Mélanie Jambeau, Ying Sun, Sina Mersmann, Marina Wagner, et al. 2016. “Toxic Gain of Function from Mutant FUS Protein Is Crucial to Trigger Cell Autonomous Motor Neuron Loss.” *The EMBO Journal* 35 (10): 1077–97.

Schwartz, Michael W, Stephen C Woods, D Porte, Randy J Seeley, and Denis G Baskin. 2000. “Central Nervous System Control of Food Intake.” *Nature* 404 (6778): 661–71.

Sellier, Chantal, Maria-Letizia Campanari, Camille Julie Corbier, Angeline Gaucherot, Isabelle Kolb-Cheynel, Mustapha Oulad-Abdelghani, Frank Ruffenach, et al. 2016. “Loss of C9ORF72 Impairs Autophagy and Synergizes with polyQ Ataxin-2 to Induce Motor Neuron Dysfunction and Cell Death.” *The EMBO Journal* 35 (12): 1276–97.

Simpson, Katherine Anne, Niamh M Martin, and Stephen R Bloom. 2009. “Hypothalamic Regulation of Food Intake and Clinical Therapeutic Applications.” *Arquivos Brasileiros de Endocrinologia E Metabologia* 53 (2): 120–28.

Sohn, Jong-Woo. 2015. “Network of Hypothalamic Neurons That Control Appetite.” *BMB Reports* 48 (4): 229–33.

Stallings, Nancy R., Krishna Puttaparthi, Katherine J. Dowling, Christina M. Luther, Dennis K. Burns, Kathryn Davis, and Jeffrey L. Elliott. 2013. “TDP-43, an ALS Linked Protein, Regulates Fat Deposition and Glucose Homeostasis.” *PloS One* 8 (8): e71793.

Stribl, Carola, Aladin Samara, Dietrich Trümbach, Regina Peis, Manuela Neumann, Helmut Fuchs, Valerie Gailus-Durner, et al. 2014. “Mitochondrial Dysfunction and Decrease in Body Weight of a Transgenic Knock-in Mouse Model for TDP-43.” *The Journal of Biological Chemistry* 289 (15): 10769–84.

Sudria-Lopez, Emma, Max Koppers, Marina de Wit, Christiaan van der Meer, Henk-Jan Westeneng, Caroline A. C. Zundel, Sameh A. Youssef, et al. 2016. “Full Ablation of C9orf72 in Mice Causes Immune System-Related Pathology and Neoplastic Events but No Motor Neuron Defects.” *Acta Neuropathologica* 132 (1). Springer Berlin Heidelberg: 145–47.

Sullivan, Peter M., Xiaolai Zhou, Adam M. Robins, Daniel H. Paushter, Dongsung Kim, Marcus B. Smolka, and Fenghua Hu. 2016. “The ALS/FTLD Associated Protein C9orf72 Associates with SMCR8 and WDR41 to Regulate the Autophagy-Lysosome Pathway.” *Acta Neuropathologica Communications* 4 (1). Acta Neuropathologica Communications: 51.

Süssmuth, S. D., V. M. Müller, C. Geitner, G. B. Landwehrmeyer, S. Iff, A. Gemperli, and Michael Orth. 2015. “Fat-Free Mass and Its Predictors in Huntington’s Disease.” *Journal of Neurology* 262 (6): 1533–40.

Swaab, Dick F. 2004. “Neuropeptides in Hypothalamic Neuronal Disorders.” *International Review of Cytology* 240 (SPEC.ISS.): 305–75.

Swinnen, Bart, and Wim Robberecht. 2014. “The Phenotypic Variability of Amyotrophic Lateral Sclerosis.” *Nature Reviews. Neurology* 10 (11). Nature Publishing Group: 661–70.

Tsujino, Natsuko, and Takeshi Sakurai. 2009. “Orexin/hypocretin: A Neuropeptide at the Interface of Sleep, Energy Homeostasis, and Reward System.” *Pharmacological Reviews* 61 (2): 162–76.

Vaisman, Nachum, Michal Lusaus, Beatrice Nefussy, Eva Niv, Doron Comaneshter, Ron Hallack, and Vivian E Drory. 2009. “Do Patients with Amyotrophic Lateral Sclerosis (ALS) Have Increased Energy Needs?” *Journal of the Neurological Sciences* 279 (1-2): 26–29.

Valassi, Elena, Massimo Scacchi, and Francesco Cavagnini. 2008. “Neuroendocrine Control of Food Intake.” *Nutrition, Metabolism, and Cardiovascular Diseases : NMCD* 18 (2): 158–68.

van der Burg, Jorien M.M., Karl Bacos, Nigel I. Wood, Andreas Lindqvist, Nils Wierup, Ben Woodman, Jaclyn I. Wamsteeker, et al. 2008. “Increased Metabolism in the R6/2 Mouse Model of Huntington’s Disease.” *Neurobiology of Disease* 29 (1): 41–51.

van Wamelen, Daniel J, N A Aziz, Raymund a C Roos, and Dick F Swaab. 2014. “Hypothalamic Alterations in Huntington’s Disease Patients: Comparison with Genetic Rodent Models.” *Journal of Neuroendocrinology* 26 (11): 761–75.

Voigt, Jörg-Peter, and Heidrun Fink. 2015. “Serotonin Controlling Feeding and Satiety.” *Behavioural Brain Research* 277 (January). Elsevier B.V.: 14–31.

Webster, Christopher P, Emma F Smith, Claudia S Bauer, Annekathrin Moller, Guillaume M Hautbergue, Laura Ferraiuolo, Monika A Myszczynska, et al. 2016. “The C9orf72 Protein Interacts with Rab1a and the ULK1 Complex to Regulate Initiation of Autophagy.” *The EMBO Journal*, June, 1–21.

Wegorzewska, Iga, Shaughn Bell, Nigel J Cairns, Timothy M Miller, and Robert H Baloh. 2009. “TDP-43 Mutant Transgenic Mice Develop Features of ALS and Frontotemporal Lobar Degeneration.” *Proceedings of the National Academy of Sciences of the United States of America* 106 (44): 18809–14.

Wijesekera, Lokesh C, and P Nigel Leigh. 2009. “Amyotrophic Lateral Sclerosis.” *Orphanet Journal of Rare Diseases* 4 (4): 3.

Wills, Anne-Marie, Jane Hubbard, Eric a Macklin, Jonathan Glass, Rup Tandan, Ericka P Simpson, Benjamin Brooks, et al. 2014. “Hypercaloric Enteral Nutrition in Patients with Amyotrophic Lateral Sclerosis: A Randomised, Double-Blind, Placebo-Controlled Phase 2 Trial.” *Lancet (London, England)* 383 (9934): 2065–72.

Wilson, Jenny L., and Pablo J. Enriori. 2015. “A Talk between Fat Tissue, Gut, Pancreas and Brain to Control Body Weight.” *Molecular and Cellular Endocrinology* 418 Pt 2 (December). Elsevier Ireland Ltd: 108–19.

Wong, Philip C., Carlos A. Pardo, David R. Borchelt, Michael K. Lee, Neal G. Copeland, Nancy A. Jenkins, Sangram S. Sisodia, Don W. Cleveland, and Donald L. Price. 1995. “An Adverse Property of a Familial ALS-Linked SOD1 Mutation Causes Motor Neuron Disease Characterized by Vacuolar Degeneration of Mitochondria.” *Neuron* 14 (6): 1105–16.

Xiao, Shangxi, Laura MacNair, Jesse McLean, Phillip McGoldrick, Paul McKeever, Serena Soleimani, Julia Keith, Lorne Zinman, Ekaterina Rogaeva, and Janice Robertson. 2016. “C9orf72 Isoforms in Amyotrophic Lateral Sclerosis and Frontotemporal Lobar Degeneration.” *Brain Research*, April. Elsevier, 1–7.

Xu, Baoji, Evan H Goulding, Keling Zang, David Cepoi, Roger D Cone, Kevin R Jones, Laurence H Tecott, and Louis F Reichardt. 2003. “Brain-Derived Neurotrophic Factor Regulates Energy Balance Downstream of Melanocortin-4 Receptor.” *Nature Neuroscience* 6 (7): 736–42.

Yadav, Vijay K., Franck Oury, Nina Suda, Zhong Wu Liu, Xiao Bing Gao, Cyrille Confavreux, Kristen C. Klemenhagen, et al. 2009. “A Serotonin-Dependent Mechanism Explains the Leptin Regulation of Bone Mass, Appetite, and Energy Expenditure.” *Cell* 138 (5). Elsevier Ltd: 976–89.

Yeo, Giles S H, and Lora K Heisler. 2012. “Unraveling the Brain Regulation of Appetite: Lessons from Genetics.” *Nature Neuroscience* 15 (10). Nature Publishing Group: 1343–49.

Zarei, Sara, Karen Carr, Luz Reiley, Kelvin Diaz, Orleiquis Guerra, Pablo Fernandez Altamirano, Wilfredo Pagani, Daud Lodin, Gloria Orozco, and Angel Chinea. 2015. “A Comprehensive Review of Amyotrophic Lateral Sclerosis.” *Surgical Neurology International* 6 (November). India: Medknow Publications & Media Pvt Ltd: 171.

Zhang, Ke, Christopher J Donnelly, Aaron R Haeusler, Jonathan C Grima, James B Machamer, Peter Steinwald, Elizabeth L Daley, et al. 2015. “The C9orf72 Repeat Expansion Disrupts Nucleocytoplasmic Transport.” *Nature* 525 (7567): 56–61.

Annex

I. Publication #4

« Serotonin 2B receptor slows disease progression and prevents degeneration of spinal cord mononuclear phagocytes in amyotrophic lateral sclerosis»

Hajer El Oussini, Hanna Bayer, Jelena Scekic-Zahirovic, **Pauline Vercruysse**, Jérôme Sinniger, Sylvie Dirrig-Grosch, Stéphane Dieterlé, Andoni Echaniz-Laguna, Yves Larmet, Kathrin Müller, Jochen H. Weishaupt, Dietmar R. Thal, Wouter van Rheenen, Kristel van Eijk, Roland Lawson, Laurent Monassier, Luc Maroteaux, Anne Roumier, Philip C. Wong, Leonard H. van den Berg, Albert C. Ludolph, Jan H. Veldink, Anke Witting, Luc Dupuis

Acta Neuropathol (2016) 131:465–480
DOI 10.1007/s00401-016-1534-4

ORIGINAL PAPER

Serotonin 2B receptor slows disease progression and prevents degeneration of spinal cord mononuclear phagocytes in amyotrophic lateral sclerosis

Hajer El Oussini[1,2] · Hanna Bayer[3] · Jelena Scekic-Zahirovic[1,2] · Pauline Vercruysse[1,2,3] · Jérôme Sinniger[1,2] · Sylvie Dirrig-Grosch[1,2] · Stéphane Dieterlé[1,2] · Andoni Echaniz-Laguna[1,2,4] · Yves Larmet[1,2] · Kathrin Müller[3] · Jochen H. Weishaupt[3] · Dietmar R. Thal[5,6] · Wouter van Rheenen[7] · Kristel van Eijk[7] · Roland Lawson[2,4] · Laurent Monassier[2,4] · Luc Maroteaux[8,9,10] · Anne Roumier[8,9,10] · Philip C. Wong[11] · Leonard H. van den Berg[7] · Albert C. Ludolph[3] · Jan H. Veldink[7] · Anke Witting[3] · Luc Dupuis[1,2]

Received: 20 October 2015 / Revised: 17 December 2015 / Accepted: 1 January 2016 / Published online: 7 January 2016

Abstract Microglia are the resident mononuclear phagocytes of the central nervous system and have been implicated in the pathogenesis of neurodegenerative diseases such as amyotrophic lateral sclerosis (ALS). During neurodegeneration, microglial activation is accompanied by infiltration of circulating monocytes, leading to production of multiple inflammatory mediators in the spinal cord. Degenerative alterations in mononuclear phagocytes are commonly observed during neurodegenerative diseases, yet little is known concerning the mechanisms leading to their degeneration, or the consequences on disease progression. Here we observed that the serotonin 2B receptor (5-HT_{2B}), a serotonin receptor expressed in microglia, is upregulated in the spinal cord of three different transgenic mouse models of ALS. In mutant SOD1 mice, this upregulation was restricted to cells positive for CD11b, a marker of mononuclear phagocytes. Ablation of 5-HT_{2B} receptor in transgenic ALS mice expressing mutant SOD1 resulted in increased degeneration of mononuclear phagocytes, as evidenced by fragmentation of Iba1-positive cellular processes. This was accompanied by decreased expression of key neuroinflammatory genes but also loss of expression of homeostatic microglial genes. Importantly, the dramatic effect of 5-HT_{2B} receptor ablation on mononuclear phagocytes was associated with acceleration of disease progression. To determine the translational relevance of these results, we studied polymorphisms in the human *HTR2B* gene, which encodes the 5-HT_{2B} receptor, in a large cohort of ALS patients. In this cohort, the C allele of SNP rs10199752 in *HTR2B* was associated with longer survival. Moreover, patients carrying one copy of the C allele of SNP rs10199752 showed increased 5-HT_{2B} mRNA in spinal cord and displayed less pronounced degeneration of Iba1

Electronic supplementary material The online version of this article (doi:10.1007/s00401-016-1534-4) contains supplementary material, which is available to authorized users.

✉ Luc Dupuis
ldupuis@unistra.fr

1 INSERM UMR-S1118, Faculté de Médecine, bat 3, 8e etage, 11 rue Humann, 67085 Strasbourg Cedex, France

2 Université de Strasbourg, Fédération de Médecine Translationnelle, Strasbourg, France

3 Department of Neurology, University of Ulm, Ulm, Germany

4 Neurology Department, Hopitaux Universitaires de Strasbourg, Strasbourg, France

5 Laboratory of Neuropathology, Institute of Pathology, University of Ulm, Ulm, Germany

6 Laboratory of Neuropathology, Department of Neuroscience, KU-Leuven, Leuven, Belgium

7 Department of Neurology, Brain Center Rudolf Magnus, University Medical Center Utrecht, Utrecht, The Netherlands

8 Inserm, UMR-S839, Paris 75005, France

9 Sorbonne Universités, UPMC University Paris 06, UMR-S839, Paris 75005, France

10 Institut du Fer à Moulin, Paris 75005, France

11 Division of Neuropathology, Department of Pathology and Neuroscience, The Johns Hopkins University School of Medicine, Baltimore, USA

positive cells than patients carrying two copies of the more common A allele. Thus, the 5-HT_{2B} receptor limits degeneration of spinal cord mononuclear phagocytes, most likely microglia, and slows disease progression in ALS. Targeting this receptor might be therapeutically useful.

Keywords Amyotrophic lateral sclerosis · Motor neuron · Serotonin · Microglia · SOD1

Introduction

Amyotrophic lateral sclerosis (ALS) is the major adult onset motor neuron disease with a lifetime risk of 1/400, and represents the third most frequent neurodegenerative disease after Alzheimer's and Parkinson's diseases. ALS is characterized by the selective degeneration of upper motor neurons in the cerebral cortex and lower motor neurons in spinal cord and brainstem, and leads to progressive paralysis and death within 3–5 years after onset [41]. A number of ALS cases are dominantly inherited and more than 20 genes have been associated with ALS, in particular *C9ORF72*, *TARDBP*, *FUS* and *SOD1* [48]. Most experimental research has involved expression of mutant SOD1 in transgenic mice, leading to development of typical ALS symptoms.

In recent years it has become increasingly clear that progression of ALS symptoms is not caused exclusively by intrinsic events within motoneurons, but rather involves many other cell types [4, 57]. In particular, mononuclear phagocytes, that collectively refers to both microglia and infiltrating monocytes [23, 28, 34, 40], are activated during ALS [57, 58, 75]. This activation is characterized by appearance of an amoeboid morphology, increased phagocytic activity and production of a number of cytokines and chemokines [52, 75]. Activation of mononuclear phagocytes could either be protective by providing support to neurons and astrocytes in response to injury and by cleaning debris through phagocytosis or deleterious by creating an inflammatory environment contributing to neuronal degeneration [51, 57]. Importantly, decreased expression of mutant SOD1 in CD11b-positive cells, i.e. in all mononuclear phagocytes, prolongs disease progression suggesting that mutant SOD1 exerts toxic action in these cells thereby accelerating disease [5]. Furthermore, decreased activation of the pro-inflammatory transcription factor NF-kappaB in microglial cells potently slowed down disease progression [26]. Mononuclear phagocytes appear themselves affected during disease progression. Indeed, the recently identified molecular signature of homeostatic microglia [7–9, 12] is heavily altered during disease progression in ALS [7, 12]. This loss of typical microglial expression patterns could be directly correlated with degeneration of mononuclear phagocytes, documented in different neurodegenerative diseases [62, 63, 74] including a transgenic model of ALS [25, 63]. Whether mononuclear phagocytes degeneration is microglia specific or also occurs in infiltrating monocytes, and whether this degeneration might be involved in neurodegeneration is not known.

Recently, we observed that serotonin 2B receptor (5-HT_{2B}R) mRNA levels were strongly upregulated in the spinal cord of a mouse model of ALS–SOD1(G86R) mice, notably at later stages and coincident with development of spasticity [15]. 5-HT_{2B}R is expressed in microglia in the CNS, with expression in a few other cell types such as brain serotonin neurons [16]. In human peripheral macrophages, 5-HT_{2B}R mediates the response to serotonin by skewing macrophages to a M2, anti-inflammatory, phenotype [14]. More relevant to ALS, we showed that 5-HT_{2B}R is the major serotonin receptor expressed on perinatal microglia and regulates chemotaxis of microglial processes in response to serotonin [44]. These findings raise the possibility that the observed 5-HT_{2B}R upregulation could be linked to microglial activation and function in the pathogenesis of ALS.

Here, we show that the lack of 5-HT_{2B}R is associated with degeneration of spinal cord mononuclear phagocytes in ALS mouse models and human patients, and slows down disease progression of ALS. This has broad consequences for our understanding of serotonin function during disease, and provides a plausible pharmacological target to modulate neuroinflammation in ALS and other neurodegenerative diseases.

Materials and methods

Patients

Two independent populations of patients were studied here. In the human genetic study, cases from the Netherlands were diagnosed with probable or definite ALS according to the revised El-Escorial Criteria by neurologists specialized in motor neuron diseases [6]. Tertiary referral centers for ALS were University Medical Center Utrecht, Academic Medical Centre Amsterdam and Radboud University Medical Center Nijmegen. All participants gave written informed consent, and approval was obtained from the relevant local ethical committees for medical research. Characteristics of ALS patients included in this genetic study are presented in Table S1. Control individuals were free of any neuromuscular disease and matched for age, gender and ethnicity ascertained through a population based study on ALS in the Netherlands [35]. Patients included in the neuropathology study were from Ulm University. All autopsy brains were collected in

accordance with local ethical committee guidelines and the federal law governing the use of human tissue for research in Germany. The characteristics of these patients are described in Table S2.

Animals

Transgenic mice were housed in the animal facility of the medicine faculty of Strasbourg University, with 12 h/12 h of light/dark and unrestricted access to food and water. In all experiments, littermates were used for comparison, and mice compared are thus in the same genetic background. Transgenic mice carrying SOD1 G86R mutation [18] and their non-transgenic littermates on a FVB/N background were genotyped and onset of symptoms was defined according to previous studies [15]. Dynactin mice expressing G59S mutation of $P150^{Glued}$ have been previously described [47], and were used according to previous studies [72]. SOD1(G37R) mice were kindly provided by Dr Don W. Cleveland and have been described previously [5]. *Htr2b*$^{-/-}$ mice in a 129S2/Sv PAS background have been described previously [49, 53]. All animal experimentation was performed in accordance with institutional guidelines, and protocols were approved by the local ethical committee from Strasbourg University (CREMEAS) under number AL/30/37/02/13 and AL/29/36/02/13 in accordance with European regulations.

Mouse breeding, survival and motor phenotyping

SOD1 (G86R) mice were crossed with *Htr2b*$^{-/-}$ mice to obtain the F1 generation. Male *Htr2b*$^{+/-}$ carrying SOD1 (G86R) transgene were then crossed with female *Htr2b*$^{+/-}$ from the F1 generation to obtain the F2 generation with the genotypes of interest. *Htr2b*$^{-/-}$ mice carrying SOD1 (G86R) transgene ($n = 16$) were compared with littermate *Htr2b*$^{+/+}$ mice carrying SOD1 (G86R) transgene ($n = 12$), *Htr2b*$^{+/-}$ mice carrying SOD1 (G86R) transgene ($n = 19$), and *Htr2b*$^{-/-}$ or *Htr2b*$^{+/+}$ littermate mice negative for SOD1 (G86R) transgene were used as control.

Mice were visually inspected daily and weekly monitored for body weight and motor symptoms from 4 weeks of age until end stage of the disease. To evaluate muscle strength, we used a gripmeter test (Bioseb, ALG01; France). Disease course and survival were assessed daily by visual inspection. The muscle force was averaged as the mean of three consecutive trials per session. Disease onset was calculated as time of peak of body weight. Disease duration was the time between the peak of body weight and death. After disease onset mice were followed daily and end stage was defined by full paralysis and when mice were unable to return after 10 s placed on the back. End stage mice were immediately euthanized.

Histological techniques

Muscle tissues and spinal cords were dissected and fixed by immersion in 4 % paraformaldehyde in 0.1 M phosphate buffer pH 7.4 overnight. The whole muscles were dissected into fibre bundles, stained using α-Bungarotoxin labeled with tetramethylrhodamine(Sigma, T195; 1:500) for nicotinic acetylcholine receptors (AchRs), anti-synaptophysin (Millipore, 5258; 1:250) and anti-neurofilament (Abcam, Ab24574, 1/100) for pre-synaptic elements, followed by fluorescent secondary antibodies anti-mouse Alexa 488 (Life Technologies, A11001), and Draq 5 for nuclei (Cell Signaling, 4084; 1:1000). Single-layer images or merged Z-Stack images (1 µm optical section, for 10 µm thickness of merged z-stacks) were acquired using a laser-scanning microscope (confocal Leica SP5 Leica Microsystems CMS GmbH) equipped with 63× oil objective (NA1.4). Excitation wavelengths were sequentially argon laser 488 nm, diode 561 nm, and helium neon laser 633 nm. Emission bandwidths are 500–550 nm for Alexa488, 570–620 nm for Alexa594, and 650–750 nm for draq5.

The lumbar parts of spinal cords were dissected and the L3–L5 region was identified according to previous studies [29]. Tissue was cryoprotected in 30 % sucrose and snap frozen in melting isopropanol in TissueTek (O.C.T.Compound, SAKURA#4583). Cryosections (Leica CM 3050S) of 16 µm were obtained for histological analysis of end stage mice (10 sections per animal). Spinal cord sections were incubated in phosphate buffered saline (PBS) 0.1 % Triton with anti-choline acetyl transferase (ChAT) (Millipore, AB144-P; diluted 1:50) for motor neuron quantification and anti-Iba1 (Abcam ab5076, 1/100) antibody followed by biotinylated species-specific secondary antibody. The staining was revealed using the ABC kit (Vectastain), by the avidin–biotin complex immunoperoxidase technique or immunofluorescence. Identical techniques and antibodies were used to stain paraffin sections of ALS patients for Iba1 immunostaining.

Quantification of histological results

Motoneuron counting was performed in L3–L5 ventral horn in every tenth section for ten sections in total per animal (160 µm thick in total, spread over 1.6 mm). Only $ChAT^+$ neurons located in a position congruent with that of motoneuron groups were counted [13]. All $ChAT^+$ profiles located in the ventral horns of immunostained sections and clearly displayed in the plane of section were counted. Total estimated motoneuron numbers were obtained using a computer-assisted microscope (Nikon Eclipse E800) and associated software (Nis Elements version 4.0). Total numbers of motoneurons and the mean area of individual cells were obtained using ImageJ freeware (http://rsbweb.nih.gov/ij/) after image acquisition at 20X under the same

exposition parameters with a digital camera (Nikon Digital Sight DS-U3) [61]. The observer was blinded to the genotype of studied mice.

To quantify ventral horn atrophy, the total surface of the ventral horn was measured using Nis Elements version 4.0.

For staining of mononuclear phagocytes, measurement of Iba1 immunoreactivity was performed on images acquired from Iba1 immunostaining at 10× magnification. A standardized rectangle was drawn in the ventral horn and the surface of Iba1 staining relative to background was calculated using the Pixel classifier algorithm of Nikon Nis-element 3.10 SP3 software, using the intensity profile measurement function. The observer was blinded to the genotype of studied mice. >10 images per animal were quantified, with $n = 5$ animals per genotype.

Iba1 positive cells morphology was defined according to previous work [63]: (i) resting phagocyte with small branched cellular processes and small cell soma, (ii) activated state with greater distal arborization, (iii) phagocytic state with increased cell soma size, and (iv) dystrophic state with fragmented cytoplasm. Iba1-immunopositive cells were categorized according to their state in each ventral horn section of the spinal cord by an observer blinded to the genotype (HEO). Percentage of each state was then calculated for each genotype of interest.

To quantify degeneration of Iba1 positive cells in ALS patients, an observer blinded to the genotype scored from 0 to 4 the occurrence of degeneration in 2–5 sections per patient, with a score of 0 for sections showing non-degenerating phagocytes. Features of microglial degeneration were according to Streit and collaborators [63]. Similar results were obtained by two independent blinded observers (HEO and LD).

Isolation of CD11b positive cells

Isolated spinal cords and brain stems from end stage SOD1 (G86R) mice were transferred into a 2 ml sterile tube with 1 ml of Hank's balanced salt solution (HBSS) (Invitrogen), then triturated to single-cell suspension using Miltenyi's Neural Tissue Dissociation Kit (P) (Miltenyi Biotec). After a final wash in HBSS containing $CaCl_2$ and $MgCl_2$, the cell suspension was incubated with anti-myelin magnetic microbeads using Myelin removal kit (Miltenyi Biotec). The cell suspension was passed onto LS columns (Miltenyi Biotec) exposed to a strong magnetic field. The flow through (demyelinated cells) was incubated with anti-CD11b magnetic microbeads using CD11b kit (Miltenyi Biotec). The cell suspension was passed onto LS columns (Miltenyi Biotec) exposed to a strong magnetic field. The flow through (non-CD11b cells) was subsequently used as a negative control and the suspension obtained once the magnetic field was switched off (CD11b cells) used as a positive fraction. Both fractions were used for gene expression analysis.

Real–time quantitative polymerase chain reaction

Total RNA was extracted from the spinal cord and the brain stem of end stage mice using TRIzol (Invitrogen). RNA was reverse transcribed using 1 µg of RNA and the iScript cDNA synthesis kit (BioRad). We performed real-time PCR using IQ SYBR green Supermix (BioRad) and data were normalized with GeNorm software [69] using two standard genes (Tata-box binding protein, and RNA polymerase 2 subunit). For microglia experiments total RNA was extracted by using RNeasy Micro Kit (Qiagen), RNA was reverse transcribed using 1 µg of RNA and the iScript cDNA synthesis kit. Quantitative PCR was performed on a CFX96 Real-time System (BioRad) using iQ SYBR Green supermix (BioRad). Relative mRNA levels were calculated with BioRad CFX Manager 3.1 using $\Delta\Delta C_t$ method.

Primer sequences are provided in Table S3.

Echocardiography

Animals were analyzed for cardiac anatomy and function on a Sonos 5500 (Hewlett Packard, USA) with a 15 MHz linear transducer (15L6). All the examinations were performed in mice anesthetized with 1–1.5 % isoflurane. The heart was first imaged in the two-dimensional (2D) mode in the parasternal long-axis view to obtain the aortic root dimensions. The aortic flow velocity and the heart rate (HR) were measured with pulsed-wave Doppler on the same section. The cardiac output (CO) was calculated from the following equation: $CO = 0.785 \times D2 \times VTI \times HR$ where D is the diameter of the aortic root and VTI is the velocity–time integral of the Doppler aortic spectrum. Left ventricular cross sectional internal diameters in end-diastole (EDLVD) and end-systole (ESLVD) were obtained by an M-mode analysis of a 2D-short axis view at the papillary muscle level. The shortening fraction was calculated as $SF = (EDLVD\text{-}ESLVD/EDLVD) \times 100$. From this view, the diastolic septum (SW) and posterior wall (PW) thicknesses were measured. The left ventricular mass (LVM) was calculated with the following formula: $LVM = 1.055 \times [(SW + PW + EDLVD)^3 - (EDLVD)^3]$. All the measurements were performed on at least three beats, according to the guidelines of the American Society of Echocardiography.

Microglial culture

Mouse microglial cells in primary culture were prepared as described previously [73]. Briefly, 1–5 day old C57Bl/6

mice were decapitated according to the guidelines of the animal research center of Ulm University, Ulm, Germany. Meninges were removed from the brains. Neopallia were dissected and dissociated by enzyme treatment (1 % trypsin, Invitrogen, 0.05 % DNAse, Worthington, 2 min) and then mechanically dissociated. The cells were centrifuged (200×*g*, 10 min), suspended in Dulbecco's modified Eagle's medium (DMEM, Invitrogen) supplemented with penicillin (100 U/ml), streptomycin (100 µg/ml) (Invitrogen) and 10 % heat-inactivated fetal bovine serum (FBS, PAA), and plated into 75-cm^2 flasks (BD Falcon) pre-coated with 1µg/ml poly-L-ornithine (Sigma). Cells from the neopallia of two brains were plated at 10 ml per flask. After 3 days, adherent cells were washed three times with Dulbecco's phosphate buffered saline (DPBS) (Invitrogen) and incubated with serum-supplemented culture media. After 7–14 days in culture, floating and loosely attached microglial cells were manually shaken off, centrifuged (200×*g*, 10 min) and seeded into 96-well plates or 6-well plates (PRIMARIA, BD Falkon) at a density of 4 × 10^4 or 6 × 10^5 cells/well, respectively, in DMEM without serum (Invitrogen) supplemented with penicillin (100 U/ml), streptomycin (100 µg/ml) (Invitrogen) and Glutamax (Invitrogen). Cells in the flasks were reincubated with serum-supplemented media after shaking. Repopulating microglial cells were removed every 3–4 days for a total of 3 weeks until fewer microglial cells were observed.

LDH and WST-1 assays

The lactate dehydrogenase (LDH) assay and water soluble tetrazolium salt (WST-1) assay were performed as described in the manual for the LDH-Cytotoxicity Assay Kit (Bio Vision) and the WST-1 Assay Kit (Quick Cell Proliferation Assay Kit; BioVision). For a positive cell death control, microglia were treated with 1 % Triton-X100 (Sigma) for 30 min. Results were expressed as a percentage of Triton treatment, with 0 % being untreated control.

HTR2B Polymorphisms in human ALS

In total 1923 cases and 2881 controls were genotyped on two different platforms; IlluminaOmniExpress (n = 3488) and Illumina2.5 M (n = 1316). Extensive quality control using standard procedures was performed as described [68]. Following this, 612,666 SNPs and 3344 individuals (1207 cases and 2137 controls) were retained on the IlluminaOmniExpress chip, and the Illumina 2.5 M chip yielded 1,481,461 single nucleotide polymorphisms (SNPs) and 1294 individuals (679 cases and 615 controls). After this extensive quality control, seven *HTR2B* SNPs were extracted and used for analyses.

Statistical analysis

All data are presented as mean ± standard error of the mean.

When the measured values were not detectable in some of the experimental points (Fig. 1), these values were considered to be null. Comparison of discrete values for two groups (Figs. 1, 2d, e, 8b, c) was performed using Student's t test. Comparison of discrete values for more than two groups (Figs. 3d, e, 4a, c, d, 5c, 6a, 7) was performed using One Way ANOVA followed by Tukey's post hoc test. Differences in survival or disease onset of animals (Fig. 2a–c) was evaluated using log rank (Mantel Cox) test. To test for the effect of dose of *Htr2b* ablation, a log rank test for trend was performed (Figure S2). For repeated measures (Figure S1), a repeated measures two way ANOVA was performed to test for the effect of age and the effect of genotype.

These statistical analyses were performed using Prism 6 (GraphPad software).

All differences were considered significant at $p < 0.05$.

To investigate the association of these seven SNPs with ALS, a logistic regression was performed in PLINK, corrected for dataset and 2 principle components. These seven SNPs are strongly correlated ($D' = 1$, and five out of seven SNPs have an R^2 between 0.7 and 1, with a minor allele frequency >0.4). Therefore the strongest correlated SNP was tested for association with survival (rs10199752). A Cox proportional hazards

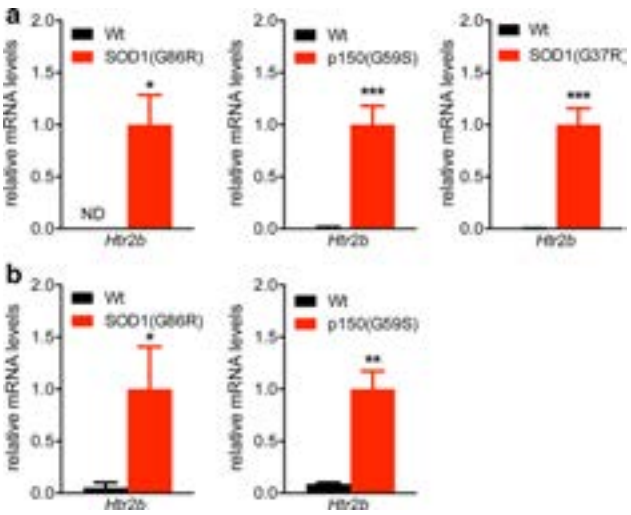

Fig. 1 Increased relative mRNA levels of 5-HT$_{2B}$ receptor in ALS mice. mRNA levels of 5-HT$_{2B}$R (Htr2b) in the spinal cord (**a**) and brainstem (**b**) of end stage SOD1 (G86R) mice (Wt N = 7, SOD11(G86R) N = 7), p150(G59S) mice (Wt N = 7, p150(G59S) N = 7), SOD1 (G37R) (Wt N = 8, SOD1(G37R) N = 7) relative to their respective wildtype (Wt) littermates. ND: not detected. *$p < 0.05$, **$p < 0.01$, ***$p < 0.001$ versus corresponding wild type, by Student's t test

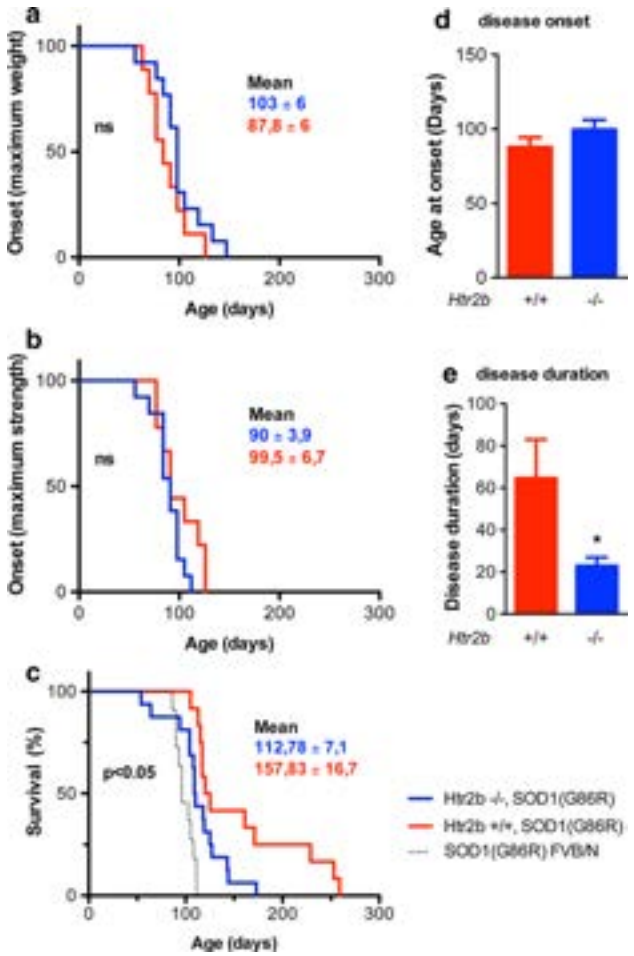

Fig. 2 The ablation of *Htr2b* in SOD1 (G86R) mice decreases life span and accelerates disease progression. Kaplan–Meier plot of disease onset, as determined by the peak weight (**a**) or the peak of grip strength (**b**), and of survival (**c**) for SOD1(G86R) mice wild type for *Htr2b* (*red*, $n = 12$) or knock-out for *Htr2b* (*blue*, $n = 16$). The mean of each group ± SEM is indicated on *each panel*. $p < 0.05$, log rank (Mantel–Cox) between *Htr2b* +/+ SOD1(G86R) mice and *Htr2b*−/−SOD1(G86R) mice in *panel* **c**. There were no significant difference (ns) in survival curves for *panels* **a** and **b.** The survival curve of SOD1 (G86R) mice in the original FVB/N background is indicated in *dashed line*. Duration of early disease (**d**, from birth to peak weight) and late disease (**e**, from peak weight to death) for SOD1(G86R) mice wild type for *Htr2b* (+/+, *red*) or knock-out for *Htr2b* (−/−, *blue*). $p < 0.05$, unpaired Student's *t* test

(coxph) regression model in R was performed with survival and death as time and event, respectively, genotype as predictor, and sex, age at onset, and site at onset as covariates. Patients with a maximum survival of 15 years were included in this analysis ($n = 1677$). This coxph regression was conducted using a dominant model, comparing a wildtype homozygous reference group versus a variant group (combined homozygous variant and heterozygous).

Results

5-HT_{2B} receptor upregulation during murine ALS

We first asked whether 5-HT_{2B}R upregulation is a general feature of ALS mouse models. For this, we measured mRNA levels of the gene encoding 5-HT_{2B}R (*Htr2b*), in spinal cord and brainstem of three different mouse models of ALS at a late stage of disease progression, i.e. when both hindlimbs were paralyzed. We used mice expressing the G86R SOD1 mutation in the murine gene (SOD1(G86R) mice), or the G37R mutation in the human gene [5]. Consistent with previous results [15], levels of *Htr2b* mRNA were strongly upregulated in spinal cord of SOD1(G86R) mice (Fig. 1a) but also of SOD1(G37R) mice (Fig. 1a). Importantly, *Htr2b* mRNA upregulation was also observed in non-SOD1 ALS mouse models, in particular in the spinal cord of mice expressing the G59S mutation in the p150 subunit of dynactin [47] (Fig. 1a). Last, *Htr2b* mRNA upregulation was also observed in the brainstem of SOD1(G86R) mice and p150(G59S) mice (Fig. 1b). Thus, 5-HT_{2B}R mRNA is upregulated in various ALS mouse models.

The lack of 5-HT_{2B} receptor accelerates disease progression in mice

To determine the effect of 5-HT_{2B}R on motoneuron disease progression, we ablated the *Htr2b* gene in SOD1(G86R) mice. We crossed SOD1(G86R) mice with $Htr2b^{-/-}$ mice generated previously [53]. After two breeding steps, we obtained SOD1(G86R); $Htr2b^{+/+}$mice, SOD1(G86R) $Htr2b^{+/-}$ mice and SOD1(G86R); $Htr2b^{-/-}$ mice, that were followed longitudinally until death. These mice were in a mixed FVB/N x 129S2/Sv PAS background. Ablation of *Htr2b* led to reduction in body weight in SOD1(G86R) mice as compared to SOD1(G86R) mice expressing *Htr2b* (Fig. S1). Complete ablation of *Htr2b* shortened survival of SOD1(G86R) mice by 30 % (Fig. 2a–c), while ablation of only one allele of *Htr2b* yielded an intermediate effect ($p < 0.05$, log rank test for trend, Fig. S2). Disease onset, as assessed either by peak of body weight [5] or by peak of grip strength, was not changed (Fig. 2a, b). Indeed, ablation of *Htr2b* did not modify the age of peak weight as a measure of disease onset (Fig. 2d), while drastically shortening disease duration after peak weight (Fig. 2e).

Since 5-HT_{2B}R has been implicated in cardiac development and function [53, 55, 56], we hypothesized that *Htr2b* ablation could affect cardiac function in SOD1(G86R) mice, leading to accelerated death. However, echocardiographic examinations did not show major reduction of cardiac contractility or output in SOD1(G86R); $Htr2b^{-/-}$ mice. In

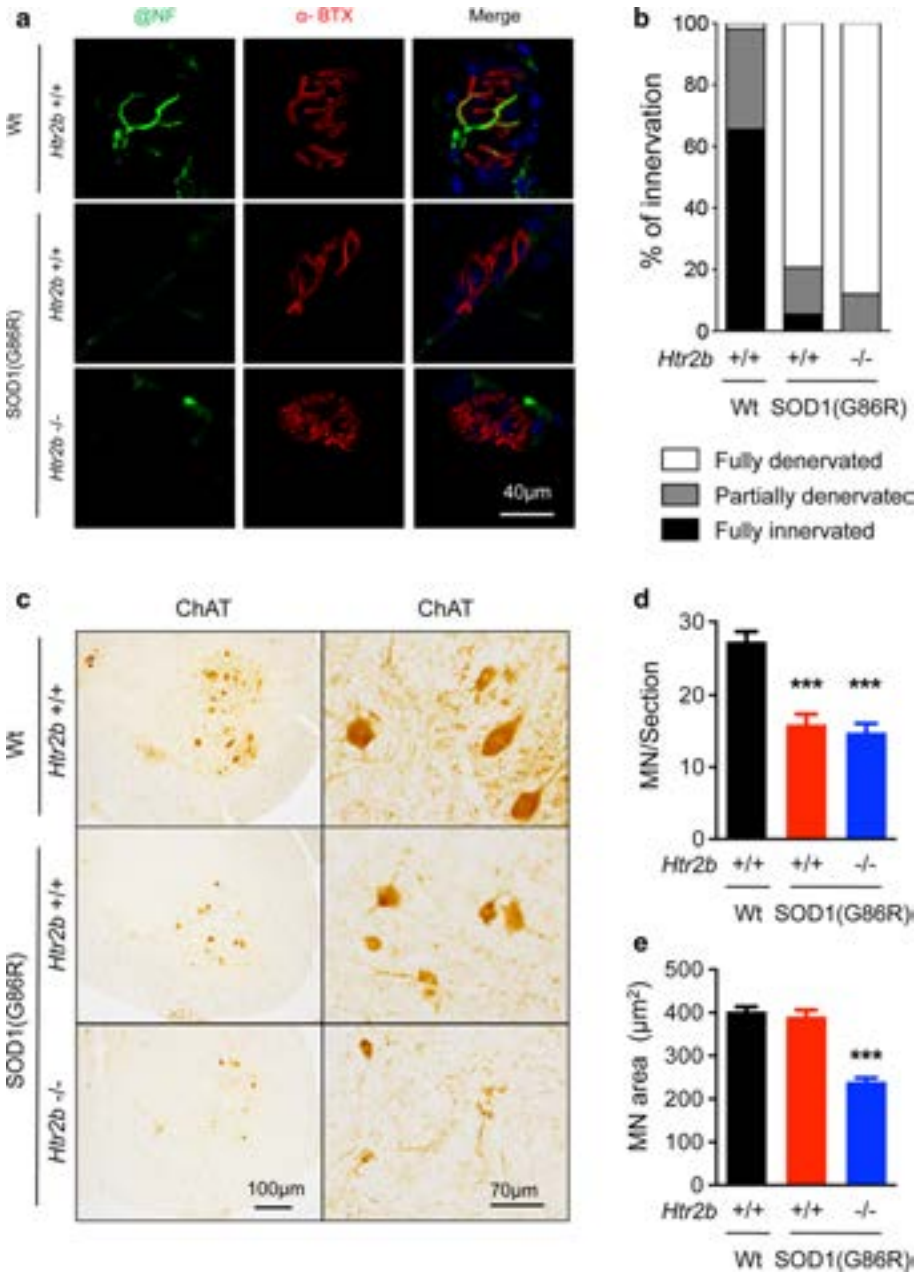

Fig. 3 The ablation of *Htr2b* in SOD1 (G86R) mice exacerbates neurodegeneration. **a** Representative confocal images of post and pre-synaptic apparatus of the neuromuscular junction in Tibialis muscle of end stage mice. Axons were labeled with anti-neurofilament (@NF, *green*), acetylcholine receptors with fluorescently labeled bungarotoxin (α-BTX, *red*) and nuclear with Draq 5 (*blue*) in wild type mice (+/+), and SOD1(G86R) mice wild type for *Htr2b* (+/+) or knock-out for *Htr2b* (−/−) at end stage. $N = 5$ for all genotypes. **b** Distribution of innervation profiles in the tibialis anterior of wild type mice (Wt), and SOD1(G86R) mice wild type for *Htr2b* (+/+) or knock-out for *Htr2b* (−/−) at end stage ($n = 5$ independent animals per genotype). **c** Representative ChAT immunohistochemistry images in wild type mice (Wt), and SOD1(G86R) mice wild type for *Htr2b* (+/+) or knock-out for *Htr2b* (−/−). Two magnifications are shown. $N = 5$ for all genotypes. Motor neuron numbers (**d**) and area (**e**) in wild type mice (Wt, *black columns*), and SOD1(G86R) mice wild type for *Htr2b* (+/+ *red columns*) or knock-out for *Htr2b* (−/− *blue columns*). ***$p < 0.001$ vs wild type, One way ANOVA followed by Tukey post hoc test. $N = 5$ for all genotypes

particular, they did not exhibit echocardiographic signs of heart failure that could explain body weight loss (Fig. S3). To determine whether SOD1(G86R); *Htr2b*$^{-/-}$ mice actually died of motoneuron disease, we examined neuromuscular junction histology in end-stage mice. All SOD1(G86R) mice examined at end-stage, irrespective of their *Htr2b* genotype, displayed heavily denervated neuromuscular junctions (Fig. 3a, b). Consistent with this, SOD1(G86R); *Htr2b*$^{+/+}$ mice displayed motoneuron degeneration similar to SOD1(G86R); *Htr2b*$^{-/-}$ mice (Fig. 3c, d), and ventral horn atrophy was not modified by the *Htr2b* genotype (Fig. S4). Motor neuron loss was similar in this mixed background to previous studies in the original FVB/N background [19, 20]. However, *Htr2b* ablation in SOD1(G86R) mice triggered atrophy of motoneuron cell bodies that was not present in SOD1(G86R); *Htr2b*$^{+/+}$ mice (Fig. 3e). Thus, consistent with its overexpression at symptom onset in SOD1(G86R) spinal cord [15], the lack of 5-HT_{2B}R potently accelerates disease progression of SOD1(G86R) mice after onset.

5-HT2B receptor is upregulated in CD11b-positive cells and is required for activation of mononuclear phagocytes during ALS

Microgliosis occurs at symptom onset in brainstem and spinal cord of transgenic models of ALS [4, 5, 57]. Since

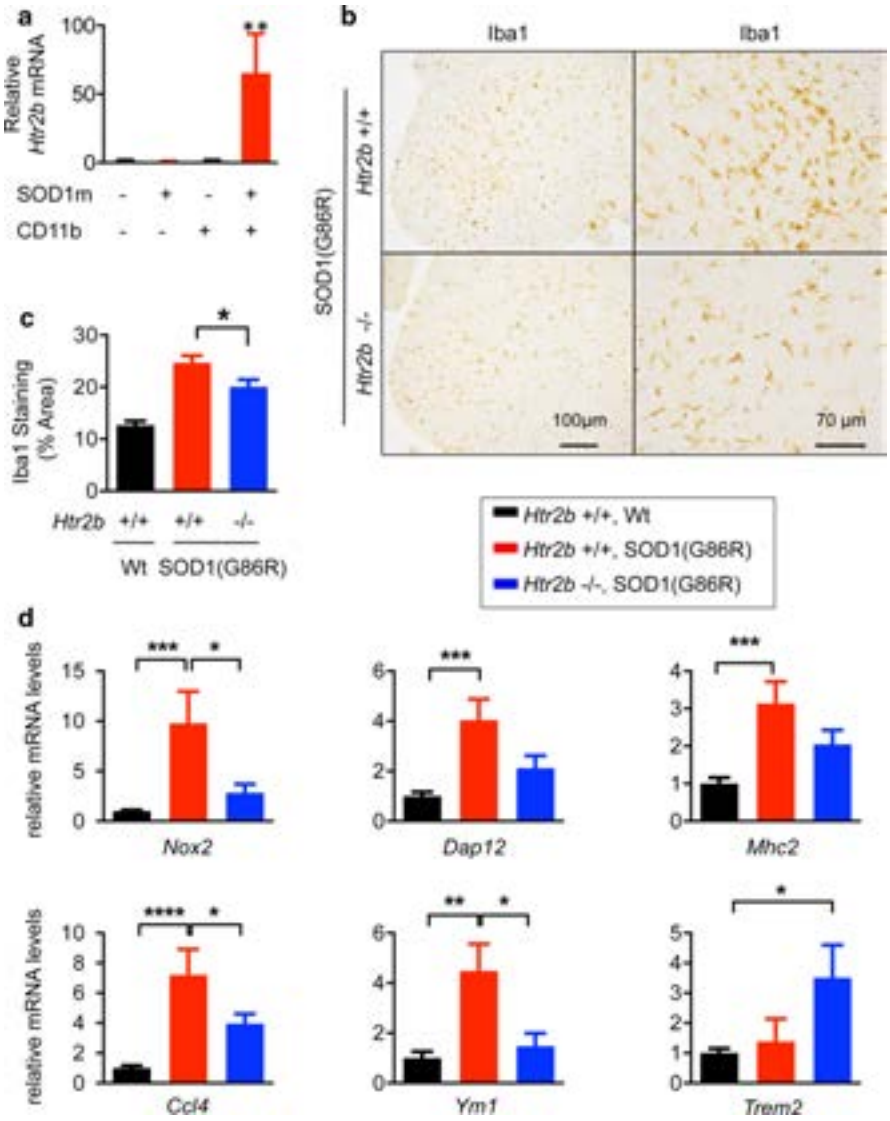

Fig. 4 The ablation of *Htr2b* in SOD1 (G86R) mice compromises activation of mononuclear phagocytes. **a** *Htr2b* mRNA levels in CD11b-positive cells ($CD11^{Pos}$) and CD11b-negative cells ($CD11b^{Neg}$) in brainstem and spinal cord of end stage SOD1(G86R) mice (SOD1) relative to wild-type littermates (Wt). $N = 5$ for all genotypes $^{**}p < 0.01$, Student's *t* test. **b** Representative Iba1 immunohistochemical images in ventral spinal cord of SOD1(G86R) mice wild type for *Htr2b* (+/+) or knock-out for *Htr2b* (−/−). $N = 5$ for all genotypes. **c** Quantification of Iba1 staining coverage in lumbar spinal cord of wild type mice (Wt, *black columns*), and SOD1(G86R) mice wild type for *Htr2b* (+/+ *red columns*) or knock-out for *Htr2b* (−/− blue columns). $^{*}p < 0.05$, One way ANOVA followed by Tukey post hoc test. $N = 5$ for all genotypes. **d** mRNA levels of the indicated genes in brainstem SOD1(G86R) mice wild type for *Htr2b* (+/+ *red columns*) or knock-out for *Htr2b* (−/− *blue columns*) relative to wild type mice (*black columns*). $^{*}p < 0.05$, $^{**}p < 0.01$; $^{***}p < 0.001$ One way ANOVA followed by Tukey post hoc test. $N = 4$–5 per genotype

5-HT_{2B}R is expressed in microglia and peripheral M2 macrophages [14, 44], increased 5-HT_{2B}R expression could reflect activation of microglia and/or of infiltrated monocytes. To address this question, we purified CD11b positive cells from late stage SOD1(G86R) mice using magnetic bead cell sorting, followed by RT-qPCR. To enable purification of CD11b positive cells from single individuals, we chose to pool brainstem and spinal cord from individual mice. Importantly, these areas are associated with strong microgliosis in mutant SOD1 models [25]. Using this procedure, we obtained CD11b positive fractions with a >300 fold enrichment in Iba1 mRNA, and corresponding 5-10 fold decrease in GFAP and ChAT mRNA content (Fig. S5). Importantly, we observed that *Htr2b* upregulation was strictly limited to mRNA enriched from CD11b positive cells (Fig. 4a). Activation of mononuclear phagocytes was reduced by *Htr2b* ablation, with decreased Iba1 staining in the spinal cord (Fig. 4b, c). Consistently, the disease-elicited induction of multiple genes involved in neuroinflammatory responses was decreased in the brainstem of the same animals (Fig. 4d). Interestingly, genes involved in the pro-inflammatory action of microglia (Fig. 4d, *Nox2, Ccl4, Mhc2*), as well as genes involved in anti-inflammatory responses (Fig. 4d, *Ym1, Dap12*) showed similar blunted expression upon *Htr2b* ablation. Notably, *Trem2*- a cell surface receptor associated with neurodegeneration—was especially upregulated in SOD1(G86R); $Htr2b^{-/-}$ brainstem (Fig. 4d). Thus, 5-HT_{2B}R is required for the activation of mononuclear phagocytes during motoneuron disease.

5-HT_{2B} receptor improves microglial survival

Searching for a role for 5-HT_{2B}R in mononuclear phagocytes, we re-examined the phenotype of these cells in SOD1(G86R); $Htr2b^{-/-}$ mice. We observed that spinal cord Iba1-positive cells of SOD1(G86R); $Htr2b^{-/-}$ mice frequently displayed

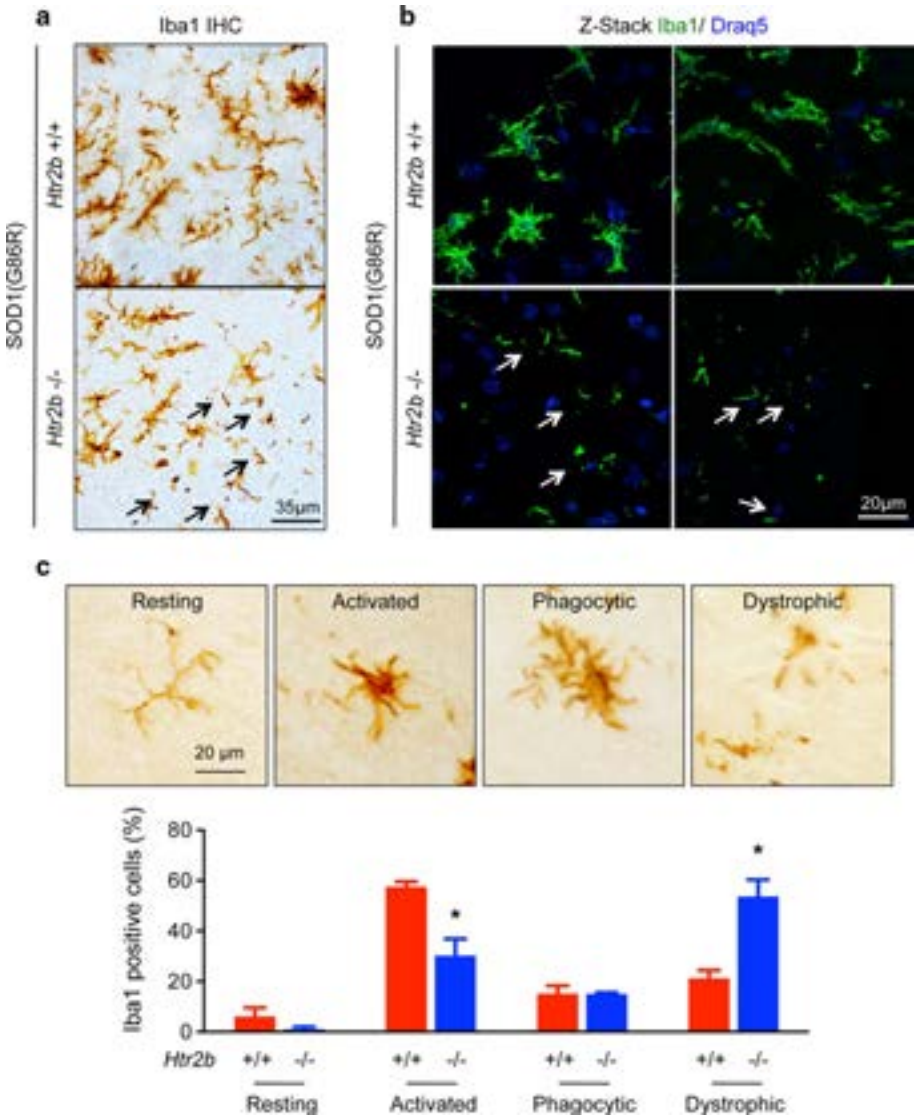

Fig. 5 The ablation of *Htr2b* in SOD1 (G86R) mice leads to degeneration of Iba1 positive cells. **a** Representative Iba 1 immunostaining in spinal cord of SOD1(G86R) mice wild type for *Htr2b* (+/+) or knock-out for *Htr2b* (−/−) showing cytorrhexia of Iba1+ cells (*arrows*). $N = 5$ for all genotypes. **b** Merged Z-stack confocal images of Iba1 immunofluorescence (*green*) counterstained with nuclear DRAQ5 staining in SOD1(G86R) mice wild type for *Htr2b* (+/+) or knock-out for *Htr2b* (−/−). Microglial cytorrhexia is shown with *arrows*. $N = 5$ for all genotypes. **c** Relative proportions of resting, activated, phagocytic and dystrophic (cytorrhexia) Iba1+ cells in SOD1(G86R) mice wild type for *Htr2b* (+/+ *red columns*) or knock-out for *Htr2b* (−/− *blue columns*). Representative examples of the different categories are illustrated. $^*p < 0.05$ vs corresponding *Htr2b* +/+ category, One way ANOVA followed by Tukey post hoc test. 10 sections per animal, with $N = 4$–5 for all genotypes

cytoplasmic fragmentation (also called cytorrhexia, Fig. 5a). This was further confirmed on z-stacks of Iba1immunostained sections obtained using confocal microscopy (Fig. 5b and Fig S6). Quantitative analysis demonstrated that about half of Iba1-positive cells displayed cytorrhexia in SOD1(G86R); *Htr2b*$^{-/-}$ mice (Fig. 5c), suggesting that the loss of *Htr2b* was associated with degeneration of mononuclear phagocytes in end stage SOD1(G86R) mice. To determine whether this degeneration of mononuclear phagocytes affected microglia and/or monocytes, we measured expression levels of genes known to be part of the homeostatic microglial signature [7–9, 12], in particular *Cx3cr1*, *Hexb, Tmem119, P2ry12, Olfml3* and *SiglecH*. All these genes displayed lower expression in SOD1(G86R) mice lacking the *Htr2b* gene than in SOD1(G86R) mice with the *Htr2b* gene (Fig. 6). The establishment of the homeostatic microglial signature is dependent upon TGFß and *Tgfbr1*, the microglial receptor of TGFß [8]. Consistent with previous work, we observed induction of TGFß and its receptor in SOD1(G86R) mice [24], and these two inductions were blunted in SOD1(G86R) mice lacking the *Htr2b* gene (Fig. 6b). Importantly expression levels of *Ly6c1*, a cell surface marker expressed on monocytes, but not microglia [9], were unaltered in SOD1(G86R) mice, irrespective of the *Htr2b genotype* (Fig. 6c). To define the relationships between 5-HT_{2B}R and microglial survival, we stimulated primary microglial cultures with 5-HT_{2B}R-targeted drugs. We selected 5-HT_{2B}R ligands classically used to target the 5-HT_{2B}R, in particular SB204741, a fairly selective antagonist of the 5-HT_{2B}R with 50 fold selectivity for 5-HT_{2B}R over other type 2 serotonin receptors, BW723C86, a preferential 5-HT_{2B}R agonist, with 50 fold selectivity for 5-HT_{2B}R over other type 2 serotonin receptors, and SB206553, an inverse agonist of both 5-HT_{2B}/5-HT_{2C}Rs [2, 43]. Microglial viability was decreased after 48 h in the presence of 1 µM of SB204741 (Fig. 7a), and increased in the presence of 3 µM of BW723C86. There was consistently more LDH

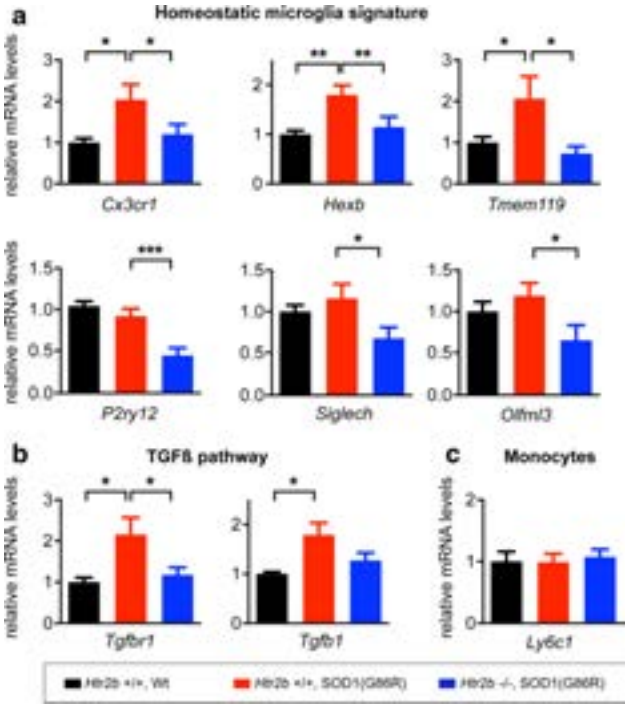

Fig. 6 The ablation of *Htr2b* in SOD1 (G86R) mice decreases expression of homeostatic microglia genes, while not affecting monocyte marker *Ly6c1*. **a–c** mRNA levels of the genes typical of the homeostatic microglia signature (**a**), TGFß pathway (**b**), and of *Ly6c1*, a monocyte marker, in brainstem of SOD1(G86R) mice wild type for *Htr2b* (+/+ *red columns*) or knock-out for *Htr2b* (−/− *blue columns*) relative to wild type mice (Wt, *black columns*). *$p < 0.05$, **$p < 0.01$; ***$p < 0.001$ One way ANOVA followed by Tukey post hoc test. $N = 7$

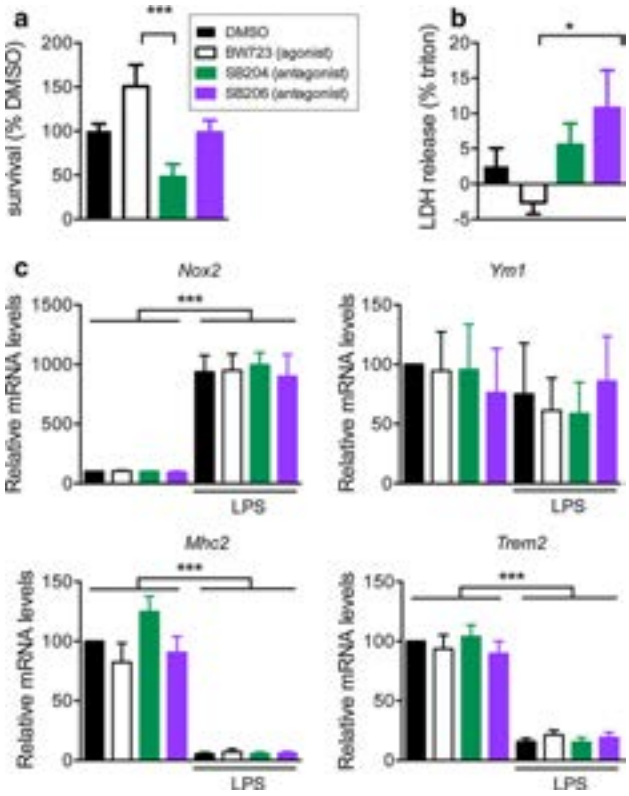

Fig. 7 Pharmacological modulation of the 5-HT_{2B} receptor modulates microglial survival in culture but not gene expression. WST-1 survival (**a**) and LDH release (**b**) assays of primary microglial cells treated with 1 µM SB204741 (5-HT_{2B} antagonist), 1 µM SB206553 (5-HT_{2B} inverse agonist), or 1 µM BW723C86 (5-HT_{2B} agonist). The WST-1 values are relative to vehicle, (DMSO). LDH release is expressed as a percentage of positive control (triton treatment), that releases all LDH contained in cells after subtracting the value of untreated cells. Note that treatment with BW723C86 (5-HT_{2B} agonist) leads to decrease in basal LDH release, leading to negative values. ***$p < 0.001$; *$p < 0.05$ as indicated by *brackets*; One way ANOVA followed by Tukey post hoc test. The experiments were performed in triplicate in three independent experiments. **c** mRNA levels of the indicated genes in primary mouse microglia incubated with 3 µM of BW723C86 (5-HT_{2B} agonist), 1 µM of SB204741 (5-HT_{2B} antagonist), 3 µM of SB206553 (5-HT_{2B} inverse agonist) relative to vehicle (DMSO) with or without 1 µg/ml LPS for 48 h. mRNA levels are given in % of control. Data are presented as mean ± SEM of $n = 3$–5 experiments ***$p < 0.001$ significantly different (One-way ANOVA followed by Tukey post hoc test)

release after 48 h in the presence of SB206553 as compared with 3 µM BW723C86 (Fig. 7b). To determine whether the 5-HT_{2B}R could also modulate microglial gene expression beyond survival, we measured mRNA levels of genes strongly modulated by *Htr2b* genotype in SOD1(G86R) mice (Fig. 4d) in primary microglia treated with 5-HT_{2B}R drugs and/or lipopolysaccharide (LPS) as a neuroinflammatory stimulus. 5-HT_{2B}R pharmacological modulation was not sufficient to alter the expression levels of *Nox2, Ym1, Mhc2* or *Trem2* whether in the absence or presence of LPS for 48 h (Fig. 7c). Thus, acute modulation of 5-HT_{2B}R modifies survival of primary microglia, but does not affect—neuroinflammatory gene expression. Taken together, our results indicate that 5-HT_{2B}R actively promotes microglial survival during neurodegeneration.

HTR2B polymorphisms associated with differential levels of 5-HT_{2B}R mRNA affect morphology of mononuclear phagocytes and survival in ALS

Next, we studied whether the *HTR2B* gene was a modifier of ALS. To this end, we interrogated genome wide association study (GWAS) results of 1886 ALS cases and 2752 controls of Dutch origin. In these samples, we identified seven different intronic SNPs. None of these SNPs showed differential frequencies between cases and controls, showing that at least in this Dutch population *HTR2B* polymorphisms are not a risk factor for ALS. However, a significant association with survival was found for SNP rs10199752 as a prototypical example of these highly correlated SNPs. We isolated patients in whom all phenotype data were available (Table S1), and used a dominant

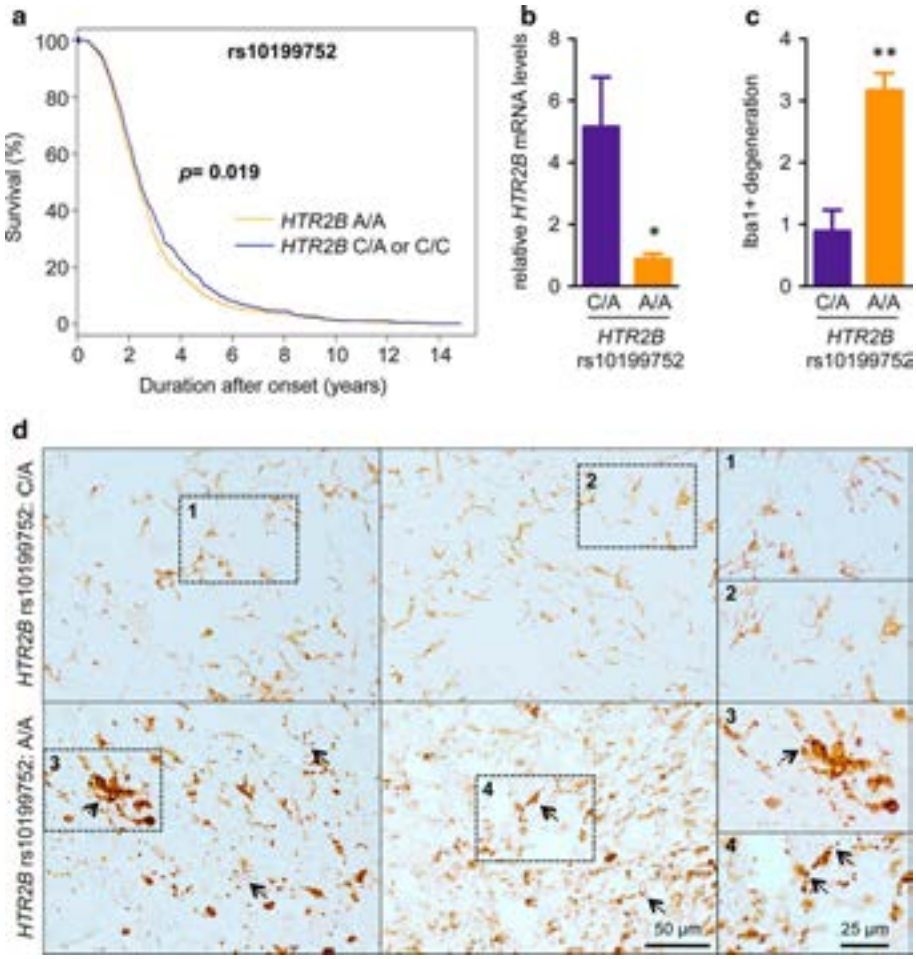

Fig. 8 *HTR2B* polymorphisms in gene expression and degeneration of Iba1 positive cells. **a** Kaplan–Meier plot for a dominant SNP model associated with patient survival. Patients with the variant genotypes (C/A and C/C, $n = 918$) have a longer survival compared to the wildtype homozygous reference group (AA, $n = 759$), hazard ratio = 0.88 (confidence interval 0.79–0.98), p value = 0.019. **b** *HTR2B* mRNA levels in the spinal cord of ALS patients with *HTR2B* C/A relative to patients with *HTR2B* A/A genotype for the rs10199752 SNP. $^{*}p < 0.05$, Student's t test. No patient with the C/C genotype was present in this cohort. **c** quantification of degeneration of Iba1+ cells. Degeneration was semi-quantitatively scored (from 0 to 4) by an observer blinded to the genotype in Iba1-stained spinal cord sections of ALS patients with *HTR2B* A/A relative to C/A genotype for the rs10199752. $^{**}p < 0.01$, Student's t test. **d** Representative Iba1 immunostaining in 4 ALS patients with *HTR2B* C/A (*upper row*) or A/A genotype (*lower row*) for the rs10199752 SNP. Magnifications of *rectangles* 1–4 is shown on the *right*. Note that microglial cells in *HTR2B* C/A carriers show the typical pattern of resident microglial cells with ramified processes (*rectangles* 1–2) whereas the A/A carriers frequently exhibited degenerating microglial cells (*arrows*), with fragmented and beaded processes (*rectangles* 3–4, *arrows*)

model to compare the survival of the variant group (combined genotypes C/A and C/C, $n = 918$) with the wild type homozygous reference group (A/A, $n = 759$). This analysis revealed that patients with the variant genotypes have a longer survival time compared to the homozygous reference group (hazard ratio = 0.88; confidence interval 0.79–0.98; p value = 0.019) (Fig. 8a). To determine whether *HTR2B* polymorphisms were associated with changes in *HTR2B* expression levels, we genotyped a cohort of autopsied ALS patients (Table S2). In this cohort, 6 patients carried an A/A genotype, and 10 patients carried a C/A genotype. There was no patient with the C/C genotype. In patients who carried the C/A genotype of rs10199752, we observed decreased spinal cord *HTR2B* mRNA levels as compared with patients carrying the A/A genotype of rs10199752 (Fig. 8b). We then performed Iba1 immunohistochemistry on lumbar spinal cord sections of these same patients and conducted a semi-quantitative evaluation of the degeneration of Iba1-positive cells (Fig. 8c). Notably, degenerating Iba1-positive cells—as evidenced by the presence of fragmented and/or beaded processes—were frequently observed in patients with the A/A genotype of rs10199752 (Fig. 8d, arrows in lower panels), but much less frequently in patients with the C/A genotype (Fig. 8d, upper panels).

Quantification revealed more frequent and severe degeneration of spinal cord Iba1 positive cells in patients with the A/A genotype than in patients with the C/A genotype (Fig. 8c). As a whole, *HTR2B* polymorphisms associated with higher spinal cord mRNA levels were also associated with increased survival and less pronounced degeneration of mononuclear phagocytes.

Discussion

Our current study provides multiple lines of evidence supporting that the 5-HT_{2B}R is a disease modifier of ALS progression by regulating survival and function of mononuclear phagocytes during neurodegeneration.

Our first important result is that *HTR2B* expression levels affect ALS progression, both in patients and in a transgenic mouse model. *Htr2b* ablation did not modify disease onset, but sharply accelerated disease progression in mutant SOD1 mice. The effect was observed despite compound transgenic mice were generated in the mixed FVB/N × 129 Sv background. The background was identical in all mice, as we used the F1 generation littermates to generate the F2 generation of interest. Interestingly, as illustrated in Fig. 2c, the mixed background increased overall survival of SOD1(G86R) mice and increased heterogeneity in survival. This effect of mixed genetic background has been previously reported, including by us [30, 38]. Accelerated death of mutant SOD1 mice ablated of *Htr2b* was due to accelerated neurodegeneration, and not to potential confounding effects on cardiac patho-physiology. Consistently, ALS patients carrying common haplotypes associated with higher spinal cord *HTR2B* mRNA expression levels survived longer than patients with low expression haplotypes. The relationship between *HTR2B* polymorphisms and survival will have to be investigated in larger cohorts, and different genetic backgrounds, but constitutes an example of a common polymorphism modifying disease progression but not disease risk. An interesting open question is whether *HTR2B* might affect other phenotypes associated with ALS. It is conceivable that *HTR2B* modulates the development of frontal symptoms commonly associated with ALS [64]. Indeed, *Htr2b*$^{-/-}$ mice were recently shown to display deficits in social interactions, as well as in learning and memory processes [59], and these processes require intact frontal lobe function. Along the same lines, the Q20* polymorphism, only found in the Finnish population, is associated with severe impulsivity [3], possibly caused by frontal lobe degeneration. Further work is thus required to elucidate the extent of the contribution of *HTR2B* in ALS-associated phenotypes, in particular in relation with frontal symptoms.

The second major result is that 5-HT_{2B}R could regulate morphology and function of central nervous mononuclear phagocytes, including microglia, in ALS. Here again we provide multiple complementary lines of evidence. Abnormalities of mononuclear phagocytes include (i) decreased overall Iba1 immunostaining, (ii) decreased induction of multiple pro- or anti-inflammatory genes, and (iii) fragmentation of Iba1-positive cells. A reasonable mechanism underlying all these different observations would be that 5-HT_{2B}R function is critical for survival of mononuclear phagocytes during prolonged neuroinflammation such as occurs in ALS. Survival of primary microglia was improved by 5-HT_{2B}R stimulation and decreased by its inhibition, consistent with previous work showing a protective function of 5-HT_{2B}R in newborn cardiomyocytes [54]. These studies will have to be extended to adult spinal cord microglia to determine the effect of aging, as well as the potential role of microglial location in their response to 5-HT_{2B}R stimulation. Our current work does not formally determine whether degenerating Iba1-positive cells are microglia and/or infiltrating monocytes. The extent of monocyte infiltration remains controversial in the field of ALS [1, 9, 12, 46, 50], contrary to Alzheimer's disease in which monocyte infiltration has been repeatedly observed [31, 32]. Our gene expression results demonstrate consistent loss of expression of multiple genes typical of homeostatic microglia while the monocyte marker *Ly6c1* remained unaffected (Fig. 6). Such loss of homeostatic microglial gene expression in whole tissue could be due to cell loss, leading to decreased proportion of microglial mRNAs. Alternatively, disease progression could also affect microglial phenotype, and a recent study performed on isolated microglia of mutant SOD1 mice observed that mutant SOD1 microglia lost their typical expression patterns with disease progression [7]. However, our in vitro experiments provide an initial proof of concept that microglial survival could be influenced by serotonergic stimulation of the 5-HT_{2B}R. Further work is required to determine the relative contributions of microglial cell death and altered microglial phenotypes in the observed degenerative phenotype in vivo as well as the importance of monocyte degeneration. Interestingly, degeneration of mononuclear phagocytes is commonly associated with human neurodegenerative diseases, and commonly referred to as microglial degeneration [63], whereas rodent models appear less affected by this phenotype. However, previous studies observed degeneration of mononuclear phagocytes in a transgenic mutant SOD1 rat [25], similar to our current results in mutant SOD1 mice carrying a wild type *Htr2b* gene. Loss of *Htr2b* almost doubled the proportion of fragmented Iba1-positive cells, showing the importance of this receptor in preventing phagocyte degeneration during disease, although detailed molecular pathways remain to be elucidated.

The processes underlying degeneration of mononuclear phagocytes during ALS remain elusive, and the

relationships between microglial activation, for instance through inflammasomes [70], and microglial survival are not understood. Paradoxically, *Trem2* was found to be upregulated in SOD1(G86R) mice in the absence of *Htr2b*. Trem2 is a scavenger receptor found on the surface of myeloid cells, and *TREM2* mutations leading to impaired phagocytic activity [42] are strong risk factors for multiple neurodegenerative diseases, including ALS [10, 27, 39]. Whether increased expression of *Trem2* in SOD1(G86R); *Htr2b*$^{-/-}$ mice is beneficial or deleterious remains unknown. However, recent work demonstrated that loss of *Trem2* leads either to microglial degeneration in different diseases of the central nervous system [11, 60, 71], or conversely to protection [37]. Thus, the exact mechanisms underlying 5-HT$_{2B}$R-mediated regulation of microglial survival and the role of scavenger receptors in this response will have to be investigated in further studies.

A major question arising from our work is whether the lack of 5-HT$_{2B}$R accelerates ALS progression through its effects on degeneration of mononuclear phagocytes. The hypothesis that degeneration of mononuclear phagocytes is directly linked to the lack of 5-HT$_{2B}$R in this cell type is plausible for several reasons. First, *Htr2b* expression has been detected in newborn brain microglia [44] although it remains low in basal conditions [7, 8, 12, 33]. *Htr2b* is also highly expressed in peripheral macrophages [14]. *Htr2b* expression was restricted to CD11b-positive cells purified from spinal cord and brainstem, thus originating from mononuclear phagocytes, either microglia or infiltrating monocytes. Second, the late occurrence of *Htr2b* upregulation [15] coincides with activation of mononuclear phagocytes in SOD1(G86R) mice. Third, the effects of *Htr2b* ablation on ALS progression are strikingly similar to interventions performed on mononuclear phagocytes. For instance, knocking out mutant SOD1 or NF-kappaB signaling from CD11b-positive cells improved disease progression, but had no effect on disease onset [5, 26]. Despite these parallels, our current results cannot exclude that at least part of the effects of *Htr2b* ablation are caused by its expression in other cell types. Besides mononuclear phagocytes, *Htr2b* is expressed at detectable levels in serotonergic neurons themselves [16], and is known to regulate serotonin release [2, 17]. It is therefore possible that the observed decrease in weight in SOD1(G86R) mice devoid of the *Htr2b* gene was due to serotonergic neurons indirectly affecting hypothalamic circuitry, consistent with our recent results (Vercruysse et al., Brain, in press). To date, no conditional knock-out model of *Htr2b* gene has been characterized. Thus, the current knowledge of the function of *Htr2b* in microglial cells remains limited to in vitro studies (this study (Fig. 7) or previous results [44]). The generation and characterization of knock-out mice in which *Htr2b* deletion is restricted to microglia will yield invaluable insights into this question.

To our knowledge, these results provide the first genetic evidence for an involvement of the serotoninergic system in ALS. We previously showed that platelet serotonin content correlated with survival [22]. Brain-derived serotonin was decreased in ALS patients and mice [15], and imaging studies consistently report dramatic reduction in the binding of 5-HT$_{1A}$ ligand [66, 67]. Pharmacological interventions targeting serotonin provided some evidence for its involvement. For instance, perinatally administered fluoxetine accelerated weight loss and disease onset in ALS rats [45], while 5-hydroxytryptophan, the serotonin precursor, delayed disease in mutant SOD1 mice [65]. Furthermore, spasticity appears linked to serotonergic abnormalities [15]. Here we provide genetic evidence that the serotonin system is involved in disease progression and microglial function. The observation that lack of *Htr2b* accelerated weight loss in ALS mice raises questions on the role of serotonin in weight loss during ALS progression [21], and our most recent results show that loss of serotonin is involved in the development of melanocortin defects (Vercruysse et al., Brain, in press).

Collectively, our results suggest that the 5-HT$_{2B}$R might be an interesting target to prolong survival of ALS patients after onset. However, this should be tempered by the known cardiovascular side effects of 5-HT$_{2B}$R agonists. Chronic use of 5-HT$_{2B}$R agonists has been associated with cardiac valvulopathies and pulmonary hypertension [36], and a therapeutic strategy targeting 5-HT$_{2B}$R should consider the balance between potential benefits and cardiovascular risks in a currently intractable and rapidly progressive disease like ALS, in which patients are most often in good cardiovascular health. Since we identify common *HTR2B* polymorphisms as differentially associated with *HTR2B* expression in the CNS, eventual clinical studies should also take into account *HTR2B* genetic variations.

Acknowledgments We thank Dr David Hicks (INCI, Strasbourg) for careful english editing. We acknowledge the technical help of Marie Jo Ruivo, Annie Picchinenna and Sébastien Freismuth. This work was supported by Fondation "Recherche sur le Cerveau" (call 2015, to LD and LMa), and the Fondation Thierry Latran (SpastALS, to LD). Research leading to these results has received funding from the European Community's Health Seventh Framework Programme (FP7/2007–2013; EuroMOTOR). This study was supported by The Netherlands Organization for Health Research and Development (Vici Scheme (to LvdB), under the frame of E-Rare-2 (to JHV) and JPND (STRENGTH, to LvdB and JHV), the ERA Net for Research on Rare Diseases (PYRAMID). This study was supported by the ALS Foundation Netherlands and the MND association (UK) (Project MinE, http://www.projectmine.com). Work in our laboratories is supported by ALS Association Investigator Initiated Award (Grants 2235, 3209 and 8075; to LD); the Frick Foundation (award 2013 to LD); Association Française contre les Myopathies (Grant #18280; to LD); Virtual Helmholtz Institute "RNA dysmetabolism in ALS and FTD" (WP2, to LD, AW and ACL). This study was supported by the ALS Foundation Netherlands and the MND association (UK) (Project MinE, http://www.projectmine.com). LMa is supported by the *Fondation pour la*

Recherche Médicale "Equipe FRM DEQ 2014039529", the French Ministry of Research (Agence Nationale pour la Recherche) ANR-12-BSV1-0015-01 and the *Investissements d'Avenir* program managed by the ANR under reference ANR-11-IDEX-0004-02.

References

1. Ajami B, Bennett JL, Krieger C, Tetzlaff W, Rossi FM (2007) Local self-renewal can sustain CNS microglia maintenance and function throughout adult life. Nat Neurosci 10:1538–1543. doi:10.1038/nn2014
2. Banas SM, Doly S, Boutourlinsky K, Diaz SL, Belmer A, Callebert J, Collet C, Launay JM, Maroteaux L (2011) Deconstructing antiobesity compound action: requirement of serotonin 5-HT2B receptors for dexfenfluramine anorectic effects. Neuropsychopharmacology 36:423–433. doi:10.1038/npp.2010.173
3. Bevilacqua L, Doly S, Kaprio J, Yuan Q, Tikkanen R, Paunio T, Zhou Z, Wedenoja J, Maroteaux L, Diaz S, Belmer A, Hodgkinson CA, Dell'osso L, Suvisaari J, Coccaro E, Rose RJ, Peltonen L, Virkkunen M, Goldman D (2010) A population-specific HTR2B stop codon predisposes to severe impulsivity. Nature 468:1061–1066. doi:10.1038/nature09629
4. Boillee S, Vande Velde C, Cleveland DW (2006) ALS: a disease of motor neurons and their nonneuronal neighbors. Neuron 52:39–59
5. Boillee S, Yamanaka K, Lobsiger CS, Copeland NG, Jenkins NA, Kassiotis G, Kollias G, Cleveland DW (2006) Onset and progression in inherited ALS determined by motor neurons and microglia. Science 312:1389–1392
6. Brooks BR, Miller RG, Swash M, Munsat TL (2000) El Escorial revisited: revised criteria for the diagnosis of amyotrophic lateral sclerosis. Amyotroph Lateral Scler Other Motor Neuron Disord 1:293–299
7. Butovsky O, Jedrychowski MP, Cialic R, Krasemann S, Murugaiyan G, Fanek Z, Greco DJ, Wu PM, Doykan CE, Kiner O, Lawson RJ, Frosch MP, Pochet N, Fatimy RE, Krichevsky AM, Gygi SP, Lassmann H, Berry J, Cudkowicz ME, Weiner HL (2015) Targeting miR-155 restores abnormal microglia and attenuates disease in SOD1 mice. Ann Neurol 77:75–99. doi:10.1002/ana.24304
8. Butovsky O, Jedrychowski MP, Moore CS, Cialic R, Lanser AJ, Gabriely G, Koeglsperger T, Dake B, Wu PM, Doykan CE, Fanek Z, Liu L, Chen Z, Rothstein JD, Ransohoff RM, Gygi SP, Antel JP, Weiner HL (2014) Identification of a unique TGF-beta-dependent molecular and functional signature in microglia. Nat Neurosci 17:131–143. doi:10.1038/nn.3599
9. Butovsky O, Siddiqui S, Gabriely G, Lanser AJ, Dake B, Murugaiyan G, Doykan CE, Wu PM, Gali RR, Iyer LK, Lawson R, Berry J, Krichevsky AM, Cudkowicz ME, Weiner HL (2012) Modulating inflammatory monocytes with a unique microRNA gene signature ameliorates murine ALS. J Clin Invest 122:3063–3087. doi:10.1172/JCI62636
10. Cady J, Koval ED, Benitez BA, Zaidman C, Jockel-Balsarotti J, Allred P, Baloh RH, Ravits J, Simpson E, Appel SH, Pestronk A, Goate AM, Miller TM, Cruchaga C, Harms MB (2014) TREM2 variant p. R47H as a risk factor for sporadic amyotrophic lateral sclerosis. JAMA Neurol 71:449–453. doi:10.1001/jamaneurol.2013.6237
11. Cantoni C, Bollman B, Licastro D, Xie M, Mikesell R, Schmidt R, Yuede CM, Galimberti D, Olivecrona G, Klein RS, Cross AH, Otero K, Piccio L (2015) TREM2 regulates microglial cell activation in response to demyelination in vivo. Acta Neuropathol 129:429–447. doi:10.1007/s00401-015-1388-1
12. Chiu IM, Morimoto ET, Goodarzi H, Liao JT, O'Keeffe S, Phatnani HP, Muratet M, Carroll MC, Levy S, Tavazoie S, Myers RM, Maniatis T (2013) A neurodegeneration-specific gene-expression signature of acutely isolated microglia from an amyotrophic lateral sclerosis mouse model. Cell Rep 4:385–401. doi:10.1016/j.celrep.2013.06.018
13. d'Errico P, Boido M, Piras A, Valsecchi V, De Amicis E, Locatelli D, Capra S, Vagni F, Vercelli A, Battaglia G (2013) Selective vulnerability of spinal and cortical motor neuron subpopulations in delta7 SMA mice. PLoS One 8:e82654. doi:10.1371/journal.pone.0082654
14. de las Casas-Engel M, Dominguez-Soto A, Sierra-Filardi E, Bragado R, Nieto C, Puig-Kroger A, Samaniego R, Loza M, Corcuera MT, Gomez-Aguado F, Bustos M, Sanchez-Mateos P, Corbi AL (2013) Serotonin skews human macrophage polarization through HTR2B and HTR7. J Immunol 190:2301–2310
15. Dentel C, Palamiuc L, Henriques A, Lannes B, Spreux-Varoquaux O, Gutknecht L, Rene F, Echaniz-Laguna A, Gonzalez de Aguilar JL, Lesch KP, Meininger V, Loeffler JP, Dupuis L (2013) Degeneration of serotonergic neurons in amyotrophic lateral sclerosis: a link to spasticity. Brain 136:483–493. doi:10.1093/brain/aws274
16. Diaz SL, Doly S, Narboux-Neme N, Fernandez S, Mazot P, Banas SM, Boutourlinsky K, Moutkine I, Belmer A, Roumier A, Maroteaux L (2012) 5-HT(2B) receptors are required for serotonin-selective antidepressant actions. Mol Psychiatry 17:154–163. doi:10.1038/mp.2011.159
17. Doly S, Valjent E, Setola V, Callebert J, Herve D, Launay JM, Maroteaux L (2008) Serotonin 5-HT2B receptors are required for 3,4-methylenedioxymethamphetamine-induced hyperlocomotion and 5-HT release in vivo and in vitro. J Neurosci 28:2933–2940. doi:10.1523/JNEUROSCI.5723-07.2008
18. Dupuis L, de Tapia M, Rene F, Lutz-Bucher B, Gordon JW, Mercken L, Pradier L, Loeffler JP (2000) Differential screening of mutated SOD1 transgenic mice reveals early up-regulation of a fast axonal transport component in spinal cord motor neurons. Neurobiol Dis 7:274–285
19. Dupuis L, Fergani A, Braunstein KE, Eschbach J, Holl N, Rene F, Gonzalez De Aguilar JL, Zoerner B, Schwalenstocker B, Ludolph AC, Loeffler JP (2009) Mice with a mutation in the dynein heavy chain 1 gene display sensory neuropathy but lack motor neuron disease. Exp Neurol 215:146–152
20. Dupuis L, Oudart H, Rene F, Gonzalez de Aguilar JL, Loeffler JP (2004) Evidence for defective energy homeostasis in amyotrophic lateral sclerosis: benefit of a high-energy diet in a transgenic mouse model. Proc Natl Acad Sci 101:11159–11164
21. Dupuis L, Pradat PF, Ludolph AC, Loeffler JP (2011) Energy metabolism in amyotrophic lateral sclerosis. Lancet Neurol 10:75–82. doi:10.1016/S1474-4422(10)70224-6
22. Dupuis L, Spreux-Varoquaux O, Bensimon G, Jullien P, Lacomblez L, Salachas F, Bruneteau G, Pradat PF, Loeffler JP, Meininger V (2010) Platelet serotonin level predicts survival in amyotrophic lateral sclerosis. PLoS One 5:e13346. doi:10.1371/journal.pone.0013346
23. ElAli A, Rivest S (2015) Microglia in Alzheimer's disease: a multifaceted relationship. Brain Behav Immun. doi:10.1016/j.bbi.2015.07.021
24. Endo F, Komine O, Fujimori-Tonou N, Katsuno M, Jin S, Watanabe S, Sobue G, Dezawa M, Wyss-Coray T, Yamanaka K (2015) Astrocyte-derived TGF-beta1 accelerates disease progression in ALS mice by interfering with the neuroprotective functions of microglia and T cells. Cell Rep 11:592–604. doi:10.1016/j.celrep.2015.03.053
25. Fendrick SE, Xue QS, Streit WJ (2007) Formation of multinucleated giant cells and microglial degeneration in rats expressing

a mutant Cu/Zn superoxide dismutase gene. J Neuroinflammation 4:9. doi:10.1186/1742-2094-4-9
26. Frakes AE, Ferraiuolo L, Haidet-Phillips AM, Schmelzer L, Braun L, Miranda CJ, Ladner KJ, Bevan AK, Foust KD, Godbout JP, Popovich PG, Guttridge DC, Kaspar BK (2014) Microglia induce motor neuron death via the classical NF-kappaB pathway in amyotrophic lateral sclerosis. Neuron 81:1009–1023. doi:10.1016/j.neuron.2014.01.013
27. Guerreiro RJ, Lohmann E, Bras JM, Gibbs JR, Rohrer JD, Gurunlian N, Dursun B, Bilgic B, Hanagasi H, Gurvit H, Emre M, Singleton A, Hardy J (2013) Using exome sequencing to reveal mutations in TREM2 presenting as a frontotemporal dementia-like syndrome without bone involvement. JAMA Neurol 70:78–84. doi:10.1001/jamaneurol.2013.579
28. Guilliams M, van de Laar L (2015) A Hitchhiker's guide to myeloid cell subsets: practical implementation of a novel mononuclear phagocyte classification system. Front Immunol 6:406. doi:10.3389/fimmu.2015.00406
29. Harrison M, O'Brien A, Adams L, Cowin G, Ruitenberg MJ, Sengul G, Watson C (2013) Vertebral landmarks for the identification of spinal cord segments in the mouse. Neuroimage 68:22–29. doi:10.1016/j.neuroimage.2012.11.048
30. Heiman-Patterson TD, Sher RB, Blankenhorn EA, Alexander G, Deitch JS, Kunst CB, Maragakis N, Cox G (2011) Effect of genetic background on phenotype variability in transgenic mouse models of amyotrophic lateral sclerosis: a window of opportunity in the search for genetic modifiers. Amyotroph Lateral Scler 12:79–86. doi:10.3109/17482968.2010.550626
31. Hickman SE, El Khoury J (2010) Mechanisms of mononuclear phagocyte recruitment in Alzheimer's disease. CNS Neurol Disord: Drug Targets 9:168–173
32. Hickman SE, El Khoury J (2013) The neuroimmune system in Alzheimer's disease: the glass is half full. J Alzheimers Dis 33(Suppl 1):S295–S302. doi:10.3233/JAD-2012-129027
33. Hickman SE, Kingery ND, Ohsumi TK, Borowsky ML, Wang LC, Means TK, El Khoury J (2013) The microglial sensome revealed by direct RNA sequencing. Nat Neurosci 16:1896–1905. doi:10.1038/nn.3554
34. Hoeffel G, Ginhoux F (2015) Ontogeny of tissue-resident macrophages. Front Immunol 6:486. doi:10.3389/fimmu.2015.00486
35. Huisman MH, de Jong SW, van Doormaal PT, Weinreich SS, Schelhaas HJ, van der Kooi AJ, de Visser M, Veldink JH, van den Berg LH (2011) Population based epidemiology of amyotrophic lateral sclerosis using capture-recapture methodology. J Neurol Neurosurg Psychiatry 82:1165–1170. doi:10.1136/jnnp.2011.244939
36. Hutcheson JD, Setola V, Roth BL, Merryman WD (2011) Serotonin receptors and heart valve disease–it was meant 2B. Pharmacol Ther 132:146–157. doi:10.1016/j.pharmthera.2011.03.008
37. Jay TR, Miller CM, Cheng PJ, Graham LC, Bemiller S, Broihier ML, Xu G, Margevicius D, Karlo JC, Sousa GL, Cotleur AC, Butovsky O, Bekris L, Staugaitis SM, Leverenz JB, Pimplikar SW, Landreth GE, Howell GR, Ransohoff RM, Lamb BT (2015) TREM2 deficiency eliminates TREM2+ inflammatory macrophages and ameliorates pathology in Alzheimer's disease mouse models. J Exp Med 212:287–295. doi:10.1084/jem.20142322
38. Jokic N, Gonzalez de Aguilar JL, Dimou L, Lin S, Fergani A, Ruegg MA, Schwab ME, Dupuis L, Loeffler JP (2006) The neurite outgrowth inhibitor Nogo-A promotes denervation in an amyotrophic lateral sclerosis model. EMBO Rep 7:1162–1167
39. Jonsson T, Stefansson H, Steinberg S, Jonsdottir I, Jonsson PV, Snaedal J, Bjornsson S, Huttenlocher J, Levey AI, Lah JJ, Rujescu D, Hampel H, Giegling I, Andreassen OA, Engedal K, Ulstein I, Djurovic S, Ibrahim-Verbaas C, Hofman A, Ikram MA, van Duijn CM, Thorsteinsdottir U, Kong A, Stefansson K (2013) Variant of TREM2 associated with the risk of Alzheimer's disease. N Engl J Med 368:107–116. doi:10.1056/NEJMoa1211103
40. Kettenmann H, Hanisch UK, Noda M, Verkhratsky A (2011) Physiology of microglia. Physiol Rev 91:461–553. doi:10.1152/physrev.00011.2010
41. Kiernan MC, Vucic S, Cheah BC, Turner MR, Eisen A, Hardiman O, Burrell JR, Zoing MC (2011) Amyotrophic lateral sclerosis. Lancet 377:942–955. doi:10.1016/S0140-6736(10)61156-7
42. Kleinberger G, Yamanishi Y, Suarez-Calvet M, Czirr E, Lohmann E, Cuyvers E, Struyfs H, Pettkus N, Wenninger-Weinzierl A, Mazaheri F, Tahirovic S, Lleo A, Alcolea D, Fortea J, Willem M, Lammich S, Molinuevo JL, Sanchez-Valle R, Antonell A, Ramirez A, Heneka MT, Sleegers K, van der Zee J, Martin JJ, Engelborghs S, Demirtas-Tatlidede A, Zetterberg H, Van Broeckhoven C, Gurvit H, Wyss-Coray T, Hardy J, Colonna M, Haass C (2014) TREM2 mutations implicated in neurodegeneration impair cell surface transport and phagocytosis. Sci Transl Med 6:243ra286. doi:10.1126/scitranslmed.3009093
43. Knight AR, Misra A, Quirk K, Benwell K, Revell D, Kennett G, Bickerdike M (2004) Pharmacological characterisation of the agonist radioligand binding site of 5-HT(2A), 5-HT(2B) and 5-HT(2C) receptors. Naunyn Schmiedebergs Arch Pharmacol 370:114–123. doi:10.1007/s00210-004-0951-4
44. Kolodziejczak M, Bechade C, Gervasi N, Irinopoulou T, Banas SM, Cordier C, Rebsam A, Roumier A, Maroteaux L (2015) Serotonin modulates developmental microglia via 5-HT receptors: potential implication during synaptic refinement of retinogeniculate projections. ACS Chem Neurosci. doi:10.1021/cn5003489
45. Koschnitzky JE, Quinlan KA, Lukas TJ, Kajtaz E, Kocevar EJ, Mayers WF, Siddique T, Heckman CJ (2014) Effect of fluoxetine on disease progression in a mouse model of ALS. J Neurophysiol 111:2164–2176. doi:10.1152/jn.00425.2013
46. Kunis G, Baruch K, Miller O, Schwartz M (2015) Immunization with a myelin-derived antigen activates the brain's choroid plexus for recruitment of immunoregulatory cells to the CNS and attenuates disease progression in a mouse model of ALS. J Neurosci 35:6381–6393. doi:10.1523/JNEUROSCI.3644-14.2015
47. Laird FM, Farah MH, Ackerley S, Hoke A, Maragakis N, Rothstein JD, Griffin J, Price DL, Martin LJ, Wong PC (2008) Motor neuron disease occurring in a mutant dynactin mouse model is characterized by defects in vesicular trafficking. J Neurosci 28:1997–2005. doi:10.1523/JNEUROSCI.4231-07.2008
48. Lattante S, Ciura S, Rouleau GA, Kabashi E (2015) Defining the genetic connection linking amyotrophic lateral sclerosis (ALS) with frontotemporal dementia (FTD). Trends Genet. doi:10.1016/j.tig.2015.03.005
49. Launay JM, Herve P, Peoc'h K, Tournois C, Callebert J, Nebigil CG, Etienne N, Drouet L, Humbert M, Simonneau G, Maroteaux L (2002) Function of the serotonin 5-hydroxytryptamine 2B receptor in pulmonary hypertension. Nat Med 8:1129–1135. doi:10.1038/nm764
50. Lewis CA, Solomon JN, Rossi FM, Krieger C (2009) Bone marrow-derived cells in the central nervous system of a mouse model of amyotrophic lateral sclerosis are associated with blood vessels and express CX(3)CR1. Glia 57:1410–1419. doi:10.1002/glia.20859
51. Liao B, Zhao W, Beers DR, Henkel JS, Appel SH (2012) Transformation from a neuroprotective to a neurotoxic microglial phenotype in a mouse model of ALS. Exp Neurol 237:147–152. doi:10.1016/j.expneurol.2012.06.011
52. Mosher KI, Wyss-Coray T (2014) Microglial dysfunction in brain aging and Alzheimer's disease. Biochem Pharmacol 88:594–604. doi:10.1016/j.bcp.2014.01.008
53. Nebigil CG, Choi DS, Dierich A, Hickel P, Le Meur M, Messaddeq N, Launay JM, Maroteaux L (2000) Serotonin 2B receptor is required for heart development. Proc Natl Acad Sci 97:9508–9513

54. Nebigil CG, Etienne N, Messaddeq N, Maroteaux L (2003) Serotonin is a novel survival factor of cardiomyocytes: mitochondria as a target of 5-HT2B receptor signaling. FASEB J 17:1373–1375. doi:10.1096/fj.02-1122fje
55. Nebigil CG, Hickel P, Messaddeq N, Vonesch JL, Douchet MP, Monassier L, Gyorgy K, Matz R, Andriantsitohaina R, Manivet P, Launay JM, Maroteaux L (2001) Ablation of serotonin 5-HT(2B) receptors in mice leads to abnormal cardiac structure and function. Circulation 103:2973–2979
56. Nebigil CG, Jaffre F, Messaddeq N, Hickel P, Monassier L, Launay JM, Maroteaux L (2003) Overexpression of the serotonin 5-HT2B receptor in heart leads to abnormal mitochondrial function and cardiac hypertrophy. Circulation 107:3223–3229. doi:10.1161/01.CIR.0000074224.57016.01
57. Philips T, Robberecht W (2011) Neuroinflammation in amyotrophic lateral sclerosis: role of glial activation in motor neuron disease. Lancet Neurol 10:253–263. doi:10.1016/S1474-4422(11)70015-1
58. Philips T, Rothstein JD (2014) Glial cells in amyotrophic lateral sclerosis. Exp Neurol 262(Pt B):111–120. doi:10.1016/j.expneurol.2014.05.015
59. Pitychoutis PM, Belmer A, Moutkine I, Adrien J, Maroteaux L (2015) Mice lacking the serotonin Htr receptor gene present an antipsychotic-sensitive schizophrenic-like phenotype. Neuropsychopharmacology. doi:10.1038/npp.2015.126
60. Poliani PL, Wang Y, Fontana E, Robinette ML, Yamanishi Y, Gilfillan S, Colonna M (2015) TREM2 sustains microglial expansion during aging and response to demyelination. J Clin Invest 125:2161–2170. doi:10.1172/JCI77983
61. Schneider CA, Rasband WS, Eliceiri KW (2012) NIH Image to ImageJ: 25 years of image analysis. Nat Methods 9:671–675
62. Streit WJ, Braak H, Xue QS, Bechmann I (2009) Dystrophic (senescent) rather than activated microglial cells are associated with tau pathology and likely precede neurodegeneration in Alzheimer's disease. Acta Neuropathol 118:475–485. doi:10.1007/s00401-009-0556-6
63. Streit WJ, Xue QS, Tischer J, Bechmann I (2014) Microglial pathology. Acta Neuropathol Commun 2:142. doi:10.1186/s40478-014-0142-6
64. Strong MJ, Yang W (2011) The frontotemporal syndromes of ALS. Clinicopathological correlates. J Mol Neurosci 45:648–655. doi:10.1007/s12031-011-9609-0
65. Turner BJ, Lopes EC, Cheema SS (2003) The serotonin precursor 5-hydroxytryptophan delays neuromuscular disease in murine familial amyotrophic lateral sclerosis. Amyotroph Lateral Scler Other Motor Neuron Disord 4(3):171–176. doi:10.1080/14660820310009389
66. Turner MR, Rabiner EA, Al-Chalabi A, Shaw CE, Brooks DJ, Leigh PN, Andersen PM (2007) Cortical 5-HT1A receptor binding in patients with homozygous D90A SOD1 vs sporadic ALS. Neurology 68:1233–1235. doi:10.1212/01.wnl.0000259083.31837.64
67. Turner MR, Rabiner EA, Hammers A, Al-Chalabi A, Grasby PM, Shaw CE, Brooks DJ, Leigh PN (2005) [11C]-WAY100635 PET demonstrates marked 5-HT1A receptor changes in sporadic ALS. Brain 128:896–905. doi:10.1093/brain/awh428
68. van Es MA, Veldink JH, Saris CG, Blauw HM, van Vught PW, Birve A, Lemmens R, Schelhaas HJ, Groen EJ, Huisman MH, van der Kooi AJ, de Visser M, Dahlberg C, Estrada K, Rivadeneira F, Hofman A, Zwarts MJ, van Doormaal PT, Rujescu D, Strengman E, Giegling I, Muglia P, Tomik B, Slowik A, Uitterlinden AG, Hendrich C, Waibel S, Meyer T, Ludolph AC, Glass JD, Purcell S, Cichon S, Nothen MM, Wichmann HE, Schreiber S, Vermeulen SH, Kiemeney LA, Wokke JH, Cronin S, McLaughlin RL, Hardiman O, Fumoto K, Pasterkamp RJ, Meininger V, Melki J, Leigh PN, Shaw CE, Landers JE, Al-Chalabi A, Brown RH Jr, Robberecht W, Andersen PM, Ophoff RA, van den Berg LH (2009) Genome-wide association study identifies 19p13.3 (UNC13A) and 9p21.2 as susceptibility loci for sporadic amyotrophic lateral sclerosis. Nat Genet 41:1083–1087. doi:10.1038/ng.442
69. Vandesompele J, De Preter K, Pattyn C, Poppe B, Van Roy N, De Paepe A, Speleman F (2002) Accurate normalization of real-time quantitative RT-PCR data by geometric averaging of multiple internal control genes. Genome Biol 3:research0034.1–research0034.11. doi:10.1186/Gb-2002-3-7-Research0034
70. Walsh JG, Muruve DA, Power C (2014) Inflammasomes in the CNS. Nat Rev Neurosci 15:84–97. doi:10.1038/nrn3638
71. Wang Y, Cella M, Mallinson K, Ulrich JD, Young KL, Robinette ML, Gilfillan S, Krishnan GM, Sudhakar S, Zinselmeyer BH, Holtzman DM, Cirrito JR, Colonna M (2015) TREM2 lipid sensing sustains the microglial response in an Alzheimer's disease model. Cell 160:1061–1071. doi:10.1016/j.cell.2015.01.049
72. Wiesner D, Sinniger J, Henriques A, Dieterle S, Muller H, Rasche V, Ferger B, Dirrig-Grosch S, Soylu-Kucharz R, Petersen A, Walther P, Linkus B, Kassubek J, Wong PC, Ludolph AC, Dupuis L (2014) Low dietary protein content alleviates motor symptoms in mice with mutant dynactin/dynein mediated neurodegeneration. Hum Mol Genet 15:2228–2240. doi:10.1093/hmg/ddu741
73. Witting A, Moller T (2011) Microglia cell culture: a primer for the novice. Methods Mol Biol 758:49–66. doi:10.1007/978-1-61779-170-3_4
74. Xue QS, Streit WJ (2011) Microglial pathology in Down syndrome. Acta Neuropathol 122:455–466. doi:10.1007/s00401-011-0864-5
75. Zhao W, Beers DR, Appel SH (2013) Immune-mediated mechanisms in the pathoprogression of amyotrophic lateral sclerosis. J Neuroimmune Pharmacol 8:888–899. doi:10.1007/s11481-013-9489-x

El Oussini and collaborators
Serotonin 2B receptor slows disease progression and prevents degeneration of spinal cord mononuclear phagocytes in amyotrophic lateral sclerosis

Supplementary Material

Supplementary Figures

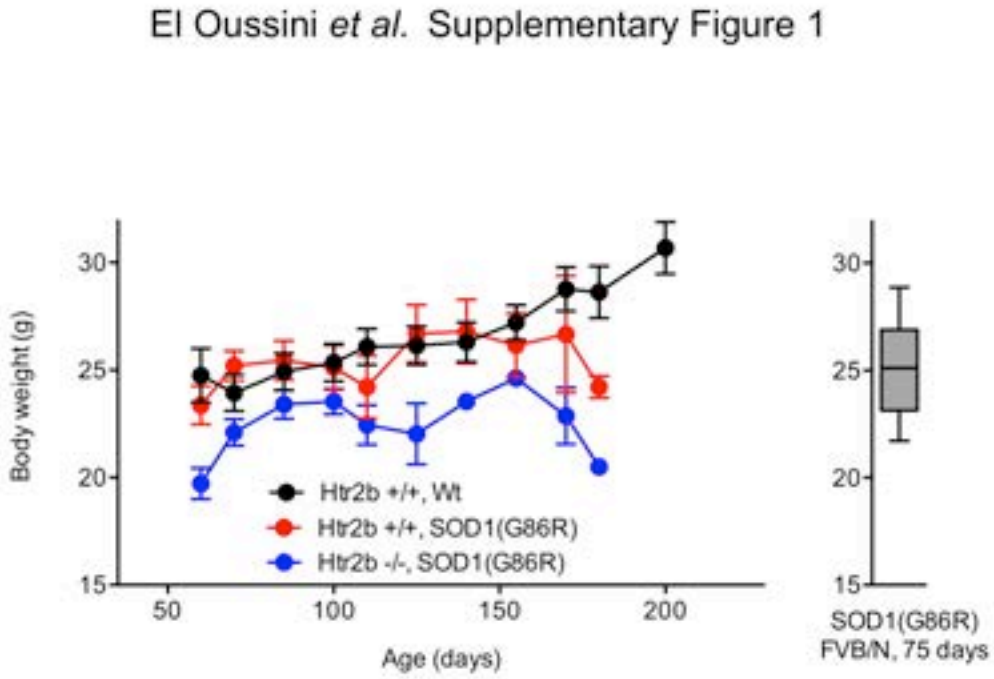

Fig. S1: *Htr2b* ablation decreases body weight in SOD1(G86R) mice
Body weight curves of SOD1(G86R) mice wild type for *Htr2b* (+/+) ,
or knock-out for *Htr2b* (-/-) and wild type littermate mice. N=10-16 per genotype.
The right panel shows the body weight of SOD1(G86R) mice in the initial FVB/N background (n=12).
P<0.05 for genotype between Htr2b -/- SOD1(G86R) and Htr2b +/+ SOD1(G86R), Repeated measures two way ANOVA.

El Oussini *et al.* Supplementary Figure 2

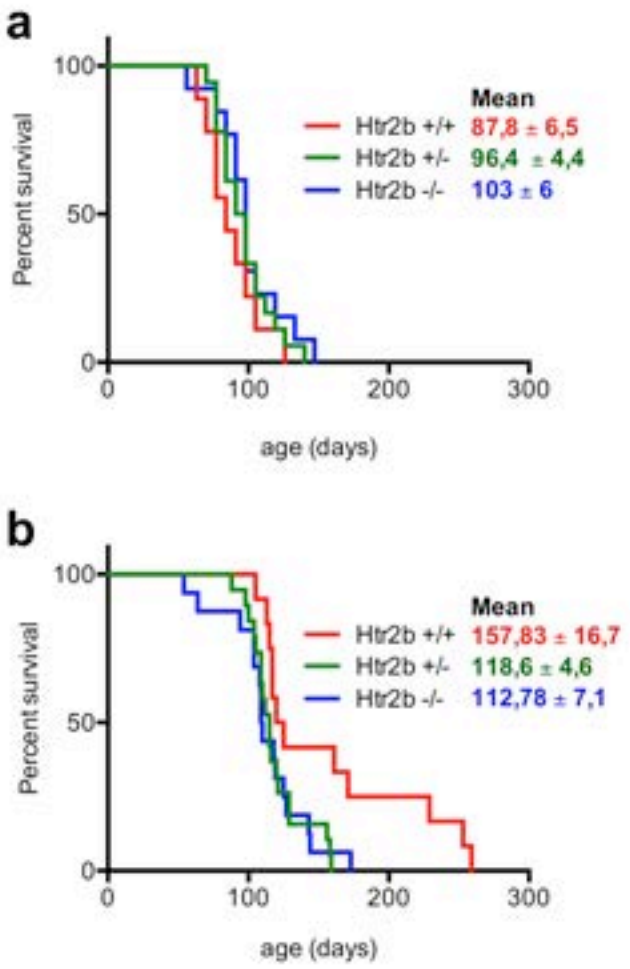

Fig. S2: *Htr2b* haploinsufficiency exacerbates SOD1(G86R) disease progression

Kaplan Meier plot of disease onset, as determined by the peak weight (a) and of survival (b) for SOD1(G86R) mice wild type for *Htr2b* (n=12, red), heterozygous for *Htr2b* (n=19, green) or homozygous for *Htr2b* (n=16, blue). The mean of each group +/- SEM is indicated on each panel.

P<0.05, log rank (Mantel cox) for panel b (+/+ vs +/- and +/+ vs -/-). The log rank test for trend has a p-value of 0.0149, showing the dose dependence of survival towards the number of functional *Htr2b* alleles.

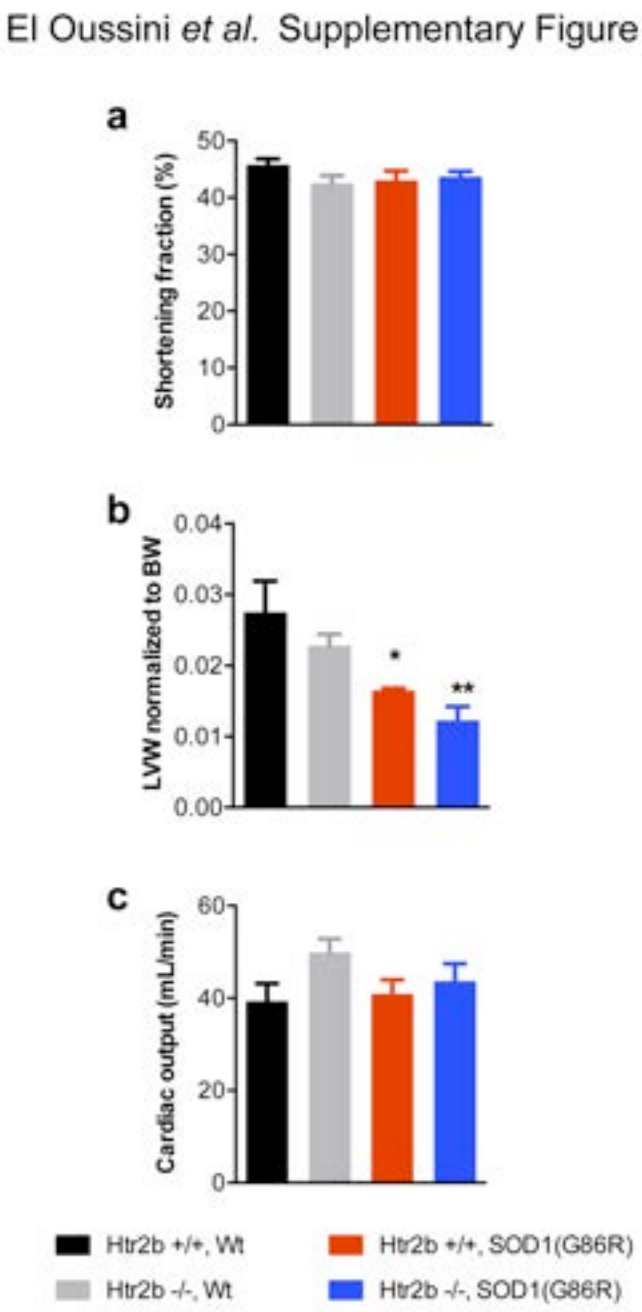

Fig. S3: *Htr2b* ablation does not exacerbate SOD1(G86R) cardiac phenotype

Shortening fraction (in %, A), left ventricular volume (LVW) and cardiac output (in mL/min) wild type mice (Htr2b +/+, Wt), mice knock-out for *Htr2b* (-/-)(Htr2b -/-, Wt) or littermate SOD1(G86R) mice wild type for *Htr2b* (+/+) , or knock-out for *Htr2b* (-/-). Note that the SOD1(G86R) genotype leads to a significant cardiac atrophy, not modified by *Htr2b* genotype.

El Oussini *et al.* Supplementary Figure 4

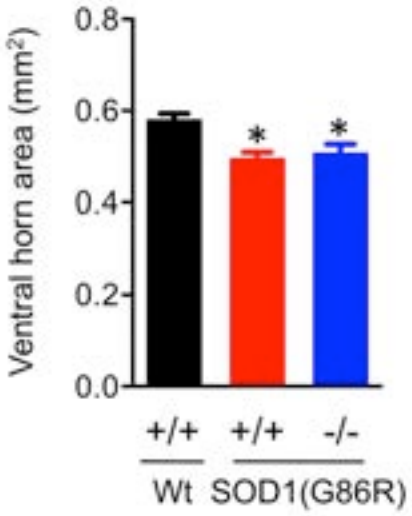

Fig. S4: *Htr2b* ablation does not modify ventral horn atrophy in SOD1(G86R)
Ventral horn area in wild type mice (Htr2b +/+, Wt), SOD1(G86R) mice wild type for *Htr2b* (+/+) , or knock-out for *Htr2b* (-/-). Note that the SOD1(G86R) genotype leads to a significant atrophy of ventral horn, not modified by *Htr2b* genotype.

Ventral horn was defined anatomically and measured in >10 sections per animal, with n=7 independent animals per genotype.
*$p<0.05$ significantly different (One-way ANOVA followed by Tukey *post hoc* test).

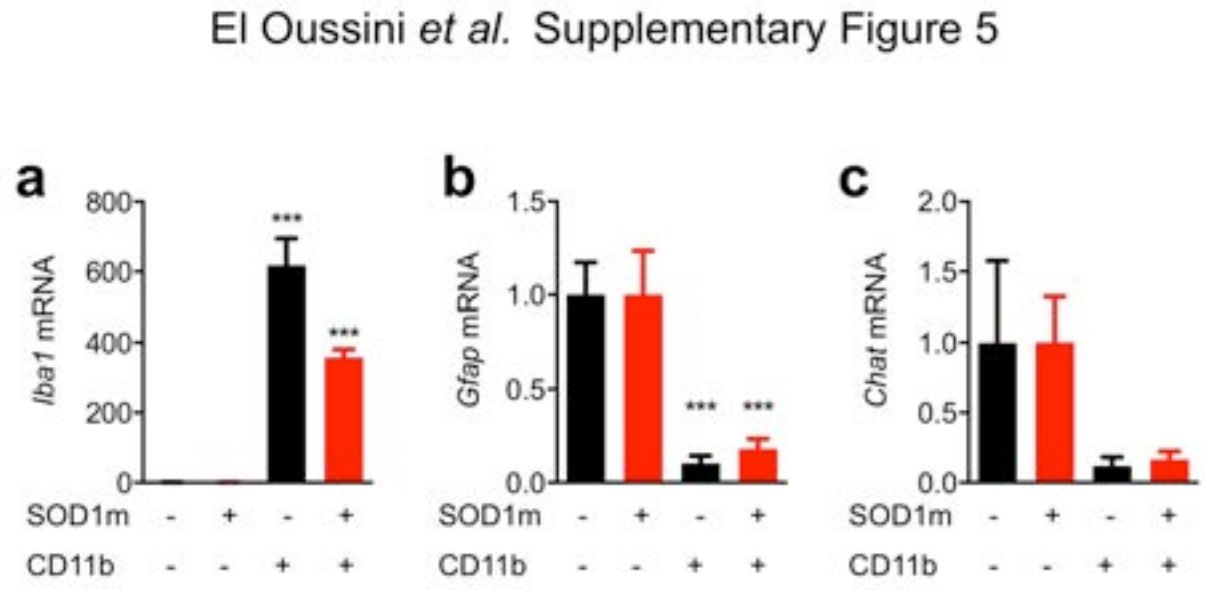

Fig. S5: controls for purification of CD11b positive cells.
Iba1 (**a**), *Gfap* (**b***) and Chat* (**c***)* mRNA levels in CD11b-positive cells ($CD11^{Pos}$) relative to CD11b-negative cells ($CD11b^{Neg}$) in brainstem and spinal cord of end stage SOD1(G86R) mice (SOD1) and control littermates (Wt). ***$p<0.01$ significantly different vs corresponding CD11b negative fraction (One-way ANOVA followed by Tukey *post hoc* test).

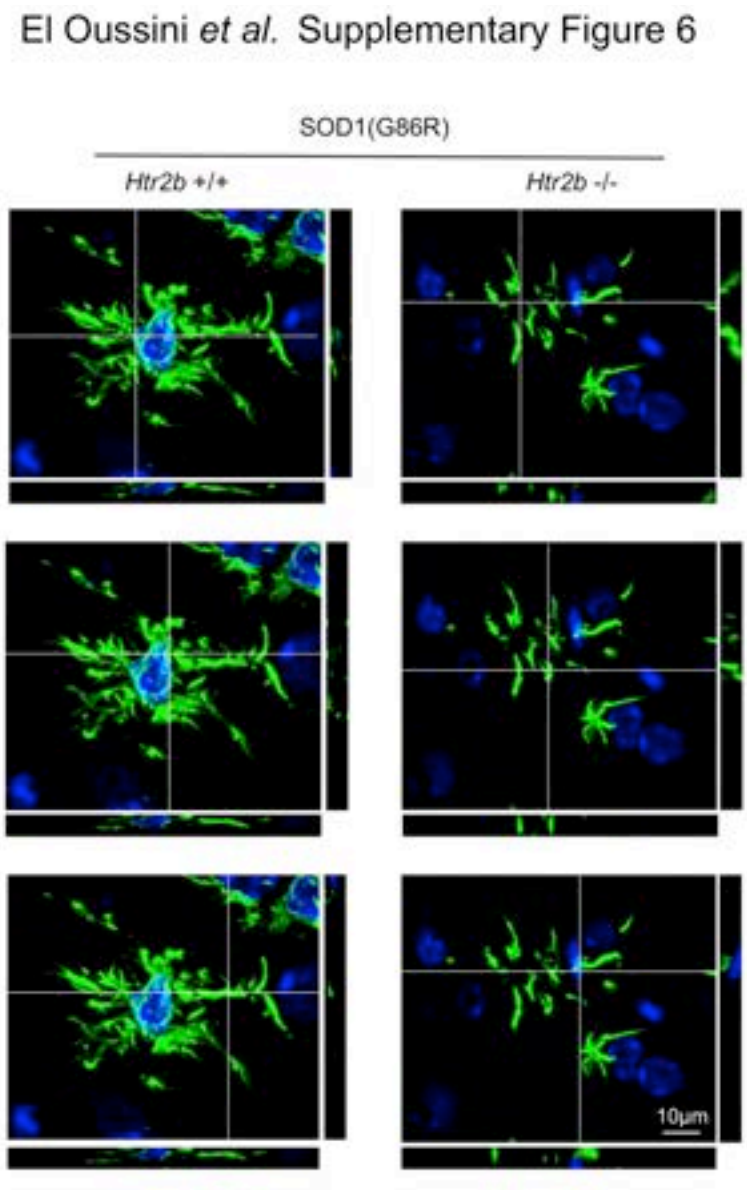

Fig. S6: side views of Iba1 immunofluorescence.
Orthogonal views of one Iba1 positive cell of a SOD1(G86R) mouse wild type for *Htr2b* (+/+) (left) and one Iba1 positive cell of a SOD1(G86R) mouse knock-out for *Htr2b* (-/-) (right).
z-stacks of 10-15µm thickness were merged and are shown in XY. Orthogonal side views are shown for XZ and YZ axes with white lines in merged images showing location of section.
Iba1 immunolabeling is shown in green, and nucleus in blue.

Table S1: Patient characteristics for survival analysis

Shown is the number of patients, gender (M=male, F=female), age at onset (AAO), age at inclusion (AAI), site of onset, Survival in years, percentage deceased.

Number	Gender (M/F)	AAO mean (range)	AAI mean (range)	Site of onset (bulbar (%))	Survival (y) mean/median	Deceased (%)
1677	998/679	62 (19-90)	66 (21-91)	563 (33.7%)	2.36/2.02 (0.0017-14.8)	80.1

Table S2: characteristics of ALS patients included in autoptic studies.

16 ALS patients were genotyped and included. 6 carried *HTR2B* A/A rs10199752 haplotype (patients 1-6) and 10 carried *HTR2B* C/A rs10199752 haplotypes (7-16).

Corresponding genotypes are indicated for each patient, as well as inclusion in qPCR and/or microglial degeneration score depending on material availability.

All patients were diagnosed with ALS, except patient 2, with a diagnosis of combined ALS and Lewy body disease (LBD). When available, the extent of TDP-43 pathology and Braak staging is indicated.

patient	rs10199752	qPCR	microglial fragmentation	age at death	Gender	diagnosis
1	A/A	+	3,5	63	m	ALS
2	A/A	+	3,5	75	m	ALS + LBD
3	A/A	+	3	66	f	ALS + AD
4	A/A	+	2	74	m	ALS (stage1/ 16% TDP-43 affected areas)
5	A/A	+	4	43	m	ALS (stage4/ 58% TDP-43 affected areas)
6	A/A	+	3	66	m	ALS
7	C/A	+	1	69	m	ALS (stage4/ 52% TDP-43 affected areas)
8	C/A	N/A	0,5	75	m	ALS (stage4/ 69% TDP-43 affected areas)
9	C/A	+	N/A	61	m	ALS (stage4/ 61% TDP-43 affected areas)
10	C/A	+	0,5	75	m	ALS (stage4/ 55% TDP-43 affected areas)
11	C/A	+	0	84	m	ALS
12	C/A	+	N/A	46	f	ALS (no TDP-43 lesions – only p62-lesions/ C9Orf72 mutation carrier)
13	C/A	+	0	25	m	ALS (stage3/ 40% TDP-43 affected areas)
14	C/A	+	N/A	76	f	ALS (stage4/ 60% TDP-43 affected areas)
15	C/A	+	1	56	f	ALS
16	C/A	N/A	0			ALS

Table S3: primers for RT-qPCR studies.
All primers are murine except where indicated.

mRNA		Sequence
Ccl4 For	Chemokine (C-C motif) ligand 4	CAA-GCC-AGC-TGT-GGT-ATT-CCT
Ccl4 Rev		GCT-GCT-CAG-TTC-AAC-TCC-AAG
Nox2 For	NADPH oxidase	ACA-CTG-ACC-TCT-GCT-CCT-GA
Nox2c Rev		AGG-CAT-CTT-GGA-ACT-CCT-GC
Mch2 For	Musculus histocompatibility 2, class II	AGG-AGA-GCC-TTA-TTC-ATC-GCT
Mch2 Rev		GAT-GGC-GCT-CTC-GTT-CTG-T
Dap12For	DNAX activation protein	TGA-CTC-TGC-TGA-TTG-CCC-TG
Dap12 Rev		GGC-GAC-TCA-GTC-TCA-GCA-AT
Ym1 For	Secretory protein precursor	GAA-GGA-CCA-TGG-AGC-AGC-TT
Ym1 Rev		GGG-GCA-CCA-ATT-CCA-GTC-TT
Hexb For	Beta-hexosaminidase subunit beta	GGA-CTT-CAG-CAT-CGA-CCA-CA
Hexb Rev		GTA-ATA-TCG-CCG-AAA-CGC-CTC
Olfml3 For	Olfactomedin-like protein 3	GAT-ATG-GTG-ACG-GAC-TGT-AGC
Olfml3 Rev		CTG-AAC-CAC-CAA-ACC-GCT-TC
Tmem119 For	Transmembrane Protein 119	ACC-CAG-AGC-TGG-TTC-CAT-AG
Tmem119 Rev		GAG-TGA-CAC-AGA-GTA-GGC-CA
Siglec-H For	Sialic acid binding Ig-like lectin H	TGC-TCT-GGG-TGC-TTA-AGT-GG
Siglec-H Rev		AAC-TCC-AGT-GTC-AGT-GAC-GG
Trem2 For	Triggering receptor expressed on myeloid cells 2	CTG-GAG-GAC-CCT-CTA-GAT-GAC
Trem2 Rev		CCA-CAG-GAT-GAA-ACC-TGC-CT
Iba1 For	Allograft inflammatory factor 1	AGC-TTT-TGG-ACT-GCT-GAA-GG
Iba1 Rev		CAG-CTC-TAG-GTG-GGT-CTT-GG
Htr2B For	5-hydroxytryptamine (serotonin) receptor 2B	GAA-GCC-ACA-GAA-GAC-AAG-CG
Htr2B Rev		GAT-TCA-GGC-TCT-CGA-AGA-TGG
ChaT For	Choline O-acetyltransferase	TAC-CTA-AGT-TGC-CAG-TGC-CC
ChaT Rev		CCC-CAA-ACC-GCT-TCA-CAA-TG
GFAP For	Glial fibrillary acidic protein	TCG-AGA-TCG-CCA-CCT-ACA-G
GFAP Rev		GTC-TGT-ACA-GGA-ATG-GTG-ATG-C
P2y12 For	Purinergic receptor P2Y, G-protein coupled 12	ACC-ACC-CCT-GTT-TTT-CCA-GTT
P2y12 Rev		AGC-CTT-GAG-TGT-TTC-TGT-AGG-G
Cx3cr1 For	Chemokine (C-X3-C motif) receptor 1	AGC-TCA-CGA-CTG-CCT-TCT-TC
Cx3cr1 Rev		GGT-TGT-TCA-TGG-AGT-TGG-CG
Ly6c1 For	Lymphocyte antigen 6 complex	ATC-TGT-GCA-GCC-CTT-CTC-TG
Ly6c1 Rev		GTA-GCA-CTG-CAG-TCC-CTG-AG
Tgfbeta1 For	Transforming growth factor, beta 1	ATG-CTA-AAG-AGG-TCA-CCC-GC
Tgfbeta1 Rev		TGC-TTC-CCG-AAT-GTC-TGA-CG
Tgfbeta1R For	Transforming growth factor receptor, beta 1	TGC-TGC-AAT-CAG-GAC-CAC-TG
Tgfbeta1R Rev		GGC-CAG-CTG-ACT-GCT-TTT-CT
HTR2B Hum For	Human 5-hydroxytryptamine (serotonin) receptor 2B, G protein-coupled	AGC-ACA-TTT-TGC-AGA-GCA-CC
HTR2B Hum Rev		GTG-CAG-TTT-ATT-TCC-CTG-TTC-CT

II. Publication #5

« Degeneration of serotonin neurons is necessary to elicit spasticity in amyotrophic lateral sclerosis»

Hajer El Oussini, Jelena Scekic-Zahirovic, **Pauline Vercruysse**, Stéphane Dieterlé, Gina Picchiarelli, Jérôme Sinniger, Caroline Rouaux & Luc Dupuis

--Manuscript in preparation--

Degeneration of serotonin neurons is necessary to elicit spasticity in amyotrophic lateral sclerosis

Hajer El Oussini[1,2], Jelena Scekic-Zahirovic[1,2], Pauline Vercruysse[1,2,3], Stéphane Dieterlé[1,2], Gina Picchiarelli[1,2], Jérôme Sinniger[1,2], Caroline Rouaux[1,2] & Luc Dupuis[1,2,*]

[1]INSERM UMR-S1118, faculté de médecine, Strasbourg, 67085 France.
[2]Université de Strasbourg, fédération de Médecine Translationnelle, Strasbourg, France.
[3]Department of Neurology, University of Ulm, Germany.

* Corresponding author: ldupuis@unistra.fr

Abstract

Amyotrophic lateral sclerosis (ALS) is characterized by the degeneration of both upper motor neurons (UMN), located in the motor cortex, and lower motor neurons in the brainstem and spinal cord. Degeneration of UMN is considered to constitute the primary cause of a number of symptoms, including spasticity, a painful symptom restricting everyday life, but participating in the maintenance a low level of motor function in impaired patients. Here we show that deleting the ALS-causing transgene selectively in brainstem serotonin neurons is sufficient to rescue the degeneration of this neuronal type and abolish spasticity. Consistently, this selective deletion worsened motor function and accelerated the onset of paralysis. These findings demonstrate that degeneration of serotonin neurons is necessary to trigger at least part of the typical symptoms commonly attributed to UMN loss. Thus the wide range of drugs targeting the serotonergic system could be useful to treat spasticity in ALS, and other neurodegenerative diseases characterized by spasticity.

Introduction

Spasticity occurs in a wide range of neurological diseases, including neurodegenerative diseases (*eg* amyotrophic lateral sclerosis, ALS or multiple sclerosis), genetic (*eg* hereditary spastic paraplegia), traumatic (*eg* spinal cord injury, SCI) or after stroke. Spasticity is characterized by involuntary muscle activity, and includes hyper-reflexia, muscles spasms, clonus and co-contraction of antagonist muscles [1-3]. Spasticity is a painful symptom and can severely restrict everyday life, but might also participate in maintaining a low level of motor function in severely impaired patients.

A number of mechanisms have been shown to participate in the development of spasticity after spinal cord injury. First, hyperreflexia might arise from increased synaptic input to motor neurons caused by remodeling of spinal pathways involving sensory afferents (Ia, Ib) or Renshaw cells [2,3]. Second, increased excitability of motor neurons themselves is able to lead to more sustained contractions in response to a sensory stimulus after SCI [2,4-6]. Such SCI-induced motor neuron hyperexcitability has been postulated to occur through BDNF-dependent downregulation of KCC2, a potassium-chloride co-transporter responsible for chloride extrusion in adult neurons [7]. Indeed BDNF application reverted both hyperreflexia and KCC2 downregulation after SCI in mice [7]. Alternatively, motor neuron hyperexcitability could be a late consequence of the deprivation of monoaminergic input to the motor neuron. Ligand-independent activity of serotonin (5-HT2B/C) and norepinephrine (alpha1) receptors could indeed be responsible for the development of spastic long lasting reflexes [8-11] and the maintenance of locomotion after partial SCI [8,12]. The sequence of events, as well as their relative importance in the development of spasticity remain however elusive.

Spasticity also occurs in amyotrophic lateral sclerosis, yet, contrary to SCI, ALS-associated spasticity has been barely studied. Spasticity in ALS is paradigmatically considered to result from the degeneration of upper motor neurons themselves [13,14]. Upper motor neurons (UMNs) are glutamatergic neurons located in layer V of motor cortex, project to spinal motor neurons through the corticospinal tract, and are the major source of descending motor commands for voluntary movement [15]. While there is a general consensus to attribute the development of spasticity to UMN degeneration in ALS, this specific question has, to our knowledge, not been addressed experimentally. Indeed, our recent work has shown that brainstem serotonin neurons degenerate in ALS mouse models and in ALS patients, and inverse agonists of the 5-$HT_{2B/C}$

receptors were potently anti-spastic in ALS mice [16]. This raised the possibility that degeneration of serotonin neurons could, at least in part, be involved in the development of ALS-associated spasticity. In this study, we took advantage of the existence of a conditional mouse model of ALS [17] to investigate the role of serotonin neurons in ALS-related spasticity. The selective rescue of serotonin neurons abolished the development of spasticity in this mouse model. These findings demonstrate that a large part of the typical symptoms attributed to UMN degeneration in ALS are in fact caused by the degeneration of another neuronal type, widely accessible to pharmacological intervention.

Results

Targeting mutant SOD1 expression in adult serotonergic neurons

To determine the role of serotonergic neurons in ALS, we used floxed SOD1(G37R) mice, that express the ALS-linked G37R mutation in the human SOD1 gene that can be excised through CRE-mediated recombination [17]. These mice have been widely used to determine the respective roles of motor neurons, microglia, astrocytes or oligodendrocytes in ALS phenotypes[17-21]. SOD1(G37R) mice were crossed with transgenic mice expressing CRE-ERT2 upon control of the Tph2 promoter (Tph2-CRE mice). SOD1(G37R) mice carrying the Tph2-CRE transgene are denoted as $G37R^{\Delta Tph2}$ mice, whereas littermate SOD1(G37R) mice without the Tph2-CRE transgene are denoted as G37R mice. Crossing Tph2-CRE mice with Rosa26 STOP YFP (YFP CRE reporter) mice, that express YFP only after CRE mediated recombination, led to robust YFP immunoreactivity after 5 days of tamoxifen treatment in virtually all Tph2 positive neurons in the brainstem (Figure 1a and Figure S1a). Contrastingly, YFP was not detected in cholinergic neurons (Figure S1b) nor in microglial cells (Figure S1b), showing that CRE activity was restricted to serotonin neurons in Tph2-CRE mice. Expression of SOD1(G37R) was decreased in microdissected raphe magnus nucleus but not in cortex or cerebellum of $G37R^{\Delta Tph2}$ mice as compared with littermate G37R mice (Figure 1b). Importantly, a subset of serotonin neurons developed large aggregates positive to human SOD1 in G37R mice, but such aggregates were not observed in $G37R^{\Delta Tph2}$ serotonin neurons, although they were readily detectable in neighbouring cells (Figure 1c). Thus, our data are consistent with a selective rescue of mutant SOD1 expression in adult serotonergic neurons of $G37R^{\Delta Tph2}$ mice.

Serotonin neuron degeneration is cell autonomous in SOD1(G37R) mice

We first asked whether rescue of mutant SOD1 expression in serotonergic neurons was sufficient to rescue serotonin neurons themselves. To this aim, we performed Tph2 immunohistochemistry in endstage $G37R^{\Delta Tph2}$ mice and littermate G37R mice (Figure 2a). Consistent with previous results, we observed that Tph2 positive neurons displayed atrophy of the cell body in the dorsal raphe and median raphe nuclei of G37R mice (Figure 2b). This atrophy was entirely reverted in $G37R^{\Delta Tph2}$ mice (Figure 2b). Tph2 immunoreactivity was generally weaker in G37R mice, as compared with $G37R^{\Delta Tph2}$ mice, as observed also using immunofluorescence (Figure 1c). We further studied the morphology of a major serotonergic tract, located in the arcuate nucleus of the hypothalamus (Figure 1d). This serotonergic tract was strongly

degenerating in G37R mice, similar to what previously observed in SOD1(G86R) mice [22], and mostly preserved in G37R$^{\Delta Tph2}$ mice (Figure 1d-e). Thus, rescuing mutant SOD1 expression in serotonergic neurons prevents their degeneration.

Rescuing serotonin neurons eliminates spasticity

Spasticity is a major symptom of ALS, and previous evidence suggested that spasticity associated with ALS was caused by constitutive activity of 5-HT$_{2B}$/5-HT$_{2C}$ receptors. In mice, the development of spasticity is visually observed by spastic contractions of tail muscles at end stage. Tail spasticity was prominently observed in 10 out of 13 G37R mice at end stage, while, contrastingly, only 1 out of 11 G37R$^{\Delta Tph2}$ mice showed this phenotype (p=0.0013, Fisher's exact test; Figure 3a). To further quantify this effect, we measured long lasting reflex (LLR) using electromyography in awake mice at end stage. This quantitative method is correlated with spasticity after spinal cord injury, and allows to measure the biological effects of classical anti-spastic drugs [9,23]. We previously showed that 5-HT$_{2B}$/5-HT$_{2C}$ inverse agonists, such as SB206553 (later referred as SB206), are able to completely block existing LLRs, suggesting their anti-spastic potential [16]. We observed that while robust LLRs are observed in end-stage G37R mice and blocked by SB206 application, such LLRs did not develop in G37R$^{\Delta Tph2}$ mice (Figure 3b, and 3c-d for quantification). Thus the degeneration of serotonin neurons is necessary to trigger spasticity in mutant SOD1 mice.

Rescuing serotonin neurons hastens onset of paralysis and worsens motor neuron atrophy

Spasticity is thought to represent a compensatory mechanism activated by motorneurons enabling to maintain their function despite loss of excitatory input. Consistent with this, the absence of spasticity in G37R$^{\Delta Tph2}$ mice was associated with worsened grip strength (Figure 4a), and with earlier onset of paralysis (Figure 4b). Indeed, G37R$^{\Delta Tph2}$ mice displayed earlier age at onset of motor symptoms (Figure 4c), but reached end stage at similar ages than G37R mice, leading to increased disease duration (Figure 4c-d). G37R$^{\Delta Tph2}$ mice displayed similar loss in motor neurons at end stage (Figure 4e-f), but motor neuron atrophy was much more pronounced (Figure 4g). Importantly, astrocytosis and microgliosis appeared normally activated in G37R$^{\Delta Tph2}$ spinal cord (Figure S2), suggesting that the most deleterious effects of rescuing spasticity were on motor neurons.

Thus, rescuing serotonin neurons accelerates disease progression and worsens motor neuron function.

Discussion

Our current study demonstrates that the degeneration of brainstem serotonin neurons is responsible for the development of spasticity in ALS mice, and that spasticity compensates for motor deficits allowing the maintenance of motor function after disease onset. These findings have important consequences for our understanding of ALS pathophysiology and management, as well as for all the diseases involving spasticity.

A first major result of the current study is that degeneration of serotonin neurons is cell autonomous in ALS. This is demonstrated by the rescue of serotonin neurons observed upon deletion of the mutant SOD1 transgene in adult serotonergic neurons. To this aim, we used a conditional CRE transgene that allowed the rescue in adult mice, thereby avoiding the potential confounding developmental effects. Multiple indexes of serotonin neuron degeneration were rescued in G37R$^{\Delta Tph2}$ mice, including decreased TPH2 immunoreactivity, decreased size of cell bodies and occurence of degenerating serotonergic fibers. This cell autonomous nature of serotonin neuron degeneration contrasts with the situation observed in motor neurons in which the local environment appears critical [17,18,24,25]. Such a difference could be due to intrinsic properties of serotonergic neurons. Indeed, we observed very few SOD1 positive aggregates in Tph2 neurons, contrasting with other cell types that accumulated large amounts of aggregated SOD1. This is consistent with our previous observation of a lack of TDP43 aggregates in serotonergic neurons of ALS patients [16] and suggests that serotonin neurons display distinct mechanisms of clearance of aggregate prone proteins than other neuronal types. Our demonstration of the cell autonomous nature of serotonergic neuron degeneration in ALS opens the way for studying mechanisms of degeneration in cultured serotonergic neurons, in particular in transdifferentiated serotonergic neurons of ALS patients, using protocols recently published [26,27].

The selective rescue of serotonin neurons in G37R$^{\Delta Tph2}$ mice allowed us to identify the primary consequences of this degeneration. Interestingly, and despite the important roles of serotonin neurons in multiple brain functions, many phenotypes developed by G37R mice were not affected. For instance, the rescue of serotonin neurons did not modify the extent of motor neuron degeneration, of astrocytosis or microgliosis. Despite the well documented role of serotonin in food intake and energy homeostasis, body weight was only affected in female but not male G37R$^{\Delta Tph2}$ mice. As a consequence, survival of G37R$^{\Delta Tph2}$ mice was not significantly different from G37R mice. It is important to mention that we performed the rescue

of serotonin neurons in adults, and alterations in motor neuron excitability and locomotor rythms, presumably serotonin dependent, were documented in embryonic or perinatal mice in others mutant SOD1 mice [28-31]. Thus, we cannot completely exclude that early, embryonic alterations in serotonin neurons contribute to other aspects of ALS pathogenesis. Last, mutant SOD1 mice, like SOD1 ALS patients, do not exhibit frontal symptoms, and our current study was thus not able to determine whether degeneration of serotonin neurons could be related with frontal symptoms in ALS and FTD. Indeed, serotonin neurons are deeply involved in the regulation of mood, social behaviour or executive functions [32-34], that could all potentially be impaired during frontal symptoms of ALS or during FTD. Thus further studies are required to study the role of serotonin neurons in frontal lobe related symptoms.

The major consequence of the rescue of serotonin neurons in G37R$^{\Delta Tph2}$ mice was a complete absence of spasticity. This was obvious from visual inspection of tail spasticity and quantified using electrophysiological characterization of long lasting reflexes in the tail muscles, a well documented measure of spasticity in rodents [8,35]. We observed that G37R$^{\Delta Tph2}$ mice developed earlier paralysis onset, associated with decreased muscle strength. This is in perfect agreement with the lack of spasticity in these mice as spasticity allows some compensatory rescue of motor function. In SCI models, similar worsening of motor function was observed after pharmacological ablation of spasticity [8,12]. It was already known that serotonergic signaling was critical in the development of ALS muscle spasms as 5-HT$_{2B/2C}$ inverse agonists are able to abolish muscle spasms [16], yet it was unclear whether the degeneration of serotonin neurons themselves was required to elicit spasticity. Indeed, spasticity in ALS is paradigmatically associated with degeneration of upper motor neurons, that are located in the motor cortex and fine tune the motor activity. Spasticity is indeed a cardinal symptom of the so-called “UMN syndrome”, presumably caused by UMN loss, and development of UMN syndrome is central to the diagnosis of ALS [13,14]. Our current data establish that this direct connection between UMN loss and spasticity is wrong, and that degeneration of serotonin neurons is essential in triggering spasticity in ALS. It is important to mention that this does not rule out that UMN loss contribute to spasticity or other symptoms of ALS, but this would have to be specifically studied using other CRE drivers.

Our model system will allow to dissect out the hierarchy of events leading to spasticity downstream of serotonin. Indeed, it will be interesting to determine whether increased mRNA levels of 5-HT$_{2B}$ receptor [16,36]

and/or altered editing of the mRNA encoding the 5-HT_{2C} receptor [8,16] return to baseline wild type levels in $G37R^{\Delta Tph2}$ mice. In spinal cord injury, spasticity has been found to involve a number of signaling mechanisms such as downregulation of the sodium/chloride transporter KCC2 [7] or the calpain-dependent cleavage of voltage gated channels [6]. Whether these mechanisms occur during ALS and are downstream of serotonin loss remains an open question.

Summarizing, our current study demonstrate that the classical view of spasticity arising from UMN loss in ALS is, at best, incomplete. The demonstration that the degeneration of serotonin neurons is necessary to elicit spasticity suggests that anti-spastic strategies should focus on the serotonergic drugs widely available to improve the treatment of this painful symptom. Multiple neurological diseases are associated with spasticity, and our current results might thus be of critical importance for treating spasticity in diseases as diverse as spinal cord injury, hereditary spastic paraplegia or ALS.

Materials and methods

Animals

Transgenic mice were housed in the animal facility of the medicine faculty of Strasbourg University, with 12h/12h of light/dark and unrestricted access to food and water. In all experiments, littermates were used for comparison. Transgenic mice carrying a floxed SOD1 G37R human transgene on a C57BL/6 background were kindly provided by Dr Don W. Cleveland[17]. As described previously, these mice carry a 12 kb genomic DNA fragment encoding the human SOD1(G37R) transgene, under its endogenous promoter, flanked by LoxP sequences and were used as heterozygous, with their non-transgenic littermates as controls. Onset of symptoms was defined according to previous studies [17]. Tph2-iCreER (referred to as Tph2 CRE) transgenic mice (Jax strain #016854) expressing a tamoxifen-inducible Cre recombinase under the control of mouse *Tph2* promoter were genotyped with their non-transgenic littermates on a C57BL/6 background. YFP CRE reporter mice were R26-stop-EYFP mice (Jax strain #006148) carrying a loxP-flanked STOP sequence followed by the Enhanced Yellow Fluorescent Protein gene (EYFP) inserted into the Gt(ROSA)26Sor locus. All animal experimentation was performed in accordance with institutional guidelines, and protocols were approved by the local ethical committee from Strasbourg University (CREMEAS) under number AL/29/36/02/13 in accordance with European regulations.

Mouse breeding, survival and motor phenotyping

SOD1 (G37R) mice were crossed with Tph2 CRE mice to obtain double transgenic mice in F1. At 56 days of age 100μL of tamoxifen/corn oil solution at a dose of 75 mg/kg body weight was administrered through oral gavage every day during 5 consecutive days on all mice. Mice single transgenic for the SOD1 (G37R) transgene (G37R, n=14) were compared with littermate double transgenic mice carrying both SOD1 (G37R) transgene and Tph2 CRE transgene ($G37R^{\Delta Tph2}$, n=15). Mice negative for SOD1 (G37R) transgene were used as controls (Wt, n=15).

Mice were visually inspected daily and weekly monitored for body weight and motor symptoms from two months of age until end stage of the disease. To evaluate muscle strength, we used a gripmeter test (Bioseb, ALG01; France). The muscle force (in Newton) was measured three times per mouse. Results are the mean of two weeks sessions. Disease course and survival were assessed daily by visual inspection. Disease onset was calculated as time of peak of body weight. Disease duration was the time between the

peak of body weight and death. After disease onset mice were followed daily and end stage was defined by full paralysis and when mice were unable to return after 10 seconds placed on the back. End stage mice were immediately euthanized.

Histological techniques

Spinal cords and brains were dissected and fixed by immersion in 4% paraformaldehyde in 0.1 M phosphate buffer pH 7.4 overnight.

The lumbar parts of spinal cords were dissected and the L3-L5 region was identified according to previous studies (Harrison *et al.*, 2013). Tissue was cryoprotected in 30% sucrose and snaps frozen in melting isopropanol in TissueTek (O.C.T.Compound, SAKURA#4583). Cryosections (Leica CM 3050S) of 16μm were obtained for histological analysis of end stage mice (10 sections per animal). Spinal cord and brains sections were incubated in phosphate buffered saline (PBS) 0.1% Triton with anti-choline acetyl transferase (ChAT) (Millipore, AB144-P; diluted 1:50) for motor neuron, Tph2 (Abcam; ab121013; diluted 1:500, human SOD1 (Abcam, ab52950; diluted 1:100) and for glial cells anti-Iba1 (Abcam; ab5076, 1:100), GFAP (Dakocytomation; Z0334; diluted 1:500) antibodies followed by biotinylated species-specific secondary antibody. The staining was revealed using the ABC kit (Vectastain), by the avidin-biotin complex immunoperoxidase technique or using fluorescent secondary antibodies for immunofluorescence.

Single-layer images or Z-Stack images (1μm optical section) were acquired using a laser-scanning microscope (confocal Leica SP5 Leica Microsystems CMS GmbH) equipped with 63× oil objective (NA1.4). Excitation wavelengths were sequentially argon laser 488nm, diode 561nm, and helium neon laser 633nm. Emission bandwidths are 500-550nm for Alexa488, 570-620nm for Alexa594, and 650-750nm for draq5.

Quantification of motor neurons in mice spinal cord

Motoneuron counting was performed in L3-L5 ventral horn in every tenth section for ten sections in total per animal (160 μm thick in total, spread over 1.6 mm). Only ChAT+ neurons located in a position congruent with that of motoneuron groups were counted [37]. All $ChAT^+$ profiles located in the ventral horns of immunostained sections and clearly displayed in the plane of section were counted. Total estimated motoneuron numbers were obtained using a computer-assisted microscope (Nikon Eclipse E800) and associated software (Nis Elements version 4.0). Total numbers of motoneurons and the mean area of individual cells were obtained using ImageJ freeware (http://rsbweb.nih.gov/ij/) after image acquisition at 20X

under the same exposition parameters with a digital camera (Nikon Digital Sight DS-U3). The observer was blinded to the genotype of studied mice.

Quantification of Iba1 and GFAP in mice spinal cord

For staining of microglia and astrocytes, measurement of Iba1 and GFAP immunoreactivity was performed on images acquired from Iba1/GFAP immunostaining at 10x magnification. A standardized rectangle was drawn in the ventral horn and the surface of staining relative to background was calculated using the Pixel classifier algorithm of Nikon Nis-element 3.10 SP3 software, using the intensity profile measurement function. The observer was blinded to the genotype of studied mice. >10 images per animal were quantified, with n=5 animals per genotype.

Quantification of Tph2 positive neurons in mice brain

For Tph2 positive neurons quantification in the brainstem we used the technics previously described [16]. At least three sections per region were selected and anatomically matched. We selected sections encomprising raphe dorsal, median raphe and raphe magnus nuclei according to Paxinos Atlas. Acquired image at 20X under the same exposition parameters with a digital camera (Nikon Digital Sight DS-U3) were taken in specific regions. Total mean area of individual cells was obtained using ImageJ freeware (http://rsbweb.nih.gov/ij/).

For quantification of axonal density in the brain, staining was processed to binary images using NIH ImageJ as described previously [38]. After changing tiff images to 8-bit images, images were inverted and processed with Feature J plugin for ImageJ (version 1.50d) to select the smallest Hessian values and « smoothing scale » of 1.0. The resulting images were transformed into binary images by thresholding. Threshold was determined on one cut of a WT animal and same threshold was applied to every image. The intensity of white pixel, referring to the axonal staining, and black pixel, referring to the, background is measured.

Real–time quantitative polymerase chain reaction

Total RNA was extracted from the spinal cord of end stage mice using TRIzol (Invitrogen). RNA was reverse transcribed using 1μg of RNA and the iScript cDNA synthesis kit (BioRad). We performed real-time PCR using IQ SYBR green Supermix (BioRad) and data were normalized with GeNorm software [39]. Two

standard genes (Tata-box binding protein, and RNA polymerase 2 subunit). Quantitative PCR was performed on a CFX96 Real-time System (BioRad) using iQ SYBR Green supermix (BioRad). Relative mRNA levels were calculated with BioRad CFX Manager 3.1 using $\Delta\Delta C_t$ method.

Electromyographical evaluation of tail spasticity

Long lasting reflex (LLR) was determined and quantitated as previously described [16]. Briefly, tail muscle spasticity was performed with percutaneous EMG wires inserted in segmental tail muscles as described for rats [35]. Paralyzed mice were kept in a chamber during the recording with the tail free to move. During EMG recording, muscle spasms were evoked with mechanical stimulation of the tail. EMG was sampled at 5 kHz (0.2mv/1s per div). For quantification, we measured LLR signal-to noise ratio intensity by a standardized rectangle that was drawn before and after (>1s) mechanical stimulation. The signal intensity ratio relative to background was calculated using the Pixel classifier algorithm of Nikon Nis-element 3.10 SP3 software, using the intensity profile measurement function. The raw signal was obtained by deducing the noise before mechanical stimulation. 3 EMG signal recordings per animal were quantified, with n=12 animals per genotype. For signal processing only positive amplitude values were analyzed. Maximal amplitude threshold measurements were obtained from LLR signal upon mechanical stimulation. For each EMG signal recording the maximum amplitude of LLR was determined.

Statistical analysis

All data are presented as mean ± standard error of the mean. Analysis was performed using Prism6 (Graph Pad software). All difference were considered significant at $p<0.05$. For the comparison of discrete values for two groups was performed using student's T test. For the comparison of discrete values for more than two groups was performed using ordinary one-way ANOVA followed Tukey's post hoc test. For survival and disease onset analysis, animals were evaluated using Log rank (Mantel Cox) test. For repeated measurement, a repeated measure two-way ANOVA was performed to test the effect of age and the genotype (Figure).

Figure and figure legends

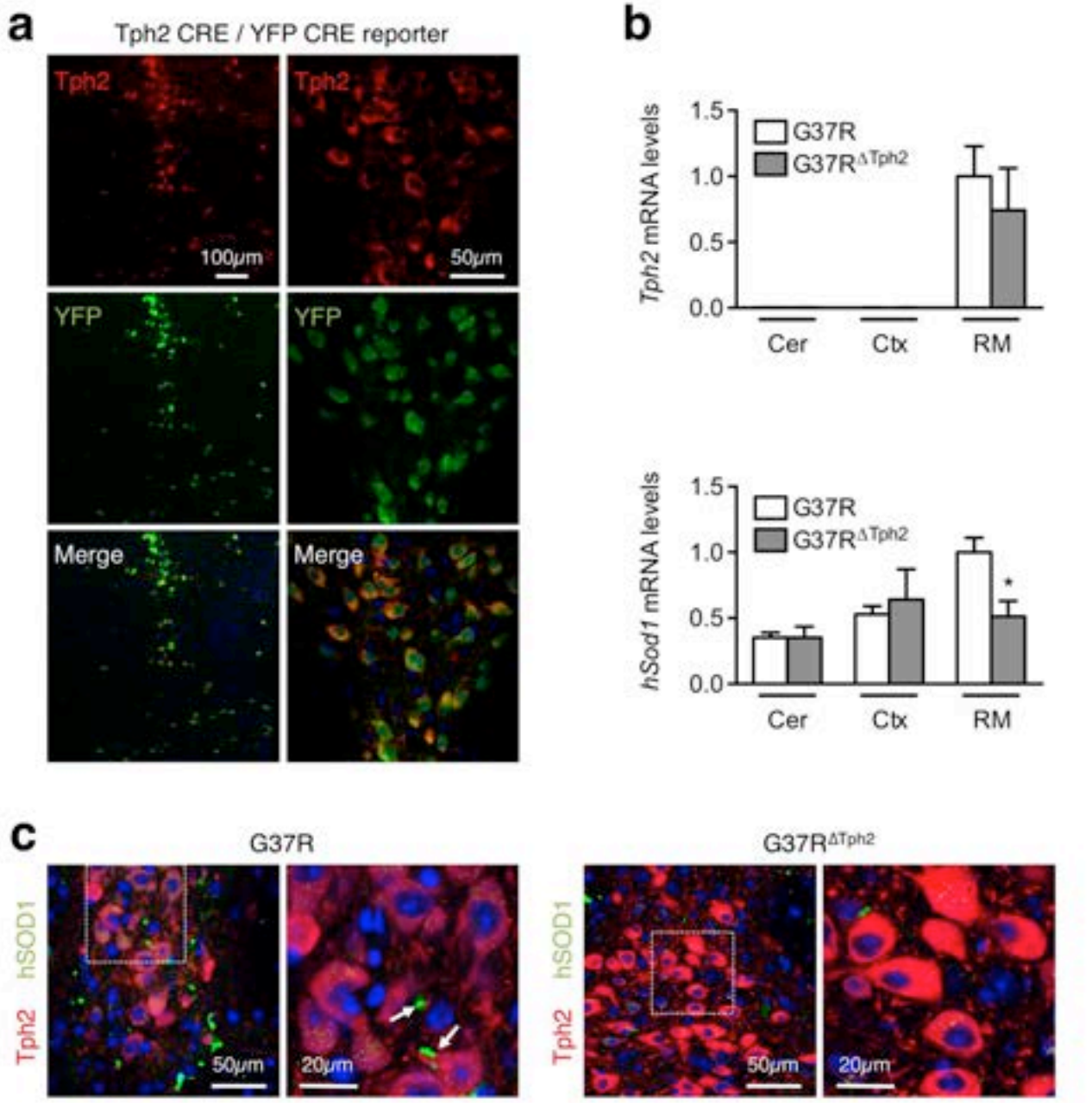

Figure 1: Efficient recombination in in adult serotoninergic neurons.

(a) Representative confocal image of serotoninergic neurons labeled with Tph2 antibody (red) and YFP (CRE reporter, green) in mice doubly transgenic for Tph2-Cre and YFP Cre reporter alleles. N=5 mice treated with Tamoxifen at 56 days of age and sacrificed one month after gavage. We observed a complete overlap between Tph2 and YFP immunoreactivities.

(b) mRNA levels of *Tph2* (upper panel) and human SOD1 (*hSOD1,* lower panel*)* in micro dissected cerebellum, cortex and raphe magnus of G37R (n=5-7) and G37R$^{\Delta Tph2}$ (n=3-6) mice one month after recombination induction. * $p<0.05$ Student's t test. Note that *Tph2* mRNA is only detected in raphe magnus, and *hSOD1* expression is selectively decreased in the raphe magnus of G37R$^{\Delta Tph2}$ mice

(c) Representative confocal image of Tph2 (red) and human SOD1 (green) immunoreactivities in G37R and G37R$^{\Delta Tph2}$ end stage mice. N=5 for all genotypes. Note the presence of bright hSOD1 positive aggregates (arrows) in G37R serotonergic neurons, but not in G37R$^{\Delta Tph2}$ serotonergic nuclei.

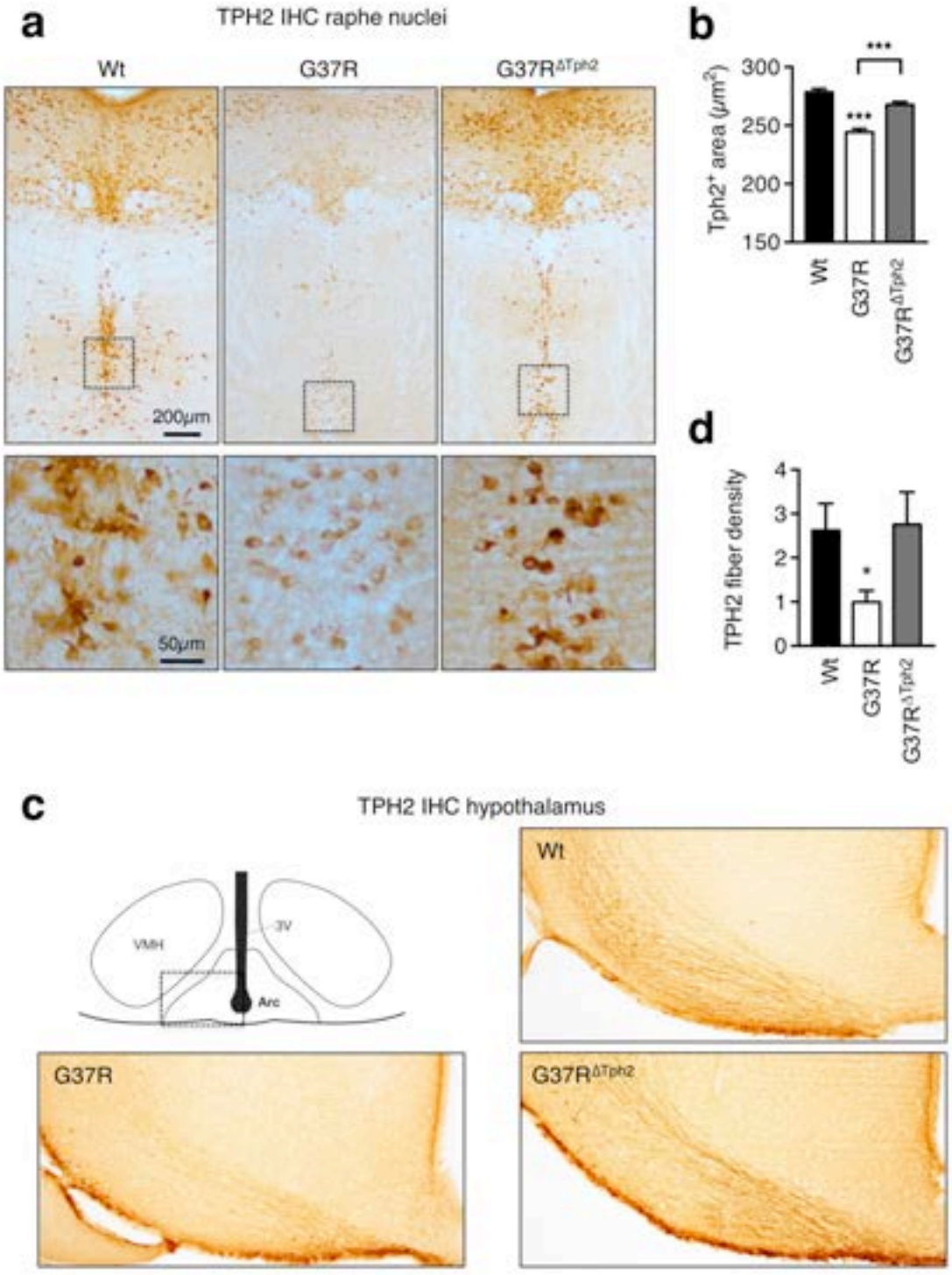

Figure 2: Serotoninergic neurons degeneration is cell autonomous in SOD1G37R mice.
(a) Representative Tph2 immunoreactivity in the brainstem (dorsal and median raphe) of Wt, G37R and G37R$^{\Delta Tph2}$ end stage mice. N=5 for all genotypes. Note that Tph2 immunoreactivity is weaker in G37R serotonergic neurons than in G37R$^{\Delta Tph2}$ serotonergic neurons.
(b) Mean area of Tph2 positive neurons in Wt (black columns), G37R (white columns) and G37R$^{\Delta Tph2}$ (grey columns) end stage mice. *** $p<0.001$ vs wild type, one way ANOVA. N=5 for all genotypes, N=4 brainstem sections/animal.
(c) Representative Tph2 immunoreactivity in the hypothalamus of of Wt, G37R and G37R$^{\Delta Tph2}$ end stage mice. A major serotonergic tract is visible in the arcuate nucleus of wild type and G37R$^{\Delta Tph2}$ mice, but almost absent in G37R mice. A scheme depicting the location of the picture is provided. *, $p<0.05$ in one way ANOVA

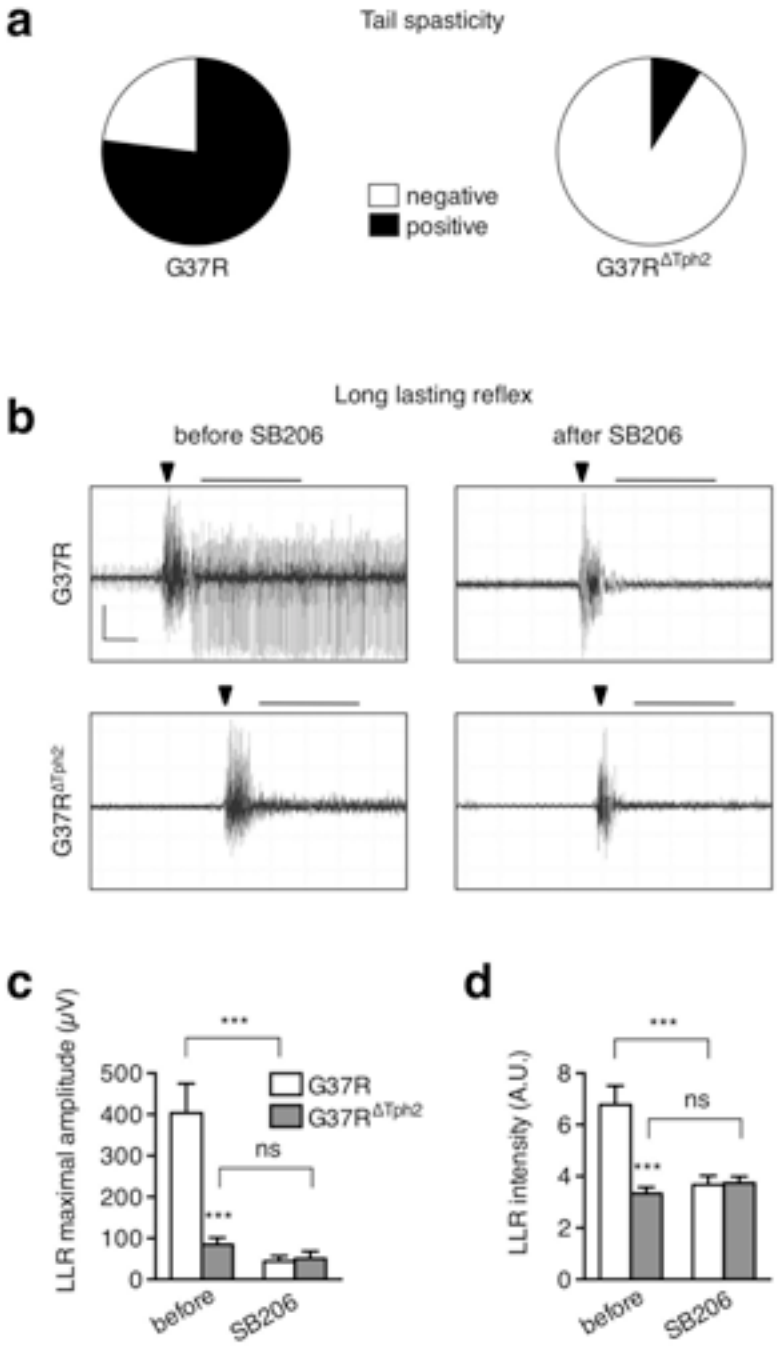

Figure 3: Rescuing serotonin neurons eliminates spasticity.

(a) Frequency of tail spasticity in G37R and G37R$^{\Delta Tph2}$ end stage mice as recorded from visual inspection.

(b) Representative recordings of long-lasting reflex (LLR) using tail EMG in G37R and G37R$^{\Delta Tph2}$ end stage mice. Recordings panel presented before and 5 minutes after SB206553 injection.

(**c-d)** Quantitative analysis of maximal LLR amplitude (μV) (c) and mean LLR signal intensity (d, A.U.) in tail EMG per animal before and 5 minutes after injection. G37R (white columns n=15); G37R$^{\Delta Tph2}$ (grey columns n=12) end stage mice. ***p<0.001 vs wild type, one way ANOVA followed by Tukey post hoc test.

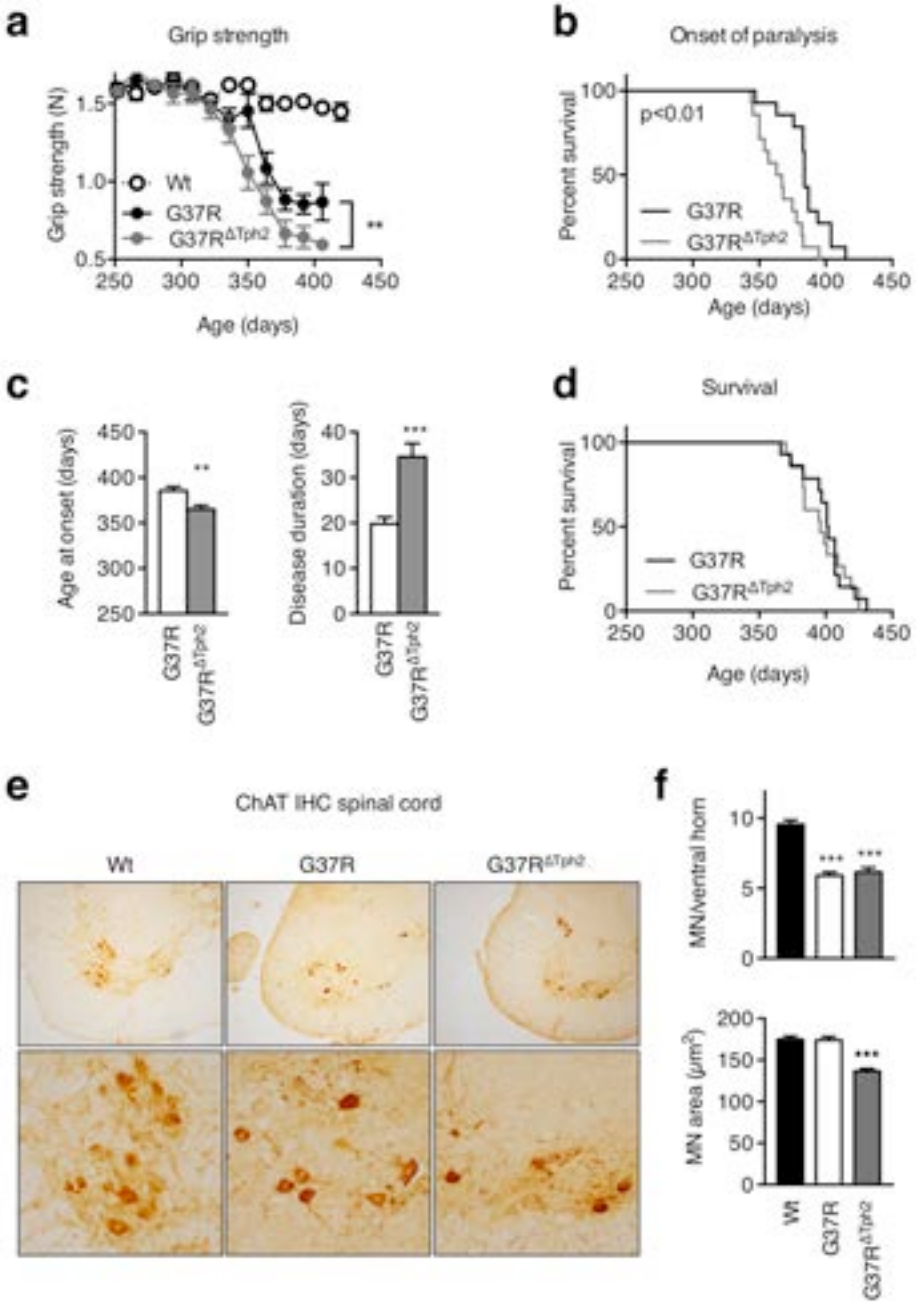

Figure 4: Rescuing serotonin neurons hastens onset of paralysis and worsens motor neuron atrophy.

(a) Muscle grip strength (Newton) curves in Wt, G37R and G37R$^{\Delta Tph2}$ mice. N=10-15 mice per genotype. **p<0.005 for genotypes between G37R and G37R$^{\Delta Tph2}$ mice, repeated two way ANOVA.

(b-d) Kaplan-Meier plot of onset of paralysis (b) and survival (d) in G37R (in black n=14) and G37R$^{\Delta Tph2}$ (in grey n=14). Representative histograms of age at disease onset (from birth to the peak of weight) and disease duration (from peak of weight to death) in G37R (white columns n=13) and G37R$^{\Delta Tph2}$ (grey columns n=11) are shown in (c). ** p<0.001, *** p<0.0001 unpaired Student's t test. Log rank test (Mantel cox) for onset of paralysis: p=0.0014; Log rank test (Mantel cox) for survival: p=0.7.

(e) Representative ChAT immunohistochemistry images in Wt, G37R and G37R$^{\Delta Tph2}$ mice. Two magnifications are shown. *N* = 5 for all genotypes.

(f) Motor neuron mean numbers and area in Wt (*black columns*), G37R (white columns) and G37R$^{\Delta Tph2}$ (grey columns) mice. ***$p < 0.001$ vs wild type, One way ANOVA followed by Tukey post hoc test. *N* = 5 and 2 section per animal for all genotypes.

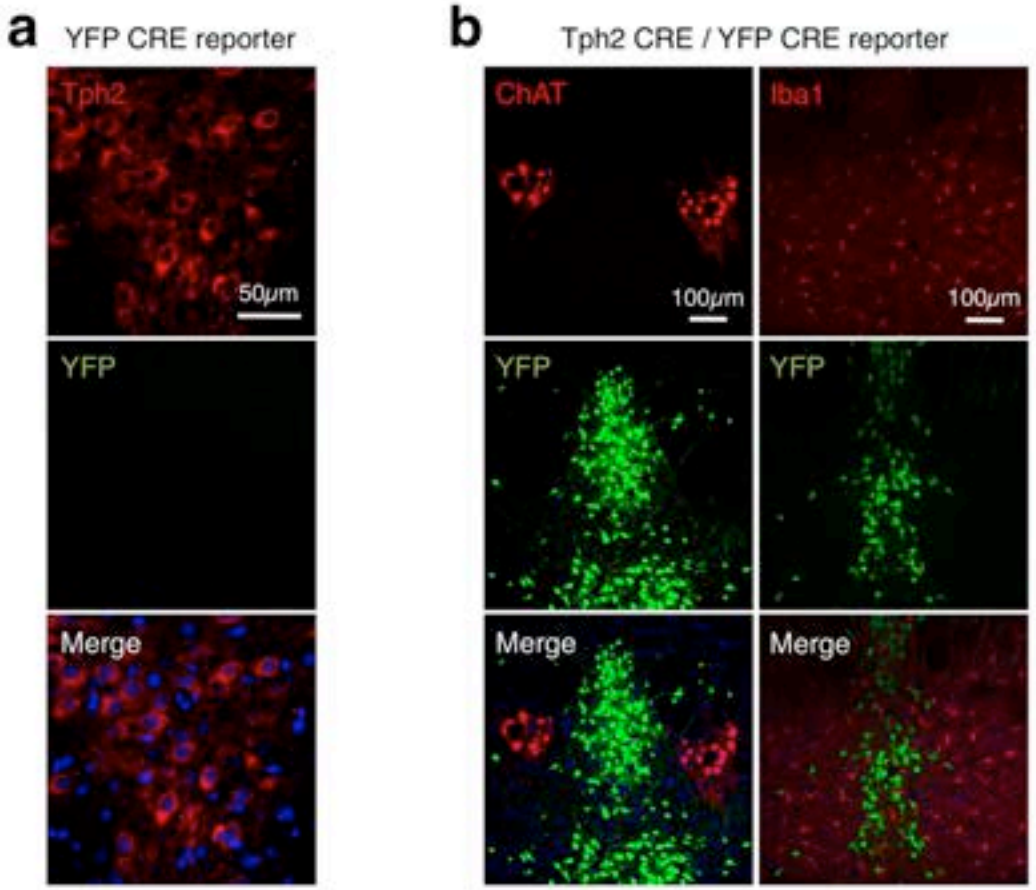

Figure S1: supplementary controls for selectivity of recombination in adult serotoninergic neurons.
(a) Representative confocal image of serotoninergic neurons labeled with Tph2 antibody (red) and YFP (CRE reporter, green) in mice single transgenic for YFP Cre reporter alleles. N=3 mice treated with Tamoxifen at 56 days of age and sacrificed one month after gavage. No leakage of YFP expression is observed
(b) Representative confocal image of cholinergic neurons labeled with Chat antibody (red, left column) or of microglia labeled with Iba1 antibody (red, right column) and YFP (CRE reporter, green) in mice doubly transgenic for Tph2-Cre and YFP Cre reporter alleles. N=5 mice treated with Tamoxifen at 56 days of age and sacrificed one month after gavage. All YFP positive cells lack ChAT or Iba1 staining.

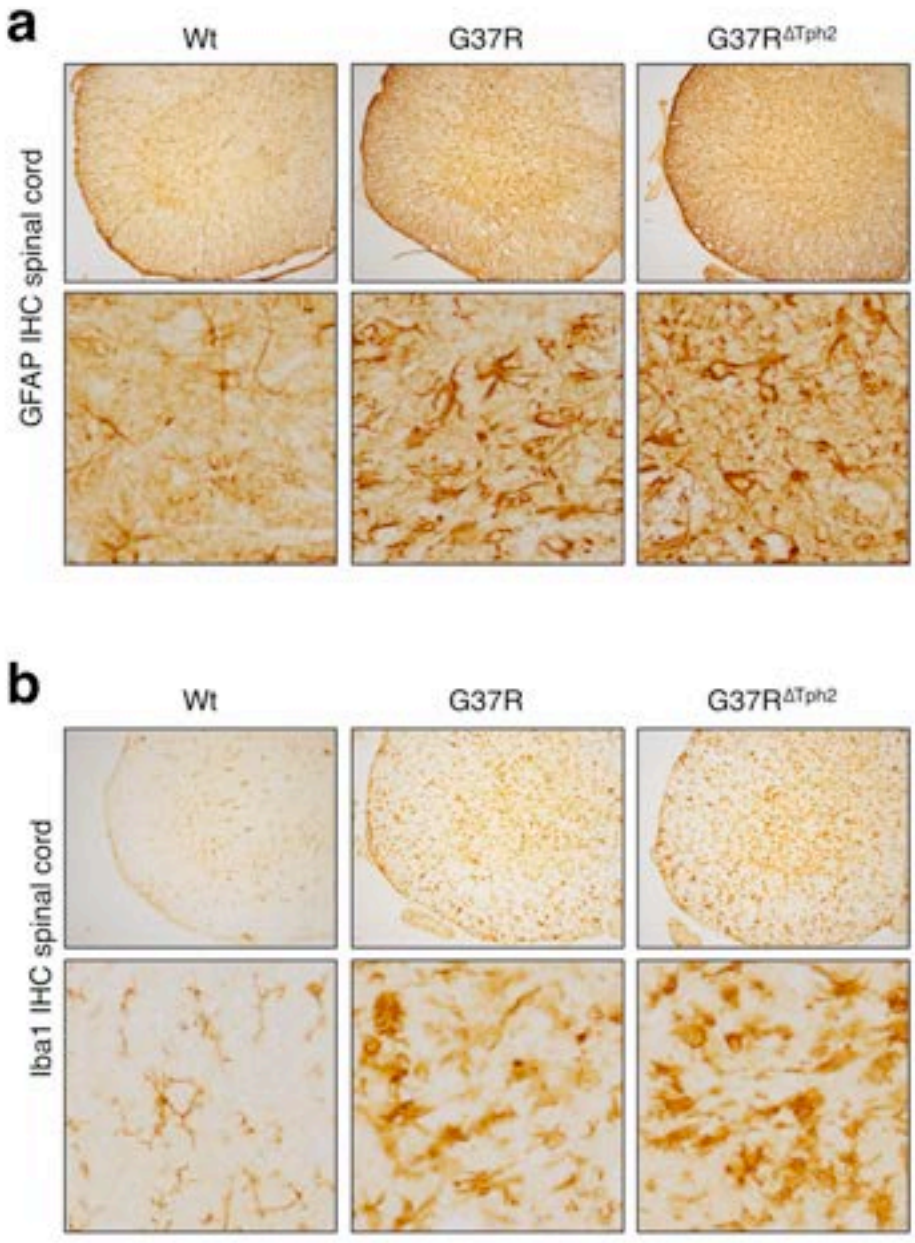

Figure S2: Rescuing serotonin neurons does not modify astrocytosis or microgliosis

(a) Representative GFAP immunohistochemistry images in Wt, G37R and G37R$^{\Delta Tph2}$ mice. Two magnifications are shown. *N* = 5 for all genotypes. Expression of human SOD1 leads to strong astrocytosis, independently of the presence of a Tph2-CRE allele.

(b) Representative Iba immunohistochemistry images in Wt, G37R and G37R$^{\Delta Tph2}$ mice. Two magnifications are shown. *N* = 5 for all genotypes. Expression of human SOD1 leads to strong microgliosis, independently of the presence of a Tph2-CRE allele.

References

1. Lance, J.W. Symposium synopsis. in *Spasticity: Disordered Motor Control* (eds Feldman, R.G., Young, R.R. & Koella, W.P.) 485-494 (Year Book Medical Publisher, Chicago, 1980).
2. Nielsen, J.B., Crone, C. & Hultborn, H. The spinal pathophysiology of spasticity--from a basic science point of view. *Acta Physiol (Oxf)* **189**, 171-80 (2007).
3. D'Amico, J.M., Condliffe, E.G., Martins, K.J., Bennett, D.J. & Gorassini, M.A. Recovery of neuronal and network excitability after spinal cord injury and implications for spasticity. *Front Integr Neurosci* **8**, 36 (2014).
4. Gorassini, M.A., Knash, M.E., Harvey, P.J., Bennett, D.J. & Yang, J.F. Role of motoneurons in the generation of muscle spasms after spinal cord injury. *Brain* **127**, 2247-58 (2004).
5. Norton, J.A., Bennett, D.J., Knash, M.E., Murray, K.C. & Gorassini, M.A. Changes in sensory-evoked synaptic activation of motoneurons after spinal cord injury in man. *Brain* **131**, 1478-91 (2008).
6. Brocard, C. *et al.* Cleavage of Na channels by calpain increases persistent Na current and promotes spasticity after spinal cord injury. *Nat Med* (2016).
7. Boulenguez, P. *et al.* Down-regulation of the potassium-chloride cotransporter KCC2 contributes to spasticity after spinal cord injury. *Nat Med* **16**, 302-7 (2010).
8. Murray, K.C. *et al.* Recovery of motoneuron and locomotor function after spinal cord injury depends on constitutive activity in 5-HT2C receptors. *Nat Med* **16**, 694-700 (2010).
9. Rank, M.M. *et al.* Adrenergic receptors modulate motoneuron excitability, sensory synaptic transmission and muscle spasms after chronic spinal cord injury. *J Neurophysiol* **105**, 410-22 (2011).
10. Murray, K.C., Stephens, M.J., Ballou, E.W., Heckman, C.J. & Bennett, D.J. Motoneuron excitability and muscle spasms are regulated by 5-HT2B and 5-HT2C receptor activity. *J Neurophysiol* **105**, 731-48 (2011).
11. D'Amico, J.M. *et al.* Constitutively active 5-HT2/alpha1 receptors facilitate muscle spasms after human spinal cord injury. *J Neurophysiol* **109**, 1473-84 (2013).
12. Fouad, K. *et al.* Locomotion after spinal cord injury depends on constitutive activity in serotonin receptors. *J Neurophysiol* **104**, 2975-84 (2010).
13. Swinnen, B. & Robberecht, W. The phenotypic variability of amyotrophic lateral sclerosis. *Nat Rev Neurol* **10**, 661-70 (2014).
14. Kiernan, M.C. *et al.* Amyotrophic lateral sclerosis. *Lancet* **377**, 942-55 (2011).
15. Lemon, R.N. Descending pathways in motor control. *Annu Rev Neurosci* **31**, 195-218 (2008).
16. Dentel, C. *et al.* Degeneration of serotonergic neurons in amyotrophic lateral sclerosis: a link to spasticity. *Brain* **136**, 483-93 (2013).
17. Boillee, S. *et al.* Onset and progression in inherited ALS determined by motor neurons and microglia. *Science* **312**, 1389-92 (2006).
18. Yamanaka, K. *et al.* Astrocytes as determinants of disease progression in inherited amyotrophic lateral sclerosis. *Nat Neurosci* **11**, 251-3 (2008).
19. Zhong, Z. *et al.* ALS-causing SOD1 mutants generate vascular changes prior to motor neuron degeneration. *Nat Neurosci* **11**, 420-2 (2008).
20. Lobsiger, C.S. *et al.* Schwann cells expressing dismutase active mutant SOD1 unexpectedly slow disease progression in ALS mice. *Proc Natl Acad Sci U S A* **106**, 4465-70 (2009).
21. Kang, S.H. *et al.* Degeneration and impaired regeneration of gray matter oligodendrocytes in amyotrophic lateral sclerosis. *Nat Neurosci* **16**, 571-9 (2013).
22. Vercruysse, P. *et al.* Alterations in the hypothalamic melanocortin pathway in amyotrophic lateral sclerosis. *Brain* **139**, 1106-22 (2016).
23. Li, Y., Li, X., Harvey, P.J. & Bennett, D.J. Effects of baclofen on spinal reflexes and persistent inward currents in motoneurons of chronic spinal rats with spasticity. *J Neurophysiol* **92**, 2694-703 (2004).
24. Boillee, S., Vande Velde, C. & Cleveland, D.W. ALS: a disease of motor neurons and their nonneuronal neighbors. *Neuron* **52**, 39-59 (2006).
25. Clement, A.M. *et al.* Wild-type nonneuronal cells extend survival of SOD1 mutant motor neurons in ALS mice. *Science* **302**, 113-7 (2003).
26. Xu, Z. *et al.* Direct conversion of human fibroblasts to induced serotonergic neurons. *Mol Psychiatry* **21**, 62-70 (2016).
27. Vadodaria, K.C. *et al.* Generation of functional human serotonergic neurons from fibroblasts. *Mol Psychiatry* **21**, 49-61 (2016).

28. Martin, E., Cazenave, W., Cattaert, D. & Branchereau, P. Embryonic alteration of motoneuronal morphology induces hyperexcitability in the mouse model of amyotrophic lateral sclerosis. *Neurobiol Dis* **54**, 116-26 (2013).
29. Amendola, J., Verrier, B., Roubertoux, P. & Durand, J. Altered sensorimotor development in a transgenic mouse model of amyotrophic lateral sclerosis. *Eur J Neurosci* **20**, 2822-6 (2004).
30. Durand, J., Amendola, J., Bories, C. & Lamotte d'Incamps, B. Early abnormalities in transgenic mouse models of amyotrophic lateral sclerosis. *J Physiol Paris* **99**, 211-20 (2006).
31. Bories, C., Amendola, J., Lamotte d'Incamps, B. & Durand, J. Early electrophysiological abnormalities in lumbar motoneurons in a transgenic mouse model of amyotrophic lateral sclerosis. *Eur J Neurosci* **25**, 451-9 (2007).
32. Puig, M.V. & Gener, T. Serotonin Modulation of Prefronto-Hippocampal Rhythms in Health and Disease. *ACS Chem Neurosci* **6**, 1017-25 (2015).
33. Challis, C. & Berton, O. Top-Down Control of Serotonin Systems by the Prefrontal Cortex: A Path toward Restored Socioemotional Function in Depression. *ACS Chem Neurosci* **6**, 1040-54 (2015).
34. Puglisi-Allegra, S. & Andolina, D. Serotonin and stress coping. *Behav Brain Res* **277**, 58-67 (2015).
35. Bennett, D.J., Sanelli, L., Cooke, C.L., Harvey, P.J. & Gorassini, M.A. Spastic long-lasting reflexes in the awake rat after sacral spinal cord injury. *J Neurophysiol* **91**, 2247-58 (2004).
36. El Oussini, H. *et al.* Serotonin 2B receptor slows disease progression and prevents degeneration of spinal cord mononuclear phagocytes in amyotrophic lateral sclerosis. *Acta Neuropathol* (2016).
37. d'Errico, P. *et al.* Selective vulnerability of spinal and cortical motor neuron subpopulations in delta7 SMA mice. *PLoS One* **8**, e82654 (2013).
38. Grider, M.H., Chen, Q. & Shine, H.D. Semi-automated quantification of axonal densities in labeled CNS tissue. *J Neurosci Methods* **155**, 172-9 (2006).
39. Vandesompele, J. *et al.* Accurate normalization of real-time quantitative RT-PCR data by geometric averaging of multiple internal control genes. *Genome Biology* **3**, research0034.1–0034.11 (2002).

Pauline VERCRUYSSE

Altérations hypothalamiques dans la Sclérose Latérale Amyotrophique

École Doctorale des Sciences de la Vie et de la Santé
STRASBOURG

Résumé

La Sclérose Latérale Amyotrophique (SLA) est une maladie neurodégénérative due à la dégénérescence des motoneurones supérieurs et inférieurs. La perte des neurones moteurs entraine une atrophie puis une paralysie progressive des muscles. En plus de la perte musculaire, une perte de poids est importante chez les patients SLA. Ce symptôme apparaît avant les premiers symptômes moteurs et est corrélé avec la survie. Ce défaut du métabolisme énergétique est en partie dû à un hypermétabolisme associé à des problèmes de prise alimentaire. L'hypothalamus est la partie du cerveau contrôlant l'ensemble du métabolisme énergétique. L'objectif de ma thèse a été de caractériser les altérations hypothalamiques dans la SLA.

Nous avons tout d'abord mis en évidence une anomalie du système mélanocortine de l'hypothalamus, et montré que cette anomalie était associée à des modifications du comportement alimentaire. Ensuite, nos travaux ont mis en évidence une atrophie de la partie postérieure de l'hypothalamus, comprenant l'aire hypothalamique latérale (LHA), des patients SLA, corrélée à la perte de poids. Finalement, nous démontré que les neurones produisant le MCH, situés dans le LHA, sont atteints dans la SLA et qu'une complémentation en MCH empêche la perte de poids dans un modèle animal de SLA

Résumé en anglais

Amyotrophic Lateral Sclerosis (ALS) is a major neurodegenerative disease characterised by a loss of upper and lower motor neurons. The loss of motor neurons leads to muscle atrophy and paralysis. Besides motor loss, weight loss is important in ALS patients. This symptom appears before first muscular symptoms and is correlated with survival. This defect of energetic metabolism is partially due to hypermetabolism associated with food intake problems. Hypothalamus is the part of brain controlling the energetic metabolism. The aim of my Ph.D. was to characterise hypothalamic alterations in ALS.

First, we have shown a default in the melanocortin system of hypothalamus, and shown that this melanocortin defect correlates with alterations in food intake behaviour. Second, we demonstrated the existence of hypothalamic atrophy in ALS patients in the posterior part of the hypothalamus, including the lateral hypothalamic area (LHA). This atrophy was correlated with weight loss. Finally, we observed that hypothalamic MCH neurons, located in the LHA, are affected in ALS, and that MCH complementation rescues weight loss in a mouse model of ALS.